BIVALVE SHELLS AS PALEO-PROXY ARCHIVES: ASSESSMENT OF THE USEFULNESS AS ENVIRONMENTAL AND CLIMATIC RECORDERS IN THE SOUTHERN HEMISPHERE

BY

HERATH MUDIYANSELAGE DILMI VINDYA HERATH

DEPARTMENT OF EARTH AND PLANETARY SCIENCES
FACULTY OF SCIENCE AND ENGINEERING
MACQUARIE UNIVERSITY
SYDNEY, AUSTRALIA

A DISSERTATION SUBMITTED IN
PARTIAL FULFILMENT OF THE REQUIREMENTS
FOR THE DEGREE OF DOCTOR OF PHILOSOPHY

SUPERVISOR:
PROFESSOR DORRIT E. JACOB

MARCH 2018

MACQUARIE
University
SYDNEY·AUSTRALIA

"It's not the strongest of the species that survive,
nor the most intelligent,
but the one most responsive to change……"
Charles Darwin

To my family, Thaththi, Ammi, Avi, Kaushi and Sarath

There is nothing more important to me in this world than you all…

TABLE OF CONTENT

CHAPTER 2

TEMPERATURE RECONSTRUCTIONS BY δ¹⁸O AND Sr/Ca USING FRESHWATER BIVALVE *Echyridella menziesii* FROM NEW ZEALAND   54

CHAPTER 4

CLIMATE SIGNALS IN THE SHELLS OF *Diplodon chilensis patagonicus* (HAAS, 1931) BIVALVES IN NORTHERN PATAGONIA, ARGENTINA

CHAPTER 5

MEDIEVAL CLIMATIC ANOMALY SIGNALS IN FOSSIL *Diplodon chilensis patagonicus* (HAAS, 1931) SHELLS FROM NORTHERN PATAGONIA

DECLARATION

I certify that the work in this thesis titled "Bivalve shells as paleo-proxy archives: assessment of the usefulness as environmental and climatic recorders in the southern hemisphere" has not previously been submitted for a degree nor has it been submitted as part or requirements for a degree to any other university or institution other than Macquarie University.

I also certify that the thesis is an original piece of research and it has been written by me. Any help and assistance that I have received in my research work and the preparation of the thesis itself have been appropriately acknowledged. In addition, I certify that all information sources and literature used are acknowledged appropriately.

Herath Mudiyanselage Dilmi Vindya Herath

Student number 43879063

SUMMARY

In contrast to other skeletal bio-carbonates, the potential of freshwater bivalves as environmental and climate archives has been less explored, despite the fact that freshwater bivalves are well-known to record environmental variables such as temperature, precipitation, primary productivity, and river discharge in multiple ways which facilitates the combination of numerous proxies that strengthens the proxy records. Although there are a large number of marine proxy studies in the southern hemisphere, the number of similar studies in freshwater environments are comparatively limited, creating a considerable lack of understanding on the past continental climate in the region. In this thesis, freshwater bivalves are studied from three different localities at similar latitudes in the southern hemisphere, namely New Zealand, Australia and South America, in order to identify the potential of five different species as new environmental proxy archives. The results show that physical and chemical characteristics in three studied species; *Echyridella menziesii*, *Alathyria profuga* and *Diplodon chilensis patagonicus* have the possibility to be used as proxies of numerous environmental and climatic variables. *Echyridella menziesii* and *Alathyria profuga* exhibit the suitability of using shell oxygen isotope ratio as a temperature proxy since temperature reconstructions using these proxies agree well ($\pm$ 2.5 and $\pm$ 3.5 °C respectively) with instrumental temperature data. Similarly, Sr/Ca in *Echyridella menziesii* and *Diplodon chilensis patagonicus* can function as a proxy of ambient temperature as both exhibit significant correlations ($r > 0.6$, $p < 0.05$) with instrumental temperature. More importantly, this study introduces the use of two different empirical equations for summer and winter which improves the reliability in summer temperature reconstructions. Further, all three species exhibit distinct growth variations in responding to regional climatic phenomena such as the Southern Annular Mode and the El Niño southern oscillation. Both *Echyridella menziesii* and *Diplodon chilensis patagonicus* show a distinctive reduction in growth during El Niño years contrary to tree ring data from these regions. Finally, fossil *Diplodon chilensis patagonicus* shells are used to evaluate the environmental conditions during medieval times (1200 – 1350 cal. yr. BP) and identified the medieval climatic anomalies as variations in Sr/Ca ratios in the shells supporting similar findings in other paleoclimate proxy archives in Argentinean Patagonia. Additionally, this provides new estimates for lifespans and growth rates for all studied species. This thesis delivers three new proxy archives which are widespread in the southern hemisphere and have the potential to improve available proxy networks, thus enhancing the precision of spatially resolved continental-scale temperature reconstructions.

ACKNOWLEDGEMENT

INTRODUCTION

The climate of Earth has undergone significant variations during the current interglacial period and is yet to be quantified at the continental scale (PAGES 2K consortium, 2013). This is largely due to lack of instrumental records beyond the last 300 years. However, paleoclimate records are preserved in marine, aquatic, and terrestrial settings from around the world that can be analysed and correlated with modern environmental parameters to improve climate models that are used to project possible future climates. These records are preserved as geological (sediments, ice cores) or biological (tree-rings, corals, molluscs) materials that document evidence of past climate variations (Cronin, 2009).

The wealth of evidence derived from the carbonate skeletons of molluscs present important information for environmental monitoring and predicting the consequences of climate change. The chemical composition of mollusc shells is determined by the chemistry of the water during shell formation which is influenced by the ambient environmental conditions. Therefore, numerous molluscs have been identified as recorders of temperature (Schöne et al., 2004a; Schöne et al., 2004b; Yan et al., 2014; Zhao et al., 2017a), precipitation (Kaandorp et al., 2005), pH (Kasemann et al., 2009; Kelemen et al., 2018), salinity (Brewster-Wingard and Ishman, 1999) and many other environmental variables. More importantly, in contrast to most archives, molluscs register environmental records from daily to annual resolution (Schöne and Surge, 2012).

Tree rings are the most commonly used continental archives that can grow for hundreds or even thousands of years and are mainly used to identify the changes in past temperature (Esper et al., 2002; Villalba et al., 2003), precipitation (Villalba et al., 1998), fire history (Holz and Veblen, 2011), and streamflow during the growing season (Lara et al., 2008). Tree rings usually record environmental data at annual resolution but mostly during the growing season. In contrast, speleothems, another frequently used terrestrial archive, span thousands to hundreds of thousands of years at a decadal or centennial resolution. These speleothems record information on drought conditions, temperature, and periods of high precipitation (Proctor et al., 2000; McDermott, 2004). Other than these major archives there are many climate archives for example corals (Hendy et al., 2002; Shen et al., 2005; Corrège, 2006), sediments (Charles et al., 1996; Lea et al., 2000), ice core (Dansgaard et al., 1993; Petit et al., 1999), pollen (Guiot et al., 1989; Davis et al., 2003), foraminifera (Waelbroeck et al., 2002; Eggins et al., 2003), ostracoda (Lister et al., 1991; De Deckker and Lord, 2017), and otoliths (Patterson, 1999; Wurster and Patterson, 2001).

Importance and challenges of mollusc shells as paleo-climatic archives

Molluscs have a significant place in paleo climatic research because of their wide biogeographic distribution, long geologic history and archaeological importance. Additionally, molluscs are among the longest-lived singular animals, with many species living up to centuries (*Arctica islandica* – 405 years; Butler et al., 2013, *Panopea abrupta* – 100-160 years; Strom et al. 2004, *Margritifera margritifera* – 127 years; Schöne et al., 2004).

The study of the incremental growth patterns in hard parts of animals is called sclerochronology (Surge and Schöne, 2015). Although the term sclerochronology was first introduced by Buddemeier et al., (1974) during a study of growth patterns in coral exoskeletons, it is currently used in studies of many calcareous aquatic organisms such as bivalves, limpets (Fenger et al., 2007), fish otoliths (Panfili et al., 2002), and coralline sponges (Fabre and Lathuiliere, 2007). Biogenic calcareous hard parts of molluscs grow continuously throughout the lifetime, influenced by the ambient environment, and are periodically interrupted by various environmental factors such as tidal cycles, seasonal cycles, and food availability (Schöne, 2008). These growth interruptions form growth lines in fast-growing portions of the carbonates and provide the key criterion for chronological research. Growth increments (distance between two adjacent growth lines) of molluscs offer invaluable information about the age and growth of the mollusc as well as different ambient environmental variations during the formation of shells such as temperature (Goodwin et al., 2001; Schöne et al., 2004b) and precipitation (Schöne et al., 2007). Other than growth rates, molluscs record environmental variables in multiple ways such as isotopic and trace element variation. This facilitates the combination of sclerochronology with geochemical data that can strengthen environmental records.

The oxygen isotope ratio ($\delta^{18}O$) is the most widely used geochemical proxy of bio carbonates and is a function of variations in the ambient water temperature and water $\delta^{18}O$ level (Urey, 1947). Numerous studies have demonstrated that molluscs precipitate their shells in oxygen isotopic equilibrium with the ambient water (Dettman et al., 1999). Therefore water temperature is related to the $\delta^{18}O_{shell}$ value of aragonitic bio-carbonates using fractionation equations introduced by Grossman and Ku (1986) and modified by Dettman, Reische & Lohmann (1999). These are used to quantitatively determine the precipitation temperature of modern and fossil bivalves (Carré et al., 2005; Foster et al., 2009; Bougeois et al., 2014).

The major weakness of this process is the use of the water $\delta^{18}O$ value which could be unknown in fossil samples. To overcome this, clumped isotope analysis of bicarbonates was introduced and successfully used on mollusc shells (Came et al., 2007; Csank et al., 2011; Wacker et al., 2014). In contrast to traditional oxygen isotope thermometry, clumped isotopes do not depend on the $\delta^{18}O_{water}$ but only varies with water temperature (Eiler, 2011; Affek, 2012), which, therefore, can be used to determine the precipitation temperature, especially in fossil samples where the $\delta^{18}O_{water}$ during shell formation is unknown. Currently, the biggest disadvantage of clumped isotopes analysis is the requirement of a large sample size that reduces the resolution in smaller mollusc species. Other than temperature, oxygen isotope ratios are also used as a proxy for river discharge (Dettman et al., 2004; Kelemen et al., 2017) and to identify the season of shellfish collection in archaeological settings (Burchell et al., 2013).

Trace element-to-calcium ratios of biogenic carbonates contain a wide range of paleoenvironmental information. Most frequently used trace elements in paleoclimatic studies are Sr, Mg, Ba and Mn. The Sr/Ca and Mg/Ca are commonly used as proxies of temperature (Yan et al., 2014; Tynan et al., 2016) while Ba/Ca is used as a proxy of salinity, precipitation and phytoplankton productivity (Gillikin et al., 2006; Izzo et al., 2016). Similarly, Mn/Ca is also used to determine the phytoplankton productivity, seasonal upwellings (Langlet et al., 2007a) and manganese cycling at the sediment-water interface (Zhao et al., 2017b). However, depending on the species, some studies conclude that the element/Ca in mollusc shells cannot be considered as reliable proxies due to the lower correlation between these and environmental variables compared to other species (Poulain et al., 2015; Geeza et al., 2018).

Aside from the environment, bivalve physiology is another factor that exerts major control over how environmental changes are recorded in the shell. There are many 'vital effects' (Urey et al., 1951), such as ontogenetic age, growth rate and metabolism that modify the chemical composition of the carbonate-secreting fluid, and thus, the biogenic hard tissues. For example, laboratory studies showed that Sr/Ca in inorganic aragonite decrease with increasing temperature (Beck et al., 1992). However, the behaviour of biogenic Sr/Ca varies significantly among different species: some show negative (Yan et al., 2014) while others have positive (Gillikin et al., 2005; Elliot et al., 2009) correlations with temperature, and some other bivalve species do not display any correlation with temperature (Freitas et al.,

2005; Schöne et al., 2011). Further, during spawning, and above and below genetically determined thermal extremes, molluscs stop growing skeletal material at regular time intervals (Schöne and Surge, 2012). These physiological effects are the major reason behind the lower correlation between chemical proxies and environmental variables in molluscs compared to corals.

These physiological effects vary among species, for example, *Tridacnidae* faithfully record environmental parameters (Yan et al., 2014; Yan et al., 2015) while *Mercenaria mercenaria* has a strong biological control on element distribution (Gillikin et al., 2005). Further, these physiological effects do not affect every biogenic calcareous carbonate at the same rate. Physiological effects on corals or foraminifera are lower than on molluscs, mainly due to the low evolutionary state of the corals and foraminifera. Therefore, a robust interpretation of geochemical proxy records from mollusc shells requires a detailed understanding of the physiology of the mollusc that produced the skeleton.

Freshwater bivalves as environmental archives

Freshwater bivalves belong to the order Unionoida and live in a wide range of geographical regions from the tropics to high latitudes and are a common constituent of archaeological sites (Campbell, 1972; Campbell, 2005; Peacock and Seltzer, 2008). These Unionoida shells typically have two different layers (Carter, 1990); outer and inner layer and unlike marine species, the outer layer in freshwater bivalves is prismatic and thinner while the inner nacreous layer covers the largest part of the shell (Fig. 1). These are usually characterised by an aragonitic shell with a nacro-prismatic microstructure, covered by a thick periostracum (Boggild, 1930; Carter, 1990).

Freshwater bivalve shells are used in environmental monitoring (Markich et al., 2002) and are an important component in ecosystems because of their filter-feeding, nutrient cycling nature and as a food source for a wide variety of organisms (Klunzinger et al., 2014). Due to the success in using marine bivalves as proxy archives, freshwater bivalves have also been studied, though with less intensity, for their potential as an environmental archive (eg; Black et al., 2010; Dettman et al., 1999; Geeza et al., 2018; Goewert et al., 2007; Kaandorp et al., 2003; Kelemen et al., 2017; O'Neil and Gillikin, 2014; Peacock and Seltzer, 2008; Ricken et al., 2003; Versteegh et al., 2009).
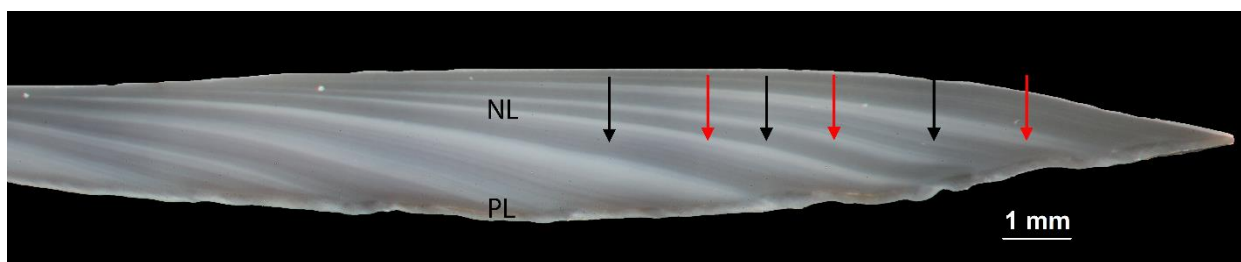
Fig. 1 Polished cross section of a freshwater bivalve *Diplodon chilensis patagonicus* shell indicating dark and light coloured bands present in the inner and outer layer of the shell. Red (black) arrows points at light (dark) bands. NL = Nacreous Layer, PL = Prismatic Layer

In contrast to relatively stable marine environments, complex variations in freshwater systems such as strong seasonality in water oxygen isotope levels, the influence of precipitation, groundwater influx and evaporation, make the use of freshwater bivalves challenging (Kelemen et al., 2018). Other major differences between marine and freshwater bivalves are the usefulness of different proxies, for example, Mg/Ca are less useful in freshwater settings due to low Mg concentrations in freshwater (Schöne et al., 2010) whereas Mn/Ca in freshwater settings are frequently studied (Langlet et al., 2007b; Kelemen et al., 2018). Ba/Ca in marine water act as a freshwater input proxy in marine species and have reduced function in freshwater studies. In contrast, Sr/Ca and oxygen isotope ratios in freshwater bivalves are as useful as in marine archives.

Each archive records environmental variability from its unique perspective of habitat, location, life history, or trophic level such that a combination of these archives provide a stronger context of the past than any data set could provide on its own. Although such multiproxy climate reconstructions remain poorly explored (Black et al., 2009), such an approach can be used to strengthen and corroborate one another. Due to similarities in resolution, freshwater bivalves can be considered as the best proxy archive to fortify tree-ring data. Continental climatic archives are currently biased towards dendrochronology because, tree ring data are annually resolved, typically span over hundreds of years, and can be extended over millennia when chronologies from dead trees are combined with living trees. However, tree rings only record environmental variabilities during the growing season that restricts the winter records.

Due to advancements in dendrochronology as a climate archive, mollusc chronologies also use the applications used in dendrochronology such as cross-dating and chronology statistics. Cross-dating is the combination of individual chronologies from different time periods to

form one master chronology using tools like COFECHA (Holmes, 1983) and ARSTAN (Cook and Peters, 1981), which are commonly used in both dendrochronology and sclerochronology. Further, chronology statistics such as R_{bar} (mean of all correlations between pairs of increment-width series) and expressed population signal (an indication of whether the common variance in the chronology is a sufficiently good expression of the common variance in the population) are also adapted in sclerochronology for chronology verification (Schöne et al., 2007; Black et al., 2010; Butler et al., 2010; Roman-Gonzalez et al., 2016). However, using dendrochronological applications on short-lived molluscs and smaller sample sizes is challenging.

Current understanding of climate variability in the southern hemisphere

Compared to the northern hemisphere, there is a lack of understanding about the climate variability over the past 1000–2000 years from the southern hemisphere (Neukom and Gergis, 2012; Chung et al., 2017). This is mainly due to the oceanic dominance at mid to high latitudes of the southern hemisphere that severely limits the availability of terrestrial archives. This limitation creates an urgent need for exploring more climate archives from the southern hemisphere. It is critical to explore more paleo-climate archives from a wide range of geographical regions, since isolating unique natural climate variabilities in different regions from anthropogenic climate change is important for reliable future climate predictions. Currently, there are only a few studies that have tested the possibility of using freshwater bivalves from the southern hemisphere as climatic archives (Kaandorp et al., 2003; Langlet et al., 2007b; Risk et al., 2010; Kelemen et al., 2017).

The major large-scale recurrent climatic phenomena that influence the climate in southern hemisphere are El Niño–Southern Oscillation (ENSO), Southern Annular Mode (SAM), and westerly winds (Fig. 2). The influence of these varies in different parts of the southern hemisphere. El Niño is a natural, coupled atmospheric-oceanic cycle that occurs in the tropical Pacific Ocean on an approximate timescale of 2–7 years (Hanley et al., 2003). During El Niño, New Zealand tends to experience stronger or more frequent winds from the west in summer, typically leading to drought in east coast areas and more rain in the west. La Niña is characterised by more north-easterly winds that tend to bring moist, rainy conditions to the northeast of the North Island. During El Niño years most of southern Australia tends to see warmer than average temperatures and eastern Australia receives

7

reduced rainfall. In contrast, La Niña produces heavy rainfall across eastern and northern Australia while cooler than normal temperatures dominate across most of mainland Australia. During El Niño events Patagonia experience above-average precipitation and increased moisture availability to plants during the growing season whereas La Niña events correspond with drought conditions (Kitzberger et al., 2001).
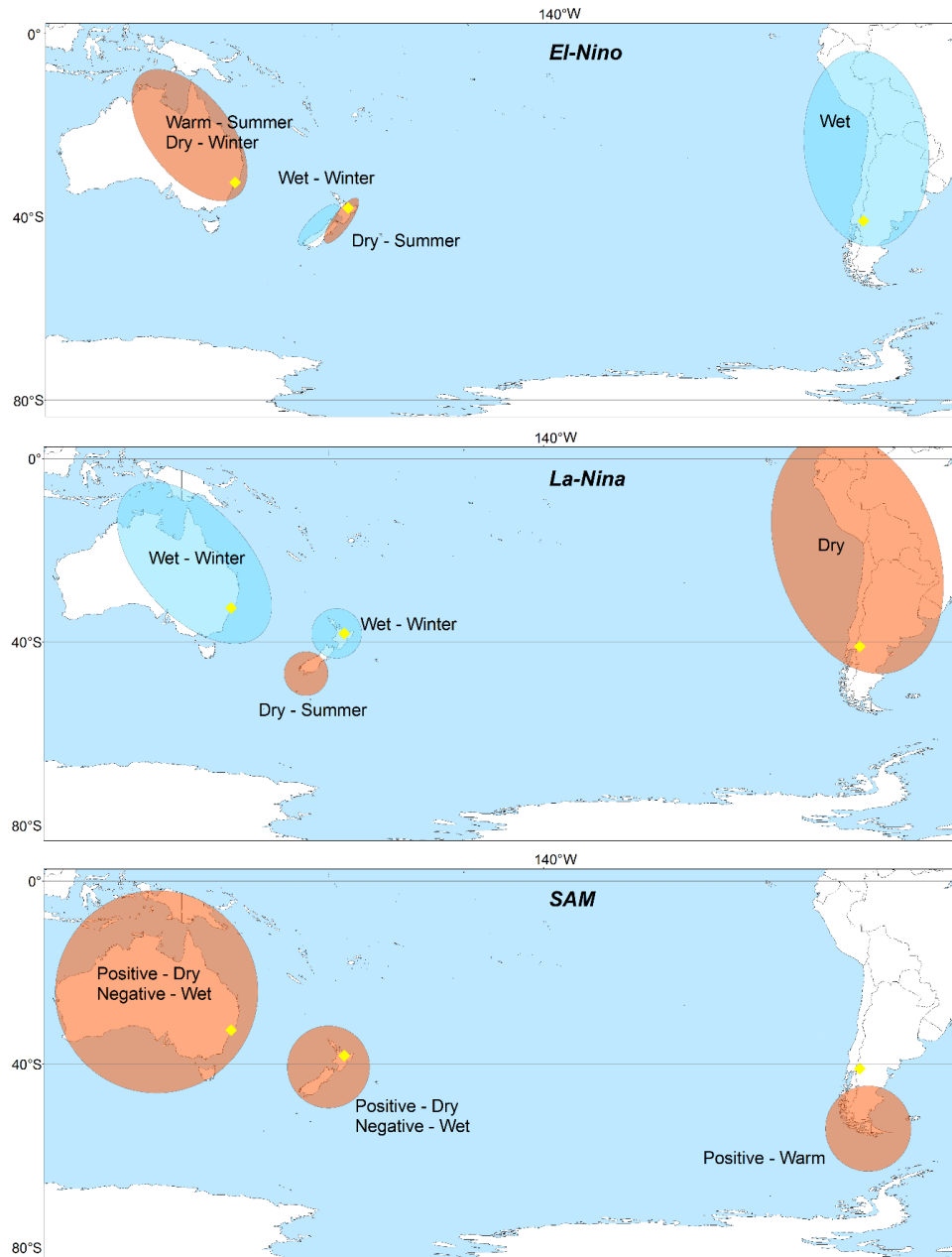
Fig. 2 Effects of El Niño, La Niña and Southern Annular Mode in different parts of South Pacific. Yellow diamonds mark the study locations considered in this thesis. Data from www.bom.gov.au and www.niwa.co.nz.

The Southern Annular Mode, also known as the Antarctic Oscillation, describes the north–south movement of the westerly wind belt that circles Antarctica, with synchronous anomalies of opposite signs over the Antarctic and the mid-latitudes centred near 45°S

(Marshall, 2003; Gillett et al., 2006). In its positive phase, the SAM is associated with relatively light winds and more settled weather over New Zealand, together with enhanced westerly winds over the southern oceans. In the negative phase, the westerlies increase over New Zealand, with the more unsettled weather, while windiness and storm activity ease over the southern oceans. The positive SAM event results in weaker than normal westerly winds and higher pressures over southern Australia, restricting the penetration of cold fronts inland. Conversely, a negative SAM event results in stronger storms and low-pressure systems over southern Australia. Although the impact of the SAM on Patagonia has not been well examined, limited studies have found that the SAM results in warming in southern South America (Thompson and Solomon, 2002; Sen Gupta and England, 2006).

Aims and structure of the thesis

Although there are a large number of carbonate proxy studies in marine environments, the number of similar studies in freshwater environments are comparatively small. This is even smaller in the south Pacific creating a lack of understanding about the past continental climate in the region. Therefore, in this thesis, freshwater bivalves are studied from three different localities in the southern hemisphere; New Zealand, Australia and Argentina to identify the potential of five different species as new environmental proxy archives.

This thesis is divided into five chapters, the First two chapters both discuss the dominant freshwater bivalve species in New Zealand; *Echyridella menziesii* (Gray 1843), and the potential of this species as a new environmental proxy archive from the southern hemisphere. Although ecology, taxonomy and the toxicology of this species has been studied previously (Roper and Hickey, 1994; Clearwater et al., 2014; Marshall et al., 2014; Cyr et al., 2016), this is the first study to our knowledge on the structure and composition of *Echyridella menziesii* shells. **Chapter 1** discusses the age and environmental relations of *Echyridella menziesii* shells from Lake Rotorua, New Zealand. This chapter is mainly focused on the biological community and has been prepared for submission to the journal 'Freshwater Science'. **Chapter 2** evaluates the potential of using *Echyridella menziesii* in temperature reconstructions using a multi-proxy approach. Due to the relatively smaller shell size in the Hyriidae family, obtaining high-resolution time series was a challenge (Chapter 3). This was overcome in this chapter by using secondary ion mass spectrometry analysis to obtain time series at weekly resolution. In contrast to the first chapter, the second chapter is mainly aimed

at a paleoclimate audience which therefore is formatted for submission to the Journal 'Palaeogeography, Palaeoclimatology, Palaeoecology'.

Despite the fact that more than 30 freshwater bivalve species are known in Australia (Walker et al., 2014), none have been studied with the intention of identifying the environmental archival potential. **Chapter 3** documents three freshwater bivalve species from eastern Australia namely *Alathyria profuga* (Gould, 1851), *Cucumerunio novaehollandiae* (Gray, 1834) and *Hyridella drapeta* (Iredale, 1934) that are studied here to identify the potential of these species as new environmental proxy archives. Further, growth analysis allows the first identification of age and growth structure of *A. profuga* and *C. novaehollandiae*. This chapter is now published in the Journal 'Marine and Freshwater Research'.

Chapter 4 describes a similar study as chapter 3, on Patagonian freshwater bivalve *Diplodon chilensis patagonicus* (Haas, 1931). The northern Patagonian region considered in this study is at a similar latitude as New Zealand and has the coldest environment compared to temperate New Zealand and semi-arid Australia. This chapter studies the suitability of *Diplodon* shells in environmental reconstructions using growth, stable isotopes and trace element variations. Further, this chapter explores the relationships between shell growth and regional climatic phenomena such as Southern Annular Mode and El Niño southern oscillation. Chapter four is also aimed at paleoclimate audience and therefore is formatted for submission to the Journal 'Palaeogeography, Palaeoclimatology, Palaeoecology'.

Finally, I present the first calibrated ages for Holocene freshwater bivalve shells in Argentinean Patagonia in **Chapter 5**. While all other chapters use living bivalve specimens, here we used fossil bivalve shells from two archaeological excavations from northern Patagonia. Calibrated ages of 27 *Diplodon chilensis patagonicus* shells were measured that provides insight on the first evidence of the medieval climatic anomalies in South America using freshwater bivalve shells. Since this chapter is especially relevant to the archaeological community, this chapter is formatted to be submitted to 'The Holocene'. All these chapters are constructed as stand alone manuscripts, (thesis by publication) and there are repetitions in each chapter especially in the introductions and methods.

References

Affek, H.P., 2012. Clumped isotope paleothermometry: principles, applications, and challenges. Reconstructing Earth's Deep-Time Climate—The State of the Art in: 101-114.

Ahmed, M., Anchukaitis, K.J., Asrat, A., Borgaonkar, H.P., Braida, M., Buckley, B.M., Büntgen, U., Chase, B.M., Christie, D.A. and Cook, E.R., 2013. Continental-scale temperature variability during the past two millennia. Nature Geoscience, 6(5): 339.

Beck, J.W., Edwards, R.L., Ito, E., Taylor, F.W., Recy, J., Rougerie, F., Joannot, P. and Henin, C., 1992. Sea-surface temperature from coral skeletal strontium/calcium ratios. Science, 257(5070): 644-647.

Black, B.A., Copenheaver, C.A., Frank, D.C., Stuckey, M.J. and Kormanyos, R.E., 2009. Multi-proxy reconstructions of northeastern Pacific sea surface temperature data from trees and Pacific geoduck. Palaeogeography, Palaeoclimatology, Palaeoecology, 278(1): 40-47.

Black, B.A., Dunham, J.B., Blundon, B.W., Raggon, M.F. and Zima, D., 2010. Spatial variability in growth-increment chronologies of long-lived freshwater mussels: implications for climate impacts and reconstructions. Ecoscience, 17(3): 240-250.

Boggild, O.B., 1930. The shell structure of the mollusks. Det Kongelige Danske Videnskabernes Selskabs Skrifter. Naturvidenskabelig og Mathematisk Afdeling, Raekke 9, 2: 231-326.

Bougeois, L., De Rafélis, M., Reichart, G.-J., De Nooijer, L.J., Nicollin, F. and Dupont-Nivet, G., 2014. A high resolution study of trace elements and stable isotopes in oyster shells to estimate Central Asian Middle Eocene seasonality. Chemical Geology, 363: 200-212.

Brewster-Wingard, G.L. and Ishman, S.E., 1999. Historical trends in salinity and substrate in central Florida Bay: a paleoecological reconstruction using modern analogue data. Estuaries, 22(2): 369-383.

Buddemeier, R.W., Maragos, J.E. and Knutson, D.W., 1974. Radiographic studies of reef coral exoskeletons: rates and patterns of coral growth. Journal of Experimental Marine Biology and Ecology, 14(2): 179-199.

Burchell, M., Cannon, A., Hallmann, N., Schwarcz, H. and Schöne, B., 2013. Refining estimates for the season of shellfish collection on the Pacific Northwest coast: Applying higyh-resolution stable oxygen isotope analysis and schlerochronology. Archaeometry, 55(2): 258-276.

Butler, P.G., Richardson, C.A., Scourse, J.D., Wanamaker, A.D., Shammon, T.M. and Bennell, J.D., 2010. Marine climate in the Irish Sea: analysis of a 489-year marine master chronology derived from growth increments in the shell of the clam *Arctica islandica*. Quaternary Science Reviews, 29(13): 1614-1632.

Butler, P.G., Wanamaker, A.D., Scourse, J.D., Richardson, C.A. and Reynolds, D.J., 2013. Variability of marine climate on the North Icelandic Shelf in a 1357-year proxy archive based on growth increments in the bivalve A*rctica islandica*. Palaeogeography, Palaeoclimatology, Palaeoecology, 373: 141-151.

Came, R.E., Eiler, J.M., Veizer, J., Azmy, K., Brand, U. and Weidman, C.R., 2007. Coupling of surface temperatures and atmospheric CO2 concentrations during the Palaeozoic era. Nature, 449(7159): 198-201.

Campbell, M., 2005. The archaeology of kakahi (*Hyridella menziesi*). Archaeology in New Zealand 48 (2): 101-112.

Campbell, V., 1972. Some Radiocarbon Dates for Aboriginal Shell Middens in the Lower Macleay River Valley, New South Wales. Mankind, 8(4): 283-286.

Carré, M., Bentaleb, I., Blamart, D., Ogle, N., Cardenas, F., Zevallos, S., Kalin, R.M., Ortlieb, L. and Fontugne, M., 2005. Stable isotopes and sclerochronology of the bivalve *Mesodesma donacium*: potential application to Peruvian paleoceanographic reconstructions. Palaeogeography, Palaeoclimatology, Palaeoecology, 228(1): 4-25.

Carter, J.G., 1990. Skeletal Biomineralization: Atlas and index, 2. Van Nostrand Reinhold Company.

Charles, C.D., Lynch-Stieglitz, J., Ninnemann, U.S. and Fairbanks, R.G., 1996. Climate connections between the hemisphere revealed by deep sea sediment core/ice core correlations. Earth and Planetary Science Letters, 142(1-2): 19-27.

Chung, C.T., Power, S.B., Santoso, A. and Wang, G., 2017. Multiyear Variability in the Tasman Sea and Impacts on Southern Hemisphere Climate in CMIP5 Models. Journal of Climate, 30(12): 4413-4427.

Clearwater, S., Wood, S., Phillips, N., Parkyn, S., Van Ginkel, R. and Thompson, K., 2014. Toxicity thresholds for juvenile freshwater mussels *Echyridella menziesii* and crayfish *Paranephrops planifrons*, after acute or chronic exposure to *Microcystis* sp. Environmental toxicology, 29(5): 487-502.

Cook, E.R. and Peters, K., 1981. The smoothing spline: a new approach to standardizing forest interior tree-ring width series for dendroclimatic studies. Tree-ring bulletin.

Corrège, T., 2006. Sea surface temperature and salinity reconstruction from coral geochemical tracers. Palaeogeography, Palaeoclimatology, Palaeoecology, 232(2): 408-428.

Cronin, T.M., 2009. Paleoclimates: understanding climate change past and present. Columbia University Press.

Csank, A.Z., Tripati, A.K., Patterson, W.P., Eagle, R.A., Rybczynski, N., Ballantyne, A.P. and Eiler, J.M., 2011. Estimates of Arctic land surface temperatures during the early Pliocene from two novel proxies. Earth and Planetary Science Letters, 304(3): 291-299.

Cyr, H., Collier, K.J., Clearwater, S.J., Hicks, B.J. and Stewart, S.D., 2016. Feeding and nutrient excretion of the New Zealand freshwater mussel *Echyridella menziesii* (Hyriidae, Unionida): implications for nearshore nutrient budgets in lakes and reservoirs. Aquatic Sciences: 1-15.

Dansgaard, W., Johnsen, S., Clausen, H., Dahl-Jensen, D., Gundestrup, N., Hammer, C., Hvidberg, C., Steffensen, J., Sveinbjörnsdottir, A. and Jouzel, J., 1993. Evidence for general instability of past climate from a 250-kyr ice-core record. Nature, 364(6434): 218-220.

Davis, B.A., Brewer, S., Stevenson, A.C. and Guiot, J., 2003. The temperature of Europe during the Holocene reconstructed from pollen data. Quaternary Science Reviews, 22(15): 1701-1716.

De Deckker, P. and Lord, A., 2017. Cyprideis torosa: a model organism for the Ostracoda? Journal of Micropalaeontology, 36(1): 3-6.

Dettman, D.L., Flessa, K.W., Roopnarine, P.D., Schöne, B.R. and Goodwin, D.H., 2004. The use of oxygen isotope variation in shells of estuarine mollusks as a quantitative record of seasonal and annual Colorado River discharge. Geochimica et Cosmochimica Acta, 68(6): 1253-1263.

Dettman, D.L., Reische, A.K. and Lohmann, K.C., 1999. Controls on the stable isotope composition of seasonal growth bands in aragonitic fresh-water bivalves (Unionidae). Geochimica et Cosmochimica Acta, 63(7): 1049-1057.

Eggins, S., De Deckker, P. and Marshall, J., 2003. Mg/Ca variation in planktonic foraminifera tests: implications for reconstructing palaeo-seawater temperature and habitat migration. Earth and Planetary Science Letters, 212(3): 291-306.

Eiler, J.M., 2011. Paleoclimate reconstruction using carbonate clumped isotope thermometry. Quaternary Science Reviews, 30(25): 3575-3588.

Elliot, M., Welsh, K., Chilcott, C., McCulloch, M., Chappell, J. and Ayling, B., 2009. Profiles of trace elements and stable isotopes derived from giant long-lived *Tridacna gigas* bivalves: potential applications in paleoclimate studies. Palaeogeography, Palaeoclimatology, Palaeoecology, 280(1): 132-142.

Esper, J., Cook, E.R. and Schweingruber, F.H., 2002. Low-frequency signals in long tree-ring chronologies for reconstructing past temperature variability. science, 295(5563): 2250-2253.

Fabre, C. and Lathuiliere, B., 2007. Relationships between growth-bands and paleoenvironmental proxies Sr/Ca and Mg/Ca in hypercalcified sponge: A micro-laser induced breakdown spectroscopy approach. Spectrochimica Acta Part B: Atomic Spectroscopy, 62(12): 1537-1545.

Fenger, T., Surge, D., Schöne, B. and Milner, N., 2007. Sclerochronology and geochemical variation in limpet shells (*Patella vulgata*): a new archive to reconstruct coastal sea surface temperature. Geochemistry, Geophysics, Geosystems, 8(7).

Foster, L., Allison, N., Finch, A., Andersson, C. and Ninnemann, U., 2009. Controls on δ18O and δ13C profiles within the aragonite bivalve *Arctica islandica*. The Holocene, 19(4): 549-558.

Freitas, P., Clarke, L.J., Kennedy, H., Richardson, C. and Abrantes, F., 2005. Mg/Ca, Sr/Ca, and stable-isotope (δ18O and δ13C) ratio profiles from the fan mussel *Pinna nobilis*: Seasonal records and temperature relationships. Geochemistry, Geophysics, Geosystems, 6(4).

Geeza, T.J., Gillikin, D.P., Goodwin, D.H., Evans, S.D., Watters, T. and Warner, N.R., 2018. Controls on magnesium, manganese, strontium, and barium concentrations recorded in freshwater mussel shells from Ohio. Chemical Geology.

Gillett, N.P., Kell, T.D. and Jones, P., 2006. Regional climate impacts of the Southern Annular Mode. Geophysical Research Letters, 33(23).

Gillikin, D.P., Dehairs, F., Lorrain, A., Steenmans, D., Baeyens, W. and André, L., 2006. Barium uptake into the shells of the common mussel (*Mytilus edulis*) and the potential for estuarine paleo-chemistry reconstruction. Geochimica et Cosmochimica Acta, 70(2): 395-407.

Gillikin, D.P., Lorrain, A., Navez, J., Taylor, J.W., André, L., Keppens, E., Baeyens, W. and Dehairs, F., 2005. Strong biological controls on Sr/Ca ratios in aragonitic marine bivalve shells. Geochemistry, Geophysics, Geosystems, 6(5).

Goodwin, D.H., Flessa, K.W., Schöne, B.R. and Dettman, D.L., 2001. Cross-calibration of daily growth increments, stable isotope variation, and temperature in the Gulf of California bivalve mollusk Chione cortezi: implications for paleoenvironmental analysis. Palaios, 16(4): 387-398.

Grossman, E.L. and Ku, T.-L., 1986. Oxygen and carbon isotope fractionation in biogenic aragonite: temperature effects. Chemical Geology: Isotope Geoscience Section, 59: 59-74.

Guiot, J., Pons, A., de Beaulieu, J.L. and Reille, M., 1989. A 140,000-year continental climate reconstruction from two European pollen records. Nature, 338(6213): 309-313.

Hanley, D.E., Bourassa, M.A., O'Brien, J.J., Smith, S.R. and Spade, E.R., 2003. A quantitative evaluation of ENSO indices. Journal of Climate, 16(8): 1249-1258.

Hendy, E.J., Gagan, M.K., Alibert, C.A., McCulloch, M.T., Lough, J.M. and Isdale, P.J., 2002. Abrupt decrease in tropical Pacific sea surface salinity at end of Little Ice Age. Science, 295(5559): 1511-1514.

Holmes, R.L., 1983. Computer-assisted quality control in tree-ring dating and measurement. Tree-ring bulletin.

Holz, A. and Veblen, T.T., 2011. Variability in the Southern Annular Mode determines wildfire activity in Patagonia. Geophysical Research Letters, 38(14).

Izzo, C., Manetti, D., Doubleday, Z.A. and Gillanders, B.M., 2016. Calibrating the element composition of *Donax deltoides* shells as a palaeo-salinity proxy. Palaeogeography, Palaeoclimatology, Palaeoecology.

Kaandorp, R.J., Vonhof, H.B., Del Busto, C., Wesselingh, F.P., Ganssen, G.M., Marmól, A.E., Pittman, L.R. and van Hinte, J.E., 2003. Seasonal stable isotope variations of the modern Amazonian freshwater bivalve *Anodontites trapesialis*. Palaeogeography, Palaeoclimatology, Palaeoecology, 194(4): 339-354.

Kaandorp, R.J., Vonhof, H.B., Wesselingh, F.P., Pittman, L.R., Kroon, D. and van Hinte, J.E., 2005. Seasonal Amazonian rainfall variation in the Miocene climate optimum. Palaeogeography, Palaeoclimatology, Palaeoecology, 221(1): 1-6.

Kasemann, S.A., Schmidt, D.N., Bijma, J. and Foster, G.L., 2009. In situ boron isotope analysis in marine carbonates and its application for foraminifera and palaeo-pH. Chemical Geology, 260(1): 138-147.

Kelemen, Z., Gillikin, D.P. and Bouillon, S., 2018. Relationship between river water chemistry and shell chemistry of two tropical African freshwater bivalve species. Chemical Geology.

Kelemen, Z., Gillikin, D.P., Graniero, L.E., Havel, H., Darchambeau, F., Borges, A.V., Yambélé, A., Bassirou, A. and Bouillon, S., 2017. Calibration of hydroclimate proxies in freshwater bivalve shells from Central and West Africa. Geochimica et Cosmochimica Acta, 208: 41-62.

Kitzberger, T., Swetnam, T.W. and Veblen, T.T., 2001. Inter-hemispheric synchrony of forest fires and the El Niño-Southern Oscillation. Global Ecology and Biogeography, 10(3): 315-326.

Klunzinger, M.W., Beatty, S.J., Morgan, D.L., Lymbery, A.J. and Haag, W.R., 2014. Age and growth in the Australian freshwater mussel, *Westralunio carteri*, with an evaluation of the fluorochrome calcein for validating the assumption of annulus formation. Age, 33(4).

Langlet, D., Alleman, L., Plisnier, P.-D., Hughes, H. and André, L., 2007a. Manganese content records seasonal upwelling in Lake Tanganyika mussels. Biogeosciences, 4(2): 195-203.

Langlet, D., Alleman, L., Plisnier, P., Hughes, H. and André, L., 2007b. Manganese content records seasonal upwelling in Lake Tanganyika mussels. Biogeosciences, 4(2): 195-203.

Lara, A., Villalba, R. and Urrutia, R., 2008. A 400-year tree-ring record of the Puelo River summer–fall streamflow in the Valdivian Rainforest eco-region, Chile. Climatic Change, 86(3-4): 331-356.

Lea, D.W., Pak, D.K. and Spero, H.J., 2000. Climate impact of late Quaternary equatorial Pacific sea surface temperature variations. Science, 289(5485): 1719-1724.

Lister, G.S., Kelts, K., Zao, C.K., Yu, J.-Q. and Niessen, F., 1991. Lake Qinghai, China: closed-basin like levels and the oxygen isotope record for ostracoda since the latest Pleistocene. Palaeogeography, Palaeoclimatology, Palaeoecology, 84(1-4): 141-162.

Markich, S.J., Jeffree, R.A. and Burke, P.T., 2002. Freshwater bivalve shells as archival indicators of metal pollution from a copper-uranium mine in tropical northern Australia. Environmental science & technology, 36(5): 821-832.

Marshall, B.A., Fenwick, M.C. and Ritchie, P.A., 2014. New Zealand Recent Hyriidae (Mollusca: Bivalvia: Unionida). Molluscan Research, 34(3): 181-200.

Marshall, G.J., 2003. Trends in the Southern Annular Mode from observations and reanalyses. Journal of Climate, 16(24): 4134-4143.

McDermott, F., 2004. Palaeo-climate reconstruction from stable isotope variations in speleothems: a review. Quaternary Science Reviews, 23(7): 901-918.

Neukom, R. and Gergis, J., 2012. Southern Hemisphere high-resolution palaeoclimate records of the last 2000 years. The Holocene, 22(5): 501-524.

Panfili, J., De Pontual, H., Troadec, H. and Wrigh, P.J., 2002. Manual of fish sclerochronology.

Patterson, W.P., 1999. Oldest isotopically characterized fish otoliths provide insight to Jurassic continental climate of Europe. Geology, 27(3): 199-202.

Peacock, E. and Seltzer, J.L., 2008. A comparison of multiple proxy data sets for paleoenvironmental conditions as derived from freshwater bivalve (Unionid) shell. Journal of Archaeological Science, 35(9): 2557-2565.

Petit, J.-R., Jouzel, J., Raynaud, D., Barkov, N.I., Barnola, J.-M., Basile, I., Bender, M., Chappellaz, J., Davis, M. and Delaygue, G., 1999. Climate and atmospheric history of the past 420,000 years from the Vostok ice core, Antarctica. Nature, 399(6735): 429-436.

Poulain, C., Gillikin, D., Thébault, J., Munaron, J.-M., Bohn, M., Robert, R., Paulet, Y.-M. and Lorrain, A., 2015. An evaluation of Mg/Ca, Sr/Ca, and Ba/Ca ratios as environmental proxies in aragonite bivalve shells. Chemical Geology, 396: 42-50.

Proctor, C., Baker, A., Barnes, W. and Gilmour, M., 2000. A thousand year speleothem proxy record of North Atlantic climate from Scotland. Climate Dynamics, 16(10): 815-820.

Risk, M.J., Burchell, M., De Roo, K., Nairn, R., Tubrett, M. and Forsterra, G., 2010. Trace elements in bivalve shells from the Río Cruces, Chile. Aquatic Biology, 10(1): 85-97.

Roman-Gonzalez, A., Scourse, J.D., Butler, P.G., Reynolds, D.J., Richardson, C.A., Peck, L.S., Brey, T. and Hall, I.R., 2016. Analysis of ontogenetic growth trends in two marine Antarctic bivalves *Yoldia eightsi* and *Laternula elliptica*: Implications for sclerochronology. Palaeogeography, Palaeoclimatology, Palaeoecology.

Roper, D.S. and Hickey, C.W., 1994. Population structure, shell morphology, age and condition of the freshwater mussel *Hyridella menziesi* (*Unionacea: Hyriidae*) from seven lake and river sites in the Waikato River system. Hydrobiologia, 284(3): 205-217.

Schöne, B.R., 2008. The curse of physiology—challenges and opportunities in the interpretation of geochemical data from mollusk shells. Geo-Marine Letters, 28(5-6): 269-285.

Schöne, B.R., Castro, A.D.F., Fiebig, J., Houk, S.D., Oschmann, W. and Kröncke, I., 2004a. Sea surface water temperatures over the period 1884–1983 reconstructed from oxygen isotope ratios of a bivalve mollusk shell (*Arctica islandica*, southern North Sea). Palaeogeography, Palaeoclimatology, Palaeoecology, 212(3): 215-232.

Schöne, B.R., Dunca, E., Mutvei, H. and Norlund, U., 2004b. A 217-year record of summer air temperature reconstructed from freshwater pearl mussels (*M. margarifitera*, Sweden). Quaternary Science Reviews, 23(16): 1803-1816.

Schöne, B.R., Page, N.A., Rodland, D.L., Fiebig, J., Baier, S., Helama, S.O. and Oschmann, W., 2007. ENSO-coupled precipitation records (1959–2004) based on shells of freshwater bivalve mollusks (*Margaritifera falcata*) from British Columbia. International Journal of Earth Sciences, 96(3): 525-540.

Schöne, B.R. and Surge, D.M., 2012. Part N, Revised, Volume 1, Chapter 14: Bivalve sclerochronology and geochemistry. Treatise online, 46: 1-24.

Schöne, B.R., Zhang, Z., Jacob, D., Gillikin, D.P., Tütken, T., Garbe-Schönberg, D. and SOLDATI, A., 2010. Effect of organic matrices on the determination of the trace element chemistry (Mg, Sr, Mg/Ca, Sr/Ca) of aragonitic bivalve shells (*Arctica*

islandica)—Comparison of ICP-OES and LA-ICP-MS data. Geochemical journal, 44(1): 23-37.

Schöne, B.R., Zhang, Z., Radermacher, P., Thébault, J., Jacob, D.E., Nunn, E.V. and Maurer, A.-F., 2011. Sr/Ca and Mg/Ca ratios of ontogenetically old, long-lived bivalve shells (*Arctica islandica*) and their function as paleotemperature proxies. Palaeogeography, Palaeoclimatology, Palaeoecology, 302(1): 52-64.

Sen Gupta, A. and England, M.H., 2006. Coupled ocean–atmosphere–ice response to variations in the Southern Annular Mode. Journal of Climate, 19(18): 4457-4486.

Shen, C.C., Lee, T., Liu, K.K., Hsu, H.H., Edwards, R.L., Wang, C.H., Lee, M.Y., Chen, Y.G., Lee, H.J. and Sun, H.T., 2005. An evaluation of quantitative reconstruction of past precipitation records using coral skeletal Sr/Ca and δ 18 O data. Earth and Planetary Science Letters, 237(3): 370-386.

Strom, A., Francis, R.C., Mantua, N.J., Miles, E.L. and Peterson, D.L., 2004. North Pacific climate recorded in growth rings of geoduck clams: a new tool for paleoenvironmental reconstruction. Geophysical Research Letters, 31(6).

Surge, D.M. and Schöne, B.R., 2015. Bivalve sclerochronology. Encyclopedia of Scientific Dating Methods: 108-115.

Thompson, D.W. and Solomon, S., 2002. Interpretation of recent Southern Hemisphere climate change. Science, 296(5569): 895-899.

Tynan, S., Opdyke, B.N., Walczak, M., Eggins, S. and Dutton, A., 2016. Assessment of Mg/Ca in *Saccostrea glomerata* (the Sydney rock oyster) shell as a potential temperature record. Palaeogeography, Palaeoclimatology, Palaeoecology.

Urey, H.C., 1947. The thermodynamic properties of isotopic substances. Journal of the Chemical Society (Resumed): 562-581.

Urey, H.C., Lowenstam, H.A., Epstein, S. and McKinney, C.R., 1951. Measurement of paleotemperatures and temperatures of the Upper Cretaceous of England, Denmark, and the southeastern United States. Geological Society of America Bulletin, 62(4): 399-416.

Villalba, R., Cook, E.R., Jacoby, G.C., D'Arrigo, R.D., Veblen, T.T. and Jones, P.D., 1998. Tree-ring based reconstructions of northern Patagonia precipitation since AD 1600. The Holocene, 8(6): 659-674.

Villalba, R., Lara, A., Boninsegna, J.A., Masiokas, M., Delgado, S., Aravena, J.C., Roig, F.A., Schmelter, A., Wolodarsky, A. and Ripalta, A., 2003. Large-scale temperature changes across the southern Andes: 20th-century variations in the context of the past 400 years, Climate Variability and Change in High Elevation Regions: Past, Present & Future. Springer, pp. 177-232.

Wacker, U., Fiebig, J., Tödter, J., Schöne, B.R., Bahr, A., Friedrich, O., Tütken, T., Gischler, E. and Joachimski, M.M., 2014. Empirical calibration of the clumped isotope paleothermometer using calcites of various origins. Geochimica et Cosmochimica Acta, 141: 127-144.

Waelbroeck, C., Labeyrie, L., Michel, E., Duplessy, J.C., McManus, J., Lambeck, K., Balbon, E. and Labracherie, M., 2002. Sea-level and deep water temperature changes derived from benthic foraminifera isotopic records. Quaternary Science Reviews, 21(1): 295-305.

Walker, K.F., Jones, H.A. and Klunzinger, M.W., 2014. Bivalves in a bottleneck: taxonomy, phylogeography and conservation of freshwater mussels (*Bivalvia: Unionoida*) in Australasia. Hydrobiologia, 735(1): 61-79.

Wanamaker, A.D., Heinemeier, J., Scourse, J.D., Richardson, C.A., Butler, P.G., Eiríksson, J. and Knudsen, K.L., 2008. Very long-lived mollusks confirm 17th century AD tephra-based radiocarbon reservoir ages for North Icelandic shelf waters. Radiocarbon, 50(3): 399-412.

Wurster, C.M. and Patterson, W.P., 2001. Late Holocene climate change for the eastern interior United States: evidence from high-resolution δ 18 O values of sagittal otoliths. Palaeogeography, Palaeoclimatology, Palaeoecology, 170(1): 81-100.

Yan, H., Shao, D., Wang, Y. and Sun, L., 2014. Sr/Ca differences within and among three Tridacnidae species from the South China Sea: Implication for paleoclimate reconstruction. Chemical Geology, 390: 22-31.

Yan, H., Sun, L., Shao, D. and Wang, Y., 2015. Seawater temperature seasonality in the South China Sea during the late Holocene derived from high-resolution Sr/Ca ratios of *Tridacna gigas*. Quaternary Research, 83(2): 298-306.

Zhao, L., Schöne, B.R. and Mertz-Kraus, R., 2017a. Controls on strontium and barium incorporation into freshwater bivalve shells (*Corbicula fluminea*). Palaeogeography, Palaeoclimatology, Palaeoecology, 465: 386-394.

Zhao, L., Walliser, E.O., Mertz-Kraus, R. and Schöne, B.R., 2017b. Unionid shells (*Hyriopsis cumingii*) record manganese cycling at the sediment-water interface in a shallow eutrophic lake in China (Lake Taihu). Palaeogeography, Palaeoclimatology, Palaeoecology.

Chapter 1

THE FRESHWATER BIVALVE *Echyridella Menziesii*: A NEW ENVIRONMENTAL ARCHIVE FROM LAKE ROTORUA, NEW ZEALAND.

Dilmi Herath[1], Susan Clearwater[2] and Dorrit Jacob[1]

[1] *Department of Earth and Planetary Science, Macquarie University, Sydney, Australia,*

[2] *National Institute of Water and Atmospheric Research, Silverdale Road, Hamilton 3216, New Zealand*

Abstract

In addition to their ecological importance, freshwater bivalves are also significant archives of continental environmental conditions and climate variations. Here we study freshwater bivalve *Echyridella menziesii* (Gray, 1843) from Lake Rotorua, New Zealand with the intention of identifying the suitability of this species as an environmental proxy archive. Shell compositional variation due to environmental variables such as water temperature and precipitation as well as different ambient water quality variables measured over a 12-month period were studied to identify the factors affecting selected element distribution in *Echyridella menziesii* shells. The Sr/Ca, and possibly Mg/Ca of *Echyridella menziesii* shells indicate strong positive correlations ($r > 0.5$, $p < 0.05$) with water and air temperature indicating the potential of these element/calcium ratios to be a proxy archive of local temperature. However, due to unlimited nutrient supply as a result of lake eutrophication, the element ratios (eg; Ba/Ca and Mn/Ca) in the shells are not affected by the primary productivity in the lake. Moreover, this study also reveals that *Echyridella menziesii* from Lake Rotorua form annual growth lines in the shell during February and live up to 25 years. Therefore, in addition to the high correlation between Sr/Ca and ambient temperature, *Echyridella menziesii* shells also fulfil the prerequisites for environmental proxy archives because the species is present in a broad biogeographic area (from 35 °S to 45 °S) in New Zealand, exhibits a long life-span and grows by regular periodic accretion of shell materials.

1.1 Introduction

Freshwater bivalves (Unionoida) are an important component in ecosystems as a result of filter-feeding, nutrient cycling and because they are a food source for a wide variety of organisms (Klunzinger et al., 2014). In addition, freshwater bivalves are used as archives of continental environmental conditions and climate variations (Black et al., 2009; Schöne and Surge, 2012; Poulain et al., 2015; Yan et al., 2015) or as indicators for environmental pollution (Jones and Walker, 1979; O'Neil and Gillikin, 2014; Markich, 2017). Different element to calcium ratios in bivalve shells have been developed as proxies for quantitative assessments of numerous environmental variables, for example temperature using Sr/Ca and Mg/Ca (Yan et al., 2014; Tynan et al., 2016), and salinity, precipitation and phytoplankton productivity using Ba/Ca (Gillikin et al., 2006; Izzo et al., 2016).

Areas most affected by climate change to date are at mid to high latitudes and/or at high elevations (Cohen et al., 2014; Wang et al., 2016). It seems critical to explore more paleo-climate archives from these regions, since isolating natural climate variability from anthropogenic climate change is important for reliable future climate predictions. Therefore, it is essential to develop more independent continental paleoclimate proxy archives to supplement these databases, since each biological archive has a unique approach to documenting environmental variability due to its habitat, location and life history such that a combination of multiple archives provides a much stronger record than any individual archive (Black et al., 2009). Although significant advancements have been made in the reconstruction of northern hemisphere climate variability, quantitative hemispherical and regional climate reconstructions are scarce from the southern hemisphere. New Zealand is one of only two land masses that extends beyond 40 ºS and has a well-established dendrochronological database (Neukom et al., 2014).

Here we study *Echyridella menziesii* (Gray, 1843) (Unionoida: Hyriidae), from Lake Rotorua, New Zealand (Fig. 1) with the intention of identifying the suitability of this species as an environmental proxy archive. Shell compositional variation due to environmental variables such as water temperature and precipitation as well as different ambient water quality variables measured over a 12-month period were studied to identify the factors affecting selected element distribution in *Echyridella menziesii* shells.

Echyridella menziesii, the dominant large freshwater mussel species out of three different species in New Zealand (Marshall et al., 2014), is abundant across a wide range of latitudes from approximately 35 °S to 45 °S. Adult *Echyridella menziesii* generally reaches a maximum shell length of approximately 10 cm (maximum height ~ 6cm), has ~ 20 g of wet flesh weight and can filter ~ 1 L of water per hour (Grimmond, 1968; Clearwater et al., 2014b). These bivalves prefer sandy to silty sediments and are commonly found in the littoral zone of lakes as well as in streams (James, 1985; James, 1987). Sediment type, adequate food supply, water velocity, and presence of fish hosts affects the density of these bivalves (James, 1985). *Echyridella menziesii* releases sperm into the water during winter to fertilize ova held in the brood pouches of the gill. The fertilized eggs subsequently develop in the brood pouch into specialized larvae called glochidia. When they are approximately 280 µm long they are released into the water during spring or summer where they will then attach to the gills, skin and fins of a fish host, such as eels (*Anguilla sp.*), koaro (*Galaxias brevipinnis*), and common bullies (*Gobiomorphus gobioides* and *G. cotidianus*) as obligate parasites for approximately two weeks (Clearwater et al., 2014b, Clearwater et al. unpublished data). After approximately two weeks the glochidia complete transformation into juvenile mussels and detach from the fish host to commence the next stage of their life cycle. Juvenile freshwater mussels are thought to inhabit well‑aerated sediments, and are known to be very sensitive to contaminants such as copper and ammonia (Clearwater et al., 2014b).

Although *Echyridella menziesii* are common in some New Zealand lakes, bivalve populations are thought to have gradually declined over the years (Clearwater et al., 2014a). Different biological (e.g., host fish declines, cyanobacterial blooms, predation, recruitment failure, invasive macrophytes) as well as physical (e.g., contaminants, hypolimnetic hypoxia, sedimentation) causes have been put forward as the reasons for these population declines (James, 1985; Roper and Hickey, 1994; Clearwater et al., 2014a). *Echyridella menziesii* is valued in the indigenous Maori culture as a traditional food source, and the shells were used as tools. Therefore, this species can be found in New Zealand freshwater shell middens, mainly in rock shelters, dating back to early periods of the last millennium (Campbell, 2005). Although ecology, taxonomy and the toxicology of these bivalves have been studied previously (Roper and Hickey, 1994; Clearwater et al., 2014a; Marshall et al., 2014; Cyr et al., 2016), to our knowledge this is the first study focused on the shells of *Echyridella menziesii*.

1.2 Study area

The Waikato River belongs to the longest river system in New Zealand, and together with the Rotorua Lake District plays an important role in supporting a significant amount of farming, forestry and generation of hydroelectricity in the North Island, New Zealand (Chapman, 1996). This river and lake system is characterised by a number of volcanic crater lakes and reservoirs including the two largest lakes in New Zealand, namely Lake Taupo in the Waikato River system and Lake Rotorua in the Rotorua Lake District (Fig. 1). Unlike Lake Taupo, which is a relatively large and deep lake (average depth; 97 m and surface area 612 km^2), Lake Rotorua (80 km north of Taupo), is a shallow lake with a mean depth of 10 m (maximum depth 45 m), surface area of 80 km^2 (Rutherford, 1984; Smith et al., 2016) and catchment area of nearly 500 km^2 (Donath et al., 2015). Both these lakes have abundant freshwater bivalve populations (James, 1985; Roper and Hickey, 1994), but the shells of Lake Rotorua mussels are generally in better condition than those at Lake Taupo, where shells tend to be severely eroded (possibly due to low water hardness) and deformed due to larval chironomid infestations (Marshall et al., 2014). Lake Rotorua was selected for this study over Lake Taupo because of better quality shells, the presence of healthy bivalve populations, and the smaller lake volume and trophic status (i.e. eutrophic) that is more representative of lakes in the North Island.

Lake Rotorua is a volcanic crater lake in the Taupo volcanic zone (Cole, 1990; Donath et al., 2015) and is geothermally active (Phillips et al., 2014). The well-known Rotorua geothermal field is located at the southern end of the lake (Heise et al., 2016; Scott et al., 2016) (Fig. 1). Hot springs are located along the southern shore of the lake while geothermal inputs flow via streams in the south. However, the lake is more dominated by groundwater flow than by stream base flow (Hamilton et al., 2016). Before European settlement in the 1880s, the catchment of Lake Rotorua was predominantly temperate rain forest which was rapidly converted into farmland and now covers almost 50 % of the catchment (Smith et al., 2016). This change in land use has been linked to water quality problems, which resulted in eutrophication during the late 20th century (Rutherford, 1984; Mueller et al., 2015; Hamilton et al., 2016). Many actions have been taken to mitigate the eutrophication in the lake, such as changing land management practices, proposing a nutrient loss limit for the catchment, preventing direct sewage input into the lake and dosing stream inflows with aluminium sulphate to bind phosphorus (Mueller et al., 2015). However, due to long transit times of

water through the groundwater system (> 50 years) (Morgenstern et al., 2015), Lake Rotorua is still considered an eutrophic lake with a three yearly average trophic level index to 2017 of 4.1 (*www.rotorualakes.co.nz/rotorua*).
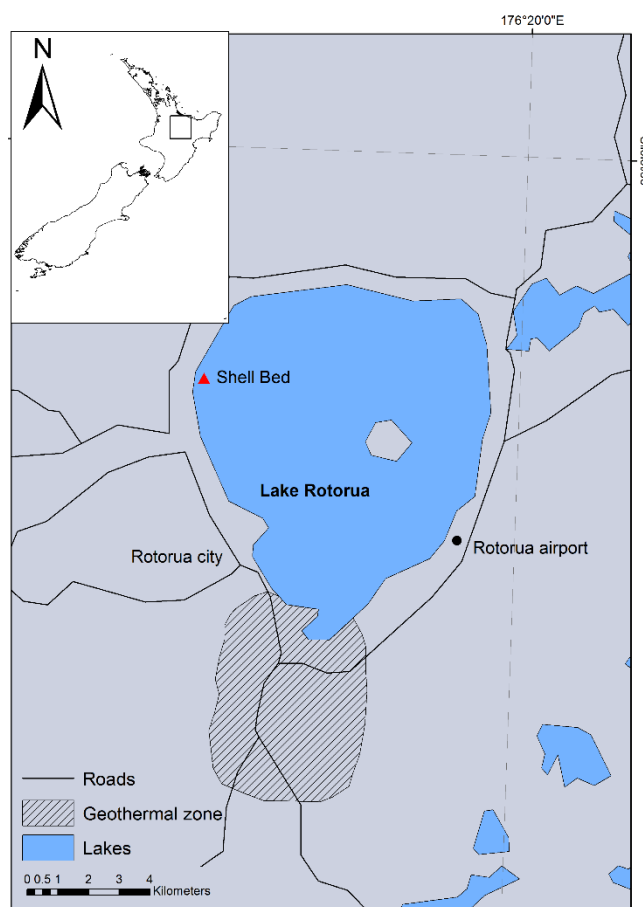
Fig. 1 Map of Lake Rotorua, New Zealand showing the location of the shell bed where bivalves and water samples were collected. Rotorua city is located south of the lake and the airport is in the east. Approximate area of the Rotorua geothermal field is marked with hashed signature. The inset shows the location of the study area in the North Island of New Zealand.

1.3 Methods

1.3.1 Bivalve, water and data collection and shell sample preparation

Bivalves were collected at the western shore near the Waiteti Stream, Ngongotaha (38° 4' S, 176° 13' E; Fig. 1). Thirty bivalves were collected alive from less than 1 m water depth in March 2016 and after that, five bivalves were collected once a month from the same location from June 2016 to July 2017 from a water depth of approximately 1 m within 50 m of a water quality sonde attached to a jetty. Temperature, pH, dissolved oxygen and chlorophyll *a* concentration of lake water from August 2016 to June 2017 was measured every five minutes

at the bivalve bed using the same sonde. More details about sonde calibration and deployment can be found in the supplementary materials at the end of the chapter.

Bivalves of a range of sizes with non-deformed shells were selected and checked visually for brood pouches. The bivalves were then frozen at -20 °C to euthanise them, the flesh was separated from the shells, and the shells were dried at room temperature. Sections of approximately 3 mm in thickness were cut from the left valve of the shell along the minimum growth axis (Fig. 2A). Sections were mounted on glass slides using metal epoxy, ground in steps with sandpaper (400, 600, 800 and 1200 grit) and eventually polished with 3 and 1 µm diamond paste. Fifty (50) polished sections were stained with Alcian Blue for 20 min at 37–40 °C (Schöne, Page et al. 2007). Digital photomicrographs of the shell sections were taken under a reflected light microscope before and after staining (Fig. 2B) and were used to measure the annual increment lengths using the freeware `imageJ` (Rueden et al., 2017). Annual growth increment data obtained from 21 well-stained shells were fitted to the Von Bertalanffy Growth (VBG) function expressed in the equation $L_t = L_{inf}[1 - e^{-K(t-t_0)}]$, where L_{inf} is the asymptotic maximum length, K is the Von Bertalanffy growth constant, t is age variable and t_0 is the length at time zero. Fisheries stock assessment methods and the data package for R (FSA, Ogle 2016) were used to fit the data into the VBG function, which uses the least square method for estimation of growth parameters. The maximum age or longevity was calculated using the equation $T_{max} = 3/K$ (Pauly, 1980).

Water samples were collected monthly at the same time and from the same location as the bivalves to provide monthly measurements of chlorophyll *a*, Total Ammonia-Nitrogen (TAN), Ca, Mg, Mn, Sr, and Ba, and Dissolved Organic Carbon (DOC) concentrations. Monthly and daily air temperature and precipitation data were obtained from The National Climate Database, New Zealand (*cliflo.niwa.co.nz*). Air temperature and precipitation data from Rotorua airport (38º 6' S, 176º 18' E; Fig. 1) which is less than 10 km from the bivalve bed and at the same elevation were used in this study. In addition, daily lake water temperature data from July 2007 to July 2016 were collected from a buoy at Lake Rotorua which is maintained by the University of Waikato and Bay of Plenty Regional Council (*monitoring.boprc.govt.nz*). The air temperatures used in this study are maximum daily temperatures since mean daily temperature from the Rotorua airport station is not available, while the daily water temperature used in this study is the average of water temperature data collected by sonde every five minutes for 24 hours.

1.3.2 Trace element analysis in shell and water samples

Polished non-stained cross-sections of three *Echyridella menziesii* shells less than five years of age and collected in June 2017 (RO 109, 106, 107) were selected for trace element analysis by Laser Ablation Inductively Coupled Plasma Mass Spectrometry (LA-ICP-MS). These shells were selected due to wider growth increments relative to other collected shells. Strontium, Mg, Mn, Ba, and Ca (measured as ^{88}Sr, ^{25}Mg, ^{55}Mn, ^{137}Ba, and ^{43}Ca) were measured *in situ* by LA-ICP-MS using an Agilent 7700 quadrupole ICP-MS coupled to a Photon Machines excimer laser (193 nm wavelength) laser ablation system. Measurements were carried out with a laser energy density of 4.00 J/cm^2 at 5 Hz with helium as the carrier gas (flow rate = 0.8 l/min). To produce trace element time series, continuous curved lines of various lengths were ablated within the thick inner nacreous layer along the direction of growth (laser spot diameter 35 μm; scanning speed 5 μm/s), after pre-ablation (laser spot diameter 65 μm; scanning speed 100 μm/s; Fig. S1). Backgrounds were measured for 60 s before each ablation.

The ^{43}Ca calculated from the stoichiometry of aragonite was used as the internal standard with NIST SRM 612 glass as the external standard. Data reduction was carried out with the commercial software `GLITTER 4.5b` (Griffin et al., 2008) while calculation of element/calcium was carried out using Microsoft Excel. NIST SRM 610 glass, U.S. Geological Survey reference glass BCR-2G and carbonate reference material MACS 3 were measured as unknowns to monitor accuracy and instrumental drift. Values for all reference materials were taken from the GeoReM database: GeoReM preferred values (Jochum et al., 2005). Detection limits (99% confidence level) for the measurements were Sr = 0.10, Mg = 2, Mn = 0.5, Ba = 0.4 µg/g. The external reproducibility for BCR-2G (n = 5), NIST SRM 610 (n = 10) and MACS 3 (n = 9) were > 90%, > 95% and 95 % for all measured elements, respectively.

Approximate calendar dates for the peak values in the Me/Ca series were assigned based on the known collection date and the growth lines, which were verified to be annual growth checks (see below). Following common practice in the literature, data between two peaks were linearly interpolated to create a monthly averaged Me/Ca time series for each measured shell (Yan et al., 2014). Only those data covering a period of 12 months from June 2017 to June 2016 simultaneous to the period of water sampling were considered for further interpretation.

The Ca, Mg, Mn, Sr, and Ba concentrations of filtered (0.45 µm) and acidified (1%) 100-ml lake water samples were measured by using ICP-MS. Total Ammonia-Nitrogen (TAN) analysis was carried out on separate filtered (0.45 µm) batches of water by using phenol/hypochlorite colourimetry on a flow injection analyser (detection limit 1 µg L^{-1}) (Lachat method). Chlorophyll *a* concentrations were measured by acetone pigment extraction, followed by spectrofluorometric measurement (method A*10200H) (detection limit 0.1 µg L^{-1}) on GF/C filtered water samples (300 ml). Dissolved organic carbon was analysed in subsamples taken from 30 ml samples filtered through pre-combusted GF/C filters into pre-combusted glass bottles. The samples were then subjected to high-temperature catalytic oxidation, followed by infrared detection (method APHA5301B) (detection limit 0.2 mg l^{-1}). All water analysis was carried out either at NIWA Hamilton (i.e., TAN, chlorophyll a, DOC) or at Hill Laboratories, Hamilton, New Zealand (i.e., metals and other elements).

1.3.3 Scanning Electron Microscope (SEM) analysis and Micro-Raman spectrometry

Broken pieces of *Echyridella menziesii* shells were etched with Ethylene Diamine Tetraacetic Acid (EDTA, 1% for 10 min) to enhance the organic-rich growth lines. Etched and non-etched samples were mounted on aluminium stubs using conductive carbon tape, coated with gold, and imaged with a JEOL 7100F field-emission scanning electron microscope at the microscope unit at Macquarie University, Sydney. An accelerating voltage of 10 kV, a sample current of 2 pA and a vacuum pressure of 5×10^{-6} mbar were used.

Raman spectra were collected at room temperature using a Horiba Jobin Yvon LabRAM HR Evolution confocal spectrometer with 473 nm laser excitation. All Raman spectra (5-10 spots per shell) were recorded in the 100–1600 cm^{-1} wavenumber range using a spectral acquisition time of 12 seconds and four accumulations. A grating with 1800 grooves/mm was used with a slit width of 100 µm to ensure a high spectral resolution of approximately 0.8 cm^{-1}.

1.4 Results

1.4.1 *Echyridella menziesii* shell structure and lifespan determination

Collected *Echyridella menziesii* shell (n = 87) lengths ranged from 38.4 to 69.5 mm, with average lengths of 57.3 ± 6.3 mm, while other average shell dimensions were: height 20.6 ± 3.4 mm, height at the umbo (perpendicular to the maximum length) 37.2 ± 5.2 mm, average maximum valve height (perpendicular to the maximum length) 41.6 ± 4.7 mm, average flesh dry weight at 60 °C was 1.0 ± 0.3 g, and average Condition Factor Index (CFI) was 2.0 ± 1.8 (where CFI = [(flesh dry weight)^3/length] x100. Out of the 32 bivalves collected from August to December 2016, only seven bivalves had brood pouches (Table S1).
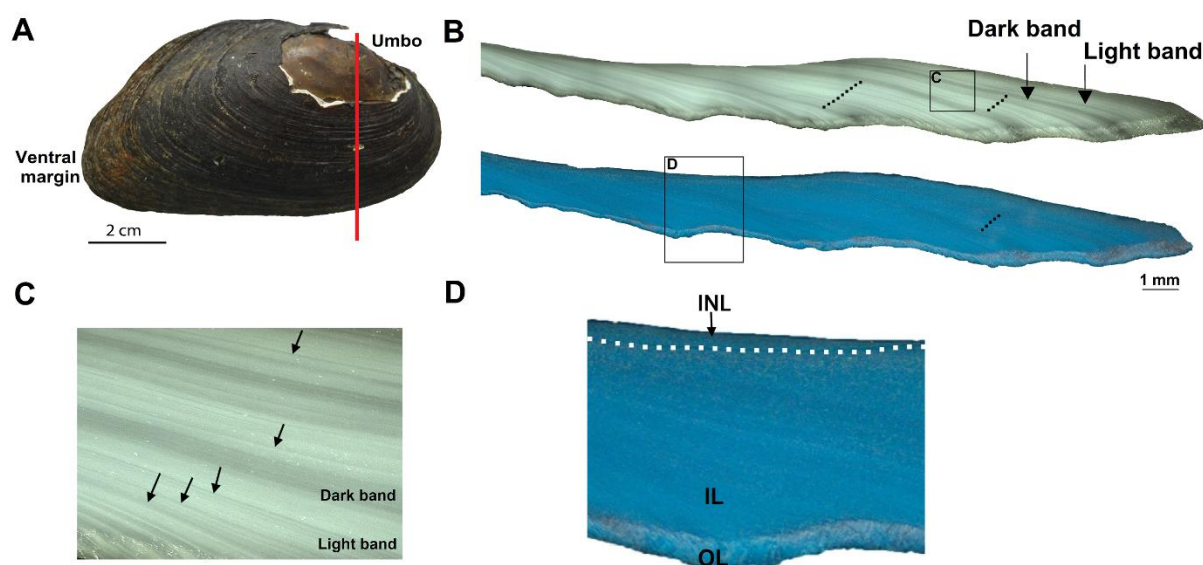
Fig. 2 (A) photograph of a representative left valve of *Echyridella menziesii* collected from Lake Rotorua indicating heavy erosion at the umbo. Red line indicates the minimum growth axis where cross‑sections for growth-analysis were made. (B) Non-stained (upper) and stained (lower) cross sections of *Echyridella menziesii* showing alternating dark and light-coloured bands. Dash lines indicate selected growth increments. (C) Inset from the non-stained shell section shows the smaller dark layers and wider light layers which are interrupted by thin dark lines (marked by arrows). (D) Inset from the stained shell section shows the two main layers of an *Echyridella menziesii* shell (OL= Outer layer, IL = Inner Layer) and the secondary nacreous layer (SNL). The white dotted line shows the margin between IL and the SNL.

The shells of *Echyridella menziesii* are covered with a dark brown periostracum; an organic membrane which is not mineralised and covers the external surface of the shell (Carter, 1990). In this sample population, the periostracum is usually heavily eroded close to the umbo exposing the outer shell layer (Fig. 2A). Dark and light coloured alternating bands are visible in shell sections (Fig. 2B) and each pair of light and dark coloured bands is bordered by a growth line which stained dark blue in some sections. Lighter coloured bands are usually

thicker than the dark bands and show many thin dark lines on either side of the dark band which were indistinct in stained sections (Fig. 2C). Since these thin lines do not appear in the stained sections, these were assumed as disturbance lines. As is typical for Unionoids, the shells consist of an outer prismatic layer (Fig. 3C) and inner nacreous layer (Fig. 3B) (Carter, 1990). Raman spectroscopic analysis verified that *Echyridella menziesii* shells are fully aragonitic (Fig. S2), consistent with the aragonitic composition of all species belonging to the subclass Palaeoheterodonta that accounts for the majority of freshwater bivalves (Taylor, 1973; Graf and Cummings, 2006). In contrast to marine shells that typically have a thick outer layer, the prismatic outer shell layer in *Echyridella menziesii* is thin, ca. 100 – 200 µm thick, while the inner nacreous layer is ca. 2 – 5 mm thick and makes up more than 90 % of the shell. In addition to these two major layers, we observed an additional secondary nacreous layer in most shell sections starting from the pallial line (where the mantle epithelium was attached) and thickening towards the umbo (Fig. 2D).

Bivalves form growth lines in their shells due to different factors such as climate, food availability or allocation of energy for reproduction (Soldati et al., 2009; Schöne and Surge, 2012; Roman-Gonzalez et al., 2016). Compared to detecting growth increments, observation of these growth lines can be challenging. In our study, 21 of the 50 *Echyridella menziesii* shells responded well to Alcian Blue staining, but growth lines in the remaining 29 shells were hardly highlighted by this treatment. Analysing the well-stained shells shows an average growth rate of 0.6 cm per year with rapid growth during the early stages of life (Fig. S3). Growth lines are easily recognisable in SEM images due to the higher amounts of organic matter in the growth line compared to other areas in the shells (Fig. 3D). The SEM images of EDTA-etched sections show a decrease in the thickness of aragonite crystals in the direct vicinity of the growth line (Fig. 3E), and relatively thicker organic interlamellar sheets (Fig. 3F).

The shell colour (dark or light) of the area closest to the ventral margin of the shell sections collected each month over a year from the same population was observed (examples from selected months are given in Fig. S4) and indicated that the shells from approximately May to December form a light band while from approximately January to April they form a dark band. Hence, the dark band forms annually during summer and one pair of dark and light bands represent one calendar year. Further, the stained shell sections indicated a regular formation of the growth line in the middle of the dark summer band or at the peak of summer (approximately February). As growth lines only stained well in a subset of samples, we chose

to use counting of the paired dark and light colour bands for age estimation of the complete sample set of 50 *Echyridella menziesii* shells. This resulted in an average lifespan of approximately 10 years with a maximum age of 22 years for this bivalve population (Fig. S5). It should be noted here that these values are the minimum age for the bivalve, since shell erosion close to the umbo removed an area equivalent to approximately 2-3 years. Bearing this in mind, it is concluded here that this population of *Echyridella menziesii* has ontogenetic ages of up to 25 years. Other studies found maximum lifespans of 33 (Roper and Hickey, 1994) and 55 years (Grimmond, 1968) for *Echyridella menziesii* using similar methods (except staining) from other parts of New Zealand (the Waikato, North Island, and in Otago, South Island respectively).
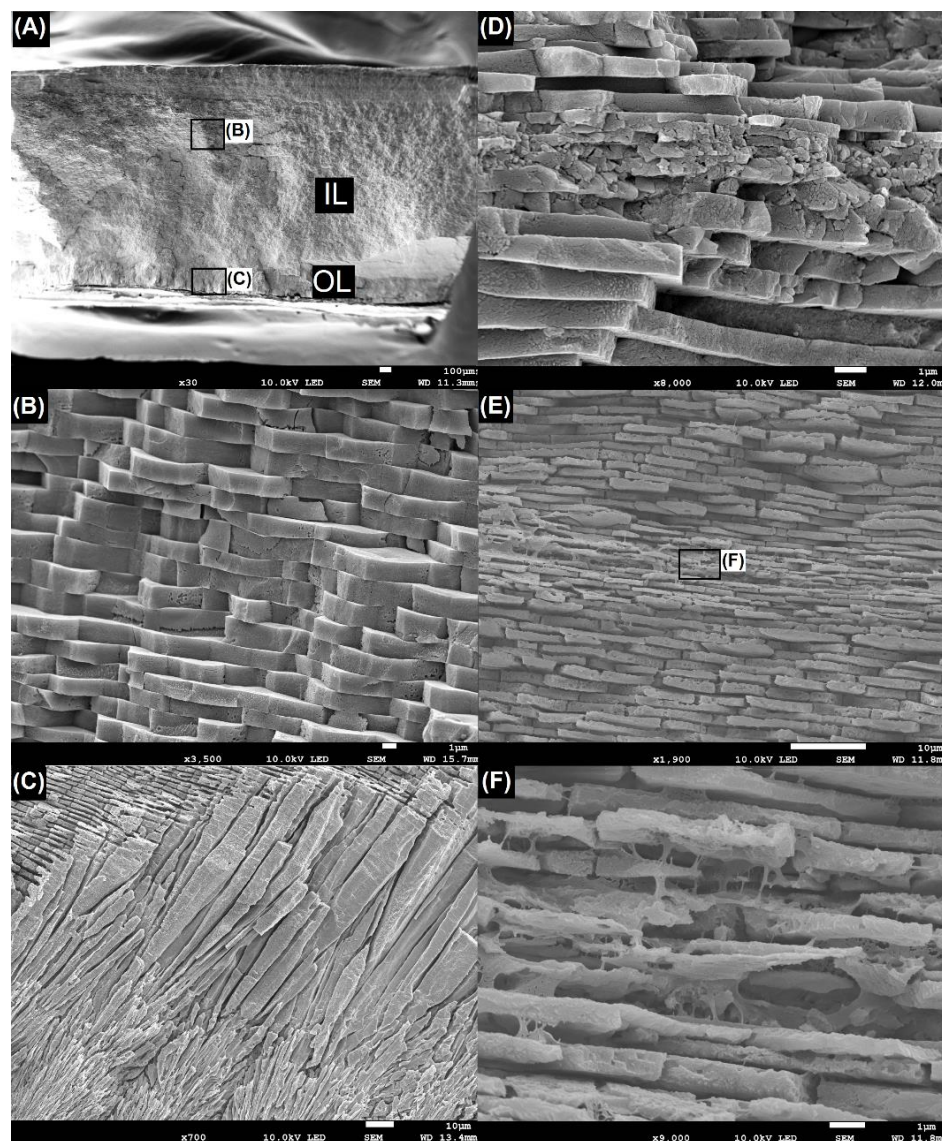
Fig. 3 Scanning electron microscope images of *Echyridella menziesii* shell (A) cross section of a shell indicating three layers (OL= Outer layer, IL = Inner layer) (B) nacreous layer (C) prismatic layer (D) organic-rich growth line (E) tablet size variation at the growth line and (F) magnification of the growth line area. (*a,b,c* and *d* are samples etched with water while *e* and *f* are etched with EDTA)

The Von Bertalanffy Growth (VBG) parameters calculated only for the well-stained samples ($n = 21$) showed a maximum asymptotic length (L_{inf}) of 9.9 cm and Von Bertalanffy growth constant (K) of 0.1 per year. The graphical representation of the VBG curve (Fig. S3) shows an exponential reduction in annual shell increment width with a high growth rate in the first three to five years of life (almost 1 cm per year) followed by smaller annual increments (approximately 0.25 cm). The maximum age indicated by the Von Bertalanffy growth analysis for this subset of samples is 30 years and thus comparable to the 25 years for the full sample set derived by increment counting.

1.4.2 Environment and water compositional variation in Lake Rotorua

Lake Rotorua belongs to the Rotorua Lake District located near the temperate east coast of the northern island, New Zealand, which contains 14 lakes. Strong seasonality in water temperature is observed in data recorded at 0.5 m depth from the water surface by the water quality buoy at Lake Rotorua (data available at *monitoring.boprc.govt.nz*). Daily water temperature from 2007 to 2016 has an average of 15.7 °C with a minimum of 8.0 °C and a maximum of 24.1 °C. Annual rainfall in the catchment is strongly affected by topography and varies from less than 1400 mm southeast of the lake to more than 2200 mm northwest of the lake (Donath et al., 2015). Precipitation rates are spread out over the year as demonstrated in the monitoring buoy data (*monitoring.boprc.govt.nz*).

Measured lake water temperature using the sonde deployed in the vicinity of the bivalves (from August 2016 to June 2017) indicates maximum temperatures of 24.7 °C in February (austral summer) and minimum temperatures of 9.6 °C in June and August (austral winter) (Fig. 4A) with an average of 16.5 °C for the year. Unfortunately, due to sonde calibration and deployment problems, the peak austral winter month of July was not included in the measurements. As recorded by the water quality buoy at Lake Rotorua, the average water temperature at 0.5 m depth for July during last 10 years was 9.5 °C (range 8.0 °C – 11.6 °C). The Pearson correlation coefficient between the buoy and sonde data for 135 days from August 2016 to December 2016 is 0.93 (p < 0.001) and the average difference between data for the same period is 1.3 °C. Measured air temperature at Rotorua airport is 2 °C warmer on average than the water temperature and follows a similar seasonal pattern (r = 0.8, p < 0.001) to lake water temperature but with more scatter (Fig. 4A). Precipitation in the area during August 2016 to June 2017 increased in austral autumn after a relatively dry summer (Fig. 4B).
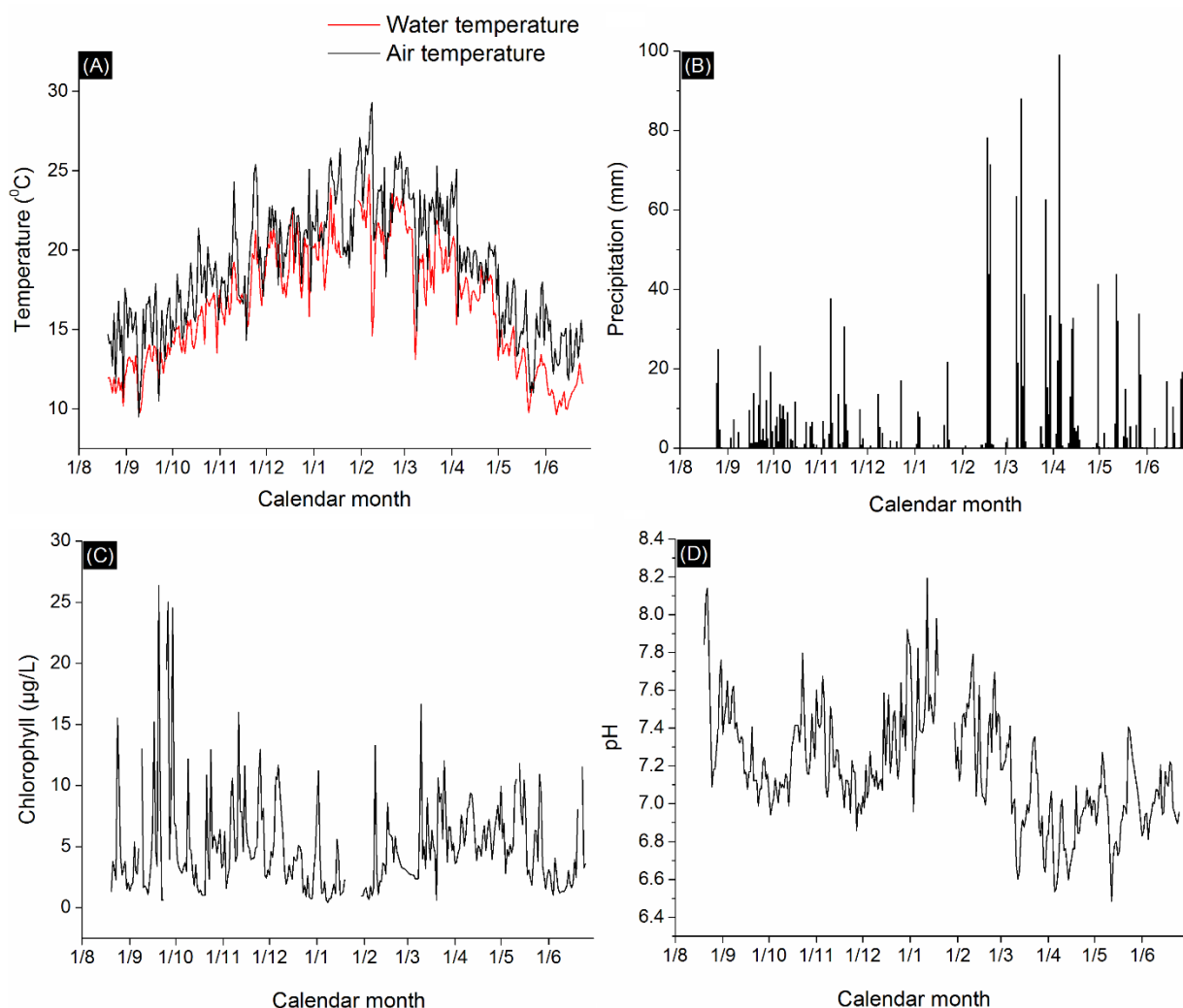
Fig. 4 Variation in measured (A) lake water and air temperature, (B) precipitation (C) chlorophyll *a* concentration*,* and (D) pH, during August 2016 and June 2017. Air temperature and precipitation data were collected daily at Rotorua airport, New Zealand (cliflo.niwa.co.nz). All other parameters listed were measured every 5 minutes using a sonde deployed close to the mussel collection point in Lake Rotorua, New Zealand and averaged to determine the daily value.

Except for Mg and Ca, whose concentrations are in the mg/l range, all other element concentrations of Lake Rotorua water are in the µg/l range (Table 1). Mn concentrations vary from less than 10 µg/l in July to over 35 µg/l in November, while all other element concentrations are relatively constant. Measured TAN and DOC remain constant throughout the year except for an increase in September while the pH is constant and neutral (average pH = 7.2) through the year (Fig. 4 and 5). Chlorophyll *a* concentrations do not show any systematic seasonal variation, but relatively high values occur at around September (austral spring) (Fig. 4 and 5).

Table 1. Trace element concentrations and different water quality parameters measured in water samples collected during a 12-month period during June 2016 to June 2017 from Lake Rotorua, New Zealand.

Month	Sr μg/l	Ba μg/l	Mg mg/l	Mn μg/l	Ca mg/l	TAN mg/m^3	DOC g/m^3	Chla g/m^3	pH
June	22	24	1.62	9.8	3.0	15	1.15	1.54	7.04
July	24	28	1.71	9.5	3.6	22	1.45	4.56	7.41
August	22	27	1.62	10.8	3.2	18	1.80	1.01	7.14
September	21	35	1.35	21.0	3.4	229	6.50	8.89	7.07
October	23	29	1.57	17.8	3.3	37	2.00	0.60	7.35
November	23	37	1.60	36.0	3.6	24	1.35	3.12	7.12
December	24	32	1.75	32.0	3.4	32.3	1.27	1.85	7.21
January	25	30	1.60	29.0	3.0	35	1.80	1.19	7.12
February	20	24	1.52	19.7	2.8	20	1.53	1.93	7.26
March	25	36	1.61	29.0	3.2	20	0.97	1.47	6.88
April	19	26	1.44	28.0	2.4	33.5	1.35	5.55	7.03
May	20	30	1.46	13.3	2.6	12.3	1.21	5.89	7.20
June	22	30	1.47	15.0	3.2	18	1.50	2.00	7.75
Average	22	29	1.56	20.8	3.1	39.7	1.83	3.04	7.19

TAN = Total Ammonia Nitrogen, DOC = Dissolved Organic Carbon, Chla = Chlorophyll *a*
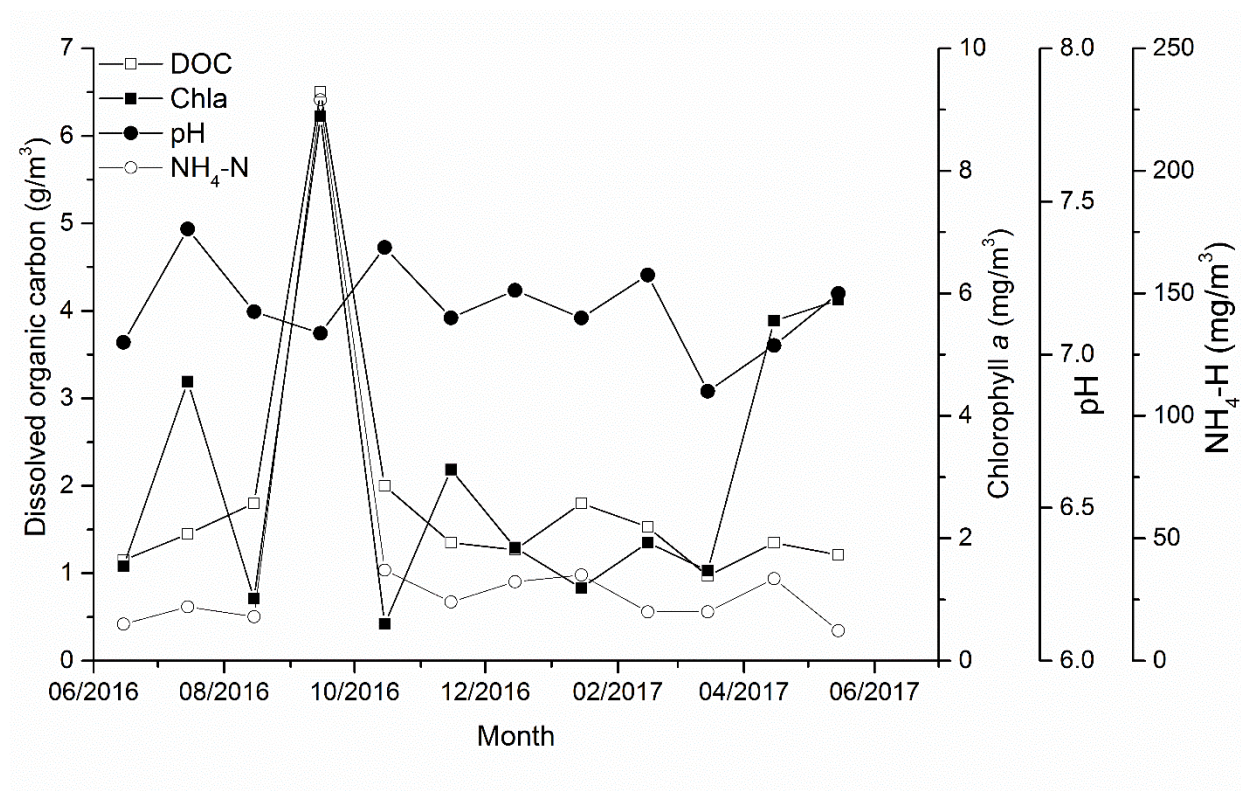
Fig. 5 Annual variation in water quality parameters in lake water collected monthly from Lake Rotorua during June 2016 and June 2017 indicating a marked increase in September. NH$_4$-N = total ammonia-nitrogen

1.4.3 Trace element concentration variations in *Echyridella menziesii* shell

The average concentrations of Sr, Mg, Ba and Mn measured in *Echyridella menziesii* shells were 1200, 24, 32 and 350 µg/g respectively. The Sr concentration in *Echyridella menziesii* shells was higher than some freshwater (Izumida et al., 2011; Bolotov et al., 2015) and marine (Takesue and van Geen, 2004; Freitas et al., 2005; Schöne et al., 2011; Yan et al., 2014) bivalve species. However, the concentrations are comparable to those found in other freshwater bivalve species for example from South Carolina, northern Patagonia and Ohio (Carroll and Romanek, 2008; Soldati et al., 2009; Geeza et al., 2018) indicating a wide range of Sr concentrations in bivalve species.

The Ba concentration in *Echyridella menziesii* shells is slightly lower than those of other freshwater bivalves (Carroll and Romanek, 2008; Bolotov et al., 2015) but several magnitudes higher than in marine bivalves (Gillikin et al., 2006; Elliot et al., 2009; Thébault et al., 2009). Since the main source of Ba in aquatic systems is the weathering of Ba-rich rocks in the surrounding environment (Montaggioni et al., 2006), freshwater contains much larger amounts of barium than seawater (50 µg/l vs. 6 µg/l) (Schroeder et al., 1972), translating into generally higher concentrations in freshwater bivalve shells than in marine shells. Similarly, the high Mn concentrations in freshwater environments (average ~ 8 µg kg^{-1}) compared to marine environments (average ~ 0.2 µg kg^{-1}) result in higher Mn contents in freshwater shells than marine bivalve shells (Barceloux and Barceloux, 1999). The Mn concentrations in *Echyridella menziesii* shells are thus higher than those recorded in marine bivalves (Carré et al., 2006; Freitas et al., 2016) but comparable to Mn concentrations of freshwater bivalves (Carroll and Romanek, 2008; Bolotov et al., 2015; Zhao et al., 2017b). In contrast, the Mg concentration in *Echyridella menziesii* and other aragonitic freshwater shells (Izumida et al., 2011; Bolotov et al., 2015; Geeza et al., 2018) is lower than the Mg concentrations in mainly calcitic marine shells (Takesue and van Geen, 2004; Foster et al., 2008; Elliot et al., 2009), largely because of crystal chemical reasons.

The monthly time series of Sr/Ca, Ba/Ca, and Mg/Ca from June 2016 to June 2017 measured in three juvenile shells are in-phase as indicated by relatively high inter-correlation (r > 0.4) and low standard deviation (SD < 1) in these time series (Table S2). In contrast, the Mn/Ca time series exhibited marked inter-specimen variation except for RO-106 and RO-109, which have reasonably high inter-correlation (r = 0.55, p < 0.05; Table S2). Further, the Sr/Ca time series of three measured shells exhibited seasonal variation with higher values in summer

and lower values in winter (Fig. 6A). Similarly, the Ba/Ca time series for two out of three shells (except RO-106) followed the same pattern (Fig. 6C) while the Mg/Ca time series had relatively stable values compared to other elements throughout the year (Fig. 6B). This seasonal pattern was clearer in the measured long-lived *Echyridella menziesii* shells in which Sr/Ca, Ba/Ca and Mg/Ca increase within the summer dark band and decrease in the light winter band (Fig. S6 and Chapter 2). In contrast, the Mn/Ca time series do not indicate seasonal variations either in young or older shells except for RO-109, in which Mn/Ca increase drastically in summer (Fig. 6D). Differences in element variation in the bivalves living in the same population can be attributed to the amount of physiological influence from the individual bivalve.
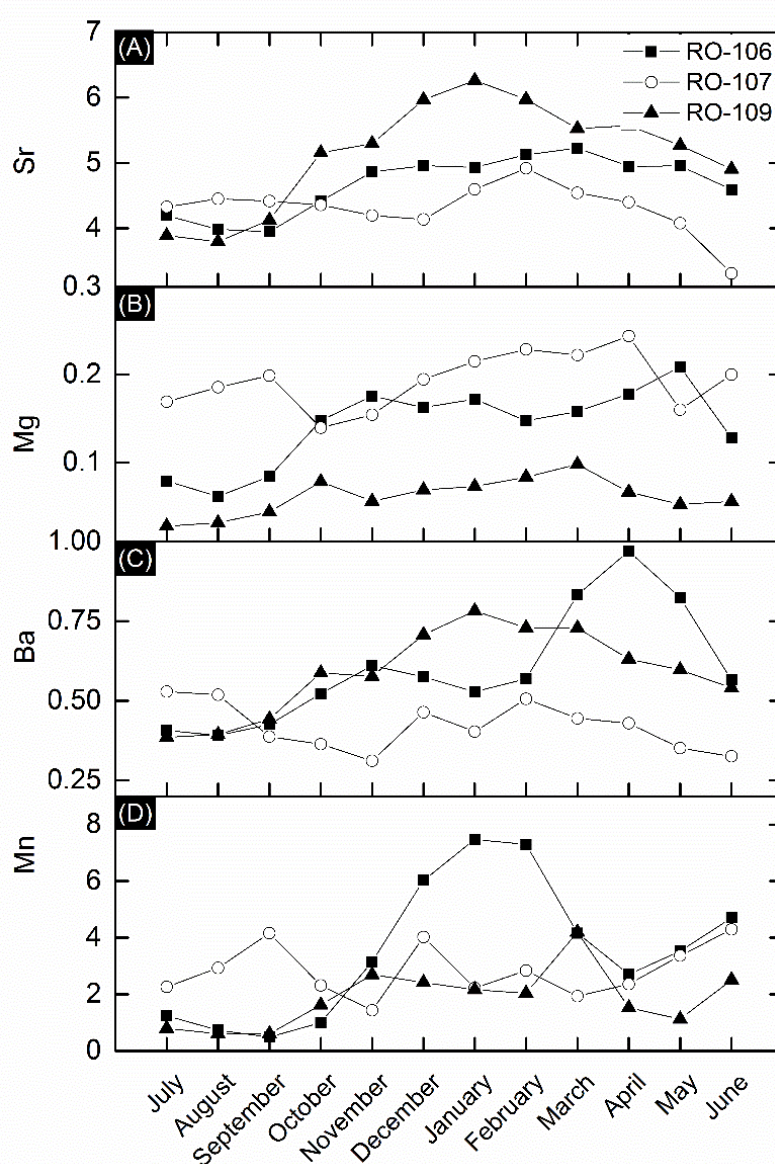
Fig. 6 Variation in trace element/calcium (in mmol/mol) of three *Echyridella menziesii* shells (RO-106, RO-107 and RO-109) collected from Lake Rotorua from July 2016 to June 2017.

All Sr/Ca time series indicate significantly positive correlations ($r > 0.5$, $p < 0.05$) with both lake water as well as with air temperature (Table 2 and Fig. 7). Similarly, the Mg/Ca time series exhibit positive correlation, but with low Pearson correlation coefficients indicating that the relationships are not strong relative to Sr/Ca. Although one of the Ba/Ca (RO-107; $r = 0.8$, $p < 0.05$) and two of the Mn/Ca (RO-106; $r = 0.7$ and RO-109; $r = 0.5$, $p < 0.05$) time series exhibits a significant positive correlation with lake water temperature, this was not observed in the other measured shells. Only a few measured shells indicate a significant correlation with either local precipitation or the respective metal concentration in the lake water (Table 2). Measured water variables such as DOC, TAN and Chlorophyll *a* do not show any significant correlations with Me/Ca ratio of the shells except between Sr/Ca in RO-=106 and DOC and Mn/Ca in RO-109 and Chlorophyll *a* which have significant negative correlations ($r > 0.5$, $p < 0.05$). Similarly, the Me/Ca time series do not indicate a significant correlation with pH variations in the lake, but almost all show a negative correlation.

Table 2. Pearson correlation coefficients between metal/calcium in three juvenile *Echyridella menziesii* shells (RO-106, RO-107 and RO-109, less than five-year-old), and selected environmental variables as well as measured physical parameters in Lake Rotorua. A Pearson $r > 0.50$ suggests a strong correlation (Cohen, 1988; Geeza et al., 2018) and are shown in bold type. At $n = 12$, $r > 0.5$ to be significant at 5% interval

Sample number	Water temp.	Air temp.	Precip.	Me$_{water}$	Chl *a*	DOC	TAN	pH
Sr/Ca RO-106	***0.74***	***0.78***	0.49	0.05	0.30	***-0.61***	0.07	-0.26
Sr/Ca RO-107	***0.61***	***0.56***	0.34	0.00	0.04	0.11	0.23	***-0.67***
Sr/Ca RO-109	***0.85***	***0.86***	0.23	0.10	0.35	-0.42	0.43	-0.21
Mg/Ca RO-106	0.49	***0.57***	0.34	-0.08	-0.08	-0.46	0.19	-0.21
Mg/Ca RO-107	0.44	***0.51***	***0.64***	-0.23	0.04	0.00	0.08	-0.31
Mg/Ca RO-109	***0.76***	***0.85***	***0.57***	0.02	-0.44	-0.30	0.34	-0.30
Ba/Ca RO-106	0.27	0.40	***0.82***	0.04	0.14	-0.42	-0.01	-0.39
Ba/Ca RO-107	***0.88***	0.05	0.13	***-0.51***	-0.15	-0.13	-0.06	-0.18
Ba/Ca RO-109	0.34	***0.90***	0.31	0.04	-0.39	-0.39	0.37	-0.30
Mn/Ca RO-106	***0.70***	***0.70***	-0.03	0.43	-0.41	-0.41	0.09	0.04
Mn/Ca RO-107	***-0.50***	-0.33	-0.38	-0.32	0.30	0.43	-0.25	0.43
Mn/Ca RO-109	***0.54***	***0.63***	0.40	***0.64***	***-0.50***	-0.46	0.06	-0.17

Water temp. = monthly lake water temperature measured by the sonde, Air temp. = monthly air temperature at Rotorua airport, Precip. = Total monthly precipitation at Rotorua airport, Me$_{water}$ = Metal concentration in water, Chl *a* = Chlorophyll *a*, DOC = dissolved organic carbon, TAN = Total Ammonia Nitrogen

1.5 Discussion

1.5.1 Shell formation and lifespan estimations of *Echyridella menziesii*

Confirming the timing of growth increment and growth line formation is essential in sclerochronological studies (Rypel et al., 2008), as they are prerequisites for the construction of the timeline of shell precipitation and for placing environmental proxy data in a precise temporal context. The maximum ontogenetic age measured for the population in Lake Rotorua of 25 years, as well as the maximum age, shown by the Von Bertalanffy growth analysis (30 years) is close to a previous study done on *Echyridella menziesii* populations in the Waikato River where a maximum age of 33 years was observed (Roper and Hickey, 1994). The Waikato River flows through the North Island approximately 40 km south west of Lake Rotorua into the Tasman Sea. However, the maximum age in our population is lower than that in another study from the Waipori River system (maximum 54 years), in the South Island of New Zealand (Grimmond, 1968). The Waipori River is situated in a colder climate (at 45 °S) than Rotorua (at 38 °S) with an annual average temperature of approximately 10 °C.

A similar increase in the lifespan in different populations of the same species with an increase in geographical latitude is reported from 1148 local populations of living marine bivalves spanning from the tropics to the polar regions (Moss et al., 2016). This increase is attributed to favourable environmental factors and lack of physical and ecological disturbances at the locations where older individuals are found (Moss et al., 2016; Moss et al., 2017). These results indicate that when the climate is favourable, *Echyridella menziesii* could live up to 54 years, similar to *Margaritifera falcata* from Western Oregon (45 °N) which reaches lifespans of up to 40 years (Black et al., 2010). However, lifespans determined here are shorter than for *Diplodon chilensis patagonicus* in Argentina at 41 °S, which reaches up to 90 years (Soldati et al., 2009). This shows that age variations of *Echyridella menziesii* are consistent with the variation in the longevity of freshwater bivalves with species, location and environmental condition (Bauer, 1992; Haag and Rypel, 2011).

1.5.2 Effects of temperature and precipitation on element incorporation into *Echyridella menziesii* shells

Sr/Ca in abiogenic aragonite is a function of temperature and decreases with increasing temperature (Beck et al., 1992). In contrast, Sr/Ca in bivalve shell aragonite show a much more variable behaviour and either increase (Gillikin et al., 2005; Elliot et al., 2009), decreases (Yan et al., 2014) or are unaffected (Freitas et al., 2005; Schöne et al., 2011) with increasing temperature, and have led to much debate over their interpretation. Similarly, the processes controlling the incorporation of Mg and its speciation in bivalve shell aragonites are also poorly understood (Foster et al., 2008). However, in contrast to Sr/Ca, Mg/Ca in molluscs (Takesue and van Geen, 2004; Freitas et al., 2005; Wanamaker Jr et al., 2008), corals (Mitsuguchi et al., 1996), and foraminifera (Elderfield and Ganssen, 2000) have been successfully identified as being positively affected by water temperature at the time of formation.

The Sr/Ca as well as Mg/Ca in *Echyridella menziesii* shells in Lake Rotorua are governed by ambient water and air temperatures as seen from the highly significant correlation between these Me/Ca time series and air temperature in most studied samples ($r > 0.5$, $p < 0.05$; Table 2). Further, our results demonstrate that both these Me/Ca increase with increasing temperature as observed in some other freshwater bivalve species (eg; *Diplodon chilensis patagonicus* and *Lampsilis cardium*) around the world (Soldati et al., 2009; Geeza et al., 2018). In contrast, the effects of temperature on Ba and Mn incorporation into the *Echyridella menziesii* shells in this population are negligible.

One of the major sources of Ba in freshwater systems is precipitation-related runoff which adds Ba by the weathering of barite-bearing siliceous rocks (Montaggioni et al., 2006). Therefore, elevated Ba/Ca in mollusc shells are typically associated with high precipitation or riverine discharge events (Gillikin et al., 2006; Montaggioni et al., 2006). However, only one of the Ba/Ca time series of *Echyridella menziesii* shells (RO-106) shows significant correlation with precipitation ($r = 0.82$, $p < 0.05$; Table 2, Fig. 7). Several causes can be suggested for these low correlations. As recorded in the water quality monitoring buoy and sonde, precipitation in Rotorua region is non-seasonal but spread throughout the winter and summer and lacks significant peaks, which provides a relatively constant level of Ba concentration in the runoff throughout the year. Furthermore, the long mean residence time (> 50 years) for groundwater in the Rotorua region (Morgenstern et al., 2015) also delay the

presence of precipitation signals in *Echyridella menziesii* shells. In addition, due to the large volume of Lake Rotorua compared to smaller lakes or streams, the amount of rainfall needed to significantly alter the Ba concentration in waters of the lake is also high. This could also reduce the Ba signal in Lake Rotorua bivalves compared to an aquatic system where rainfall and overland flow has a high influence over Ba concentration as well as a coastal coral reef affected by nearby large river discharges during storm events.
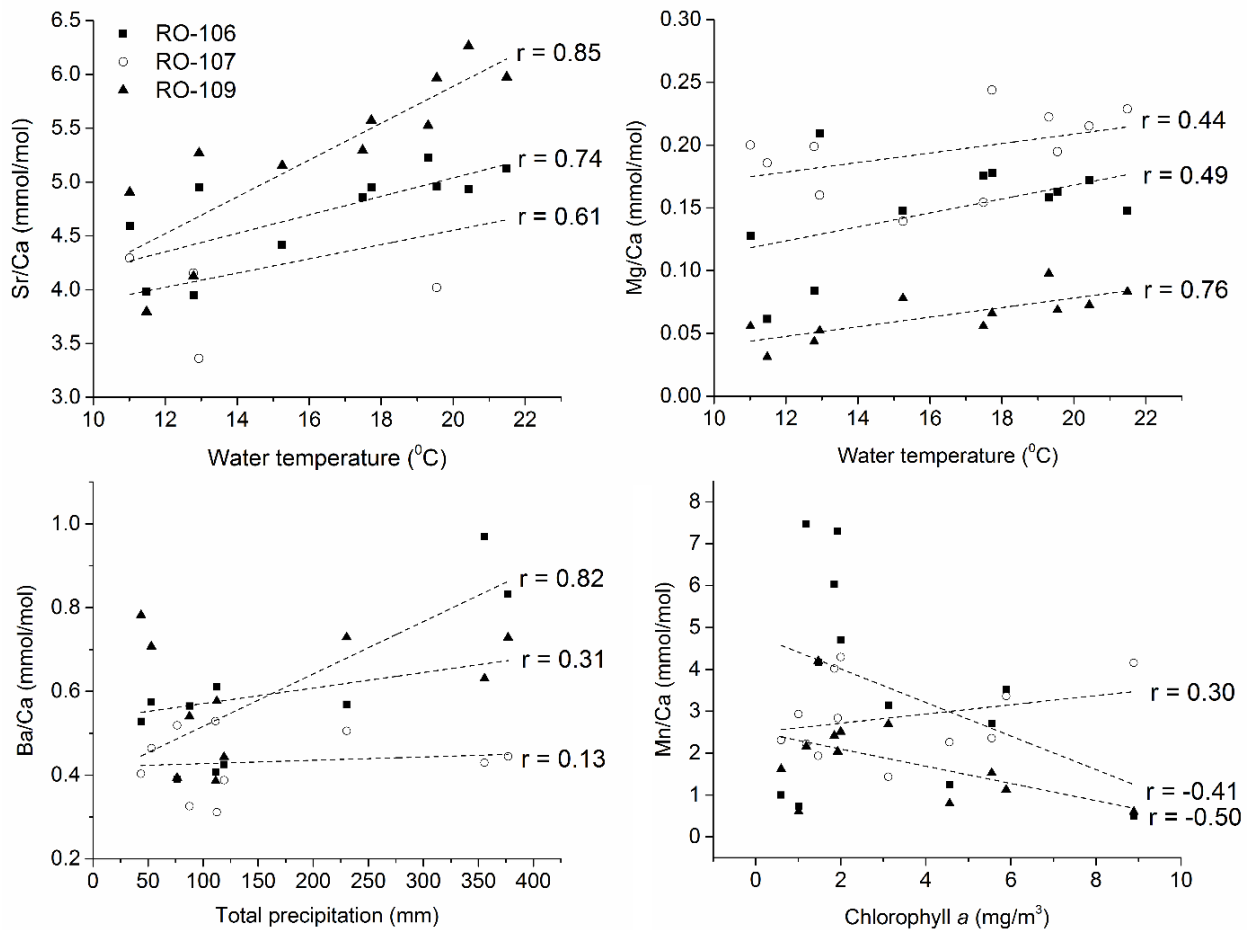
Fig. 7 Biplots of Sr/Ca and Mg/Ca of three juvenile *Echyridella menziesii* shells (RO-106, RO-107 and RO-109, < 5 years old) against monthly lake water temperature from July 2016 to June 2017, biplot of Ba/Ca against precipitation and Mn/Ca against chlorophyll *a*. Dash lines represent the linear regression line for each shell with their respective Pearson correlation coefficients at the end.

1.5.3 Primary productivity influence on element incorporation

Primary productivity and nutrient loads in the ambient aquatic environment are identified as two of the major controlling factors of shell composition (Thébault et al., 2009; Thomsen et al., 2013; Zhao et al., 2017a) shell growth rates (Marali and Schöne, 2015), and shell shape (Telesca et al., 2018) in bivalves. Chlorophyll *a* concentration in lake water is an indicator

of the primary productivity in the natural environment as it is the major pigment in live algal and plant cells (Hoek et al., 1995). High total N is associated with higher nutrient loads as well as primary production (Jeppesen et al., 2005). However, none of the element distributions in *Echyridella menziesii* shells was affected by food and nutrient supply in the lake as suggested by the low correlation values (r < 0.5, p < 0.05) between Me/Ca in shell and chlorophyll *a* concentration, TAN or DOC content in Lake Rotorua (Table 2).

Although Lake Rotorua has its maximum nutrient production occurring around summer or early autumn (Burnet and Davis, 1980), neither monthly water samples nor the sonde data show an increase in chlorophyll *a* concentration, TAN or DOC content in Lake Rotorua during summer (Fig. 4, Table 1). Further, the water quality monitoring buoy in the middle of the lake has not captured a seasonal variation in chlorophyll *a* levels in the lake for the past decade (data available at *monitoring.boprc.govt.nz*). Major nutrient sources in Lake Rotorua have been identified as the extensive cattle farming areas in the catchment (Hamilton, 2003). In addition, Lake Rotorua is a polymictic, eutrophic lake which experiences high internal nutrient release rates due to the large pool of nutrients accumulated in the bottom sediments as a result of several decades of high rates of external loading (Burger et al., 2007). Therefore, nutrient concentrations are not a limiting factor in Lake Rotorua and this could be cause for the observed non-seasonality in nutrient levels and low correlations, since the effects of nutrients on shell growth are negligible in environments with unlimited nutrient supply (Schöne et al., 2004; Dunca et al., 2005). Similarly, no relationship between Sr/Ca or Ba/Ca and primary productivity were observed by other authors who suggest that these elements come exclusively from the ambient water in the dissolved format in contrast to digestion of phytoplankton or algae (Gillikin et al., 2006; Zhao et al., 2017a).

1.5.4 *Echyridella menziesii*; a new environmental archive from Lake Rotorua, New Zealand

The trace element geochemistry of biogenic carbonates is commonly used as indicators of environmental conditions particularly water temperature, precipitation, primary productivity and salinity at the time of shell formation. Most frequently used trace element proxies of temperature in paleoclimatic studies are Sr and Mg (Dodd, 1965; Klünder et al., 2008; Yan et al., 2014; Tynan et al., 2016), since, similar to *Echyridella menziesii* shells, Sr/Ca and Mg/Ca in many different bio-carbonates such as corals, foraminifera and molluscs are controlled by water temperature during shell formation. This study demonstrates the

potential of Sr/Ca in *Echyridella menziesii* shells as a proxy of water temperature based on the significant positive correlation as well the annual cycles observed in the shells. The possibility for Mg/Ca is also observed but with less clarity.

Barium/Ca in bio-carbonates are commonly used as a proxy of primary productivity due to ingestion of phytoplankton by bivalves (Thébault et al., 2009), the oceanic barium cycle (Chan et al., 1977; Gillikin et al., 2006) or precipitation related runoff (Montaggioni et al., 2006). In contrast, the Ba/Ca in *Echyridella menziesii* shells in this population show only low correlations here and cannot be considered a proxy for either primary productivity or precipitation. This is likely an effect of non-seasonal precipitation and a long eutrophic history of Lake Rotorua.

Similar to Ba/Ca, Mn/Ca are also used in literature as a proxy of primary productivity as well as an indication of seasonal upwellings (Langlet et al., 2006), and Mn inputs into coastal environments (Barats et al., 2007). However, Mn/Ca in *Echyridella menziesii* shells show only low correlations with these variables (Table 2). Further, significant heterogeneity observed among Mn/Ca in studied shells suggests the possibility of high biological control over Mn incorporation into the shell (Elliot et al., 2009), which required further study. Long-term monitoring and more details on primary productivity of the lake could contribute to the possibility of using Ba/Ca and Mn/Ca proxies in future.

1.6 Conclusions

Echyridella menziesii; a widespread, large freshwater bivalve in New Zealand has been studied to identify the growth and trace element composition of the shell. *Echyridella menziesii* from Lake Rotorua form annual growth bands in the shell during summer and live up to 25 years. Therefore, *Echyridella menziesii* shells fulfil the prerequisites for environmental proxy archives because the species is present in a broad biogeographic area (from 35 ^{o}S to 45 ^{o}S) in New Zealand, exhibits a long life-span and grows by regular periodic accretion of shell materials. Additionally, Sr/Ca, and possibly Mg/Ca indicate strong positive correlations with water and air temperature indicating the suitability of these element/calcium ratios to perform as a proxy of ambient temperature. In contrast, due to non-seasonal precipitation and long eutrophic history of Lake Rotorua, Ba/Ca in *Echyridella menziesii* shells in this population cannot be considered as a reliable proxy.

Although the results of this study must be confirmed with more shell samples and long chronologies (Chapter 2), this can serve as a guideline to subsequent comprehensive studies. More importantly, *Echyridella menziesii* can now be considered one of the first freshwater bivalve species identified as a potentially suitable environmental archive from Oceania.

1.7 References

Barats, A., Amouroux, D., Pécheyran, C., Chauvaud, L. and Donard, O., 2007. High-Frequency Archives of Manganese Inputs To Coastal Waters (Bay of Seine, France) Resolved by the LA− ICP− MS Analysis of Calcitic Growth Layers along Scallop Shells (*Pecten maximus*). Environmental science & technology, 42(1): 86-92.

Barceloux, D. and Barceloux, D., 1999. Manganese. Journal of Toxicology: Clinical Toxicology, 37(2): 293-307.

Bauer, G., 1992. Variation in the life span and size of the freshwater pearl mussel. Journal of animal ecology: 425-436.

Beck, J.W., Edwards, R.L., Ito, E., Taylor, F.W., Recy, J., Rougerie, F., Joannot, P. and Henin, C., 1992. Sea-surface temperature from coral skeletal strontium/calcium ratios. Science, 257(5070): 644-647.

Black, B.A., Copenheaver, C.A., Frank, D.C., Stuckey, M.J. and Kormanyos, R.E., 2009. Multi-proxy reconstructions of northeastern Pacific sea surface temperature data from trees and Pacific geoduck. Palaeogeography, Palaeoclimatology, Palaeoecology, 278(1): 40-47.

Black, B.A., Dunham, J.B., Blundon, B.W., Raggon, M.F. and Zima, D., 2010. Spatial variability in growth-increment chronologies of long-lived freshwater mussels: implications for climate impacts and reconstructions. Ecoscience, 17(3): 240-250.

Bolotov, I., Pokrovsky, O., Auda, Y., Bespalaya, J., Vikhrev, I., Gofarov, M., Lyubas, A., Viers, J. and Zouiten, C., 2015. Trace element composition of freshwater pearl mussels *Margaritifera spp.* across Eurasia: Testing the effect of species and geographic location. Chemical Geology, 402: 125-139.

Burger, D., Hamilton, D., Pilditch, C. and Gibbs, M., 2007. Benthic nutrient fluxes in a eutrophic, polymictic lake. Hydrobiologia, 584(1): 13-25.

Burnet, A.M.R. and Davis, J.M., 1980. Primary production in Lakes Rotorua, Rerewhakaaitu, and Rotoiti, North Island. New Zealand. 1973–78. New Zealand journal of marine and freshwater research, 14(3): 229-236.

Campbell, M., 2005. The archaeology of kakahi (*Hyridella menziesi*). Archaeology in New Zealand 48 (2): 101-112.

Carré, M., Bentaleb, I., Bruguier, O., Ordinola, E., Barrett, N.T. and Fontugne, M., 2006. Calcification rate influence on trace element concentrations in aragonitic bivalve shells: evidences and mechanisms. Geochimica et Cosmochimica Acta, 70(19): 4906-4920.

Carroll, M. and Romanek, C.S., 2008. Shell layer variation in trace element concentration for the freshwater bivalve *Elliptio complanata*. Geo-Marine Letters, 28(5-6): 369-381.

Carter, J.G., 1990. Skeletal Biomineralization: Atlas and index, 2. Van Nostrand Reinhold Company.

Chan, L., Drummond, D., Edmond, J. and Grant, B., 1977. On the barium data from the Atlantic GEOSECS expedition. Deep Sea Research, 24(7): 613-649.

Chapman, M., 1996. Human impacts on the Waikato river system, New Zealand. GeoJournal, 40(1-2): 85-99.

Clearwater, S., Wood, S., Phillips, N., Parkyn, S., Van Ginkel, R. and Thompson, K., 2014a. Toxicity thresholds for juvenile freshwater mussels *Echyridella menziesii* and crayfish *Paranephrops planifrons*, after acute or chronic exposure to *Microcystis* sp. Environmental toxicology, 29(5): 487-502.

Clearwater, S.J., Thompson, K.J. and Hickey, C.W., 2014b. Acute toxicity of copper, zinc, and ammonia to larvae (Glochidia) of a native freshwater mussel *Echyridella*

menziesii in New Zealand. Archives of environmental contamination and toxicology, 66(2): 213-226.

Cohen, J., 1988. Statistical power analysis for the behavioral sciences 2nd edn. Erlbaum Associates, Hillsdale.

Cohen, J., Screen, J.A., Furtado, J.C., Barlow, M., Whittleston, D., Coumou, D., Francis, J., Dethloff, K., Entekhabi, D. and Overland, J., 2014. Recent Arctic amplification and extreme mid-latitude weather. Nature geoscience, 7(9): 627-637.

Cole, J., 1990. Structural control and origin of volcanism in the Taupo volcanic zone, New Zealand. Bulletin of volcanology, 52(6): 445-459.

Cyr, H., Collier, K.J., Clearwater, S.J., Hicks, B.J. and Stewart, S.D., 2016. Feeding and nutrient excretion of the New Zealand freshwater mussel *Echyridella menziesii* (Hyriidae, Unionida): implications for nearshore nutrient budgets in lakes and reservoirs. Aquatic Sciences: 1-15.

Dodd, J.R., 1965. Environmental control of strontium and magnesium in Mytilus. Geochimica et Cosmochimica Acta, 29(5): 385-398.

Donath, F.M., Daughney, C.J., Morgenstern, U., Cameron, S.G. and Toews, M.W., 2015. Hydrochemical interpretation of groundwater-surface water interactions at catchment and local scales, Lake Rotorua catchment, New Zealand. Journal of Hydrology, 54(1): 11.

Dunca, E., Schöne, B.R. and Mutvei, H., 2005. Freshwater bivalves tell of past climates: But how clearly do shells from polluted rivers speak? Palaeogeography, Palaeoclimatology, Palaeoecology, 228(1): 43-57.

Elderfield, H. and Ganssen, G., 2000. Past temperature and $\delta\,^{18}$O of surface ocean waters inferred from foraminiferal Mg/Ca ratios. Nature, 405(6785): 442.

Elliot, M., Welsh, K., Chilcott, C., McCulloch, M., Chappell, J. and Ayling, B., 2009. Profiles of trace elements and stable isotopes derived from giant long-lived *Tridacna gigas* bivalves: potential applications in paleoclimate studies. Palaeogeography, Palaeoclimatology, Palaeoecology, 280(1): 132-142.

Foster, L., Finch, A., Allison, N., Andersson, C. and Clarke, L., 2008. Mg in aragonitic bivalve shells: Seasonal variations and mode of incorporation in *Arctica islandica*. Chemical Geology, 254(1): 113-119.

Freitas, P., Clarke, L.J., Kennedy, H., Richardson, C. and Abrantes, F., 2005. Mg/Ca, Sr/Ca, and stable-isotope (δ^{18}O and δ^{13}C) ratio profiles from the fan mussel *Pinna nobilis*: Seasonal records and temperature relationships. Geochemistry, Geophysics, Geosystems, 6(4).

Freitas, P.S., Clarke, L.J., Kennedy, H. and Richardson, C.A., 2016. Manganese in the shell of the bivalve *Mytilus edulis*: Seawater Mn or physiological control? Geochimica et Cosmochimica Acta, 194: 266-278.

Geeza, T.J., Gillikin, D.P., Goodwin, D.H., Evans, S.D., Watters, T. and Warner, N.R., 2018. Controls on magnesium, manganese, strontium, and barium concentrations recorded in freshwater mussel shells from Ohio. Chemical Geology.

Gillikin, D.P., Dehairs, F., Lorrain, A., Steenmans, D., Baeyens, W. and André, L., 2006. Barium uptake into the shells of the common mussel (*Mytilus edulis*) and the potential for estuarine paleo-chemistry reconstruction. Geochimica et Cosmochimica Acta, 70(2): 395-407.

Gillikin, D.P., Lorrain, A., Navez, J., Taylor, J.W., André, L., Keppens, E., Baeyens, W. and Dehairs, F., 2005. Strong biological controls on Sr/Ca ratios in aragonitic marine bivalve shells. Geochemistry, Geophysics, Geosystems, 6(5).

Graf, D.L. and Cummings, K.S., 2006. Palaeoheterodont diversity (Mollusca: *Trigonioida+ Unionoida*): what we know and what we wish we knew about freshwater mussel evolution. Zoological Journal of the Linnean Society, 148(3): 343-394.

Griffin, W., Powell, W., Pearson, N. and O'reilly, S., 2008. GLITTER: data reduction software for laser ablation ICP-MS. Laser Ablation-ICP-MS in the earth sciences. Mineralogical association of Canada short course series, 40: 204-207.

Grimmond, N.M.W., 1968. Observations on growth and age of *Hyridella menziesi* Gray (MolluscaBivalvia) in a freshwater tidal lake, University of Otago.

Haag, W.R. and Rypel, A.L., 2011. Growth and longevity in freshwater mussels: evolutionary and conservation implications. Biological Reviews, 86(1): 225-247.

Hamilton, D.P., 2003. An historical and contemporary review of water quality in the Rotorua lakes. Proceedings Rotorua Lakes: 3-15.

Hamilton, D.P., Collier, K.J. and Howard-Williams, C., 2016. Lake restoration in New Zealand. Ecological Management & Restoration, 17(3): 191-199.

Heise, W., Caldwell, T., Bertrand, E., Hill, G., Bennie, S. and Palmer, N., 2016. Imaging the deep source of the Rotorua and Waimangu geothermal fields, Taupo Volcanic Zone, New Zealand. Journal of Volcanology and Geothermal Research, 314: 39-48.

Hoek, C., Mann, D. and Jahns, H.M., 1995. Algae: an introduction to phycology. Cambridge university press.

Izumida, H., Yoshimura, T., Suzuki, A., Nakashima, R., Ishimura, T., Yasuhara, M., Inamura, A., Shikazono, N. and Kawahata, H., 2011. Biological and water chemistry controls on Sr/Ca, Ba/Ca, Mg/Ca and δ ^{18}O profiles in freshwater pearl mussel *Hyriopsis* sp. Palaeogeography, Palaeoclimatology, Palaeoecology, 309(3): 298-308.

Izzo, C., Manetti, D., Doubleday, Z.A. and Gillanders, B.M., 2016. Calibrating the element composition of *Donax deltoides* shells as a palaeo-salinity proxy. Palaeogeography, Palaeoclimatology, Palaeoecology.

James, M., 1985. Distribution, biomass and production of the freshwater mussel, *Hyridella menziesi* (Gray), in Lake Taupo, New Zealand. Freshwater biology, 15(3): 307-314.

James, M., 1987. Ecology of the freshwater mussel *Hyridella menziesi* (Gray) in a small oligotrophic lake. Archiv für Hydrobiologie, 108(3): 337-348.

Jeppesen, E., Søndergaard, M., Jensen, J.P., Havens, K.E., Anneville, O., Carvalho, L., Coveney, M.F., Deneke, R., Dokulil, M.T. and Foy, B., 2005. Lake responses to reduced nutrient loading–an analysis of contemporary long-term data from 35 case studies. Freshwater Biology, 50(10): 1747-1771.

Jochum, K.P., Nohl, U., Herwig, K., Lammel, E., Stoll, B. and Hofmann, A.W., 2005. GeoReM: a new geochemical database for reference materials and isotopic standards. Geostandards and Geoanalytical Research, 29(3): 333-338.

Jones, W. and Walker, K., 1979. Accumulation of iron, manganese, zinc and cadmium by the Australian freshwater mussel *Velesunio ambiguus* (Phillipi) and its potential as a biological monitor. Marine and Freshwater Research, 30(6): 741-751.

Klünder, M.H., Hippler, D., Witbaard, R. and Frei, D., 2008. Laser ablation analysis of bivalve shells–archives of environmental information.

Klunzinger, M.W., Beatty, S.J., Morgan, D.L., Lymbery, A.J. and Haag, W.R., 2014. Age and growth in the Australian freshwater mussel, *Westralunio carteri*, with an evaluation of the fluorochrome calcein for validating the assumption of annulus formation. Age, 33(4).

Langlet, D., Alleman, L., Plisnier, P.D., Hughes, H. and André, L., 2006. Mn seasonal upwellings recorded in Lake Tanganyika mussels. Biogeosciences Discussions, 3(5): 1453-1471.

Marali, S. and Schöne, B.R., 2015. Oceanographic control on shell growth of *Arctica islandica* (Bivalvia) in surface waters of Northeast Iceland—Implications for paleoclimate reconstructions. Palaeogeography, Palaeoclimatology, Palaeoecology, 420: 138-149.

Markich, S., 2017. Sensitivity of the glochidia (larvae) of freshwater mussels (Bivalvia: *Unionida: Hyriidae*) to cadmium, cobalt, copper, lead, nickel and zinc: Differences

between metals, species and exposure time. The Science of the total environment, 601: 1427.

Marshall, B.A., Fenwick, M.C. and Ritchie, P.A., 2014. New Zealand Recent Hyriidae (Mollusca: Bivalvia: Unionida). Molluscan Research, 34(3): 181-200.

Mitsuguchi, T., Matsumoto, E., Abe, O., Uchida, T. and Isdale, P.J., 1996. Mg/Ca thermometry in coral skeletons. Science, 274(5289): 961-963.

Montaggioni, L.F., Le Cornec, F., Corrège, T. and Cabioch, G., 2006. Coral barium/calcium record of mid-Holocene upwelling activity in New Caledonia, South-West Pacific. Palaeogeography, Palaeoclimatology, Palaeoecology, 237(2): 436-455.

Morgenstern, U., Daughney, C.J., Leonard, G., Gordon, D., Donath, F.M. and Reeves, R., 2015. Using groundwater age and hydrochemistry to understand sources and dynamics of nutrient contamination through the catchment into Lake Rotorua, New Zealand. Hydrology and Earth System Sciences, 19(2): 803-822.

Moss, D.K., Ivany, L.C., Judd, E.J., Cummings, P.W., Bearden, C.E., Kim, W.J., Artruc, E.G. and Driscoll, J.R., 2016. Lifespan, growth rate, and body size across latitude in marine Bivalvia, with implications for Phanerozoic evolution, Proc. R. Soc. B. The Royal Society, pp. 20161364.

Moss, D.K., Ivany, L.C., Silver, R.B., Schue, J. and Artruc, E.G., 2017. High-latitude settings promote extreme longevity in fossil marine bivalves. Paleobiology, 43(3): 365-382.

Mueller, H., Hamilton, D.P. and Doole, G.J., 2015. Response lags and environmental dynamics of restoration efforts for Lake Rotorua, New Zealand. Environmental Research Letters, 10(7): 074003.

Neukom, R., Gergis, J., Karoly, D.J., Wanner, H., Curran, M., Elbert, J., González-Rouco, F., Linsley, B.K., Moy, A.D. and Mundo, I., 2014. Inter-hemispheric temperature variability over the past millennium. Nature Climate Change, 4(5): 362-367.

O'Neil, D.D. and Gillikin, D.P., 2014. Do freshwater mussel shells record road-salt pollution? Scientific reports, 4.

Ogle, D., 2016. FSA: Fisheries Stock Analysis. R package version 0.8. 7, 2016.

Pauly, D., 1980. On the interrelationships between natural mortality, growth parameters, and mean environmental temperature in 175 fish stocks. ICES Journal of Marine Science, 39(2): 175-192.

Phillips, N.R., Stewart, M., Olsen, G. and Hickey, C.W., 2014. Human health risks of geothermally derived metals and other contaminants in wild-caught food. Journal of Toxicology and Environmental Health, Part A, 77(6): 346-365.

Poulain, C., Gillikin, D., Thébault, J., Munaron, J.-M., Bohn, M., Robert, R., Paulet, Y.-M. and Lorrain, A., 2015. An evaluation of Mg/Ca, Sr/Ca, and Ba/Ca ratios as environmental proxies in aragonite bivalve shells. Chemical Geology, 396: 42-50.

Roman-Gonzalez, A., Scourse, J.D., Butler, P.G., Reynolds, D.J., Richardson, C.A., Peck, L.S., Brey, T. and Hall, I.R., 2016. Analysis of ontogenetic growth trends in two marine Antarctic bivalves *Yoldia eightsi* and *Laternula elliptica*: Implications for sclerochronology. Palaeogeography, Palaeoclimatology, Palaeoecology.

Roper, D.S. and Hickey, C.W., 1994. Population structure, shell morphology, age and condition of the freshwater mussel *Hyridella menziesi* (Unionacea: Hyriidae) from seven lake and river sites in the Waikato River system. Hydrobiologia, 284(3): 205-217.

Rueden, C.T., Schindelin, J., Hiner, M.C., DeZonia, B.E., Walter, A.E. and Eliceiri, K.W., 2017. ImageJ2: ImageJ for the next generation of scientific image data. arXiv preprint arXiv:1701.05940.

Rutherford, J., 1984. Trends in Lake Rotorua water quality. New Zealand journal of marine and freshwater research, 18(3): 355-365.

Rypel, A.L., Haag, W.R. and Findlay, R.H., 2008. Validation of annual growth rings in freshwater mussel shells using cross dating. Canadian Journal of Fisheries and Aquatic Sciences, 65(10): 2224-2232.

Schöne, B.R., Dunca, E., Mutvei, H. and Norlund, U., 2004. A 217-year record of summer air temperature reconstructed from freshwater pearl mussels (*M. margarifitera*, Sweden). Quaternary Science Reviews, 23(16): 1803-1816.

Schöne, B.R. and Surge, D.M., 2012. Part N, Revised, Volume 1, Chapter 14: Bivalve sclerochronology and geochemistry. Treatise online, 46: 1-24.

Schöne, B.R., Zhang, Z., Radermacher, P., Thébault, J., Jacob, D.E., Nunn, E.V. and Maurer, A.-F., 2011. Sr/Ca and Mg/Ca ratios of ontogenetically old, long-lived bivalve shells (*Arctica islandica*) and their function as paleotemperature proxies. Palaeogeography, Palaeoclimatology, Palaeoecology, 302(1): 52-64.

Schroeder, H.A., Tipton, I.H. and Nason, A.P., 1972. Trace metals in man: strontium and barium. Journal of Chronic Diseases, 25(9): 491-517.

Scott, B., Mroczek, E., Burnell, J., Zarrouk, S., Seward, A., Robson, B. and Graham, D., 2016. The Rotorua Geothermal Field: an experiment in environmental management. Geothermics, 59: 294-310.

Smith, V.H., Wood, S.A., McBride, C., Atalah, J., Hamilton, D. and Abell, J., 2016. Phosphorus and nitrogen loading restraints are essential for successful eutrophication control of Lake Rotorua, New Zealand. Inland Waters, 6(2): 273-283.

Soldati, A., Jacob, D., Schöne, B., Bianchi, M. and Hajduk, A., 2009. Seasonal periodicity of growth and composition in valves of *Diplodon chilensis patagonicus* (d'Orbigny, 1835). Journal of Molluscan Studies, 75(1): 75-85.

Takesue, R.K. and van Geen, A., 2004. Mg/Ca, Sr/Ca, and stable isotopes in modern and Holocene Protothaca staminea shells from a northern California coastal upwelling region. Geochimica et Cosmochimica Acta, 68(19): 3845-3861.

Taylor, J.D., 1973. The structural evolution of the bivalve shell. Palaeontology, 16(3): 519-534.

Telesca, L., Michalek, K., Sanders, T., Peck, L.S., Thyrring, J. and Harper, E.M., 2018. Blue mussel shell shape plasticity and natural environments: a quantitative approach. Scientific reports, 8(1): 2865.

Thébault, J., Chauvaud, L., L'Helguen, S., Clavier, J., Barats, A., Jacquet, S., Pécheyran, C. and Amouroux, D., 2009. Barium and molybdenum records in bivalve shells: Geochemical proxies for phytoplankton dynamics in coastal environments? Limnology and Oceanography, 54(3): 1002-1014.

Thomsen, J., Casties, I., Pansch, C., Körtzinger, A. and Melzner, F., 2013. Food availability outweighs ocean acidification effects in juvenile *Mytilus edulis*: laboratory and field experiments. Global change biology, 19(4): 1017-1027.

Tynan, S., Opdyke, B.N., Walczak, M., Eggins, S. and Dutton, A., 2016. Assessment of Mg/Ca in *Saccostrea glomerata* (the Sydney rock oyster) shell as a potential temperature record. Palaeogeography, Palaeoclimatology, Palaeoecology.

Wanamaker Jr, A.D., Kreutz, K.J., Wilson, T., Borns Jr, H.W., Introne, D.S. and Feindel, S., 2008. Experimentally determined Mg/Ca and Sr/Ca ratios in juvenile bivalve calcite for *Mytilus edulis*: implications for paleotemperature reconstructions. Geo-Marine Letters, 28(5-6): 359-368.

Wang, Q., Fan, X. and Wang, M., 2016. Evidence of high-elevation amplification versus Arctic amplification. Scientific reports, 6.

Yan, H., Shao, D., Wang, Y. and Sun, L., 2014. Sr/Ca differences within and among three Tridacnidae species from the South China Sea: Implication for paleoclimate reconstruction. Chemical Geology, 390: 22-31.

Yan, H., Sun, L., Shao, D. and Wang, Y., 2015. Seawater temperature seasonality in the South China Sea during the late Holocene derived from high-resolution Sr/Ca ratios of *Tridacna gigas*. Quaternary Research, 83(2): 298-306.

Zhao, L., Schöne, B.R. and Mertz-Kraus, R., 2017a. Controls on strontium and barium incorporation into freshwater bivalve shells (*Corbicula fluminea*). Palaeogeography, Palaeoclimatology, Palaeoecology, 465: 386-394.

Zhao, L., Walliser, E.O., Mertz-Kraus, R. and Schöne, B.R., 2017b. Unionid shells (*Hyriopsis cumingii*) record manganese cycling at the sediment-water interface in a shallow eutrophic lake in China (Lake Taihu). Palaeogeography, Palaeoclimatology, Palaeoecology.

1.8 Supplementary Material – Chapter 1

1.8.1 Supplementary - Methodology

Sonde calibration and settings

From June to August Eureka Manta 2 sondes were deployed, then on 18 August 2016 Exosondes were used for the remainder of the monitoring (further detail is provided below). The sondes were calibrated and fitted with fully charged batteries at the NIWA Hamilton Laboratory immediately prior to deployment at the lake

The Eureka Manta 2 sondes measured pH, temperature, DO and chlorophyll *a* every hour from 22 June 2016-7 July 2016, and then every five minutes from 21 July 2016 to 3 August 2016. From 22 August 2016, the Exosondes were couriered to NIWA Rotorua with a cap on the sonde containing pH 4 standard buffer (which assists subsequent data analysis by indicating the start of deployment when the cap was removed at the site). From 18 August 2016 to March 2017 the exosondes were set to take measurements every 10 minutes. Each measurement consisted of readings every 1 second for 30 seconds. In March 2017 the data recording was changed to only record the average of the readings every 10 minutes. On return to the lab, measurements were taken to evaluate whether significant drift in the calibration of the probes had occurred.

pH calibration and post-deployment readings

The pH probe was calibrated pre-deployment in pH 4, 7 and 10 standard buffers. After calibration, a pre-deployment pH reading was taken in the pH 7 standard buffer. After deployment for a month, the sonde was capped and couriered back to NIWA Hamilton. At the laboratory, a manual pH reading was taken for a post-deployment measure in the pH 7 standard after wiping the sensor face (just as the automated sensor wipe would do during deployment).

Dissolved oxygen calibration and post-deployment readings

The DO probe measuring percentage dissolved oxygen (rather than the other DO measures) was calibrated by preparing a flask with a small amount of aerated (shaken) tap water and placing the sensor end of the sonde in this moist oxygen-saturated environment (not sealed) for 30 minutes. Barometric pressure in the laboratory at NIWA Hamilton was used in this process and the probe calibrated to 100 per cent saturation.

Distilled water reading of the temperature, DO, conductivity and pH probes.

All the sensors were placed in distilled water pre-deployment and temperature, DO, conductivity and pH, was recorded to be followed by another manual reading at the end of the deployment. Distilled water from a reverse osmosis unit was always used for this step and pH was highly variable.

1.8.2 Supplementary –Tables

Table S1. Notes on mussels observed to have brood pouches.

Date collected	Mussel-ID	Brood pouch? Yes/No	Brood pouch size	Brood pouch colour
18/8/16	8-8	Yes	S	W
22/9/16	9-4	Yes	S	W
20/10/16	10-5	Yes	F	PY
20/10/16	10-6	Yes	F	Y
21/11/16	11-5	Yes	F	Y-O
21/11/16	11-6	Yes	S	Y
15/12/16	12-6	Yes	F	Y

For brood pouch size: F = full; S = slight. For brood pouch colour PY = pale yellow, Y = yellow, Y-O = yellow-orange, O= orange, W = white. Orange is characteristic of a brood pouch containing mature glochidia, and a white brood pouch may indicate a ripe male mussel.

Table S2. Inter-correlations between Me/Ca time series for the monitoring year (June 2016 to June 2017) in three measured shells (RO 106, 107 and 109) of young mussels (< 5 years old) and the standard deviation (stdv) of each time series

Sr	106	107	109	stdv
106	1			0.44
107	0.43	1		0.38
109	0.89	0.48	1	0.82
Mg	106	107	109	
106	1			0.18
107	0.38	1		0.07
109	0.60	0.65	1	0.13
Ba	106	107	109	
106	1			0.04
107	0.36	1		0.02
109	0.74	0.60	1	0.02
Mn	106	107	109	
106	1			2.47
107	0.04	1		0.93
109	0.55	-0.29	1	1.04

1.8.3 Supplementary – Figures
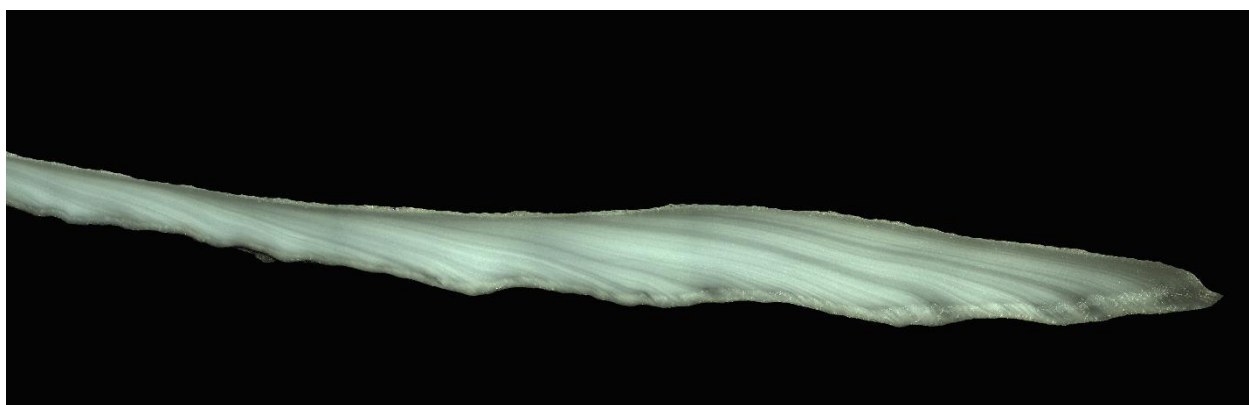
Fig. S1 Microphotograph image of a cross section of a shell (opaque white) from a less than 5 year old *Echyridella menziesii* (RO-109) collected from Lake Rotorua, indicating the location of LA-ICP-MS curve (dashed line) in the nacreous layer. The dark and granular area in the lower half of the image, and the clear granular area in the upper half, is the resin holding the cross section.
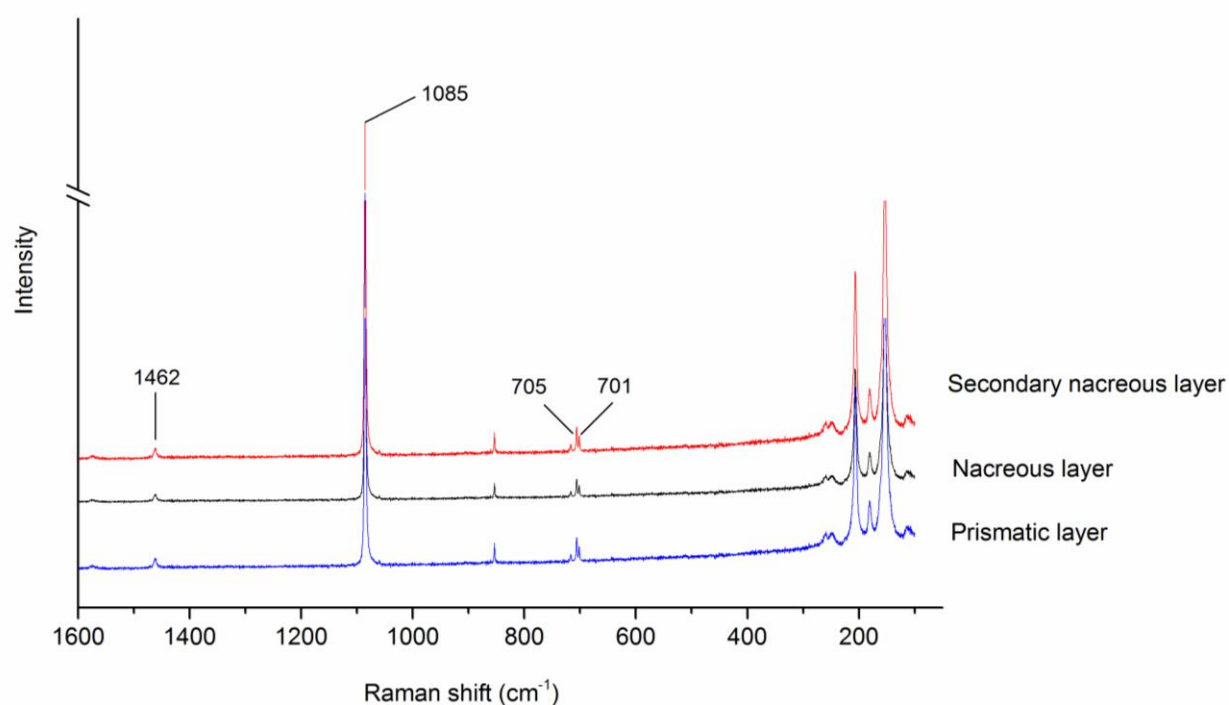
Fig. S2 Representative Raman spectrums from three layers of *Echyridella menziesii* shell indicating that the shell is composed of aragonite. Note that the intensity axis is braked to enhance the peaks.
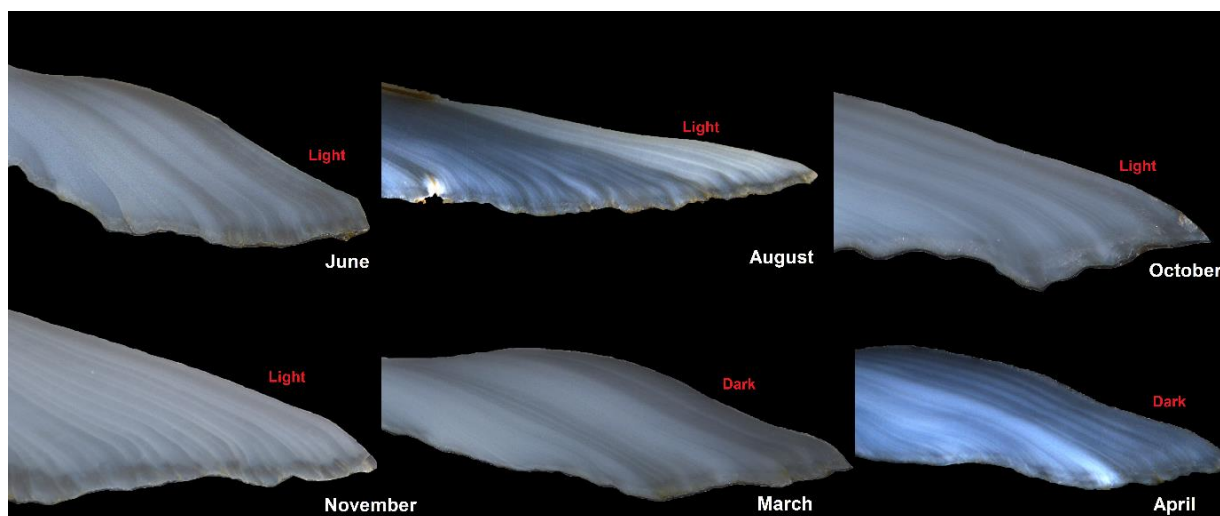
Fig. S3 Microphotographs of the ventral margin of selected polished sections of *Echyridella menziesii* shells from Lake Rotorua. The images identify the area precipitated at specific months which enables the creation of a time line for the dark band formation.
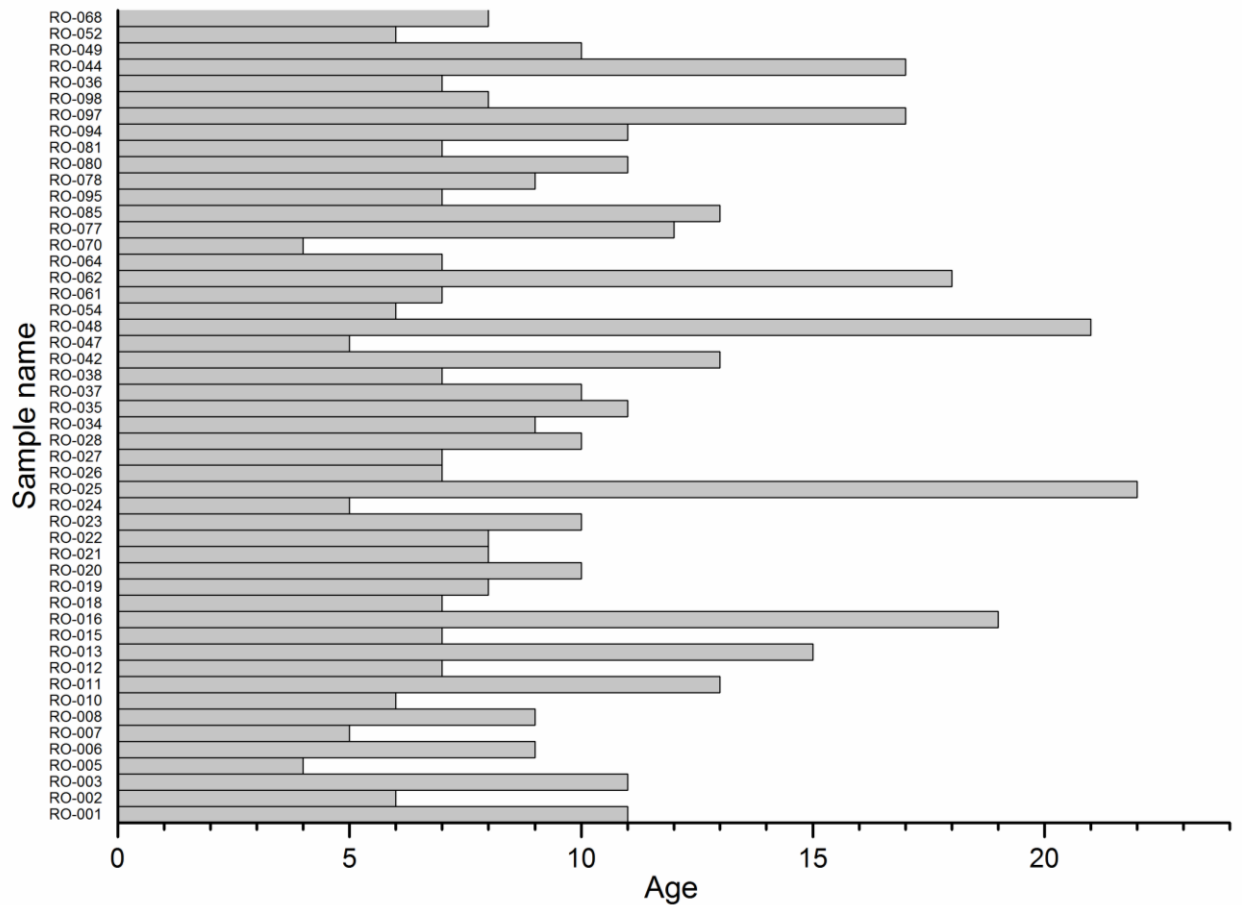
Fig. S4 Measured ages of fifty *Echyridella menziesii* shells collected from Lake Rotorua, New Zealand showing the variation in ages among shells
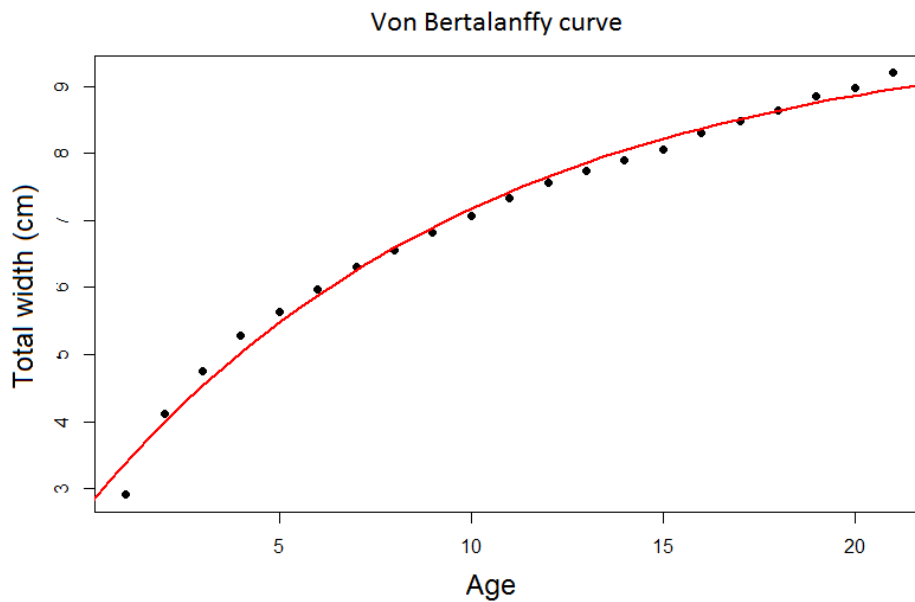
Fig. S5 Von Bertalanffy curve for 21 well-stained *Echyridella menziesii* shells from Lake Rotorua (*n* = 21). The maximum asymptotic length (L_{inf}) is 9.9 cm and average growth rate (K) is 0.1 cm per year.

52
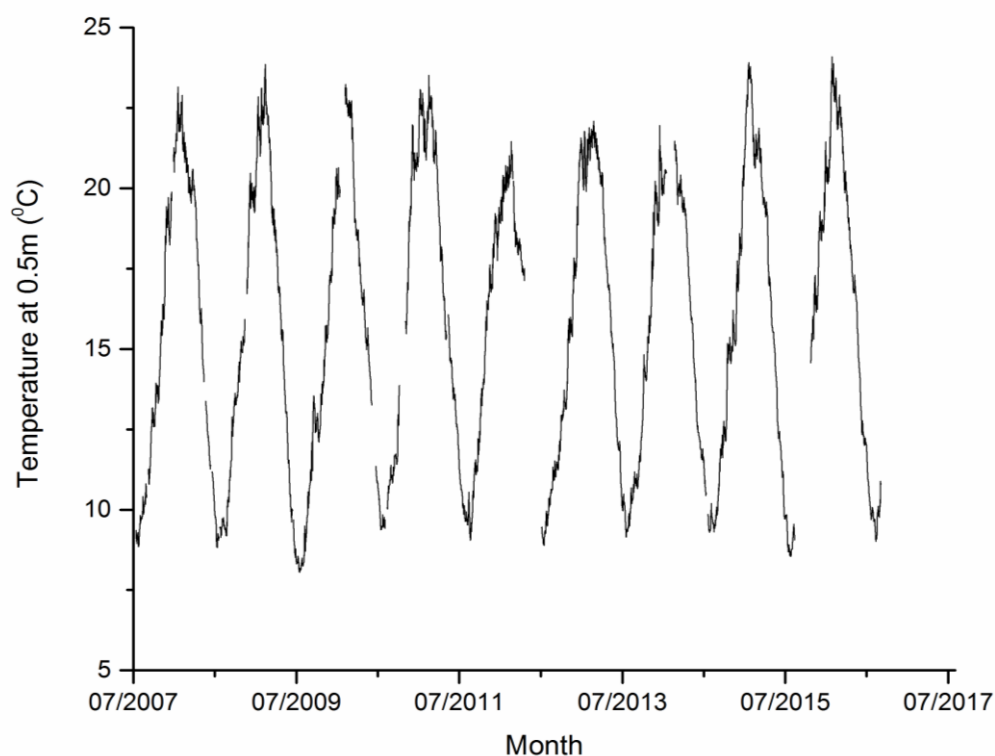
Fig. S6 Daily water temperature variation in Lake Rotorua, New Zealand recorded at 0.5 m below the water surface by a water quality buoy deployed by the University of Waikato.
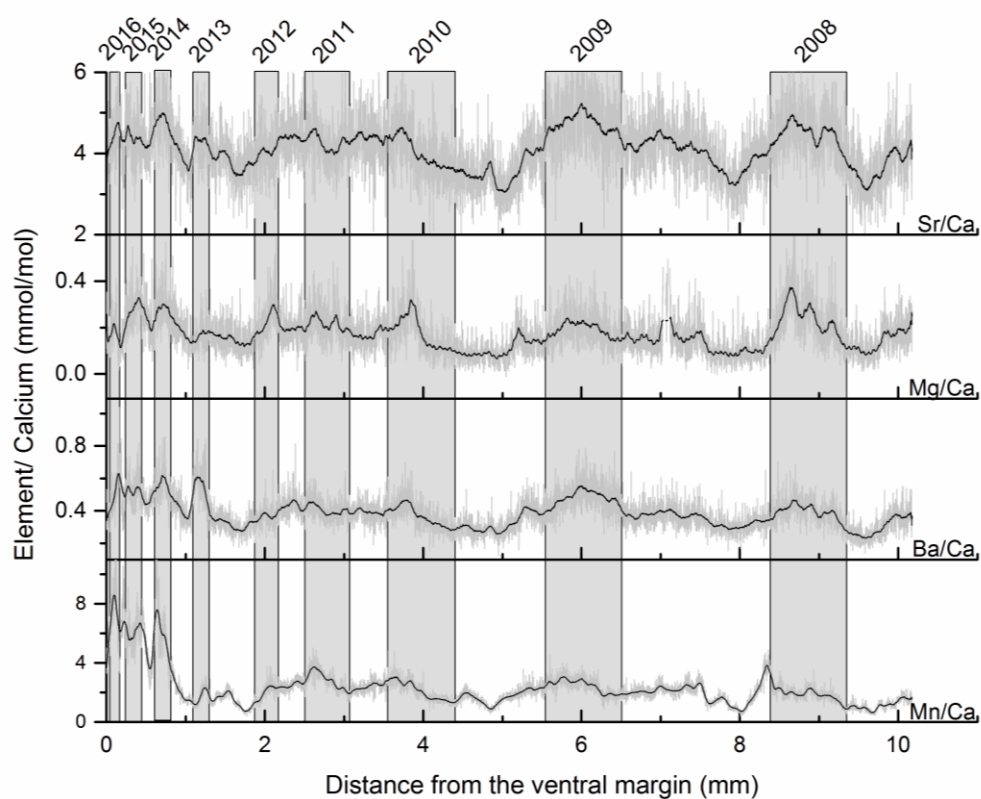
Fig. S7 Trace element/calcium variation (mmol/mol) along the nacreous middle layer of a long-lived *Echyridella menziesii* shell collected Lake Rotorua. Shaded areas mark the approximate location of the dark summer growth increment.

Chapter 2

TEMPERATURE RECONSTRUCTIONS BY δ^{18}O AND Sr/Ca USING FRESHWATER BIVALVE *Echyridella menziesii* FROM NEW ZEALAND

Dilmi Herath[1], Richard Stern[2], Susan Clearwater[3] and Dorrit Jacob[1]

[1] Department of Earth and Planetary Science, Macquarie University, Sydney, Australia,

[2] Department of Earth and Atmospheric Sciences, University of Alberta, Edmonton, Alberta T6G 2E3, Canada

[3] National Institute of Water and Atmospheric Research, Silverdale Road, Hamilton 3216, New Zealand

Abstract

High-resolution records of past environmental conditions from a geographically widespread area can considerably improve regional climate models. Here we explore the possibility of using the freshwater bivalve *Echyridella menziesii* from Lake Rotorua, New Zealand as a temperature proxy archive using a multi-proxy approach. Carbonate clumped isotopes, oxygen isotopes and Sr/Ca analysis are used to obtain annual, monthly and weekly temperature reconstructions. Results show that oxygen isotope ratios and Sr/Ca ratios in *Echyridella menziesii* shells record temperature variability at the weekly resolution and carbonate clumped isotopes at annual resolution. In addition, Ba/Ca ratios are identified as a possible proxy for primary productivity. Further, drastic reductions in *Echyridella menziesii* shell growth rates are recognized as indicators of El-Niño events. Southern hemisphere climate reconstructions are biased towards dendrochronology and lack the input from other terrestrial archives. *Echyridella menziesii;* the dominant large freshwater bivalve species in New Zealand between 35 °S and 45 °S and also present in shell middens, can now complement in identifying local environmental variables as well as regional climate systems from the southern hemisphere.

2.1 Introduction

Hemispheric-scale climate models require long-term and high-resolution records of past environmental conditions from a geographically widespread area (Neukom et al., 2014). Tree-rings are the most widely used continental climate archives to reconstruct numerous environmental variables including temperature, precipitation, fire history, and river discharge (Cook et al., 2006; Fowler et al., 2012; Villalba et al., 2012). However, additional archives that can reinforce and validate tree-ring climate reconstructions are poorly examined (Black et al., 2009). Due to similarities in their resolution, incremental accretion of calcium carbonate, long lifetimes and global distribution, the skeletal hard parts of molluscs are often found to be suitable archives to complement tree-ring data. Therefore, various physical and chemical characteristics of mollusc shells have been used in the reconstruction of climatic and environmental variables such as temperature, precipitation, salinity, river discharge, and primary productivity (Schöne et al., 2004b; Gillikin et al., 2006b; Schöne et al., 2007; Wanamaker et al., 2011; Kelemen et al., 2017).

Since environmental variables are recorded in the shells in multiple ways such as growth, isotope and trace element variations, molluscs provide an added advantage in using multiproxy approaches to obtain past environmental records with the possibility of assigning calendar dates (Schöne et al., 2004a). Growth rate, oxygen isotope ratio and trace element-to-calcium ratios are frequently used proxies for environmental reconstructions. Oxygen isotope ratios ($\delta^{18}O$) of biogenic carbonates have been successfully used as a proxy of temperature, river discharge, salinity, growth rate and growth cessation temperature (Urey et al., 1951; Dettman et al., 1999; Ricken et al., 2003; Rosales et al., 2004). Similarly, carbonate clumped isotopes have also been increasingly used as a proxy of past temperature (Eiler, 2011; Affek, 2012) and in paleo biology to understand the physiology of extinct animals (Eagle et al., 2011). Additionally, strontium, magnesium, barium and manganese ratios with calcium in molluscs are also frequently utilized as proxies of environmental conditions such as temperature, salinity, precipitation and primary productivity (Gillikin et al., 2006a; Langlet et al., 2007; Yan et al., 2014b; Tynan et al., 2016; Geeza et al., 2018).

Although marine bivalves are frequently used in environmental reconstructions, the potential of freshwater bivalves as proxy archives has been examined in just a few studies (Kaandorp et al., 2003; Ricken et al., 2003; Peacock and Seltzer, 2008; Black et al., 2010; Geeza et al.,

2018), because in contrast to relatively stable marine environments, complex variations in freshwater systems such as strong seasonality in water oxygen isotope levels, the influence of precipitation, groundwater influx and evaporation, make the use of freshwater bivalves challenging. Here we explore the possibility of using the freshwater bivalve *Echyridella menziesii* from Lake Rotorua, New Zealand (Fig. 1) as a temperature proxy archive using a multi-proxy approach. High-resolution oxygen isotopes and trace element analysis are used here to obtain monthly and weekly temperature reconstructions using *Echyridella menziesii* shells.

2.1.1 Effects of regional climate systems on New Zealand

Major regional-scale recurrent climatic phenomena that influence the climate in New Zealand are El Niño–Southern Oscillation (ENSO), Southern Annular Mode (SAM), and westerly winds (Toggweiler, 2009; Villalba et al., 2012; Jones et al., 2016; Lim et al., 2016). During El Niño events which have a 2-7 years frequency (Wang et al., 2017), New Zealand typically experiences stronger or more frequent winds from the west in summer, leading to drier-than-normal conditions in east coast areas and more rain than normal in the west (*www.niwa.co.nz*). La Niña events are associated with more north easterly winds which tend to bring moist, rainy conditions to the northeast of the North Island where Lake Rotorua is located while warmer than normal temperatures typically occur over much of the country. The ENSO has been recorded in *Agathis australis* tree-ring chronologies from New Zealand for more than 4500 years, and although amplitude and frequency have varied over the years, the twentieth century is considered as the most ENSO-active century of the past 500 years (Fowler et al., 2012). The positive phase of SAM is typically associated with relatively light winds, lower than normal rainfall and higher than normal temperatures occurring throughout western parts of the North and South Islands. However, these temperature and precipitation anomalies along the east coast of the country are weak and are not statistically significant (Renwick and Thompson, 2006). Similar to ENSO, SAM is also recorded by tree ring proxy archives for the last millennium from New Zealand and exhibits a positive trend since approximately 1940, driven by stratospheric ozone depletion (Abram et al., 2014).

The two most frequently used terrestrial climate archives in New Zealand are tree rings and speleothems. Speleothems are typically used in long-term climate reconstructions (Hellstrom et al., 1998; Lorrey et al., 2008), and in New Zealand, these are yet to be used as proxy archives for ENSO and SAM. This is probably due to the decadal to centennial resolution in

speleothems. Tree rings in New Zealand have been frequently studied because of the temperate climate and widespread *Nothofagus* forests and in contrast to speleothems, tree rings from New Zealand are commonly used as a proxy of ENSO (Gergis and Fowler, 2009; Fowler et al., 2012). These show that tree ring growth rates increase during El Niño and decrease during La Nina events (Fowler et al., 2008; Gergis and Fowler, 2009).

2.2 Study area

Rotorua is a shallow lake with a mean depth of 10 m (maximum depth 45 m), a surface area of 80 km^2 (Rutherford, 1984; Smith et al., 2016) and a catchment of nearly 500 km^2 (Donath et al., 2015). Since it has a high surface to volume ratio, the lake is easily and frequently mixed by the wind which results in multiple thermal stratification events during summer (Rutherford, 1984). Further, Lake Rotorua is a volcanic crater lake in the Taupo volcanic zone therefore, the lake has extensive natural geothermal activity (Phillips et al., 2014) and like many volcanic lakes in New Zealand, is dominated by groundwater flow rather than stream base flow (Hamilton et al., 2016) and a long mean residence time (> 50 years) for this groundwater (Morgenstern et al., 2015). The well-known Rotorua geothermal field consists of hot springs and geothermal stream inflows located along the southern shore of the lake (Fig. 1B) (Heise et al., 2016; Scott et al., 2016). Lake Rotorua was selected for the study because of the presence of an abundant and accessible population of freshwater bivalves with non-deformed shells along the western shore of the lake (Chapter 1).

Rotorua, along with Taupo and Hamilton belongs to the central north island temperate climate zone in New Zealand which is sheltered by elevated country to the south and east and has less wind than many other parts of New Zealand. Strong seasonality in water temperature was shown in data recorded at 0.5 m depth from the water surface (Chapter 1). Daily water temperature data from 2007 to 2016 has an average of 15 ^{o}C with a minimum of 8 ^{o}C during July and maximum of 24 ^{o}C during February (data available at *monitoring.boprc.govt.nz*). Measured air temperature in Rotorua airport also follows the same seasonal pattern with a slightly lower annual average of 13 ^{o}C (*cliflo.niwa.co.nz*). In contrast, precipitation in the area is non-seasonal and spread throughout the year with less than 1400 mm southeast of the lake to more than 2200 mm northwest of the lake (Donath et al., 2015).

2.3 Methods

2.3.1 Bivalve collection and shell sample preparation

Echyridella menziesii (Gray 1843) (family Hyriidae) is the dominant large freshwater bivalve species in New Zealand and is distributed throughout the country. These bivalves prefer sandy to silty substrate and are commonly found in the littoral zone of the lakes as well as in streams and rivers (James, 1985; James, 1987). Adult *Echyridella menziesii* reaches a maximum shell length of approximately 6 cm (height ~ 4cm), have ~ 20 g of wet flesh weight and can filter ~ 1 L of water per hour (Clearwater et al., 2014).

Echyridella menziesii were collected live from the western shore of Lake Rotorua at Ngongotaha (38.07 °S, 176.22 °E, Fig 1B) from less than 1 m water depth. Bivalve specimens of a range of sizes with non-deformed shells were selected and were then frozen at -20 °C to euthanise them. The flesh was separated from the shells, and the shells were then dried for 10 days at room temperature (approximately 21 °C). Sections of approximately 3 mm in thickness were cut with a low speed saw from the left valve of the bivalve shell along the maximum growth axis. These sections were mounted in 1 inch round mounts using EpoFix Resin and progressively polished in automated Struers system finishing with 3 and 1 µm diamond pastes. Digital photomicrographs of the shell sections were taken under a reflected light microscope before and after chemical analysis (Fig. S1). Another set of approximately 3 mm sections were cut from the same shells and processed following the methods described in Chapter 1 for the growth analysis.

2.3.2 Chronology construction and growth analysis

Observation of *Echyridella menziesii* from the same population at Lake Rotorua collected each month over a year identified that dark and light bands form in the shells during summer and winter respectively (Chapter 1). Shell annual increment lengths of 46 *Echyridella menziesii* shells were measured along the complete shell sections on the photomicrographs with the computer software `imageJ` (Rasband, 1997). In the absence of distinctive growth lines, the width of an individual annual increment was defined as the perpendicular distance between the start of two adjacent light bands (Fig. S1). Due to the relatively lower number of total annual increments (average = 10), only visual cross-matching was possible in the

present study and software tools such as SHELLCORR (Scourse et al., 2006) or COFECHA (Holmes, 1983) could not be used.
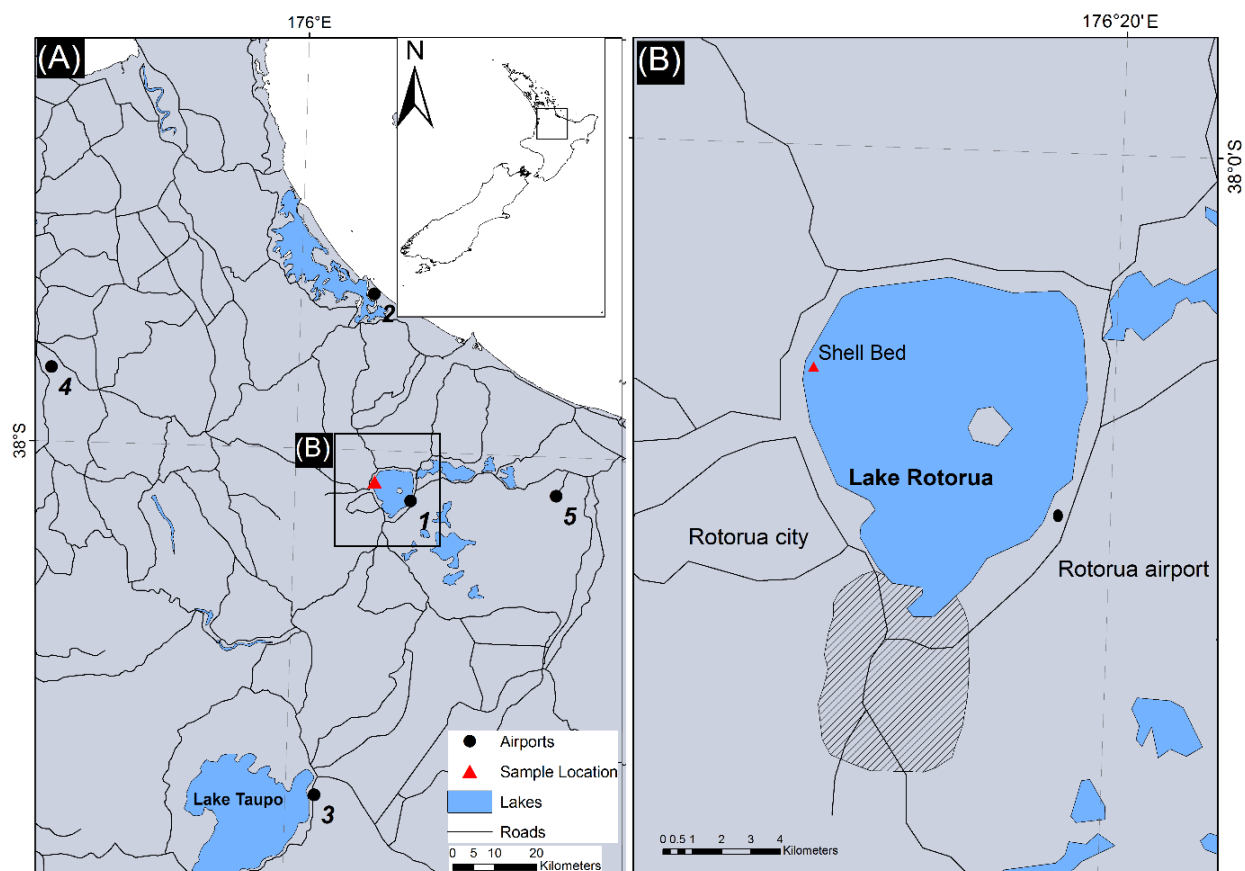
Fig. 1 (A) Map of northern New Zealand indicating the location of Lake Rotorua and the five regional airport sites where air temperature data was collected and used in this study. 1. Rotorua 2. Tauranga 3. Taupo 4. Hamilton and 5. Kawerau airports. (B) Inset from (A) indicating the sampling location where live mussels and water samples were collected. Rotorua city is located south of the lake and the airport is on the eastern shore. The black striped area marks the approximate location of the Rotorua geothermal field.

The software package ARSTAN for windows (version 44h3) (Cook and Holmes, 1996), was used to build the master chronology where ARSTAN power transforms and detrends individual increment-width series (using a negative exponential function) and applies a biweight robust mean function to the indices to build the chronology. The standardised master chronology produced by ARSTAN was selected for all further analysis. Additionally, ARSTAN was also used to calculate the Expressed Population Signal (EPS) which indicates whether the common variance in the chronology is a sufficiently good expression of the common variance in the population. Since the average age of *Echyridella menziesii* in this population was 10 years (Chapter 1), a window length of 5 years with no window overlap was selected for the EPS calculations.

2.3.3 Stable isotope analysis by SIMS

Two *Echyridella menziesii* shells collected on November 2016 from Lake Rotorua (RO-063, RO-066) were selected for the stable isotope analysis. These shells were selected because these have relatively broader growth increments compared to other collected shells. Shell samples exposed as polished sections were prepared for Secondary Ion Mass Spectrometry (SIMS) oxygen isotope analysis at the Canadian Centre for Isotopic Microanalysis (CCIM), University of Alberta. The shell sections were cast together in epoxy along with a calcite reference materials (RM) into a CCIM mount M1450. The mount was then lightly polished with diamond compounds to achieve a uniformly flat surface. After cleaning with soap and de-ionised water, the mount was coated with gold before Scanning Electron Microscopy (SEM) using the CCIM Zeiss EVO MA15 instrument, operating at 20 kV and $3 - 4$ nA beam current. Oxygen isotope ratios ($^{18}O/^{16}O$) were determined using the IMS-1280 multi-collector ion microprobe at CCIM. Primary beam conditions included the use of 20 keV 133Cs$^+$ ions focused to form a probe with diameter ~12 µm and beam current ~ 2.0 nA which was rastered during analysis to form a sampled area ~15 x 20 µm (Fig. S2). The primary beam was rastered 20 x 20 µm for 30 s before analysis to clean the surface of Au and contaminants and to implant Cs. The normal incidence electron gun was utilised for charge compensation. Negative secondary ions were extracted through 10 kV into the secondary column (Transfer section). Conditions for the Transfer section included an entrance slit width of 122 µm, field aperture of 5 x 5 mm, and a field aperture-to-sample magnification of 100 x. Automated tuning of the secondary ions in the Transfer section preceded each analysis. The energy slit was fully open. Both ^{16}O- and ^{18}O- were analysed simultaneously in Faraday cups (L'2 using 1010 Ω amplifier, and H'2 with 1011 Ω) at mass resolutions of 2000 and 2275, respectively. Mean count rates for ^{16}O- and ^{18}O- were typically 2.0×10^9 and 4×10^6 counts/s, respectively, determined over a 75 s counting interval. The analytical protocol interspersed analyses of unknowns with in-house end-member calcite reference materials (CCIM calcite S0161 with $\delta^{18}O_{VSMOW}$ = +25.40 ‰; R. Stern, unpublished data) in a 4:1 ratio. Instrumental Mass Fractionation (IMF) for ^{18}O-/^{16}O- was ~ -2.6 ‰, determined precisely for each analytical session by utilizing all the replicate analyses of the RMs. The standard deviation of multiple measurements of ^{18}O-/^{16}O- ratios in S0161 was ± 0.10 ‰, after small corrections for systematic within-session IMF drift (<0.4 ‰). Final uncertainties are reported at 95% confidence level (2σ) and propagate within-spot counting errors, between-spot errors to account for geometric effects, and between-session error that accounts

for uncertainty in the mean IMF for the session. The total uncertainties in $\delta^{18}O_{VSMOW}$ calcite average about ±0.26 ‰ (2σ) per spot.

The oxygen isotope content of three different shells of *Echyridella menziesii* (RO-19, RO-109 and RO-106) collected from the same population as RO-063, RO-066 in Lake Rotorua was measured using Isotope Ratio Mass Spectrometry (IRMS). The detailed methodology is provided in the supplementary materials.

Measured lake water temperature and water $\delta^{18}O$ ratios ($\delta^{18}O_{water}$) were used to calculate the predicted $\delta^{18}O$ values in the shell ($\delta^{18}O_{predict}$) with the following equation (Grossman and Ku, 1986; Dettman et al., 1999);

$$1000 \ln(\alpha) = 2.2559 \, (106 \, T - 2) + 0.715 \tag{1}$$

Where T is in Kelvin and α is the fractionation coefficient between water and aragonite which is given by the following equation;

$$\alpha_{\text{(aragonite - water)}} = \frac{1000 + \delta^{18}O_{aragonite}(VSMOW)}{1000 + \delta^{18}O_{water}(VSMOW)} \tag{2}$$

Where $\delta^{18}O_{aragonite}$ was calculated relative to Vienna Standard Mean Ocean Water (VSMOW) standard which was then converted into Vienna Pee Dee Belemnite (VPDB) scale by using; $O_{(VPDB)} = (O_{(VSMOW)} \times 0.97001) - 29.99$.

2.3.4 Clumped isotope analysis of *Echyridella menziesii* shells

Two *Echyridella menziesii* shells (RO-109 and RO-107) characterised for trace elements by LA-ICPMS and measured using IRMS were selected for clumped isotope analysis at the stable isotope laboratory at Goethe University Frankfurt. These two shells were selected due to the wider growth increments for the year 2016 which facilities obtaining a larger powder sample. Powdered samples (~ 30mg) were collected from the ventral margin taking care to sample within the last growth increment by using a hand drill. Clumped isotope analyses were made using a fully automated gas extraction and purification line connected to a ThermoFisher MAT 253 gas-source isotope-ratio mass spectrometer. Homogenised carbonate powder was reacted at 90 °C with > 105% phosphoric acid. Analyte CO_2 was measured against Oztech reference gas [$\delta^{18}O$ = +25.01 ‰ (VSMOW) and $\delta^{13}C$ = -3.63 ‰

(VPDB)] using a dual inlet system. Sample and reference gases were adjusted to mass 44 signals of 16,000 ± 150 mV. Measurements contain ten acquisitions consisting of ten cycles with an ion integration time of 20 s each, resulting in a total analysis time of about 3 h; the corresponding shot-noise limit is ~ 0.008 ‰. Before each acquisition, peak centring, background determination and pressure adjustments to 16 V at mass 44 were made. Empirical transfer functions (ETFs) were determined using gases of various bulk isotope compositions equilibrated at 25 °C and at 1000 °C, respectively. For further details on the method and the temperature calculations, see Wacker et al. (2014) and Bajnai et al., (2018).

2.3.5 Stable isotope analysis of lake water

Water samples for oxygen isotopic analysis at the Environmental Stable Isotope Laboratory, NIWA, New Zealand were collected monthly from June 2016 to June 2017 from the same location as bivalve shells. Carbon dioxide-water equilibration took place (with shaking) at 24°C for a minimum of 18 h, during which the small amount of CO_2 in the headspace of the vial was isotopically equilibrated with oxygen from the H_2O in the water sample. The very small amount of CO_2 in the headspace ensures complete transfer of the ^{18}O information during equilibration (Duhr and Hilkert, 2004). The stable isotope ratios of CO_2 were then measured on a GasBench II. Values of $\delta^{18}O$ from the CO_2 gas were calculated by Isodat software (Thermo Fisher Scientific). Reference materials VSMOW2, SLAP2 and GISP, were run in duplicate at the start of each sample batch. Data from VSMOW2 and SLAP2 were used to normalise all $\delta^{18}O$ values. Data from the analysis of GISP were used to check accuracy and precision. Samples were typically analysed in sets of 10, bracketed by two laboratory standards - Evans Bay SeaWater (EB SW) and ultrapure water (DIW). These two laboratory standards were used to check for precision. Two other water laboratory standards were used as a further check on precision (Antarctic Snow and Ruapehu Snow).

2.3.6 Trace element analysis by LA-ICPMS

Polished cross-sections of five *Echyridella menziesii* shells collected on November 2016 (RO-63, 66, 67, 25 and 21) were used for trace element analysis. Except for the two samples used for stable isotope analysis other shells were selected randomly to include old and young shells. Strontium, Mg, Mn, Ba and Ca intensities (measured as ^{88}Sr, ^{25}Mg, ^{55}Mn, ^{137}Ba and ^{43}Ca) were measured *in situ* by Laser Ablation Inductively Coupled Plasma Mass

Spectrometry (LA-ICP-MS) using an Agilent 7700 quadrupole ICP-MS coupled to a Photon Machines excimer laser (193 nm wavelength) laser ablation system. Measurements and reference materials followed the same procedure as Chapter 1.

The Sr/Ca series from the two shells (RO-63 and RO-66) for which oxygen isotope data were available were aligned with the oxygen isotope series of the same shell for absolute dating of these series (Fig. S2). Since all Sr/Ca series show high inter-correlation (Table S1), it was assumed that the three shells without oxygen isotope data also behave similarly to RO-63 and RO-66. Therefore, the calendar months were assigned to the peak values in these three shells, and the data in-between peaks were linearly interpolated between the seasonal peaks to assign the months (Yan et al., 2014a). Since no extended growth break was observed in summer it was assumed that *Echyridella menziesii* shells grow throughout the year. All other Me/Ca series were then assigned calendar months by aligning them to Sr/Ca series since all measurements were taken simultaneously. Combining time series from several shells of various ontogenetic age can eliminate the problems of individual growth hiatuses and increase the probability of capturing the full range of environmental conditions (Kelemen et al., 2017). Therefore, the monthly averaged master Me/Ca time series were created by taking the average of 5 *Echyridella menziesii* shells, covering data from July 2001 to July 2015.

2.3.7 Environmental data collection and statistical analysis

Daily lake water temperature at different depths from 2007 to 2015 were collected by a buoy at Lake Rotorua which is maintained by the University of Waikato and Bay of Plenty Regional Council (*monitoring.boprc.govt.nz*). All water temperature data used in this study are measured at 0.5 m depth from the surface unless the depth is mentioned. Since lake water temperature data are not available before 2007, all analysis considering Me/Ca master series were done by using air temperature data from Rotorua airport (Fig. 1). Annual, monthly and daily mean air temperature and total precipitation from 2000 to 2016 were obtained from The National Climate Database, New Zealand (*cliflo.niwa.co.nz*). Additional air temperature data from four locations around Lake Rotorua (Hamilton, Taupo, Kawerau, and Tauranga airports, Fig. 1) were also obtained from The National Climate Database. Sea Surface Temperature (SST) from Gisborne (approximately 160 km southeast of Lake Rotorua) was obtained from the KNMI Climate Explorer (*climexp.knmi.nl/start.cgi*). Data for the southern

annular mode index and Niño 3.4 SST index were obtained from NOAA ESRL Physical Sciences Division database (*www.esrl.noaa.gov*).

Ordinary least square regression and stepwise multiple regression among the master chronology and annual climatic variables as well as linear regression analysis among geochemical time series and all environmental variables collected from the area were calculated using the statistical software R (Team, 2017). The risk of multicollinearity among predictor variables was examined by calculating the correlations among pairs of these variables and found that correlations among predictor variables were weak. The standardised master chronology was also compared with the summer SAM index as well as the ENSO index of the calendar year (*www.esrl.noaa.gov*).

2.4 Results

2.4.1 Growth analysis of *Echyridella menziesii* shells

The master growth chronology of *Echyridella menziesii* created by using ARSTAN covers 21 years from 1995 to 2015 and shows variation in shell growth with distinctive years of below (1997, 2002, 2009 and 2015) and above (2000; Fig. 2) average growth. The shell growth of *Echyridella menziesii* is influenced by temperature as well as precipitation in the Rotorua region. This was indicated by the linear regression analysis which found a positive correlation between the master chronology and the annual average temperature as well as precipitation (r = 0.41, p < 0.05 and r = 0.38, p < 0.05). Further, the correlation between the master chronology and total wet days per year in Rotorua was significant and positive (r = 0.5, p < 0.05; Table 1 and Fig. S3). Multiple regression analysis confirmed that *Echyridella menziesii* shells prefer high temperature and precipitation during growth since the combination of these two variables explain 34 % of shell growth (r = 0.58, p <0.05). These correlation values are comparable to those found in other bivalve studies around the world, for example, *Panopea abrupta* (Black et al., 2009) and *Margaritifera margaritifera* (Schöne et al., 2004b). Notably, ENSO explains the *Echyridella menziesii* shells growth more than temperature and precipitation; 42 % (r = -0.65, p <0.05) which is also the case in tree-ring chronologies from New Zealand (Fowler et al., 2008). This reveals the dominant influence of regional climate events on the shell growth of *Echyridella menziesii.* However, in contrast to temperature and precipitation, ENSO has a negative correlation with *Echyridella menziesii*

shells growth (Table 1). Both SAM (r = 0.04, p < 0.5) and SST at Gisborne (r = 0.1, p < 0.05) indicate no correlation with shell growth of *Echyridella menziesii.*

Table 1. Regression coefficients between master chronology, $\delta^{18}O$ and Me/Ca ratios of *Echyridella menziesii* shells against selected climatic and environmental variables. At n = 21, r > 0.43 to be significant at 5% interval

	n	R^2	r
Master chronology vs annual temperature	21	0.16	0.41
Master chronology vs annual precipitation	18	0.14	0.38
Master chronology vs wet days	18	0.25	*0.50*
Master chronology vs annual temperature + precipitation	18	0.34	*0.58*
Master chronology vs Niño 3.4	21	0.42	*-0.65*
Master chronology vs sonuthern annular mode index	21	0.04	0.21
Master chronology vs Sea surface temperature in Gisborne	21	0.10	0.32
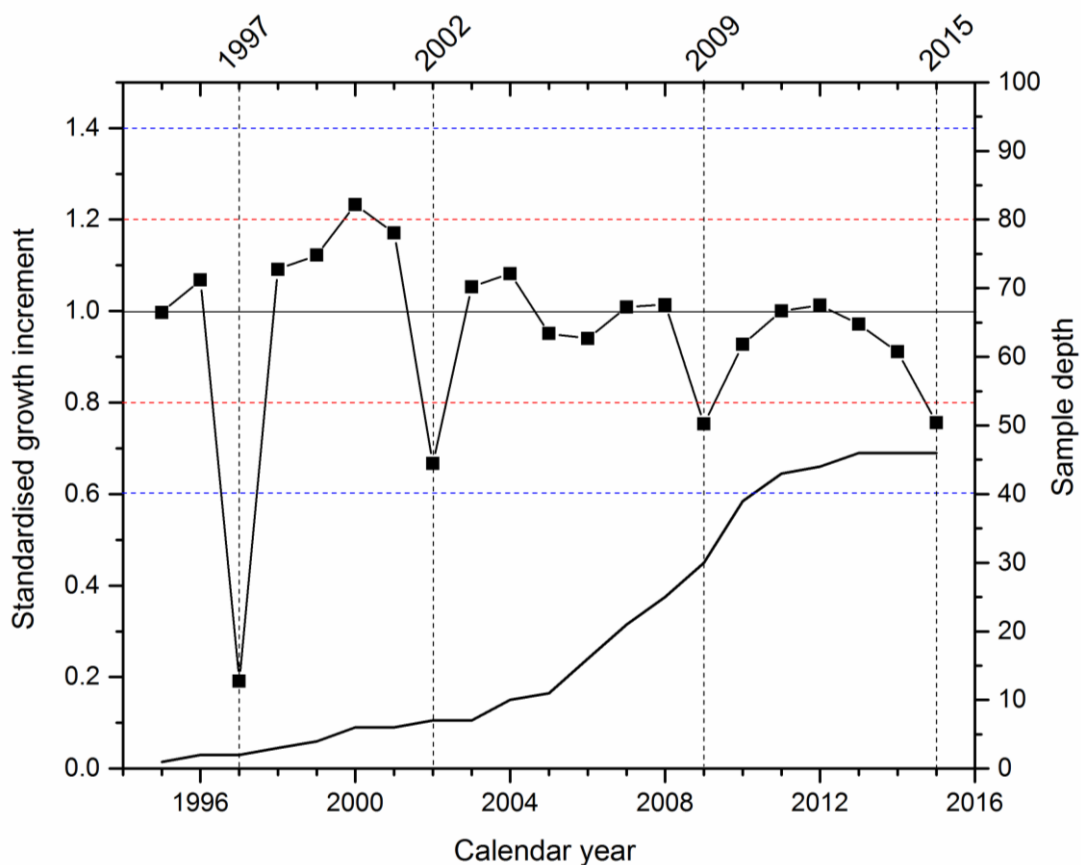
Fig. 2 Master growth chronology for the *Echyridella menziesii* shells collected from Lake Rotorua, New Zealand (*n* = 46) created using ARSTAN. Black dash lines indicate the drastic decrease in growth during strong and moderate El Nino years while red and blue dash lines indicate 1SD and 2SD values respectively (1SD = 0.2, 2SD = 0.4).

A critical threshold EPS value of 0.85 (Wigley et al., 1984) was introduced for dendrochronology which typically consists of longer chronologies (expanding into centuries) than a typical mollusc chronology (less than 100 years). Although the running EPS of the master chronology of *Echyridella menziesii* shells is lower than the threshold of 0.85 for tree rings at high sample depths, the EPS is higher than the threshold at lower sample depths (25 shells or less; Fig. S4). The low EPS values can be mainly attributed to the false identification and missing increments during cross-matching. The smaller average age of the population (10 years) meant that only visual cross-matching was possible in the present study and software tools such as SHELLCORR (Scourse et al., 2006) or COFECHA (Holmes, 1983) could not be used. Use of bivalve populations with longer lifespans could avoid these problems and would increase the EPS. Nevertheless, all shells in this population had distinctive synchronous growth reductions in 1997, 2002, 2009 and 2015.

2.4.2 Clumped isotope composition in *Echyridella menziesii* shells

Clumped isotope analysis resulted in Δ_{47} values of 0.690 ± 0.018 and 0.687 ± 0.005 for the two *Echyridella menziesii* shells RO-107 and RO-109 respectively (3 replicates each) (Table 2). These clumped isotope ratios observed for *Echyridella menziesii* are plotted with measured Δ_{47} values in literature from modern freshwater bivalves from Greenland (Csank et al., 2011b) as well as other molluscs such as marine bivalves (Henkes et al., 2013; Petrizzo et al., 2014; Wacker et al., 2014), gastropods (Csank et al., 2011a; Henkes et al., 2013) and oysters (Eagle et al., 2013) (Fig. 3).

Calculated temperature values of 18 ± 4 ℃ and 19 ± 2 ℃ (RO-107 and RO-109 respectively) were found by using the Wacker et al. (2014) calibration curve. The temperature calculations using the calibration curve introduced by Kelson et al. (2017) resulted in relatively higher temperatures (22 ± 4 ℃ and 23 ± 2 ℃ for RO-107 and RO-109 respectively). However, all these values are within the temperature range of Lake Rotorua for over a year (8 - 24 °C with an average of 15 °C).
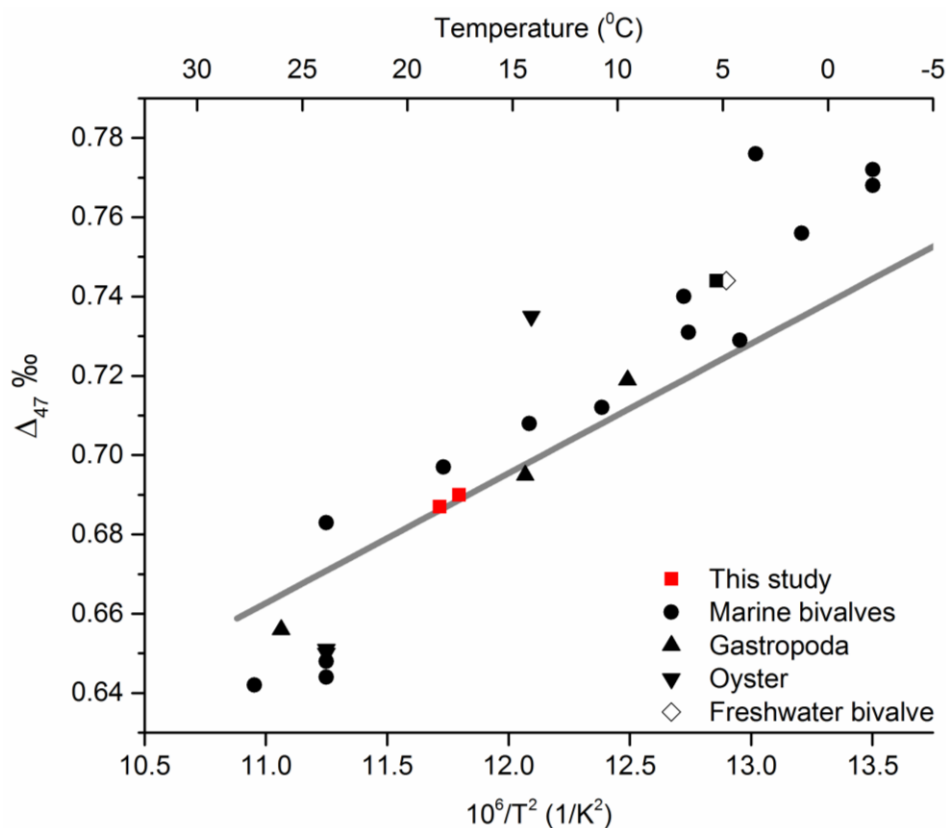
Fig. 3 Δ_{47} mean values of analysed *Echyridella menziesii* shells (red squares) and recorded Δ_{47} values of different selected molluscs in literature plotted against the growth temperatures. The linear regression line (in grey) expresses the calibration equation determined by Wacker et al. (2014) used in this study; $\Delta_{47} = 0.0327$ (± 0.0026) x $10^6/T^2 + 0.3030$ (± 0.0308) with Δ_{47} in ‰ and T in K.

2.4.3 Oxygen isotope composition in *Echyridella menziesii* shells

Echyridella menziesii shells have an average $\delta^{18}O$ values of -3.6 $\pm$ 0.1 ‰ as indicated by four bulk samples measured using IRMS; two replicates of RO-19 resulted in values of -3.61 and -3.68 $\pm$ 0.10 ‰ while RO-109 and RO-107 resulted in -3.65 and -3.75 $\pm$ 0.20 ‰ respectively (Table 2). These values are consistent with the predicted $\delta^{18}O$ ($\delta^{18}O_{predict}$) from July 2008 to July 2015 which varied between -5.22 ‰ and -1.87 ‰ with an average of -3.50 ‰ (Fig. 4A). The $\delta^{18}O_{shell}$ measured using SIMS in both measured shells (RO-63 and RO-66) varied from -7.06 ‰ to -3.72 ‰ with an average of -6.16 ‰ (Table 2, Fig. 4A).
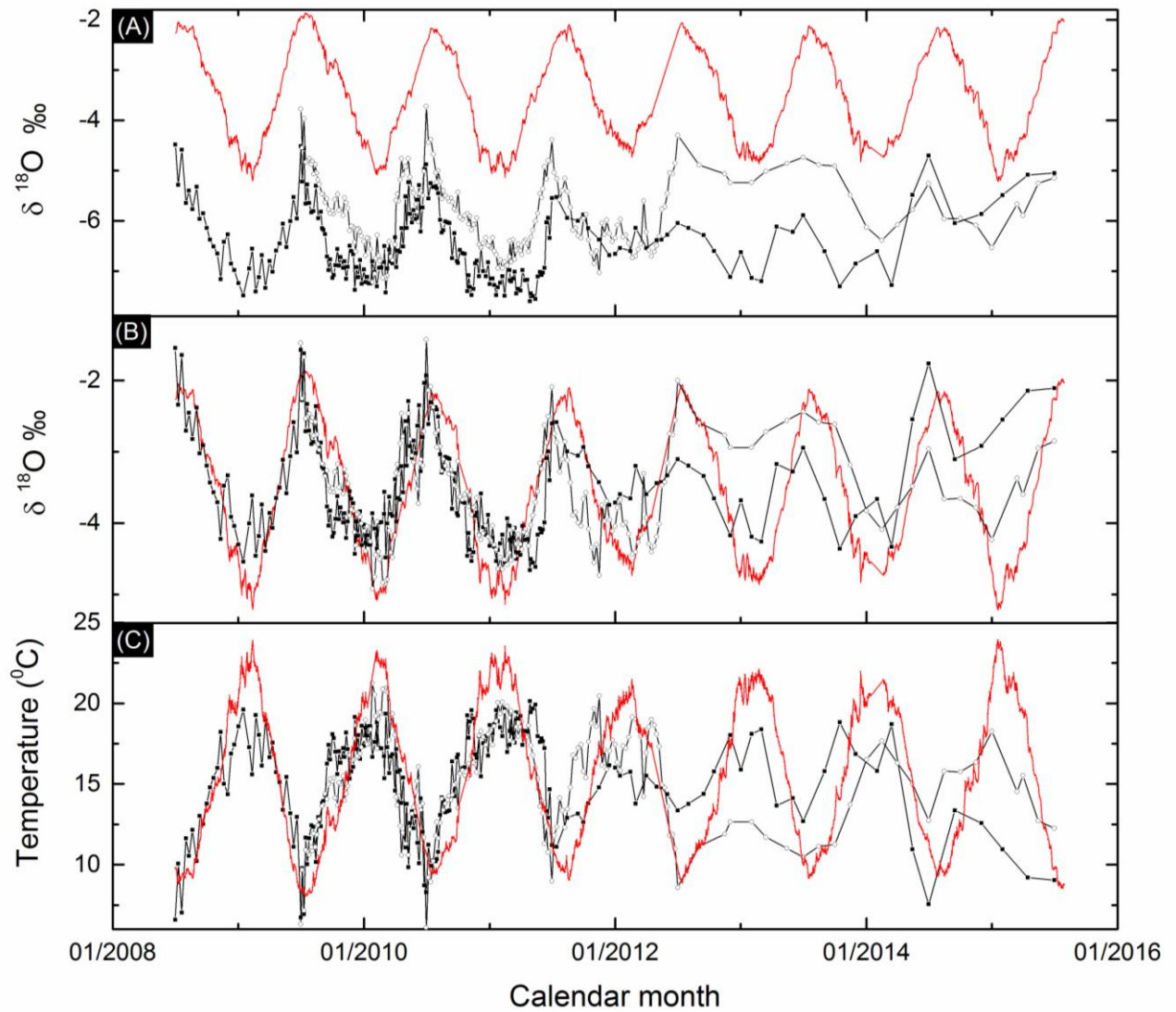
Fig. 4 (A) Variation in δ ^{18}O in two measured (using SIMS) *Echyridella menziesii* shells (RO63 - filled squares and RO-66 – circles) along the direction of growth and the δ ^{18}O$_{predicted}$ (in red). (B) The δ ^{18}O$_{adjested}$ for two shells (in black) agrees well with the δ ^{18}O$_{predicted}$ (in red). (C) Calculated temperature using two shells (in black) also agrees well with the measured lake water temperature (in red).

Both shells measured by SIMS indicated seasonal variation in δ^{18}O levels along the direction of growth (Fig. 4) and resulted in higher values during winter and lower values during summer when dates were assigned to these data series. The high sampling resolution achieved by SIMS analysis (20 µm) contributed to the collection of enough samples from the annual growth increments of *Echyridella menziesii* (600 µm in average, Chapter 1) to observe a clear seasonal pattern. However, smaller growth increments at ontogenetically older parts (100 µm Chapter 1), cause inaccurate seasonality due to insufficient sampling resolution that is evident by the non-seasonal behaviour of δ^{18}O$_{shell}$ series after approximately 2013. The δ^{18}O$_{shell}$ variation in *Echyridella menziesii* shells was significantly influenced by lake water temperature while the influence of local precipitation was negligible since a strong

negative correlation was recorded between $\delta^{18}O_{shell}$ and air and lake water temperature (r > -0.6, p < 0.05; Table 3). In contrast, when compared to total daily precipitation in the area, it indicated that the $\delta^{18}O_{shell}$ do not correlate with total ambient precipitation (r < 0.05, p < 0.05; Table 3).

Table 2. Measured $\delta^{18}O$ (±0.1), Δ_{47} (±0.01) and average element concentrations of *Echyridella menziesii* shells from Lake Rotorua.

Sample no.	$\delta^{18}O_{IRMS}$‰	$\delta^{18}O_{SIMS}$‰	Δ_{47}	Sr (µg/g)	Mg (µg/g)	Ba (µg/g)	Mn (µg/g)
RO-19.1	-3.61	-	-	-	-	-	-
RO-19.2	-3.68	-	-	-	-	-	-
RO-109	-3.65	-	0.687	1368	24	180	323
RO-107	-3.75	-	0.690	1091	46	254	404
RO-63	-	-6.46	-	1070	33	157	360
RO-66	-	-5.85	-	1147	18	163	476
RO-67	-	-	-	1274	38	225	1147
RO-25	-	-	-	1050	40	150	711
RO-21	-	-	-	1058	40	150	700

The $\delta^{18}O_{shell}$ measured using SIMS shows a systematic offset from the $\delta^{18}O_{predict}$, which is 2.9 ‰ in RO-63 and 2.3 ‰ in RO-66, similar to other bio-carbonate studies using SIMS; for example 5.45 ‰ in Arctic bivalves (Vihtakari et al., 2016) and 2.0 and 2.9 ‰ in bamboo coral (Saenger et al., 2017). Since it was identified that an analytical issue is responsible for this offset in *Echyridella menziesii* shells (see below), the offset was corrected by adding the instrumental shift to the $\delta^{18}O_{shell}$ series. This adjusted oxygen isotope values ($\delta^{18}O_{adjusted}$) agreed well with the predicted oxygen isotope values from 2008 to 2013 (Fig. 4B). Lake water temperature was then calculated by using $\delta^{18}O_{adjusted\ and}$ was then found to be in good agreement with measured lake water temperature (± 2.5 ˚C) between 2008 and 2013 (Fig. 4C).

The measured $\delta^{18}O$ values for lake water ($\delta^{18}O_{water}$) at the collection site varied from -6.4 ‰ to -3.4 ‰ from June 2016 to June 2017 (Fig. S5). Typically, $\delta^{18}O$ values in freshwater systems display seasonal cycles mainly due to the seasonal variation in amount and composition of different source waters (Versteegh et al., 2010). For example, $\delta^{18}O_{water}$ in rainwater, groundwater and surface runoff can alter extensively due to factors such as evaporation, latitude, elevation and different pathways of the rain-bringing air masses (Poage and Chamberlain, 2001; Mayr et al., 2007). However, the $\delta^{18}O_{water}$ of Lake Rotorua did not show seasonal variation but remained stable around the average value of -4.5 ‰ throughout the year except for an uncharacteristic decrease in September (Fig. S5). The average value

is consistent with past measurements of $\delta^{18}O_{water}$ from the lake where values of -3.0 and -4 to -4.5 ‰ were recorded (Stewart and Taylor, 1981; Northcote et al., 1992).

Table 3. Regression coefficients between $\delta^{18}O$ and Me/Ca ratios of *Echyridella menziesii* shells against selected climatic and environmental variables from Lake Rotorua and the surrounding region.

	n	R^2	r	slope
Water temperature vs $\delta^{18}O$ RO-063	216	0.57	-0.75	
Air temperature vs $\delta^{18}O$ RO-063	216	0.50	-0.71	
Total precipitation vs $\delta^{18}O$ RO-063	216	0.00	0.04	
Water temperature vs $\delta^{18}O$ RO-066	209	0.47	-0.68	
Air temperature vs $\delta^{18}O$ RO-066	209	0.42	-0.65	
Total precipitation vs $\delta^{18}O$ RO-066	209	0.00	0.05	
Air temperature vs Sr/Ca	168	0.40	0.63	0.08±0.01
Air temperature vs Mg/Ca	168	0.06	0.26	0.004±0.01
Air temperature in Hamilton vs Sr/Ca	168	0.40	0.62	0.08±0.01
Air temperature in Taupo vs Sr/Ca	168	0.40	0.62	0.07±0.01
Air temperature in Whakatane vs Sr/Ca	168	0.40	0.62	0.08±0.01
Air temperature in Tauranga vs Sr/Ca	168	0.40	0.62	0.08±0.01
Sea surface temperature in Gisborne vs Sr/Ca	159	0.38	0.61	0.07±0.01
Total precipitation vs Ba/Ca	168	0.00	-0.03	-0.00±0.01
Water temperature vs weekly resolution $\delta^{18}O$	170	0.59	-0.77	-0.12±0.01
Air temperature vs weekly resolution Sr/Ca	92	0.64	0.80	0.08±0.01

2.4.4 Trace element variations in *Echyridella menziesii* shells

Average trace element concentrations of five *Echyridella menziesii* shells demonstrate that Sr has the highest concentration (~1100 µg/g) while Mg has the lowest (~ 40 µg/g; Table 2). These values are consistent with other freshwater bivalve studies from around the world (Carroll and Romanek, 2008; Soldati et al., 2009; Izumida et al., 2011; Bolotov et al., 2015; Zhao et al., 2017; Geeza et al., 2018). In the present study, all measured trace element series show stable Me/Ca throughout the bivalve's lifetime, whereas only Mn shows an abrupt concentration increase at ontogenetically older parts (Fig. S6). The monthly averaged Me/Ca master time series exhibits seasonal variations, and apart from Mn, all other elements are generally in phase (Fig. 5). In contrast to the $\delta^{18}O_{shell,}$ Me/Ca time series indicate higher values at austral summer and lower values at austral winter (Fig. S2).

The Sr/Ca in *Echyridella menziesii* shells was most strongly influenced by the air temperature in the region as indicated by the significant positive correlation (r = 0.63, p <

0.05) with air temperature from Rotorua airport, while in comparison Mg/Ca time series had a weaker correlation (r = 0.26, p < 0.05; Table 3). The regression analysis between Sr/Ca series and air temperature is parameterised by the following equation.

$$Sr/Ca \text{ (mmol/mol)} = 0.08 \times T \text{ (°C)} + 3.11 \qquad\qquad (3)$$

Both Ba/Ca and Mn/Ca time series had no significant correlation with either temperature or precipitation data from Rotorua airport (Table 3). However, the Ba/Ca increased in phase with Sr/Ca and the maximums coincide with the dark bands of the shell section which emphasise seasonal variation.
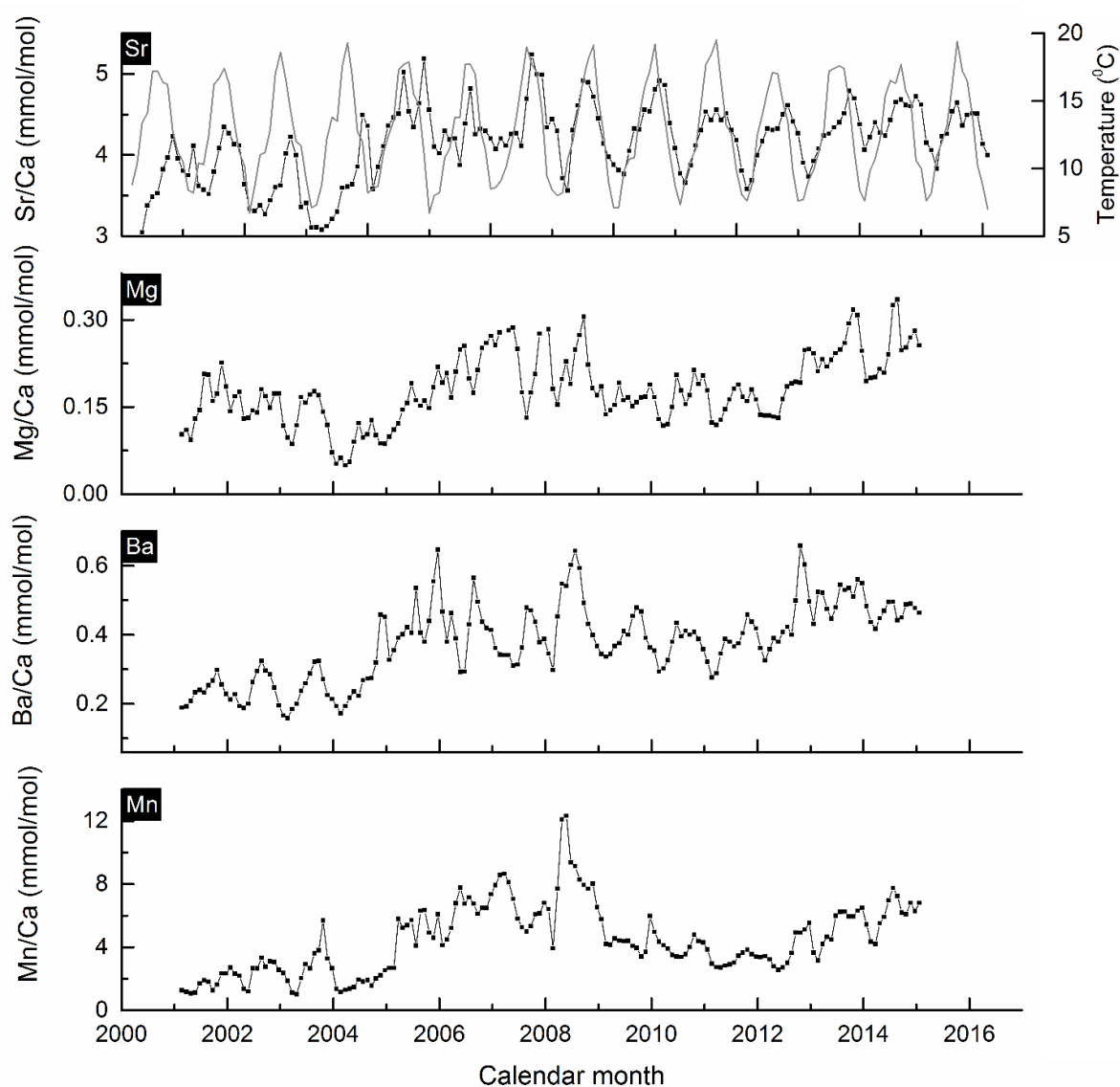
Fig. 5 Seasonal variation in trace element/calcium in the master series created by averaging five *Echyridella menziesii* shells showing the increase in Sr/Ca, Ba/Ca and Mg/Ca during summer. Grey continues line indicate instrumental air temperature measured at Rotorua airport.

2.5 Discussion

2.5.1 Temperature reconstructions using oxygen isotopes and Sr/Ca in *Echyridella menziesii* shells

Since oxygen isotope fractionation in bio-carbonates depends on both water temperature and $\delta^{18}O_{water}$ (Urey, 1947), conventional oxygen isotope thermometry has a built-in limitation because of its association with $\delta^{18}O_{water}$. For example, the use of oxygen isotope thermometry in fossil samples where the $\delta^{18}O_{water}$ during shell precipitation is unknown is generally challenging because $\delta^{18}O_{water}$ can vary over geologic timescales (Affek, 2012). Furthermore, use of oxygen isotope thermometry in freshwater systems is also difficult due to seasonal variations in $\delta^{18}O_{water}$ as a result of precipitation and the influence of evaporation (Mayr et al., 2007). Carbonate clumped-isotope thermometry does not depend on the $\delta^{18}O_{water}$ but only varies with water temperature (Eiler, 2007; Affek, 2012), since it is based on the temperature dependence of the abundance of ^{13}C-^{18}O bonds in the carbonate lattice (Ghosh et al., 2006). Therefore, carbonate clumped-isotope thermometry has been successfully used in temperature reconstructions in various calcareous organisms such as bivalves, shallow water corals, land snail shells, foraminifera and coccoliths (Tripati et al., 2010; Eiler, 2011; Thiagarajan et al., 2011; Zaarur et al., 2011; Henkes et al., 2013; Saenger et al., 2017).

Studies on carbonate clumped isotope thermometry of bivalve shells are limited (Eagle et al., 2013; Henkes et al., 2013; Petrizzo et al., 2014; Wacker et al., 2014) while studies on freshwater bivalve shells are rare (Csank et al., 2011b; Tobin et al., 2014). To our knowledge, this is the first study that explores the potential of carbonate clumped isotope thermometry using bivalve shells in Oceania. Due to the large sample sizes necessary for clumped isotope analysis (> 0.5 mg), the best possible temporal resolution that could be achieved for *Echyridella menziesii* shells in this study was an annual resolution. Analysis indicates that the clumped isotopes in *Echyridella menziesii* shells demonstrated in shell formation temperatures of 18 ± 4 °C and 19 ± 2 °C which are within the annual temperature range (15 ± 5 °C) of Lake Rotorua. This provides the first results suggesting that carbonate clumped isotopes of *Echyridella menziesii* shells have the potential to be a proxy for water temperature, albeit at lower temporal resolution than conventional $\delta^{18}O$, and the ability to complement information obtained from better-known techniques such as conventional oxygen isotope thermometry.

Analysis of $\delta^{18}O$ of mollusc shell carbonates has a significant place in paleoclimate reconstructions as this can be used to estimate the temperature of the ambient water at the time of shell formation (Urey, 1947; Epstein et al., 1953; Grossman and Ku, 1986; Wanamaker et al., 2011; Schöne and Surge, 2012; Schöne and Gillikin, 2013; Peharda et al., 2017; Prendergast et al., 2017). Since the $\delta^{18}O$ in *Echyridella menziesii* shells precipitate in equilibrium with ambient $\delta^{18}O_{water}$, these also have the possibility to act as a thermometer. Oxygen isotope thermometry of bivalves usually have an accuracy of $1 - 3$ °C, for example, *Arctica islandica* from the northwest coast of Scotland; ± 1.2 °C (Foster et al., 2009), Oyster shells from western China; $\pm 1.6 - 3.2$ °C (Bougeois et al., 2014). The stable isotope ratio in *Echyridella menziesii* shells also has potential as a proxy for the lake water temperature since the reconstructed water temperature has an accuracy of ± 2.5 °C. Reconstructed temperature using *Echyridella menziesii* shells are more accurate at or around 15 °C (annual average temperature in the lake) where the accuracy is within ± 1 °C (Fig. S7) and deviates more from the measured values at higher or lower temperature levels. Water temperatures around 15 °C are common during summer in Lake Rotorua and likely present the optimum growth conditions for *Echyridella menziesii* in this lake, this may be the reason for the higher accuracy of shell-derived temperatures in this temperature range.

One of the biggest challenges in oxygen isotope analysis of bio-carbonates is the insufficient temporal resolution at the slow-growing portions of the shell (Goodwin et al., 2003). Due to the requirement of powder samples, the IRMS analysis usually has a sampling resolution of approximately 100 µm and/or 50 - 30 µg. In species such as *Echyridella menziesii* where the annual growth increments at the adult stages of life are less than 100 µm per year, powder sampling techniques will sample shell material precipitated in a larger than expected period which limits the reliability of the proxy. In contrast, SIMS analysed *in-situ* samples at 20 µm intervals during this study which enables the collection and analysis of $\delta^{18}O$ values at weekly resolution. More importantly, this high resolution in $\delta^{18}O$ data also assists the absolute dating of Me/Ca series at weekly resolution.

Some bio-carbonates show significant correlations ($r > 0.9$) between Sr/Ca and the water temperature (DeLong et al., 2011; Yan et al., 2014a) while others do not show strong correlations (Sosdian et al., 2006; Bolton et al., 2014; Xu et al., 2015). However, due to the relatively high correlation between the Sr/Ca and the measured air temperature in Rotorua airport ($r = 0.63$, $p < 0.05$), Sr/Ca in *Echyridella menziesii* shells can be considered a useful

temperature proxy. Since Lake Rotorua is known to have extensive geothermal activity and thermal stratification (Rutherford et al., 1989), the Sr/Ca master series was compared with lake water temperature at different depths during 2012 to 2016, which also resulted in the same relationship.

More importantly, Sr/Ca in *Echyridella menziesii* shells can be a temperature proxy in a wider region as evident by the consistent relationships between the Sr/Ca and the air temperature in a 100 km radius from Lake Rotorua (Table 1, Fig. S8). These results suggest that *Echyridella menziesii* collected from Rotorua can be used as a temperature proxy at least in the northern New Zealand region of approximately $15, 000 \text{ km}^2$ around Lake Rotorua. Further, a similar relationship was also observed between Sr/Ca master series and SST from Gisborne (Table 3, Fig. S9). In contrast, the Sr/Ca master series does not show any correlation with regional climatic indices such as SAM and NINO 3.4 (Table 3, Fig. S9). Due to the relatively low correlation between Mg/Ca and air temperature ($r = 0.2$ relative to $r = 0.6$ of Sr/Ca; Table 3), the Mg/Ca of *Echyridella menziesii* shells is not a useful proxy of water temperature in this population.

Weekly resolved oxygen isotope data from ontogenetically younger areas of the shell (formed earlier in life) enabled the assignment of calendar dates of the Me/Ca series also at a weekly resolution. The Sr/Ca proxy showed a significant improvement in the correlation with the water temperature at weekly resolution ($r = 0.80$, $p < 0.05$) from July 2009 to July 2011, compared to the complete master series ($r = 0.63$, $p < 0.05$) and we were able to identify detailed changes in the weekly water temperature variations in the Lake Rotorua (Fig. S10). This suggests that *Echyridella menziesii* can provide an archival record of environmental variability at a weekly resolution using both oxygen isotope ratio and Sr/Ca proxies.

2.5.2 No vital effects for oxygen isotopic ratios in *Echyridella menziesii* shells

As suggested by numerous studies in the past, molluscan carbonate precipitates in oxygen isotope equilibrium with ambient water (Dettman et al., 1999). Although some studies report species-specific disequilibrium (Steuber, 1999; de Winter et al., 2017), and offsets of -0.37 ‰ (*Astarte borealis;* Muller-Lupp et al., 2003) or 2 ‰ (*Eurhomalea exalbida;* Yan et al., 2012) relative to predicted data, these can be attributed to the differences in monitoring stations and shell collection sites (Kelemen et al., 2017). Similarly, carbonate clumped

isotopes do not exhibit species-specific behaviour as evident by the consistency among most of the published calibrations within the temperature range of approximately 0 to 40 °C (Eiler, 2011). Further, if there is a disequilibrium effect seen in Δ_{47}, it should be accompanied by even larger deviations from equilibrium in the bulk isotopic composition (Henkes et al., 2013). The *Echyridella menziesii* shells precipitate in an oxygen isotope equilibrium with ambient water as suggested by the accurate water temperature reconstructions that were found in during this study using clumped isotopes. This was also supported by the similarities between the average $\delta^{18}O_{predicted}$ value which is -3.5 ± 0.1 ‰ and the values from the four IRMS analysis (-3.6 ± 0.1 ‰).

Since *Echyridella menziesii* shells precipitate in equilibrium with ambient water, the cause for the observed offset between $\delta^{18}O_{shell}$ and $\delta^{18}O_{predicted}$ could be due to a physiological and/or an analytical effect. The IRMS use a chemical reaction to release oxygen isotopes while SIMS uses sputtering techniques which preferentially removes the lighter isotope (Vihtakari et al., 2016). This would result in lower $\delta^{18}O$ levels than what is expected from the IRMS fractionation equations. In this case, it would result in a constant offset similar to that observed in *Echyridella menziesii,* and this can be put forward as the main reason behind the observed offset between $\delta^{18}O_{shell}$ and $\delta^{18}O_{predicted}$. This analytical issue can be resolved by measuring the oxygen isotope ratios of different bio-carbonate samples where the $\delta^{18}O$ levels are known, using both SIMS and IRMS, and determining the offsets for specific analytical conditions. Measurements of known carbonate materials are currently being undertaken at the Canadian Centre for Isotopic Microanalysis, University of Alberta and the instrument offset is not yet determined. However, once the instrument offset is calculated, it will be added to the $\delta^{18}O_{shell}$ to obtain the correct $\delta^{18}O$ levels for *Echyridella menziesii* shells.

2.5.3 Variation in Ba/Ca in *Echyridella menziesii* shells

Ba/Ca time series of bio-carbonates has a typical sinusoidal variation which, in marine bio-carbonates, is characteristically disturbed by irregularly distributed peaks several magnitudes higher than background levels (Gillikin et al., 2006a; Thébault et al., 2009). These background peaks are often interpreted as reflecting the ingestion of Ba-rich phytoplankton by bivalves during periods of high food availability (Thébault et al., 2009). Consequently, as found in *Echyridella menziesii,* the Ba/Ca in freshwater bivalve shells tend to increase during summer when the primary production in the lake is at maximum. This allows the use

of Ba/Ca in freshwater bivalve shells to be used as a proxy for primary productivity in lake environments.

The background sinusoidal peaks observed in bio-carbonates are also attributed to the increase in Ba concentration in water due to weathering of barite-bearing siliceous rocks in the surrounding area (Montaggioni et al., 2006). Therefore, the Ba/Ca in freshwater bivalve shells typically shows a high correlation with local precipitation that was not observed in *Echyridella menziesii.* The lower correlations that we found between regional precipitation and the Ba/Ca in *Echyridella menziesii,* could be attributed to the non-seasonal distribution of precipitation in Rotorua. In contrast to *Echyridella menziesii,* a high correlation between Ba/Ca and the temperature is also observed in some freshwater species, but the reason for this is debatable (Geeza et al., 2018). These results suggest that although the Ba/Ca in *Echyridella menziesii* shells can be developed to use as a primary productivity proxy, it cannot be used as a proxy of precipitation due to a poor correlation between the two factors. Furthermore, the relatively low correlations observed between the Mn/Ca and environmental variables suggest that it cannot be used as a proxy for environmental variability at least for the *Echyridella menziesii* population considered during this study.

2.5.4 Regional climatic signals recorded in *Echyridella menziesii* shells

As shown by the positive correlation between the precipitation and the shell growth chronology (Table 1; Fig. S4), *Echyridella menziesii* prefers high precipitation while low precipitation hinders shell growth. During El Niño years, drier conditions occur for much of the North Island where a significant decrease in rainfall is observed with annual precipitation levels dropping by almost 400 mm per year (Ummenhofer and England, 2007). This reduced precipitation during El Niño events is expected to decrease the *Echyridella menziesii* shell growth. The strongest recorded El Niño events in New Zealand occurred during 2015-2016 and 1997-1998 (*www.niwa.co.nz*). Notably, these are the years the *Echyridella menziesii* shells show the lowest growth in the master chronology (Fig. 2). Further, 2009-2010 and 2002-2003 are also considered moderately strong El Niño years which are also marked by lower than average growth rates. In contrast, strong La Nina years such as 2010-2011, 2007-2008 and 1999-2000 indicate no distinct variation in *Echyridella menziesii* shell growth. This suggests that a drastic reduction in *Echyridella menziesii* shell growth can be considered as a strong indicator for El Niño events which governs the climate in the southern hemisphere.

The negative phase of the SAM in New Zealand brings more wind and more precipitation from high latitudes, and below average temperatures, while the positive phase is characterised by low precipitation and above average temperatures (Gordon, 1986; Mullan, 1995). Almost all negative SAM years such as 1996, 2000, 2007 and 2011 (*www.cpc.ncep.noaa.gov*) record higher than average growth in *Echyridella menziesii* shells as expected. However, some negative SAM years which are also considered moderate El Niño years, such as 2002 and 2009 show lower growth rates (Fig. 2). This indicates that although precipitation variations induced by SAM influence higher shell growth in *Echyridella menziesii,* those influences are overshadowed during El Niño events. This was also confirmed by the lower correlation between SAM index and growth chronology (Table 1).

In contrast to *Echyridella menziesii,* tree growth increase during El Niño events and decreases in La Nina events as recorded in *Agathis australis* tree-ring chronologies from New Zealand (Fowler et al., 2008; Gergis and Fowler, 2009). This identified that trees have opposite responses to ENSO events to *Echyridella menziesii* where growth rates are lower during ENSO events. Hence, the combined use of tree ring and *Echyridella menziesii* shell archives in the future could lead to a more detailed reconstruction of ENSO. Furthermore, in contrast to continual growth throughout the year of *Echyridella menziesii* shells, *Agathis australis* growth is mainly restricted to spring and early summer (Fowler et al., 2012). Therefore, these shells can be used to reconstruct weekly resolved temperature variations throughout ENSO events, while tree ring reconstructions usually are restricted to their growing season that excludes the winter months.

These climatic phenomena usually have long frequencies varying from 5-7 years in ENSO to decadal and inter-decadal frequencies in Pacific decadal oscillation (Mantua and Hare, 2002; Wang et al., 2017). Since the master growth chronology of *Echyridella menziesii* is only 21 years in length, it is not enough to identify the frequencies of these global climatic events based on this sample suite. However, since this study reliably identified the occurrence of some isolated ENSO events, it suggests the potential to use these shells in the future. Since *Echyridella menziesii* is recorded to live more than 50 years (Grimmond, 1968), these long-lived populations could deliver a wealth of information on regional climate variations in the southern Pacific region.

2.6 Conclusions

This study was conducted as an exploration into the possibility of using the freshwater bivalve *Echyridella menziesii* from Lake Rotorua, New Zealand as a temperature proxy archive using a multi-proxy approach. Carbonate clumped isotope, high-resolution oxygen isotope and trace element analysis were used here to obtain monthly and weekly temperature reconstructions using freshwater bivalves from Oceania.

Results demonstrate that *Echyridella menziesii* shells can archive environmental variability using numerous physical and geochemical proxies. The stable oxygen isotopes, clumped isotopes and Sr/Ca in these shells act as temperature proxies while Ba/Ca is a primary productivity proxy. Further, a marked decrease in growth rate is a strong indicator of the El-Nino events in the South Pacific Ocean. Although the results of this study are promising, it is noted here that the chemical analysis is from a small sample size (n < 5) and recommend more analyses before these proxies are used for regional temperature reconstructions.

The study also identified *Echyridella menziesii* as the first freshwater bivalve species from the southern hemisphere to be recognised as a temperature proxy using carbonate clumped isotopes. Further, this is the first climate proxy study using carbonate clumped thermometry from Oceania. Because of the oceanic dominance in the southern hemisphere, there is a wealth of climate archival data available from oceanic archives, such as corals, oceanic sediments and marine molluscs. Nevertheless, hemispheric-scale climate reconstructions lack the input from continental archives except for tree-ring data making continental climate data biased towards dendrochronology. However, as described in this chapter, shells of *Echyridella menziesii,* the dominant large freshwater bivalve species in New Zealand found from 35 ºS to 45 ºS and also available in shell middens, can complement the identification of local environmental variables as well as regional climate systems from the southern hemisphere.

2.7 References

Abram, N.J., Mulvaney, R., Vimeux, F., Phipps, S.J., Turner, J. and England, M.H., 2014. Evolution of the Southern Annular Mode during the past millennium. Nature Climate Change, 4(7): 564-569.

Affek, H.P., 2012. Clumped isotope paleothermometry: principles, applications, and challenges. Reconstructing Earth's Deep-Time Climate—The State of the Art in: 101-114.

Bajnai, D., Fiebig, J., Tomašových, A., Garcia, S.M., Rollion-Bard, C., Raddatz, J., Löffler, N., Primo-Ramos, C. and Brand, U., 2018. Assessing kinetic fractionation in brachiopod calcite using clumped isotopes. Scientific reports, 8(1): 533.

Black, B.A., Copenheaver, C.A., Frank, D.C., Stuckey, M.J. and Kormanyos, R.E., 2009. Multi-proxy reconstructions of northeastern Pacific sea surface temperature data from trees and Pacific geoduck. Palaeogeography, Palaeoclimatology, Palaeoecology, 278(1): 40-47.

Black, B.A., Dunham, J.B., Blundon, B.W., Raggon, M.F. and Zima, D., 2010. Spatial variability in growth-increment chronologies of long-lived freshwater mussels: implications for climate impacts and reconstructions. Ecoscience, 17(3): 240-250.

Bolotov, I., Pokrovsky, O., Auda, Y., Bespalaya, J., Vikhrev, I., Gofarov, M., Lyubas, A., Viers, J. and Zouiten, C., 2015. Trace element composition of freshwater pearl mussels *Margaritifera spp.* across Eurasia: Testing the effect of species and geographic location. Chemical Geology, 402: 125-139.

Bolton, A., Goodkin, N., Hughen, K., Ostermann, D., Vo, S. and Phan, H., 2014. Paired Porites coral Sr/Ca and δ 18 O from the western South China Sea: Proxy calibration of sea surface temperature and precipitation. Palaeogeography, Palaeoclimatology, Palaeoecology, 410: 233-243.

Bougeois, L., De Rafélis, M., Reichart, G.-J., De Nooijer, L.J., Nicollin, F. and Dupont-Nivet, G., 2014. A high resolution study of trace elements and stable isotopes in oyster shells to estimate Central Asian Middle Eocene seasonality. Chemical Geology, 363: 200-212.

Carroll, M. and Romanek, C.S., 2008. Shell layer variation in trace element concentration for the freshwater bivalve *Elliptio complanata*. Geo-Marine Letters, 28(5-6): 369-381.

Clearwater, S.J., Thompson, K.J. and Hickey, C.W., 2014. Acute toxicity of copper, zinc, and ammonia to larvae (Glochidia) of a native freshwater mussel *Echyridella menziesii* in New Zealand. Archives of environmental contamination and toxicology, 66(2): 213-226.

Cook, E. and Holmes, R., 1996. Guide for computer program ARSTAN. The international tree-ring data bank program library version, 2(0): 75-87.

Cook, E.R., Buckley, B.M., Palmer, J.G., Fenwick, P., Peterson, M.J., Boswijk, G. and Fowler, A., 2006. Millennia-long tree-ring records from Tasmania and New Zealand: A basis for modelling climate variability and forcing, past, present and future. Journal of Quaternary Science, 21(7): 689-699.

Csank, A.Z., Tripati, A.K., Patterson, W.P., Eagle, R.A., Rybczynski, N., Ballantyne, A.P. and Eiler, J.M., 2011a. Estimates of Arctic land surface temperatures during the early Pliocene from two novel proxies. Earth and Planetary Science Letters, 304(3): 291-299.

Csank, A.Z., Tripati, A.K., Patterson, W.P., Eagle, R.A., Rybczynski, N., Ballantyne, A.P. and Eiler, J.M., 2011b. Estimates of Arctic land surface temperatures during the early

Pliocene from two novel proxies. Earth and Planetary Science Letters, 304(3-4): 291-299.

de Winter, N.J., Goderis, S., Dehairs, F., Jagt, J.W., Fraaije, R.H., Van Malderen, S.J., Vanhaecke, F. and Claeys, P., 2017. Tropical seasonality in the late Campanian (late Cretaceous): Comparison between multiproxy records from three bivalve taxa from Oman. Palaeogeography, Palaeoclimatology, Palaeoecology.

DeLong, K.L., Flannery, J.A., Maupin, C.R., Poore, R.Z. and Quinn, T.M., 2011. A coral Sr/Ca calibration and replication study of two massive corals from the Gulf of Mexico. Palaeogeography, Palaeoclimatology, Palaeoecology, 307(1): 117-128.

Dettman, D.L., Reische, A.K. and Lohmann, K.C., 1999. Controls on the stable isotope composition of seasonal growth bands in aragonitic fresh-water bivalves (*Unionidae*). Geochimica et Cosmochimica Acta, 63(7): 1049-1057.

Donath, F.M., Daughney, C.J., Morgenstern, U., Cameron, S.G. and Toews, M.W., 2015. Hydrochemical interpretation of groundwater-surface water interactions at catchment and local scales, Lake Rotorua catchment, New Zealand. Journal of Hydrology, 54(1): 11.

Duhr, A. and Hilkert, A.W., 2004. Automated H_2/H_2O equilibration for for δD determination on aqueous samples using Thermo Scientific GasBench II. .

Eagle, R., Eiler, J.M., Tripati, A.K., Ries, J., Freitas, P., Hiebenthal, C., Wanamaker, A.D., Taviani, M., Elliot, M. and Marenssi, S., 2013. The influence of temperature and seawater carbonate saturation state on 13C−18O bond ordering in bivalve mollusks. Biogeosciences, 10: 4591.

Eagle, R.A., Tütken, T., Martin, T.S., Tripati, A.K., Fricke, H.C., Connely, M., Cifelli, R.L. and Eiler, J.M., 2011. Dinosaur body temperatures determined from isotopic (13C-18O) ordering in fossil biominerals. Science, 333(6041): 443-445.

Eiler, J.M., 2007. "Clumped-isotope" geochemistry—The study of naturally-occurring, multiply-substituted isotopologues. Earth and Planetary Science Letters, 262(3): 309-327.

Eiler, J.M., 2011. Paleoclimate reconstruction using carbonate clumped isotope thermometry. Quaternary Science Reviews, 30(25): 3575-3588.

Epstein, S., Buchsbaum, R., Lowenstam, H.A. and Urey, H.C., 1953. Revised carbonate-water isotopic temperature scale. Geological Society of America Bulletin, 64(11): 1315-1326.

Foster, L., Allison, N., Finch, A., Andersson, C. and Ninnemann, U., 2009. Controls on $\delta 18O$ and $\delta 13C$ profiles within the aragonite bivalve *Arctica islandica*. The Holocene, 19(4): 549-558.

Fowler, A.M., Boswijk, G., Gergis, J. and Lorrey, A., 2008. ENSO history recorded in *Agathis australis* (kauri) tree rings. Part A: kauri's potential as an ENSO proxy. International Journal of Climatology, 28(1): 1-20.

Fowler, A.M., Boswijk, G., Lorrey, A.M., Gergis, J., Pirie, M., McCloskey, S.P., Palmer, J.G. and Wunder, J., 2012. Multi-centennial tree-ring record of ENSO-related activity in New Zealand. Nature Climate Change, 2(3): 172.

Geeza, T.J., Gillikin, D.P., Goodwin, D.H., Evans, S.D., Watters, T. and Warner, N.R., 2018. Controls on magnesium, manganese, strontium, and barium concentrations recorded in freshwater mussel shells from Ohio. Chemical Geology.

Gergis, J.L. and Fowler, A.M., 2009. A history of ENSO events since AD 1525: implications for future climate change. Climatic Change, 92(3-4): 343-387.

Ghosh, P., Adkins, J., Affek, H., Balta, B., Guo, W., Schauble, E.A., Schrag, D. and Eiler, J.M., 2006. 13 C−18 O bonds in carbonate minerals: A new kind of paleothermometer. Geochimica et Cosmochimica Acta, 70(6): 1439-1456.

Gillikin, D.P., Dehairs, F., Lorrain, A., Steenmans, D., Baeyens, W. and André, L., 2006a. Barium uptake into the shells of the common mussel (*Mytilus edulis*) and the potential for estuarine paleo-chemistry reconstruction. Geochimica et Cosmochimica Acta, 70(2): 395-407.

Gillikin, D.P., Lorrain, A., Bouillon, S., Willenz, P. and Dehairs, F., 2006b. Stable carbon isotopic composition of *Mytilus edulis* shells: relation to metabolism, salinity, $\delta^{13}C$ DIC and phytoplankton. Organic Geochemistry, 37(10): 1371-1382.

Goodwin, D.H., Schöne, B.R. and Dettman, D.L., 2003. Resolution and fidelity of oxygen isotopes as paleotemperature proxies in bivalve mollusk shells: models and observations. Palaios, 18(2): 110-125.

Gordon, N.D., 1986. The southern oscillation and New Zealand weather. Monthly weather review, 114(2): 371-387.

Grimmond, N.M.W., 1968. Observations on growth and age of *Hyridella menziesi* Gray (MolluscaBivalvia) in a freshwater tidal lake, University of Otago.

Grossman, E.L. and Ku, T.-L., 1986. Oxygen and carbon isotope fractionation in biogenic aragonite: temperature effects. Chemical Geology: Isotope Geoscience Section, 59: 59-74.

Hamilton, D.P., Collier, K.J. and Howard-Williams, C., 2016. Lake restoration in New Zealand. Ecological Management & Restoration, 17(3): 191-199.

Heise, W., Caldwell, T., Bertrand, E., Hill, G., Bennie, S. and Palmer, N., 2016. Imaging the deep source of the Rotorua and Waimangu geothermal fields, Taupo Volcanic Zone, New Zealand. Journal of Volcanology and Geothermal Research, 314: 39-48.

Hellstrom, J., McCulloch, M. and Stone, J., 1998. A detailed 31,000-year record of climate and vegetation change, from the isotope geochemistry of two New Zealand speleothems. Quaternary Research, 50(2): 167-178.

Henkes, G.A., Passey, B.H., Wanamaker Jr, A.D., Grossman, E.L., Ambrose Jr, W.G. and Carroll, M.L., 2013. Carbonate clumped isotope compositions of modern marine mollusk and brachiopod shells. Geochimica et Cosmochimica Acta, 106: 307-325.

Holmes, R.L., 1983. Computer-assisted quality control in tree-ring dating and measurement. Tree-ring bulletin.

Izumida, H., Yoshimura, T., Suzuki, A., Nakashima, R., Ishimura, T., Yasuhara, M., Inamura, A., Shikazono, N. and Kawahata, H., 2011. Biological and water chemistry controls on Sr/Ca, Ba/Ca, Mg/Ca and $\delta^{18}O$ profiles in freshwater pearl mussel *Hyriopsis* sp. Palaeogeography, Palaeoclimatology, Palaeoecology, 309(3): 298-308.

James, M., 1985. Distribution, biomass and production of the freshwater mussel, *Hyridella menziesi* (Gray), in Lake Taupo, New Zealand. Freshwater biology, 15(3): 307-314.

James, M., 1987. Ecology of the freshwater mussel *Hyridella menziesi* (Gray) in a small oligotrophic lake. Archiv für Hydrobiologie, 108(3): 337-348.

Jones, J.M., Gille, S.T., Goosse, H., Abram, N.J., Canziani, P.O., Charman, D.J., Clem, K.R., Crosta, X., De Lavergne, C. and Eisenman, I., 2016. Assessing recent trends in high-latitude Southern Hemisphere surface climate. Nature Climate Change, 6(10): 917.

Kaandorp, R.J., Vonhof, H.B., Del Busto, C., Wesselingh, F.P., Ganssen, G.M., Marmól, A.E., Pittman, L.R. and van Hinte, J.E., 2003. Seasonal stable isotope variations of the modern Amazonian freshwater bivalve *Anodontites trapesialis*. Palaeogeography, Palaeoclimatology, Palaeoecology, 194(4): 339-354.

Kelemen, Z., Gillikin, D.P., Graniero, L.E., Havel, H., Darchambeau, F., Borges, A.V., Yambélé, A., Bassirou, A. and Bouillon, S., 2017. Calibration of hydroclimate proxies in freshwater bivalve shells from Central and West Africa. Geochimica et Cosmochimica Acta, 208: 41-62.

Kelson, J.R., Huntington, K.W., Schauer, A.J., Saenger, C. and Lechler, A.R., 2017. Toward a universal carbonate clumped isotope calibration: Diverse synthesis and preparatory

methods suggest a single temperature relationship. Geochimica et Cosmochimica Acta, 197: 104-131.

Langlet, D., Alleman, L., Plisnier, P.-D., Hughes, H. and André, L., 2007. Manganese content records seasonal upwelling in Lake Tanganyika mussels. Biogeosciences, 4(2): 195-203.

Lim, E.P., Hendon, H.H., Arblaster, J.M., Delage, F., Nguyen, H., Min, S.K. and Wheeler, M.C., 2016. The impact of the Southern Annular Mode on future changes in Southern Hemisphere rainfall. Geophysical Research Letters, 43(13): 7160-7167.

Lorrey, A., Williams, P., Salinger, J., Martin, T., Palmer, J., Fowler, A., Zhao, J.X. and Neil, H., 2008. Speleothem stable isotope records interpreted within a multi-proxy framework and implications for New Zealand palaeoclimate reconstruction. Quaternary International, 187(1): 52-75.

Mantua, N.J. and Hare, S.R., 2002. The Pacific decadal oscillation. Journal of oceanography, 58(1): 35-44.

Mayr, C., Lücke, A., Stichler, W., Trimborn, P., Ercolano, B., Oliva, G., Ohlendorf, C., Soto, J., Fey, M. and Haberzettl, T., 2007. Precipitation origin and evaporation of lakes in semi-arid Patagonia (Argentina) inferred from stable isotopes (δ ^{18}O, δ ^{2}H). Journal of Hydrology, 334(1): 53-63.

Montaggioni, L.F., Le Cornec, F., Corrège, T. and Cabioch, G., 2006. Coral barium/calcium record of mid-Holocene upwelling activity in New Caledonia, South-West Pacific. Palaeogeography, Palaeoclimatology, Palaeoecology, 237(2): 436-455.

Morgenstern, U., Daughney, C.J., Leonard, G., Gordon, D., Donath, F.M. and Reeves, R., 2015. Using groundwater age and hydrochemistry to understand sources and dynamics of nutrient contamination through the catchment into Lake Rotorua, New Zealand. Hydrology and Earth System Sciences, 19(2): 803-822.

Mueller-Lupp, T., Erlenkeuser, H. and Bauch, H.A., 2003. Seasonal and interannual variability of Siberian river discharge in the Laptev Sea inferred from stable isotopes in modern bivalves. Boreas, 32(2): 292-303.

Mullan, A., 1995. On the linearity and stability of Southern Oscillation-climate relationships for New Zealand. International Journal of Climatology, 15(12): 1365-1386.

Neukom, R., Gergis, J., Karoly, D.J., Wanner, H., Curran, M., Elbert, J., González-Rouco, F., Linsley, B.K., Moy, A.D. and Mundo, I., 2014. Inter-hemispheric temperature variability over the past millennium. Nature Climate Change, 4(5): 362-367.

Northcote, T., Hendy, C., Nelson, C. and Boubee, J., 1992. Tests for migratory history of the New Zealand common smelt (*Retropinna retropinna* (Richardson)) using otolith isotopic composition. Ecology of freshwater fish, 1(1): 61-72.

Peacock, E. and Seltzer, J.L., 2008. A comparison of multiple proxy data sets for paleoenvironmental conditions as derived from freshwater bivalve (Unionid) shell. Journal of Archaeological Science, 35(9): 2557-2565.

Peharda, M., Thébault, J., Markulin, K., Schöne, B.R., Janeković, I. and Chauvaud, L., 2017. Contrasting shell growth strategies in two Mediterranean bivalves revealed by oxygen-isotope ratio geochemistry: The case of *Pecten jacobaeus* and *Glycymeris pilosa*. Chemical Geology.

Petrizzo, D.A., Young, E.D. and Runnegar, B.N., 2014. Implications of high-precision measurements of 13C–18O bond ordering in CO2 for thermometry in modern bivalved mollusc shells. Geochimica et Cosmochimica Acta, 142: 400-410.

Phillips, N.R., Stewart, M., Olsen, G. and Hickey, C.W., 2014. Human health risks of geothermally derived metals and other contaminants in wild-caught food. Journal of Toxicology and Environmental Health, Part A, 77(6): 346-365.

Poage, M.A. and Chamberlain, C.P., 2001. Empirical relationships between elevation and the stable isotope composition of precipitation and surface waters: Considerations for studies of paleoelevation change. American Journal of Science, 301(1): 1-15.

Prendergast, A., Versteegh, E. and Schöne, B., 2017. New research on the development of high-resolution palaeoenvironmental proxies from geochemical properties of biogenic carbonates. Elsevier.

Rasband, W., 1997. ImageJ software. National Institutes of Health: Bethesda, MD, USA, 2012.

Renwick, J. and Thompson, D., 2006. The southern annular mode and New Zealand climate. Water Atmos, 14(2): 24-25.

Ricken, W., Steuber, T., Freitag, H., Hirschfeld, M. and Niedenzu, B., 2003. Recent and historical discharge of a large European river system–oxygen isotopic composition of river water and skeletal aragonite of *Unionidae* in the Rhine. Palaeogeography, Palaeoclimatology, Palaeoecology, 193(1): 73-86.

Rosales, I., Robles, S. and Quesada, S., 2004. Elemental and oxygen isotope composition of Early Jurassic belemnites: salinity vs. temperature signals. Journal of Sedimentary Research, 74(3): 342-354.

Rutherford, J., 1984. Trends in Lake Rotorua water quality. New Zealand journal of marine and freshwater research, 18(3): 355-365.

Rutherford, J., Pridmore, R. and White, E., 1989. Management of phosphorus and nitrogen inputs to Lake Rotorua, New Zealand. Journal of water resources planning and management, 115(4): 431-439.

Saenger, C., Gabitov, R.I., Farmer, J., Watkins, J.M. and Stone, R., 2017. Linear correlations in bamboo coral δ 13 C and δ 18 O sampled by SIMS and micromill: Evaluating paleoceanographic potential and biomineralization mechanisms using δ [11]B and Δ_{47} composition. Chemical Geology, 454: 1-14.

Schöne, B.R., Castro, A.D.F., Fiebig, J., Houk, S.D., Oschmann, W. and Kröncke, I., 2004a. Sea surface water temperatures over the period 1884–1983 reconstructed from oxygen isotope ratios of a bivalve mollusk shell (*Arctica islandica*, southern North Sea). Palaeogeography, Palaeoclimatology, Palaeoecology, 212(3): 215-232.

Schöne, B.R., Dunca, E., Mutvei, H. and Norlund, U., 2004b. A 217-year record of summer air temperature reconstructed from freshwater pearl mussels (*M. margarifitera*, Sweden). Quaternary Science Reviews, 23(16): 1803-1816.

Schöne, B.R. and Gillikin, D.P., 2013. Unraveling environmental histories from skeletal diaries—advances in sclerochronology. Palaeogeography, Palaeoclimatology, Palaeoecology, 373: 1-5.

Schöne, B.R., Page, N.A., Rodland, D.L., Fiebig, J., Baier, S., Helama, S.O. and Oschmann, W., 2007. ENSO-coupled precipitation records (1959–2004) based on shells of freshwater bivalve mollusks (*Margaritifera falcata*) from British Columbia. International Journal of Earth Sciences, 96(3): 525-540.

Schöne, B.R. and Surge, D.M., 2012. Part N, Revised, Volume 1, Chapter 14: Bivalve sclerochronology and geochemistry. Treatise online, 46: 1-24.

Scott, B., Mroczek, E., Burnell, J., Zarrouk, S., Seward, A., Robson, B. and Graham, D., 2016. The Rotorua Geothermal Field: an experiment in environmental management. Geothermics, 59: 294-310.

Scourse, J., Richardson, C., Forsythe, G., Harris, I., Heinemeier, J., Fraser, N., Briffa, K. and Jones, P., 2006. First cross-matched floating chronology from the marine fossil record: data from growth lines of the long-lived bivalve mollusc *Arctica islandica*. The Holocene, 16(7): 967-974.

Smith, V.H., Wood, S.A., McBride, C., Atalah, J., Hamilton, D. and Abell, J., 2016. Phosphorus and nitrogen loading restraints are essential for successful eutrophication control of Lake Rotorua, New Zealand. Inland Waters, 6(2): 273-283.

Soldati, A., Jacob, D., Schöne, B., Bianchi, M. and Hajduk, A., 2009. Seasonal periodicity of growth and composition in valves of *Diplodon chilensis patagonicus* (d'Orbigny, 1835). Journal of Molluscan Studies, 75(1): 75-85.

Sosdian, S., Gentry, D.K., Lear, C.H., Grossman, E.L., Hicks, D. and Rosenthal, Y., 2006. Strontium to calcium ratios in the marine gastropod *Conus ermineus*: Growth rate effects and temperature calibration. Geochemistry, Geophysics, Geosystems, 7(11).

Steuber, T., 1999. Isotopic and chemical intra-shell variations in low-Mg calcite of rudist bivalves (*Mollusca-Hippuritacea*): disequilibrium fractionations and late Cretaceous seasonality. International Journal of Earth Sciences, 88(3): 551-570.

Stewart, M. and Taylor, C., 1981. Environmental isotopes in New Zealand hydrology 1 introduction: The role of oxygen—18. New Zealand journal of science, 24: 295-311.

Team, R.C., 2017. R: A language and environment for statistical computing. Vienna, Austria: R Foundation for Statistical Computing; 2017.

Thébault, J., Chauvaud, L., L'Helguen, S., Clavier, J., Barats, A., Jacquet, S., Pécheyran, C. and Amouroux, D., 2009. Barium and molybdenum records in bivalve shells: Geochemical proxies for phytoplankton dynamics in coastal environments? Limnology and Oceanography, 54(3): 1002-1014.

Thiagarajan, N., Adkins, J. and Eiler, J., 2011. Carbonate clumped isotope thermometry of deep-sea corals and implications for vital effects. Geochimica et Cosmochimica Acta, 75(16): 4416-4425.

Tobin, T.S., Wilson, G.P., Eiler, J.M. and Hartman, J.H., 2014. Environmental change across a terrestrial Cretaceous-Paleogene boundary section in eastern Montana, USA, constrained by carbonate clumped isotope paleothermometry. Geology, 42(4): 351-354.

Toggweiler, J., 2009. Shifting westerlies. Science, 323(5920): 1434-1435.

Tripati, A.K., Eagle, R.A., Thiagarajan, N., Gagnon, A.C., Bauch, H., Halloran, P.R. and Eiler, J.M., 2010. 13C–18O isotope signatures and 'clumped isotope'thermometry in foraminifera and coccoliths. Geochimica et Cosmochimica Acta, 74(20): 5697-5717.

Tynan, S., Opdyke, B.N., Walczak, M., Eggins, S. and Dutton, A., 2016. Assessment of Mg/Ca in *Saccostrea glomerata* (the Sydney rock oyster) shell as a potential temperature record. Palaeogeography, Palaeoclimatology, Palaeoecology.

Ummenhofer, C.C. and England, M.H., 2007. Interannual extremes in New Zealand precipitation linked to modes of Southern Hemisphere climate variability. Journal of Climate, 20(21): 5418-5440.

Urey, H.C., 1947. The thermodynamic properties of isotopic substances. Journal of the Chemical Society (Resumed): 562-581.

Urey, H.C., Lowenstam, H.A., Epstein, S. and McKinney, C.R., 1951. Measurement of paleotemperatures and temperatures of the Upper Cretaceous of England, Denmark, and the southeastern United States. Geological Society of America Bulletin, 62(4): 399-416.

Versteegh, E.A., Vonhof, H.B., Troelstra, S.R., Kaandorp, R.J. and Kroon, D., 2010. Seasonally resolved growth of freshwater bivalves determined by oxygen and carbon isotope shell chemistry. Geochemistry, Geophysics, Geosystems, 11(8).

Vihtakari, M., Renaud, P.E., Clarke, L.J., Whitehouse, M.J., Hop, H., Carroll, M.L. and Ambrose Jr, W.G., 2016. Decoding the oxygen isotope signal for seasonal growth patterns in Arctic bivalves. Palaeogeography, Palaeoclimatology, Palaeoecology, 446: 263-283.

Villalba, R., Lara, A., Masiokas, M.H., Urrutia, R., Luckman, B.H., Marshall, G.J., Mundo, I.A., Christie, D.A., Cook, E.R. and Neukom, R., 2012. Unusual Southern Hemisphere tree growth patterns induced by changes in the Southern Annular Mode. Nature Geoscience, 5(11): 793-798.

Wacker, U., Fiebig, J., Tödter, J., Schöne, B.R., Bahr, A., Friedrich, O., Tütken, T., Gischler, E. and Joachimski, M.M., 2014. Empirical calibration of the clumped isotope paleothermometer using calcites of various origins. Geochimica et Cosmochimica Acta, 141: 127-144.

Wanamaker, A.D., Kreutz, K.J., Schöne, B.R. and Introne, D.S., 2011. Gulf of Maine shells reveal changes in seawater temperature seasonality during the Medieval Climate Anomaly and the Little Ice Age. Palaeogeography, Palaeoclimatology, Palaeoecology, 302(1): 43-51.

Wang, C., Deser, C., Yu, J.-Y., DiNezio, P. and Clement, A., 2017. El Niño and Southern Oscillation (ENSO): A Review, Coral Reefs of the Eastern Tropical Pacific. Springer, pp. 85-106.

Wigley, T.M., Briffa, K.R. and Jones, P.D., 1984. On the average value of correlated time series, with applications in dendroclimatology and hydrometeorology. Journal of Climate and Applied Meteorology, 23(2): 201-213.

Xu, Y.-Y., Pearson, S. and Kilbourne, K.H., 2015. Assessing coral Sr/Ca–SST calibration techniques using the species *Diploria strigosa*. Palaeogeography, Palaeoclimatology, Palaeoecology, 440: 353-362.

Yan, H., Shao, D., Wang, Y. and Sun, L., 2014a. Sr/Ca differences within and among three Tridacnidae species from the South China Sea: Implication for paleoclimate reconstruction. Chemical Geology, 390: 22-31.

Yan, H., Wang, Y. and Sun, L., 2014b. High resolution oxygen isotope and grayscale records of a medieval fossil giant clam (*Tridacna gigas*) in the South China Sea: physiological and paleoclimatic implications. Acta Oceanologica Sinica, 33(8): 18-25.

Yan, L., Schöne, B.R. and Arkhipkin, A., 2012. Eurhomalea exalbida (Bivalvia): A reliable recorder of climate in southern South America? Palaeogeography, Palaeoclimatology, Palaeoecology, 350: 91-100.

Zaarur, S., Olack, G. and Affek, H.P., 2011. Paleo-environmental implication of clumped isotopes in land snail shells. Geochimica et Cosmochimica Acta, 75(22): 6859-6869.

Zhao, L., Walliser, E.O., Mertz-Kraus, R. and Schöne, B.R., 2017. Unionid shells (*Hyriopsis cumingii*) record manganese cycling at the sediment-water interface in a shallow eutrophic lake in China (Lake Taihu). Palaeogeography, Palaeoclimatology, Palaeoecology.

2.8 Supplementary materials – Chapter 2

2.8.1 Supplementary methods

Oxygen isotope analysis by isotope ratio mass spectrometry (IRMS)

Drilled *Echyridella menziesii* shell samples from RO-19, 109 AND 107 with weights of around 1 mg were obtained. Shell samples were transferred into 5.9 ml Labco Exetainer vials, flushed with He gas, reacted with 0.2 ml of 99.9 % phosphoric acid and finally heated to 70 ${}^{\circ}$C before being rested for two hours. Analyses of oxygen isotopes of RO-19 was carried using a SerCon 20-22 stable isotope ratio mass spectrometer equipped with a carbonate device at the Research School of Earth Sciences, The Australian National University. The $\delta^{18}O$ values are reported relative to the Vienna Pee-Dee Belemnite (VPDB) reference material based internal reference material (ANU-M1), calibrated Carrara marble and NBS-18. External precision (1 SD) was better than ± 0.1 ‰ based on multiple measurements of the ANU-M1 and other secondary reference materials. Analyses of oxygen isotopes of RO-109 and 107 were carried using a Thermo Scientific MAT 253 gas source mass spectrometer at the stable isotope laboratory at Goethe University, Frankfurt.

2.8.2 Supplementary tables

Table S1. Inter-correlation values between measured Sr/Ca time series in five *Echyridella menziesii* shells.

	RO-63	RO-66	RO-67	RO-25	RO-21
RO-63	1				
RO-66	0.609501	1			
RO-67	0.340575	0.436741	1		
RO-25	0.03866	-0.14734	0.0643	1	
RO-21	0.156082	0.122503	0.446007	-0.25884	1

2.8.3 Supplementary figures
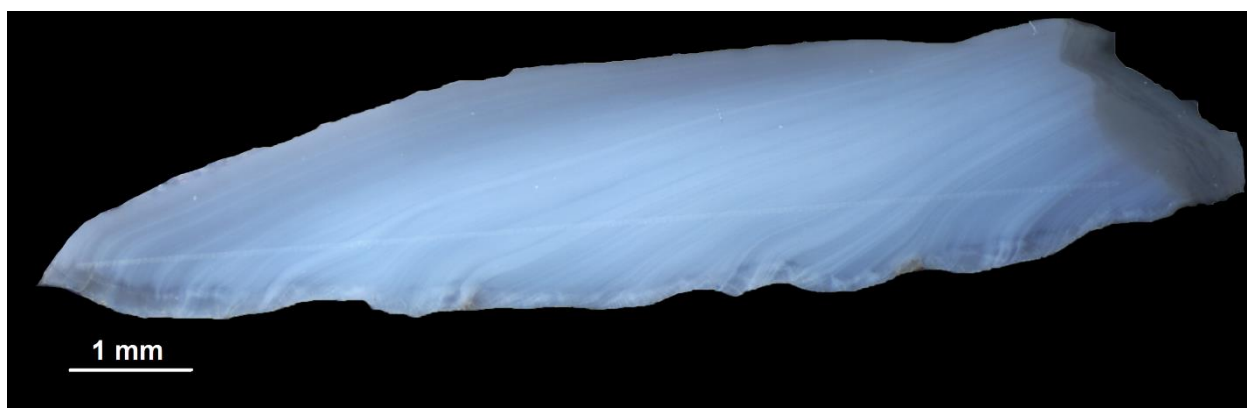
Fig. S1 Photograph of a shell section through the maximum growth axis showing the location of the trace element and oxygen isotope analysis. The outer surface of the shell (covered in periostr acum) is at the bottom of the image, and the outer growing edge is on the left.
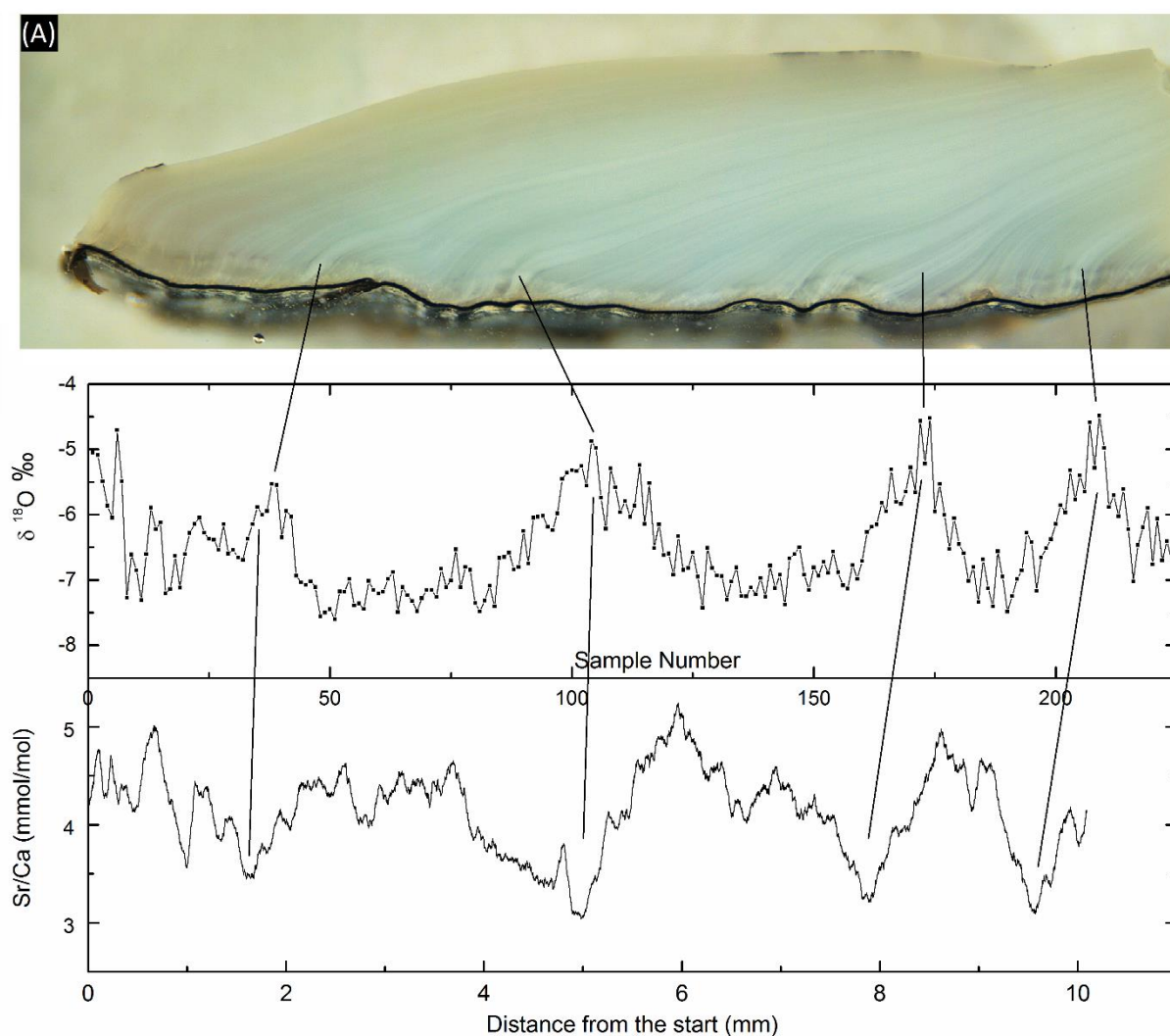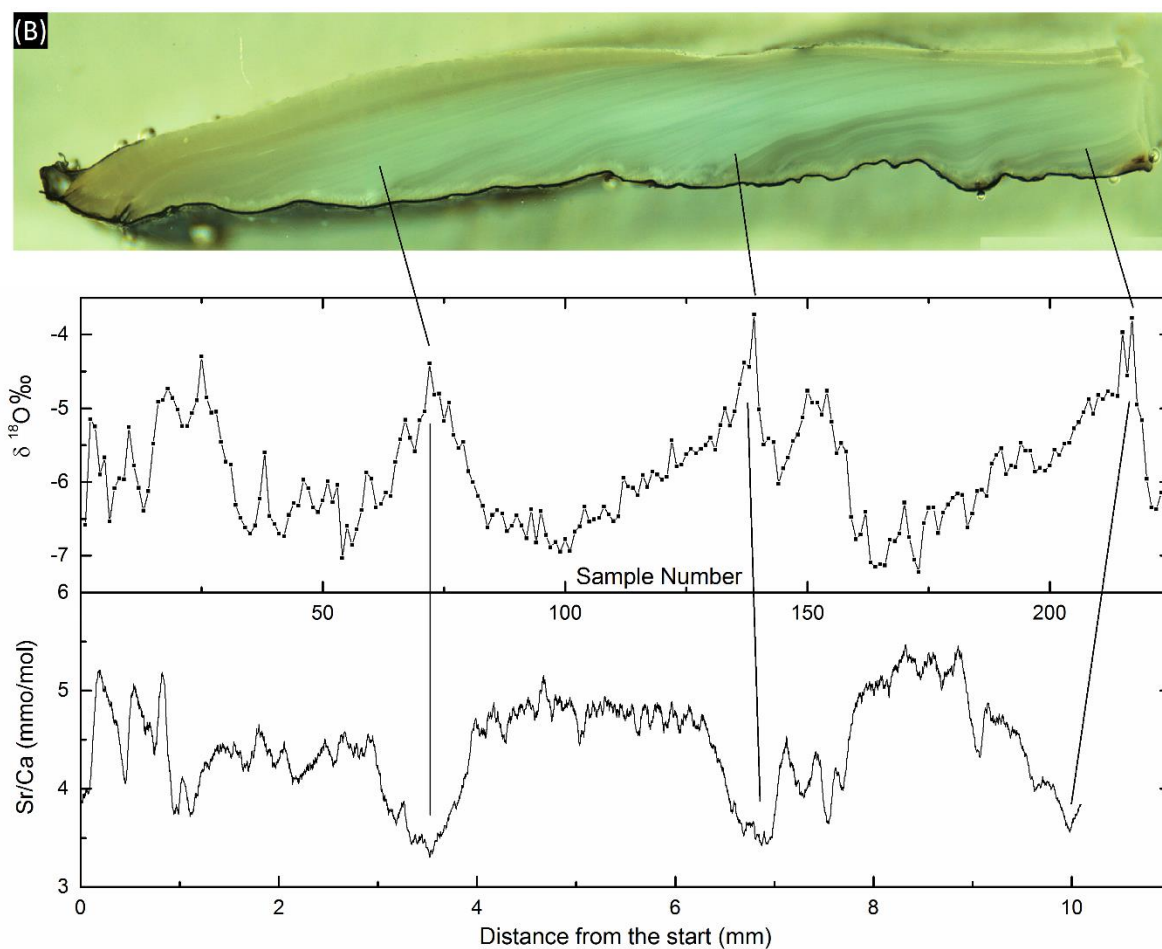
Fig. S2 Graph showing the coinciding and opposite variations in δ $^{18}O_{shell}$ and Sr/Ca ratio in *Echyridella menziesii* shell (A) RO-66 and (B) RO-63 and the alignment of the data with the location on the shell section.
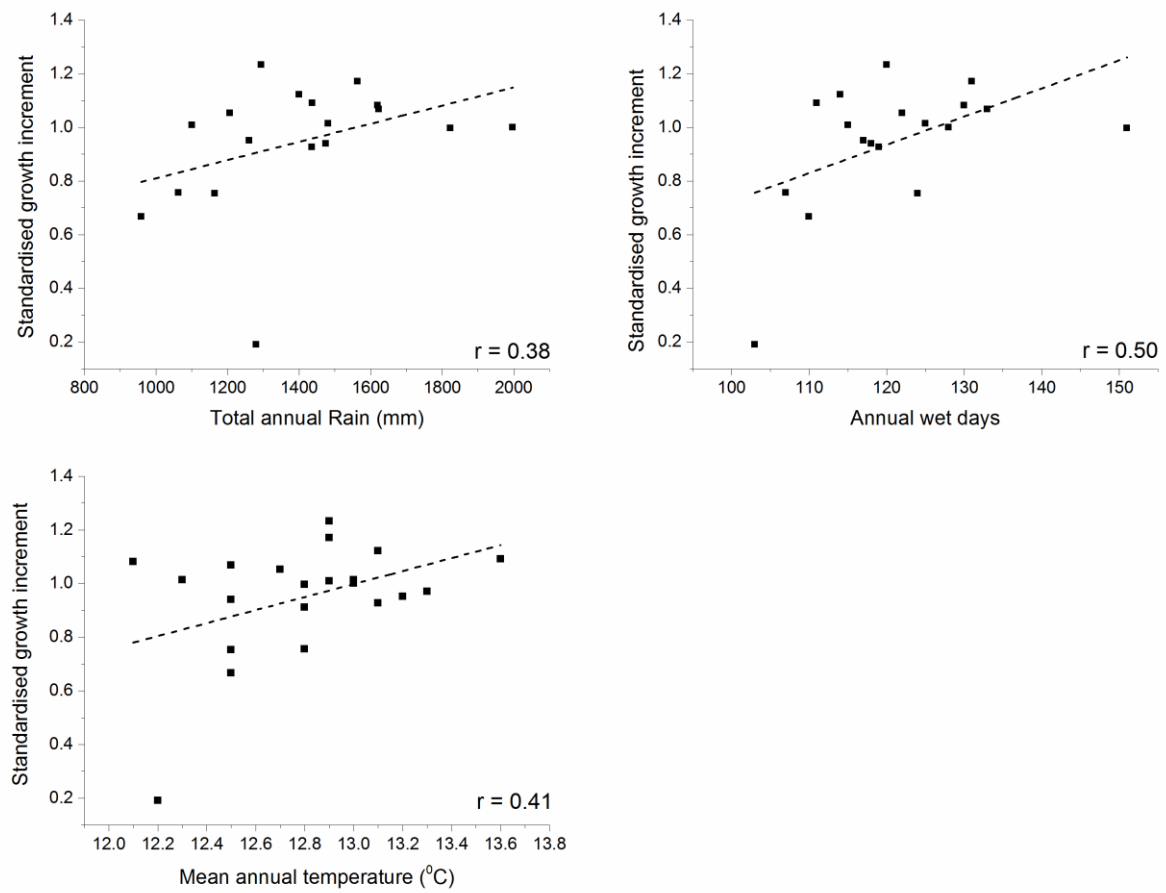
Fig. S3 Bi-plots showing the correlation between standardised growth increment and total annual rainfall, total annual wet days and mean annual air temperature in the Rotorua region. Dash lines represent the linear regression line
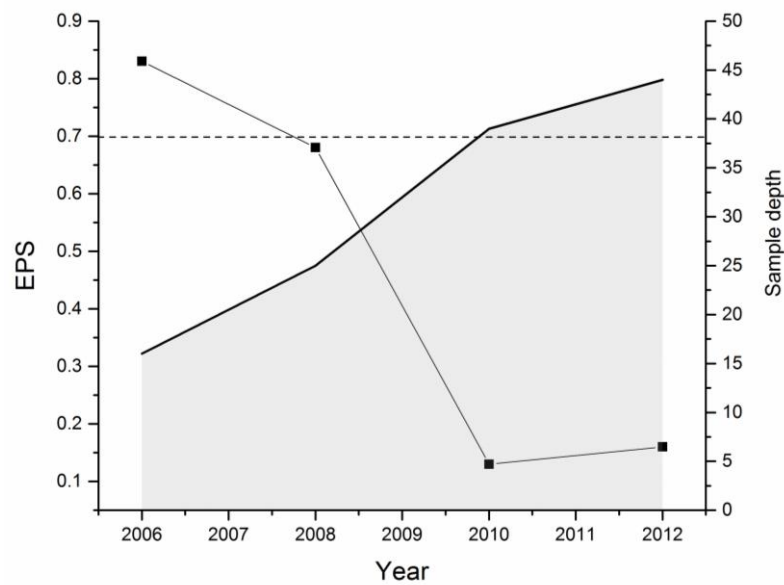
Fig. S4 Expressed Population Signal (EPS) variation in the master chronology of 46 *Echyridella menziesii* shells showing the drop in EPS value at higher sample depths.

90
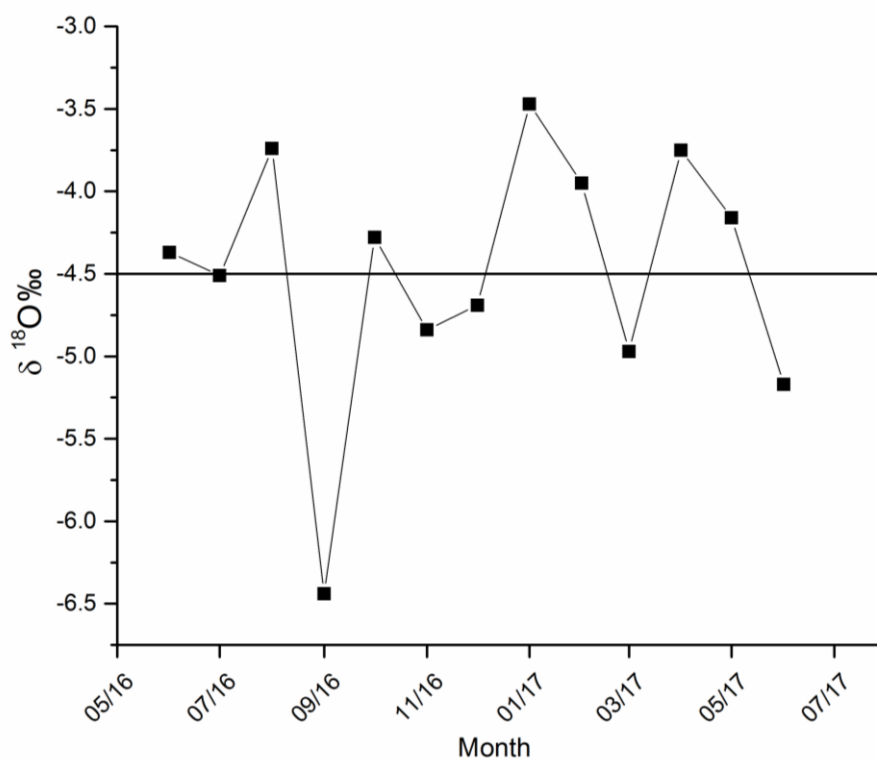
Fig. S5 Variation in δ ^{18}O levels measured in Lake Rotorua, New Zealand during June 2016 to June 2017.
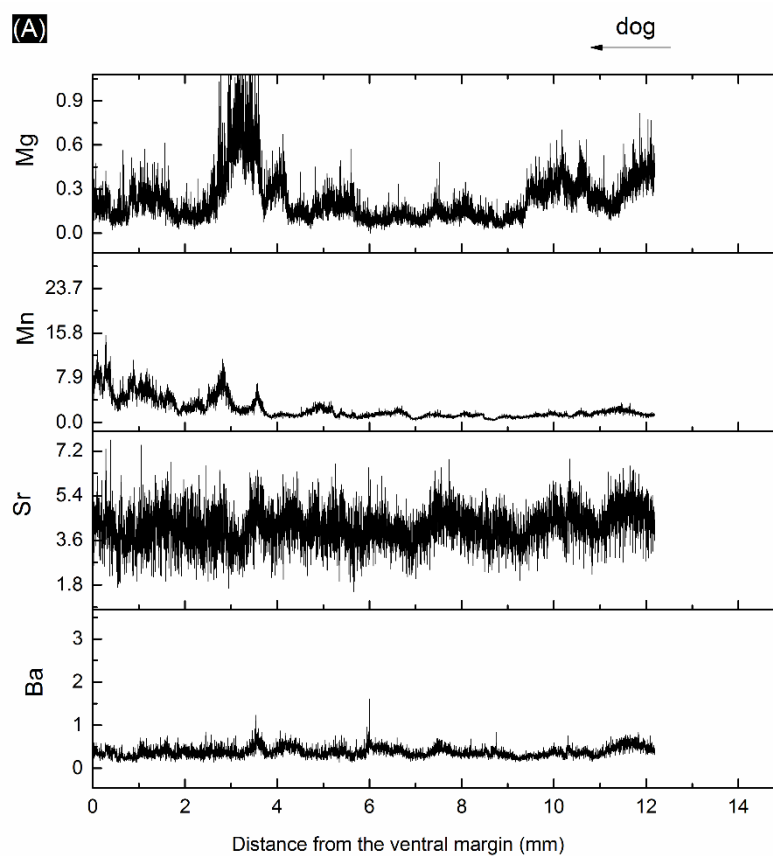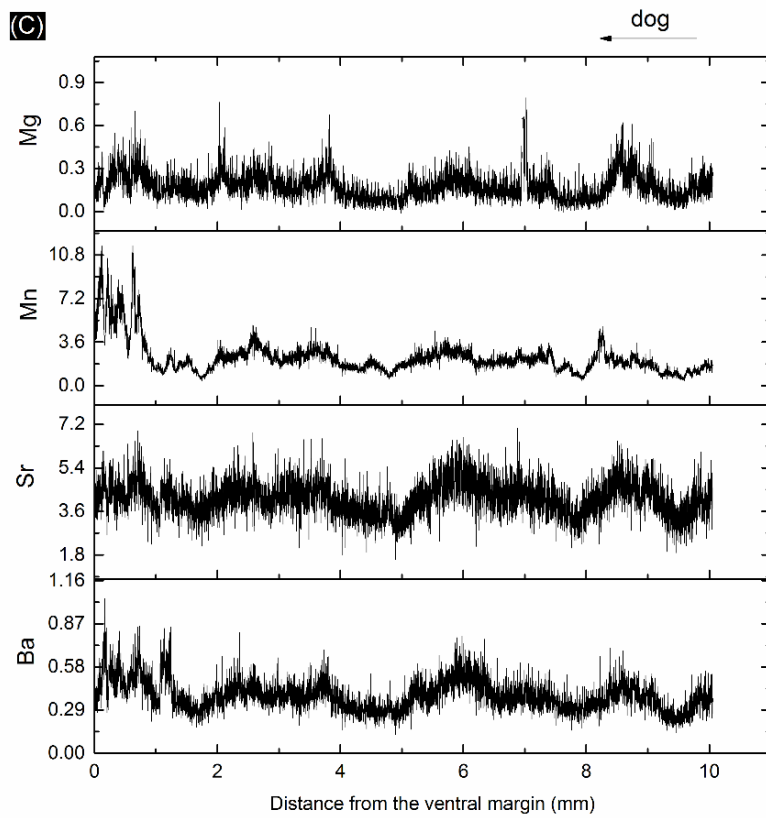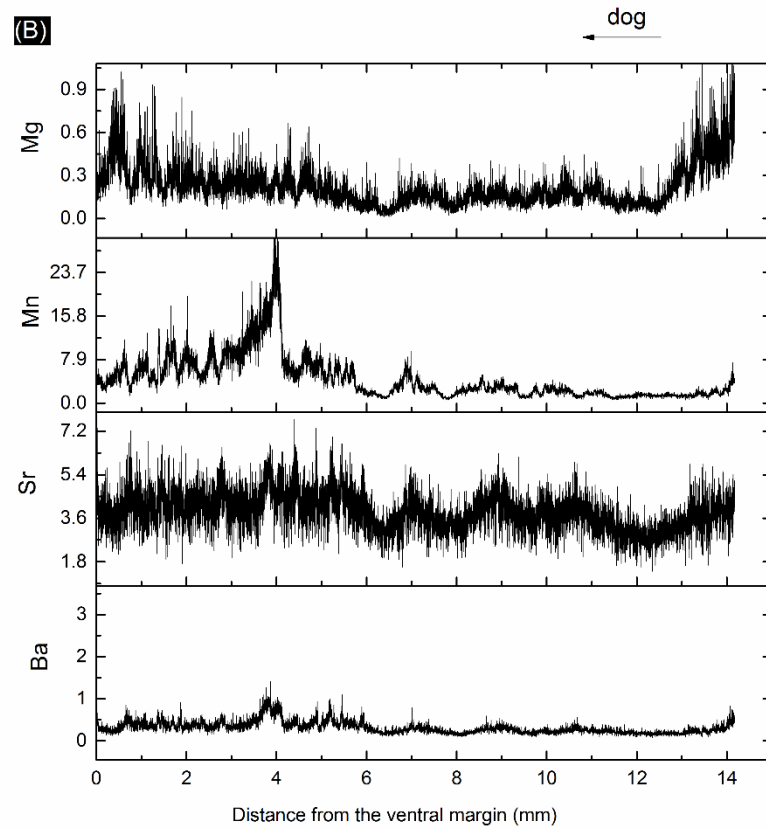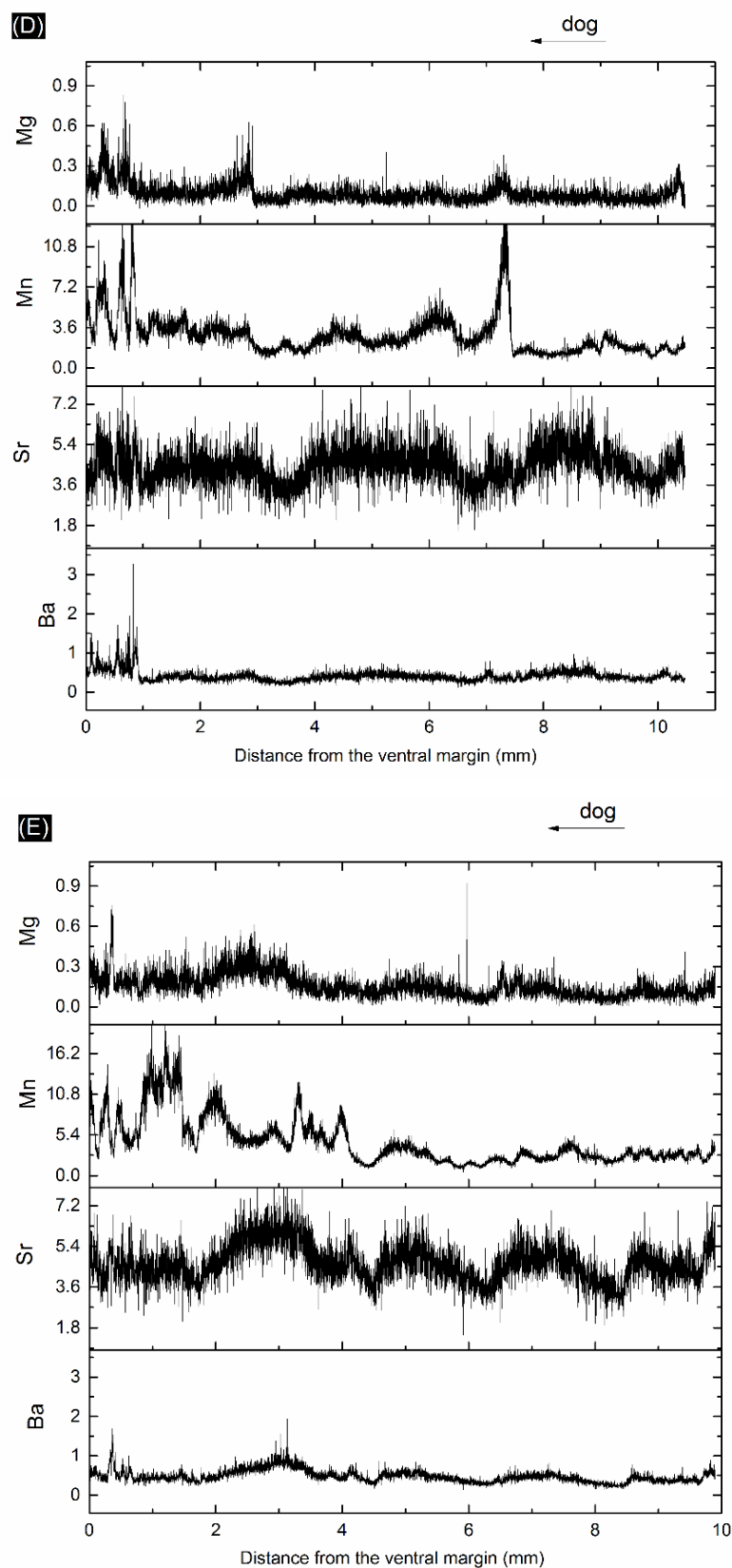
Fig. S6 The variations in measured Me/Ca ratios in five *Echyridella menziesii* shells (A) RO-21, (B) RO- 25, (C) RO-63, (D) RO-66 and (E) RO-67. All Me/Ca ratios are in mmol/mol, dog = direction of growth
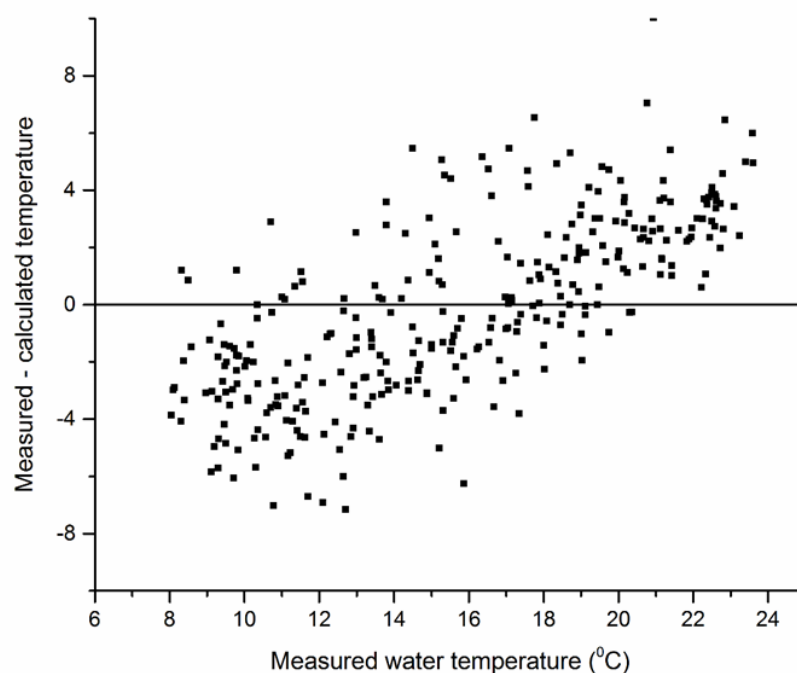
Fig. S7 The plot of measured water temperature in Lake Rotorua against the difference between the measured and calculated temperature. The figure indicates that the calculated temperature is more accurate at around 15
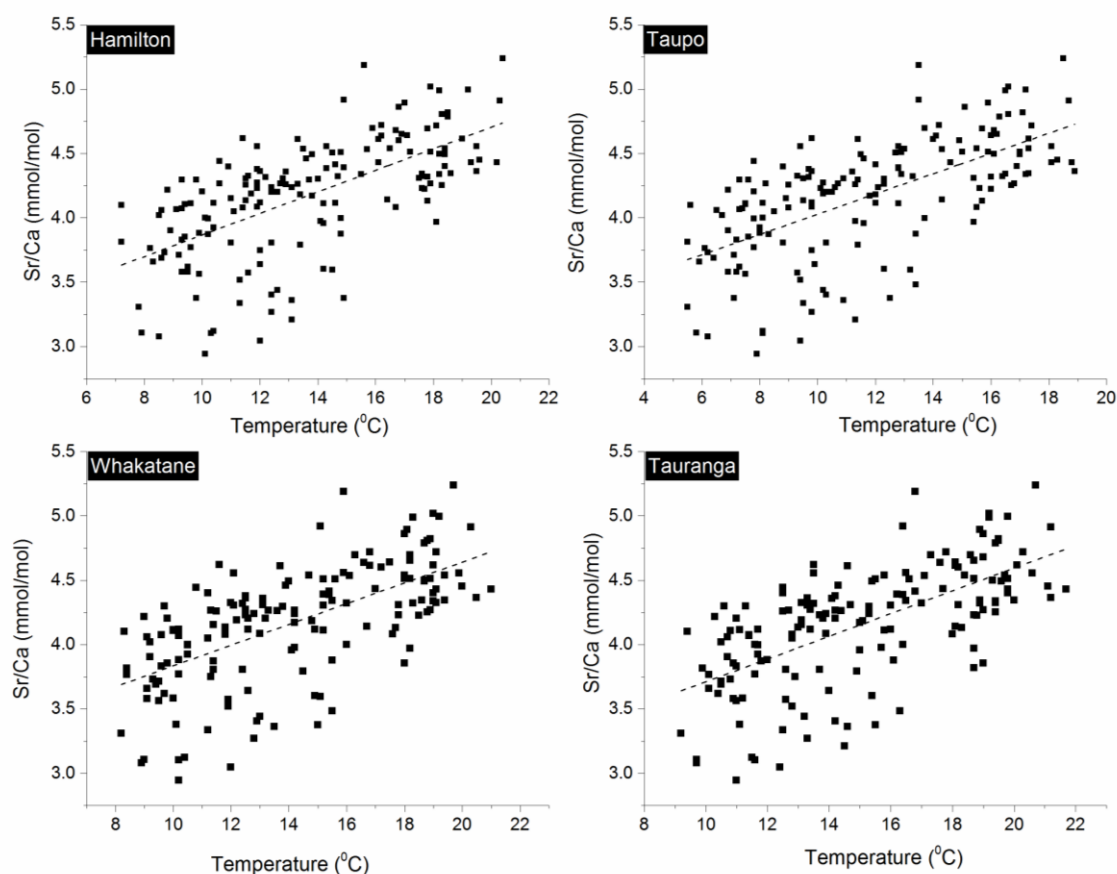
°C.

Fig. S8 Biplots of Sr/Ca ratios calculated by averaging five *Echyridella menziesii* shells collected from Lake Rotorua, New Zealand against monthly air temperature from Hamilton, Taupo, Kawerau, and Tauranga

airports (at 100 km radius from Lake Rotorua). All element/Ca are in mmol/mol. Dash lines represent the linear regression line.
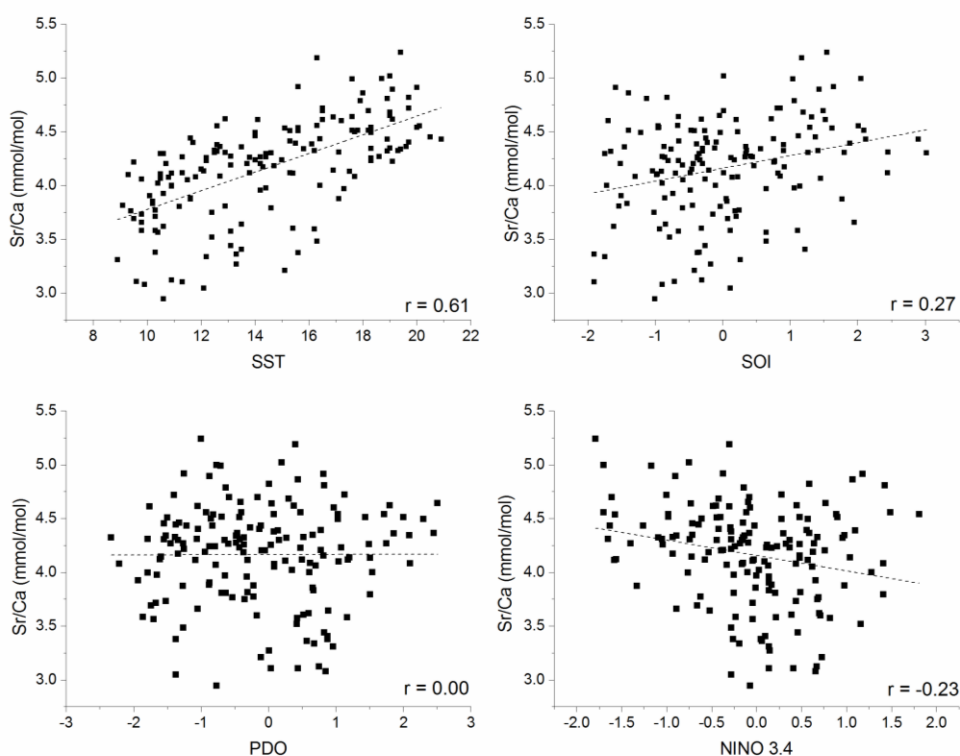
Fig. S9 Bi-plots showing the correlation between Sr/Ca and El-Nino southern oscillation index (NINO 3.4), Sothern Oscillation Index (SOI), Pacific Inter-decadal Oscillation (PIO) and Sea Surface Temperature (SST) at Gisborne (approximately 160 km southeast of Lake Rotorua). Dash lines represent the linear regression line.
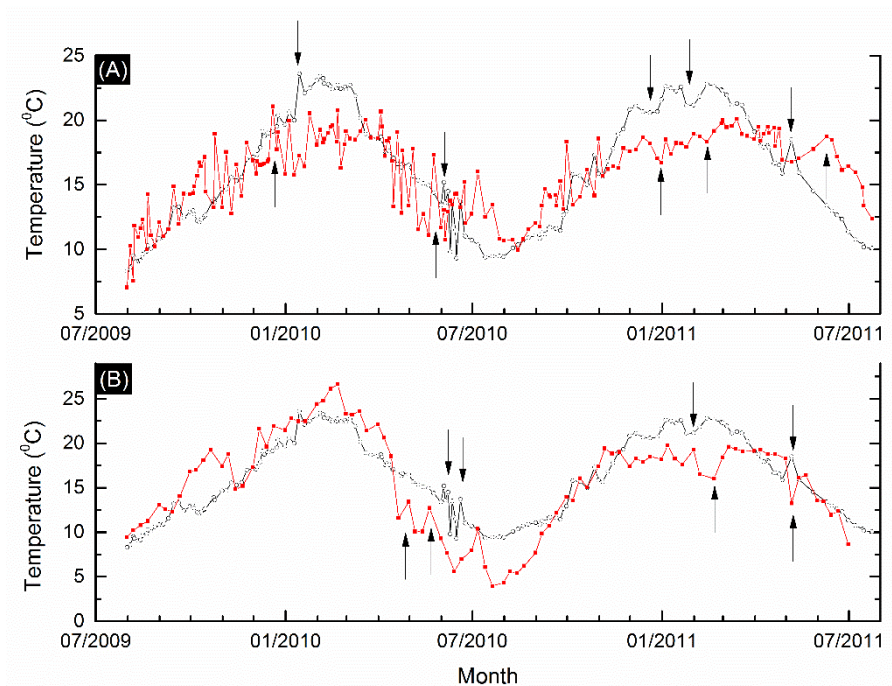
Fig S10. Comparison between instrumental lake water temperature from Lake Rotorua (black) and calculated temperature using (A) oxygen isotopes and (B) Sr/Ca ratios. The figure indicates that at weekly resolution both were able to identify detailed changes in the weekly water temperature variations in the Lake Rotorua. Arrows point towards the similarities in the data series. Small discrepancies observed between the time series
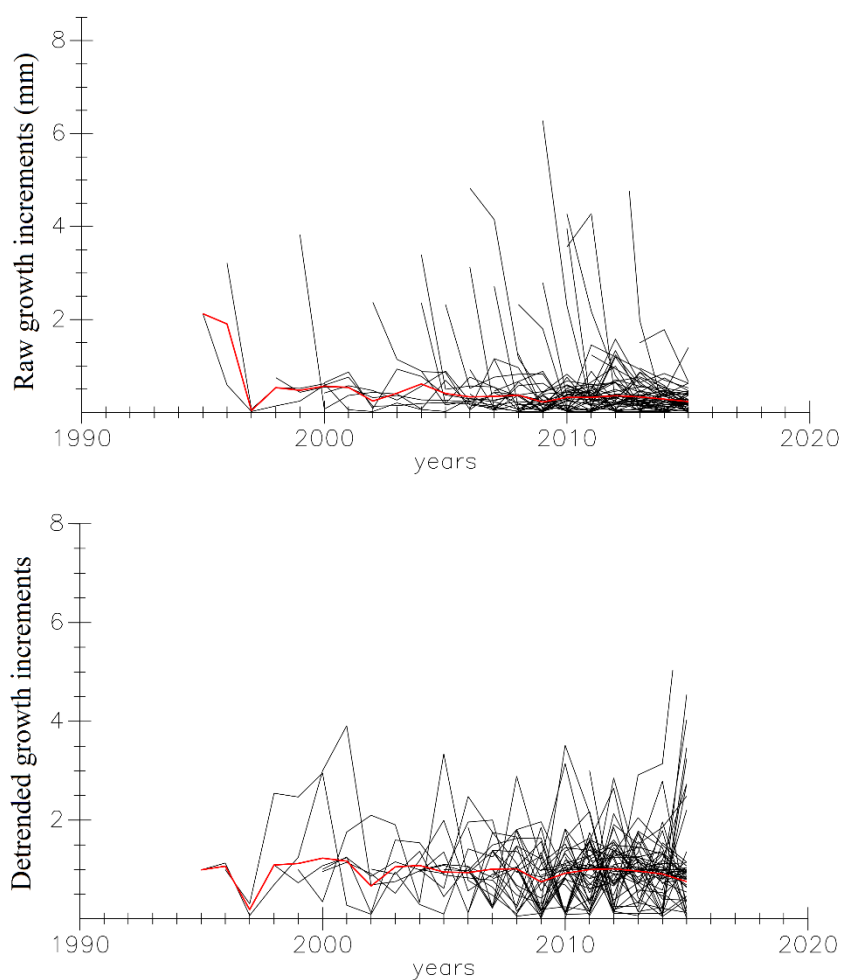
Chapter 3

THE POTENTIAL OF THREE EAST AUSTRALIAN FRESHWATER BIVALVE SPECIES AS ENVIRONMENTAL PROXY ARCHIVES

Dilmi Herath[1], Dorrit Jacob[1], Hugh Jones[2], Stewart Fallon[3]

[1] Department of Earth and Planetary Science, Macquarie University, North Ryde, Sydney, Australia.

[2] NSW Office of Environment and Heritage, Sydney, Australia.

[3] Research School of Earth Sciences, Australian National University, Canberra, ACT, Australia.

Abstract

Freshwater mussels in Australia are rarely studied for their life history and potential as paleoclimate proxy archives. Therefore, three freshwater mussel species from the Williams River, Hunter Valley, Australia, namely *Alathyria profuga*, *Cucumerunio novaehollandiae* and *Hyridella drapeta* were studied to identify the potential of these species as new environmental proxy archives from Australian freshwater bodies. Growth analysis revealed that *A. profuga* and *C. novaehollandiae* produce distinctive growth lines, which allow the first identification of age and growth structure of these species. Oxygen isotope ratio in *A. profuga* shells, as well as high resolution element concentrations in all three species, show cyclic, annual variations. The high correlation between growth rates and the combined winter air temperature and annual rainfall as well as accurate temperature reconstruction using oxygen isotopic values in the shells suggest that *A. profuga* has good potential as an environmental proxy archive. However, low correlation observed between Sr/Ca and temperature limited the usefulness of Sr/Ca in *A. profuga* shells as a water temperate proxy. In contrast, growth rates and element ratios of *C. novaehollandiae* do not indicate a significant relationship with environmental variables suggesting that this species together with *H. drapeta* is probably not suitable for paleo-climatic studies.

3.1 Introduction

Freshwater mussels (Order Unionida) are vulnerable to rapid environmental changes due to their sedentary, benthic habit and (as adults) weak dispersal capability (Jones and Byrne, 2014). These characteristics combined with their incremental shell growth and wide geographic coverage give them the potential to inform on past environmental and climatic conditions in a regional and continental context. Compared to corals and marine species, freshwater mussels in Australia are less frequently studied for their life history and potential as paleoclimate proxy archives, despite the fact that more than 32 species are known (Walker et al., 2014). The most commonly studied Australian genera are *Velesunio* (Walker, 1981; Humphrey and Simpson, 1985; Jones and Byrne, 2014; Markich, 2017) and *Hyridella* (Jeffree et al., 1995; Byrne and Vesk, 2000; Walker et al., 2001b; Walker, 2016), predominantly for their distribution, abundance, life history and ecological importance in rivers and lakes. Lastly, Humphrey and Simpson (1985) studied the trophic status of *Velesunio angasi* and correlation of shell growth rates with dissolved oxygen and chlorophyll *a* concentrations in the water.

Growth and composition of the shells of long-lived mussels are increasingly used in the study of seasonal to inter annual paleoclimate variability (Schöne and Gillikin, 2013; Butler and Schöne, 2017). In freshwater environments, trace element to calcium ratios in the shells can give information on water temperature (Sr/Ca ratios: Zhao, Schöne *et al.* 2017), precipitation rates, primary productivity and pH values (Ba/Ca ratios: Carroll and Romanek 2008; Mn/Ca ratios: Langlet, Alleman *et al.* 2007; Kelemen, Gillikin *et al.* 2018). In addition, stable carbon and oxygen isotope data in bivalve shells have been successfully used to reconstruct river discharge rates, water temperatures (Dettman, Reische *et al.* 1999; Kelemen, Gillikin *et al.* 2017) and Dissolved Inorganic Carbon (DIC) contents (McConnaughey and Gillikin 2008). Furthermore, freshwater mussels are also successfully used as archival indicators of heavy metal pollution in the world (Zuykov et al., 2013; O'Neil and Gillikin, 2014), as well as in Australia (Jones and Walker, 1979; Markich et al., 2002; Markich, 2017).

Freshwater mussels have been a traditional food source for Aboriginal Australians for millennia (Negri and Jones, 1995), resulting in abundant shell middens across Australia (Campbell, 1972). A better understanding of modern shells in general and of the genera present in shell middens is essential for providing a basis for deciphering the environmental information preserved in fossil shells. Additionally, mussel populations are under threat in

most freshwater systems in Australia, even in strongholds with high mussel diversity and abundance (Jones and Byrne, 2010), and better knowledge of their life history and other parameters will support protective measures in the future.

In this study, shells of three common freshwater mussel species from the Hunter Basin close to Australia's East coast, *Alathyria profuga* (Gould, 1851), *Cucumerunio novaehollandiae* (Gray, 1834) and *Hyridella drapeta* (Iredale, 1934), are studied to identify their potential as environmental proxy archives. *A. profuga* is abundant in the Hunter, Manning and Shoalhaven Rivers, and occurs sporadically in the Macleay River (Fig. 1). It belongs to the same genus as *A. jacksoni* which is often found in middens from the Murray-Darling Basin; west of the Hunter Basin (Garvey, 2015). We report the first sclerochronology, $\delta^{18}O$ and trace element data on these species with a focus on *A. profuga* as the species which we found to have the best potential for future paleo-environmental research.
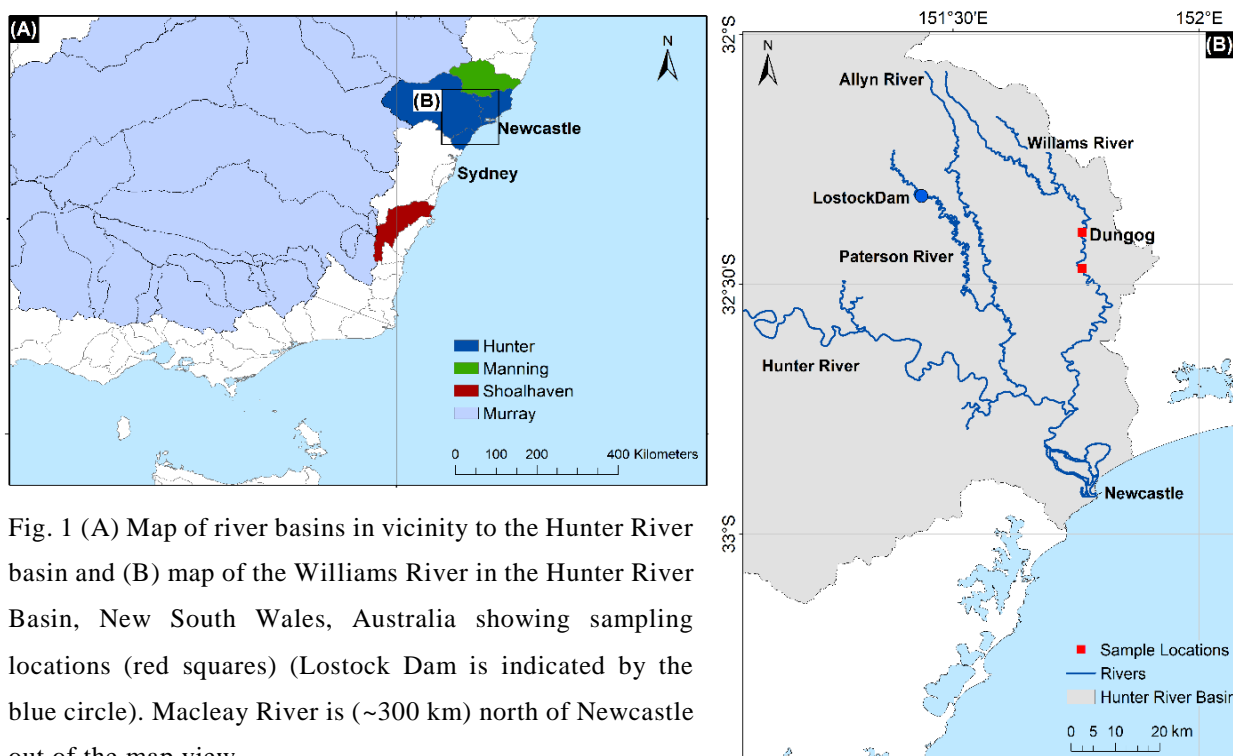
Fig. 1 (A) Map of river basins in vicinity to the Hunter River basin and (B) map of the Williams River in the Hunter River Basin, New South Wales, Australia showing sampling locations (red squares) (Lostock Dam is indicated by the blue circle). Macleay River is (~300 km) north of Newcastle out of the map view.

3.2 Materials and methods

3.2.1 Sample collection and preparation

Samples of three different mussel species, namely *Alathyria profuga* (n=15)*, Cucumerunio novaehollandiae* (n=6) *and Hyridella drapeta* (n=28), were collected alive from the Williams River near Dungog, NSW, Australia (Fig. 1B) in October 2015. The Williams River is an eutrophic river (Nolan et al., 1995) draining an agricultural catchment of over 1000 km^2 in

the north-eastern Hunter Valley (Erskine, 2001), which is dominated by dairying and beef cattle production. The river has a large-capacity, gravel bed channel with a relatively steep gradient, in-channel benches and various types of gravel and bedrock bars (Erskine and Livingstone, 1999). The Hunter Valley has a temperate climate with temperatures ranging from -5 to > 40 °C and averaging around 20 °C in summer. Average annual rainfall is 750 mm with rainfall distribution slightly skewed to summer months (Wells et al., 2008).

Alathyria is a freshwater mussel genus endemic to Australia, belonging to the family Hyriidae (subfamily Velesunioninae), and is closely related to *Velesunio*; a genus that occupies more than 60 river basins across Australia, has a limited distribution in the coastal rivers of New South Wales, but is widespread in inland drainages (Walker et al., 2014). Four species of *Alathyria* are found in Australia (*A. profuga, A. jacksoni, A. pertexta* and *A. condola*) and all are restricted to the eastern part of the continent (Walker et al., 2014). *A. profuga* is found throughout the Shoalhaven, Hunter, Manning and Macleay River basins (Fig. 1B) in New South Wales (Jones and Byrne, 2010). It has a moderately large (maximum length 120 mm), heavy oval shell (Fig. 2A) with a 'unionid' type hinge with blade-like lateral teeth and erect, grooved pseudo-cardinal teeth (McMichael and Hiscock, 1958). Brooding occurs in the austral winter and glochidial release peaks in spring-summer (Jones et al., 1986). A wide range of fish are used as glochidial hosts with flathead gudgeons (*Philypnodon grandiceps*) and Australian smelt (*Retropinna semoni*) being important host fish for this species (Walker et al., 2014).

Cucumerunio novaehollandiae (subfamily Hyriinae,) is a large, distinctive Australian freshwater mussel species with an elongate-elliptical shell (Fig. 2B) bearing strong lachrymose sculpture (McMichael and Hiscock, 1958). These animals attain 200 mm in length, favour fast-flowing water over stable bottoms in gravel-bed streams, and are often found in glides at the base of riffles or on the outer bends of channels (Jones and Byrne, 2010). *C. novaehollandiae* spawn late in the austral summer and is a winter brooder with a tightly synchronised seasonal cycle (Jones et al., 1986). This mussel uses a range of fish species as hosts, especially Australian bass (*Percalates novemaculeata*) (Walker et al., 2014).

Hyridella drapeta (subfamily Hyriinae) occurs in most coastal rivers of southeast Australia, from southeast Queensland to the Otway Ranges, Victoria and is associated with habitats of slow-moderate current velocity (Walker et al., 2014). The shells are oval and a dull leaden

grey to brown colour, medium-sized (attaining a maximum length of 90 mm), with a delicate beak sculpture (Walker et al., 2001a) (Fig. 2C) and, similarly to *A. profuga*, brooding in this species occurs from the late austral winter throughout the warmer months, and glochidia are released throughout the warmer months (Walker, 2016). *H. drapeta* is a host generalist, utilising a range of fish species (Walker et al., 2014).

All three species belong to the subclass Palaeoheterodonta, characterised by an aragonitic shell consisting of three layers with a nacro-prismatic microstructure, covered by a thick organic periostracum (Fig. 2) (Taylor, 1973; Graf and Cummings, 2006).

All mussels were collected live from less than 2 m water depth, soft parts were removed, and shells were air-dried. Sections of approximately 3 mm in thickness were cut with a low speed saw from the left valve along the minimum growth axis (Fig. 2). The sections were mounted on glass slides using metal epoxy, ground with sandpaper in steps (400, 600, 800 and 1200 grit) and eventually polished with 3 and 1 µm diamond pastes. Polished sections were stained with Alcian Blue (Schöne et al., 2007) for 20 minutes at 37–40 °C. This staining procedure uses a mixture of acetic acid, glutaraldehyde and Alcian Blue to lightly etch the shell, fixate the organic growth lines and stain the glycoproteins in the shell, thus enhancing the growth lines. Digital photomicrographs of the shell sections were taken, before and after staining, under a reflected light microscope and were used to measure the growth increment lengths using the software Panopea (©Peinl and Schöne 2004).

A growth increment is defined as the distance perpendicular between two adjacent growth lines (sharp blue lines in the stained samples, Fig. 2A bottom, marked with arrows). Since all animals were live-collected in October 2015, the last growth line was used as the reference to match growth curves from different animals. Each series of growth increments was first visually cross-matched with each other and verified using the visual correlation tool SHELLCORR (Scourse et al., 2006). SHELLCORR generates a graphical output showing lagged running correlations (window width 21 years) between growth-increment series to cross-match series from different shells (representative examples are shown in Fig S1). This procedure enables identifying missing and false growth increments that can occur in individuals (Kesler and Downing, 1997).
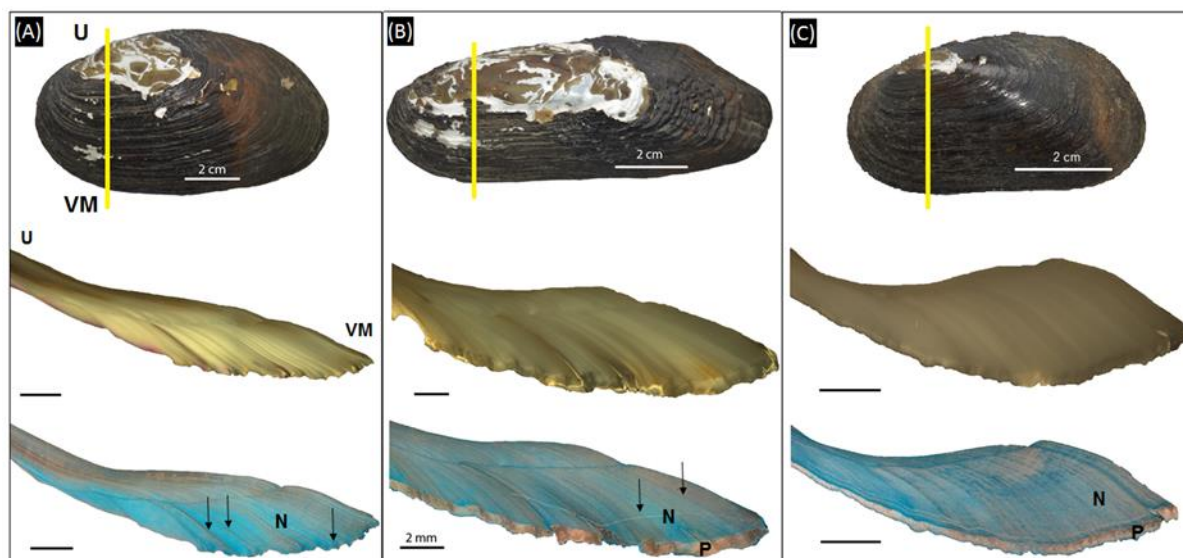
Fig. 2 Left valves (top), polished shell sections (centre) and stained polished shell sections (bottom) for the three mussel species studied. (A) *Alathyria profuga* with extensive shell erosion close to the umbo. The polished shell section (centre) shows dark- and light-coloured alternating growth increments. Alcian Blue stained shell section (bottom) shows growth lines in dark blue (arrows) and growth increments in light blue. (B) *Cucumerunio novaehollandiae*, with shell erosion at the umbo. (C) *Hyridella drapeta*. Scale bar is 2 mm. VM = Ventral Margin, U = Umbo, N = Nacreous layer, P = Prismatic layer. The yellow line indicates the minimum growth direction which is used to cut the section.

3.2.2 Growth increment analysis

The series of growth increments from individual shells demonstrated a strong decrease in growth rate with increasing age of the animal, which is typical for growth increments in bivalve shells (Rypel et al., 2008; Schöne, 2008). Following methods routinely applied in sclerochronology (Schöne and Surge, 2012), this ontogenetic trend was removed by detrending the data series of cumulative growth increment widths by fitting a polynomial regression using the statistical software R (R-core Team, 2017). Each time series was systematically fitted with models of increasing complexity and the improvement was tested using Akaike's Information Criterion (AIC) to determine the best fitting model. Almost all growth series could be fitted with second-order polynomial equations apart from two shells (AP02 and AP15), which were fitted with third-order polynomial equations. Autocorrelation function plots and Durbin-Watson tests revealed no evidence of autocorrelation (Fox and Weisberg, 2011).

In order to remove the age-related growth trend from the measured data, Growth Indices (GI) were calculated by dividing measured growth increments by predicted polynomial growth values for each year. Years with higher growth than predicted by the model result in GI > 1

while GI < 1 represent years of slower than predicted growth (Fritts et al., 2017). Subsequently, the GI data were standardized by subtracting the mean of the GI time series and dividing it by the standard deviation of the GI time series (Schöne, 2003) to yield Standardized Growth Indices values (SGI). A master shell chronology was calculated for *A. profuga* as the average of time series from 15 shells, while 6 shells were used for *C. novaehollandiae*. *H. drapeta* shells did not show clear-enough growth lines to allow for a growth increment chronology.

Chronology statistics including Expressed Population Signal (EPS) and mean series intercorrelation (R_{bar}) were calculated with the software ARSTAN, which is routinely used in dendrochronology (Cook and Holmes, 1996). The values for EPS indicate whether the common variance in the chronology is a sufficiently good expression of the common variance in the population while R_{bar} indicates the strength of the common signal in the chronology. R_{bar} of 0.5 and higher are typically accepted in sclerochronology to indicate a strong enough common signal in a given population of shell (Black et al., 2016). In dendrochronology values of 0.85 and above are usually regarded as the threshold above which the chronology is considered sufficiently robust for climate reconstruction (Wigley et al., 1984). However, EPS values in bivalve sclerochronology are often lower than 0.85 and values of 0.7 or higher are considered as sufficient (Featherstone et al., 2017).

3.2.3 Trace element analyses

Strontium, barium, manganese and calcium concentrations (measured as ^{88}Sr, ^{137}Ba, ^{55}Mn and ^{43}Ca) of four *A. profuga* shells and one shell each of *C. novaehollandiae* and *H. drapeta* was measured *in situ* using Laser Ablation Inductively Coupled Plasma-Mass Spectrometry (LA-ICP-MS). A laser ablation system consisting of an Agilent 7700 quadrupole ICP-MS coupled to a Photon Machines excimer laser (193 nm wavelength) was used. Measurements were carried out with laser energy densities of 4.05 J/cm^2 at a frequency of 5 Hz using helium as the carrier gas (flow rate – 0.8 l/min). After pre-ablation (50 µm spot size at 125 µm/s), continuous curved lines were ablated with a laser spot diameter of 30 µm at 5 µm/s. Lines were placed along the central parts of the nacreous shell layer parallel to the direction of growth and perpendicular to the growth lines from ventral margin to umbo (Fig. S2). Background measurements were carried out for 60 s prior to each ablation. ^{43}Ca was used as the internal standard whilst NIST SRM 612 glass was used as the external standard; data reduction was carried out with the commercial software GLITTER 4.5b (Griffin et al.,

2008). USGS BCR-2G and NIST SRM 610 were measured as secondary reference materials with data taken from the GeoReM preferred values (Jochum et al., 2005). Detection limits (at 99 % confidence level) were Sr = 0.02 µg/g, Ba = 0.20 µg/g and Mn = 0.30 µg/g. The relative standard deviation after repeated measurements of USGS BCR-2G (n=4) was < 1.5 % for Sr, Ba and Mn and the reproducibility of USGS BCR-2G was > 96 % for all measured elements. All element concentrations were converted to molar element to ^{43}Ca ratios.

3.2.4 Stable isotope analyses

The nacreous shell layers of four *A. profuga* shells (AP04, AP10, AP08 and AP11) were sampled using a Micromill (400 µm drill bit) by drilling trenches parallel to the growth lines from the ventral margin to the umbo at approximately 100 µm intervals (Fig. S2). The nacreous shell layer was selected because it is thicker than the prismatic layer in this species and allowed powder sample collection at reasonably high resolution. Sampling was carried out along the centre of the shell section to avoid potential alteration near the inner and outer margins of the shell and care was taken to keep sampling within individual annual growth increments. Collecting enough powder for analysis (~ 1mg) resulted in slightly variable sampling intervals and thus, the temporal resolution of the dataset for some parts of the shell and small growth increments in AP04, AP08 and AP11 towards the ventral margin could not be sampled.

Samples with weights of around 1 mg were transferred into 5.9 ml Labco Exetainer vials, flushed with He gas, reacted with 0.2 ml of 99.9 % m/m phosphoric acid and heated to 70 °C before being rested for two hours. Analyses of oxygen and carbon isotopes were carried using a SerCon 20-22 stable isotope ratio mass spectrometer equipped with a carbonate device at the Research School of Earth Sciences, The Australian National University. The $\delta^{18}O$ values are reported relative to the Vienna Pee-Dee Belemnite (VPDB) reference material based internal reference material (ANU-M1), calibrated Carrara marble and NBS-18. External precision (1 SD) was better than ± 0.1 ‰ based on multiple measurements of the ANU-M1 and other secondary reference materials.

Water temperature was related to the $\delta^{18}O$ value of the shell using the following equation (Grossman and Ku, 1986), as modified by Dettman, Reische & Lohmann (1999):

$$T (^{o}C) = 20.6 - 4.34 (\delta^{18}O_{sample} - [\delta^{18}O_{water} - 0.27]) \tag{1}$$

We used an average value of $\delta^{18}O_{water}$ = -3.5 ‰ obtained from two river water samples (WR-01 = -3.6 ‰ and WR- 02 = -3.4 ‰) collected in October 2016 from the Williams River at Dungog Railway Bridge (Fig. 1B) and measured at the stable isotope facility at Macquarie University, Sydney following standard methods.

3.2.5 Environmental data collection and statistical analysis

Monthly air temperatures at Lostock Dam, NSW, (ca. 50 km from Dungog and approximately 100 m elevation, Fig. 1B), precipitation, water level and water discharge of the Williams River at Dungog, NSW for the period of 1970 to 2015 were obtained from the Australian Government Bureau of Meteorology website (*http://www.bom.gov.au/climate/data/*).

3.2.6 Statistical analysis

Trends and seasonality in the $\delta^{18}O$ series were described by fitting sinusoidal periodic components to model seasonal variation (Bliss, 1970) with a penalised cubic regression spline to model nonlinear trends in time (Wood, 2006; Foster, 2010). The relationship of $\delta^{18}O$ with temperature was examined by fitting a regression of $\delta^{18}O$ against maximum daily temperature, adjusting for correlated errors (Pinheiro and Bates, 2000). Wald statistics were used to evaluate the significance of model terms and regression diagnostics were used to check the model fits (Fox and Weisberg, 2011).

ARIMA time series models (Brockwell and Davis, 2006) were used to identify and describe trends, seasonality and periodicity in the trace element profiles. Molar trace element to calcium ratios were log-transformed before analysis to remove skewness and to stabilise the variance. Preliminary identification of trends and periodicity was undertaken by examining time series plots that were smoothed using locally-weighted polynomial regression (lowess), and plots of the autocorrelation function (ACF) and partial autocorrelation function (PACF) for each series. More details on these statistical model fitting procedures can be found in the electronic supplementary material.

Multiple linear regression models for the master chronologies (*A. profuga* and *C. novaehollandiae*) were developed using the statistical software package R (R-core Team, 2017) to investigate the influence of individual environmental variables on shell growth. A forward stepwise selection procedure using Akaike's Information Criterion as the selection

criterion (the R function, stepAIC) was used to determine the best combination of environmental variables. Akaike's Information Criterion was used to select the best combination of environmental variables that explained the most variation in shell growth (Venables and Ripley, 2002). The correlations between pairs of environmental variables were examined using pairwise correlation analysis (Kleinbaum, 1998) and highly correlated variables were removed from the analysis. Correlations among predictor variables were weak except for water level and river discharge (therefore, only river discharge was selected as the predictor variable to represent both), and only uncorrelated combinations of predictors were used in regression models.

3.3 Results
3.3.1 Shell size and age structure

A. profuga was the dominant mussel species in the Williams River in this study, with lengths ranging from 9.5 to 12.0 cm and height of around 5.5 cm (Fig. 2A, Table 2). *C. novaehollandiae* were the largest shells (Fig. 2B), while *H. drapeta* represented the smallest (Fig. 2C). Shell height and weight were significantly positively correlated with shell length for all three species (r values are all > 0.8, $p < 0.01$). The shells of *A. profuga* and *C. novaehollandiae* were strongly eroded at the umbo, and often more than half of the periostracum was destroyed in these shells (Fig. 2 top). Light- and dark-coloured alternating layers were clearly visible within each growth increment of most shell sections (Fig. 2 middle).

Bivalves form growth lines in their shells due to different factors such as climate, food availability or allocation of energy for reproduction (Soldati et al., 2009; Schöne and Surge, 2012; Roman-Gonzalez et al., 2016). Many species in the Hyriidae family are confirmed to form annual growth lines, for example, *Westralunio carteri* (Klunzinger et al. 2014), *Velesunio angasi* (Humphrey and Simpson 1985) and *Diplodon chilensis patagonicus* (Soldati, et al. 2009). The annual nature of these lines are typically verified by Sr/Ca (Gillikin et al., 2005; Elliot et al., 2009; Yan et al., 2014) and/or by $\delta^{18}O$ values (Versteegh et al., 2010). Similar to studies in the literature, regular Sr/Ca maxima coinciding with the growth lines in *A. profuga* and in *C. novaehollandiae* shells and seasonal variation in $\delta^{18}O$ values (see below) confirmed that growth lines in shells of both species form annually towards the end of summer.

Cyclic patterns of $\delta^{18}O$ values in the four measured *A. profuga* shells (Fig. 3) show high $\delta^{18}O$ values (low temperatures) in the light-coloured growth increments and low $\delta^{18}O$ values (high temperatures) in the dark shell growth increments (Fig. S3). This confirms the formation of dark increments in summer, while lighter coloured increments form in winter supporting literature findings for other freshwater mussels (Soldati et al., 2009). Dark bands are generally thicker than light-coloured bands showing that growth rates are higher in summer than in winter for *A. profuga* shells. Furthermore, the number of pairs of maximum and minimum, i.e. one full annual cycle, matches the number of growth lines in the section (Fig. 3 and S3) and, in addition to the evidence from Sr/Ca confirms the growth lines to be annual in this species. Notably, growth lines form at the end of each dark increment and before the light-coloured increment, hence towards the end of austral summer (Fig. S3).
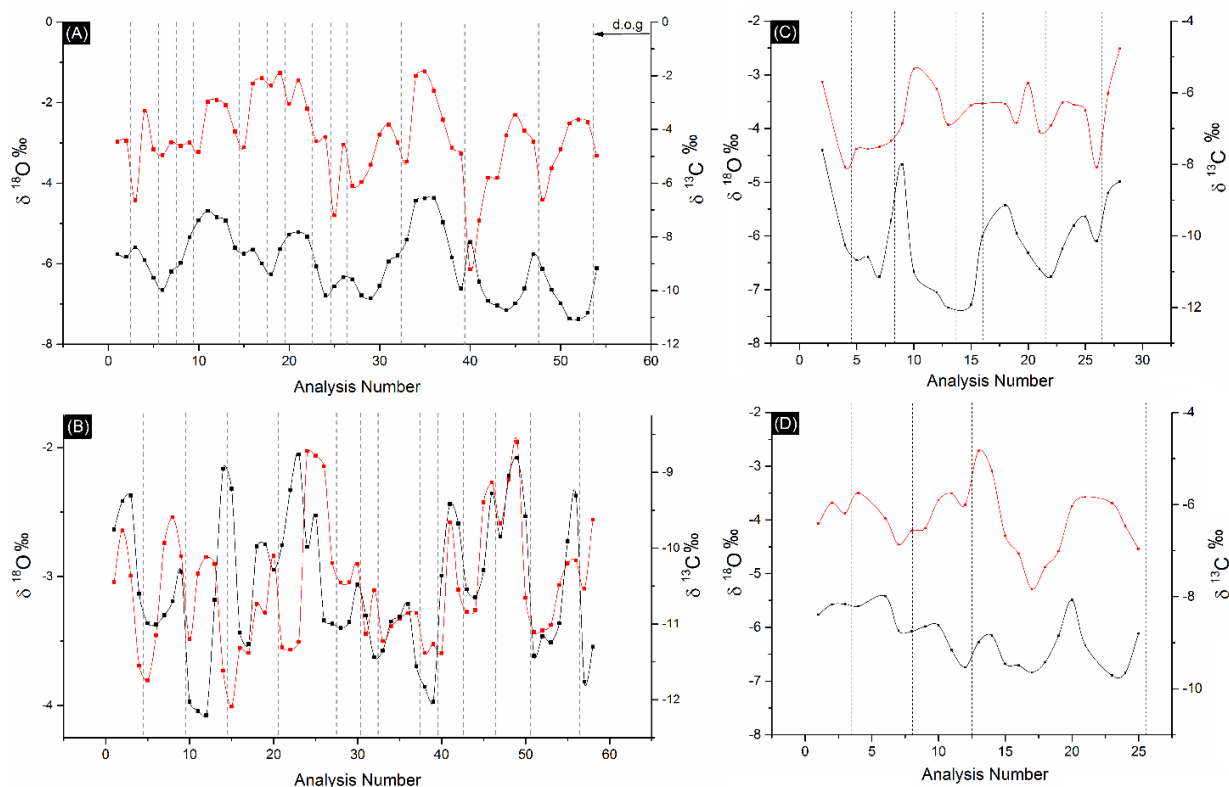
Fig. 3 $\delta^{18}O$ (red line) and $\delta^{13}C$ (black line) variation in four *Alathyria profuga* shells (A) AP04, (B) AP10, (C) AP-08 and AP14 indicating seasonal patterns along the direction of growth. Locations of the growth lines are indicated by the dashed lines. (dog = direction of growth)

Growth line analysis of the entire sample set of *A. profuga* shells (15 shells), resulted in an average lifetime of 25 years with the oldest animal being 33 years of age and the youngest 18 years old (Table 1). It should be noted, however, that these are minimum values as strong shell erosion at the umbo erased about 3-4 years from the record in each shell. Notably, this average age is similar to lifespans of 30 years derived using external ring counts for a different species of the same genus from the Murray River (*A. Jacksoni*; Walker, 1981).

Annual growth rates are high in the first 5 years of life with an average rate of 1.3 cm per year, subsequently decreasing to 0.3 cm per year, equalling an average growth rate of 0.5 cm per year over the entire lifespan.

Growth line counting in *C. novaehollandiae* shells, taking into account umbo erosion, resulted in an average minimum lifespan of 36 years (range 30-47 years) for the sample population (n=6; Table 2). In contrast to *A. profuga* the annual growth rate in this species does not reduce drastically but decreases by half from 0.5 cm per year in the first 5 years of life to 0.25 cm per year after approximately the 5th year of life. Unfortunately, growth lines in *H. drapeta* were too diffuse to identify them reliably across the whole shell (Fig. 2C bottom). However, Sr/Ca in measured *H. drapeta* shells indicated more than 30 maxima, which could be annual cycles, but await confirmation in future studies.

Table 1. Summary of physical characteristics (averages, with ranges in parentheses) of three freshwater mussel species collected from the Williams River. (NA = Not Available).

	A. profuga	*C. novaehollandiae*	*H. drapeta*
Number of Samples	15	6	28
Length (cm)	11.0 (9.5 - 12.0)	14.9 (14.5 - 15.5)	6.2 (4.9 - 7.5)
Width (cm)	5.5 (5.0 - 6.1)	5.7 (5.3 - 6.1)	3.3 (2.6 -3.9)
Dry weight (g)	42.8 (30.7 - 59.3)	46.1 (36.2 - 53.8)	7.8 (3.1 -14.2)
% Shell erosion	~50	~55	~25
Estimated age	25 (18 - 33)	36 (30-47)	NA

3.3.2 Strength of the master chronologies and correlation with environmental variables

The mean series intercorrelation (R_{bar}), an indicator of synchronous population growth, is 0.6 for raw increment widths in *A. profuga*, indicating the high strength in the common signal of the chronology. Although the raw running EPS (10 year window, no overlap) was lower than the commonly used threshold of 0.85 for tree rings (Wigley, Briffa et al. 1984) for most parts of the chronology (Fig. S4), it is overall above 0.7, which is often taken as the threshold value applicable to sclerochronology in bivalve shells (Featherstone et al., 2017), thus, suggesting the common variance in the chronology is a sufficiently good expression of that of the population. Hence, the master chronology of *A. profuga* is sufficiently robust for environmental and climatic reconstructions. In contrast, the R_{bar} value for *C.*

novaehollandiae shells was relatively low (R_{bar} = 0.3), and the running EPS was close to zero (EPS < 0.5) for the complete chronology (Fig. S5), suggesting that the master chronology of this population of *C. novaehollandiae* is unsuitable for such reconstructions.

Although the complete age range for the *A. profuga* sample population spans 33 years (Fig. 4A), based on sufficient sample depth (> 5 samples per year; Fig. 4A), an expressed population signal of higher than 0.7 (Fig. S4) and the average age of the population of 25 years, a master chronology of 26 years (1990 - 2015) was constructed and used for further analysis. A provisional master chronology was created for *C. novaehollandiae*, constructed as the average of 6 SGI series, covered 47 years (Fig. 4B) and indicated distinct variations from the average growth rate in the years 1985, 1994, 2003 and 2006 (Fig. 4B), although at too low EPS value to be considered significant.
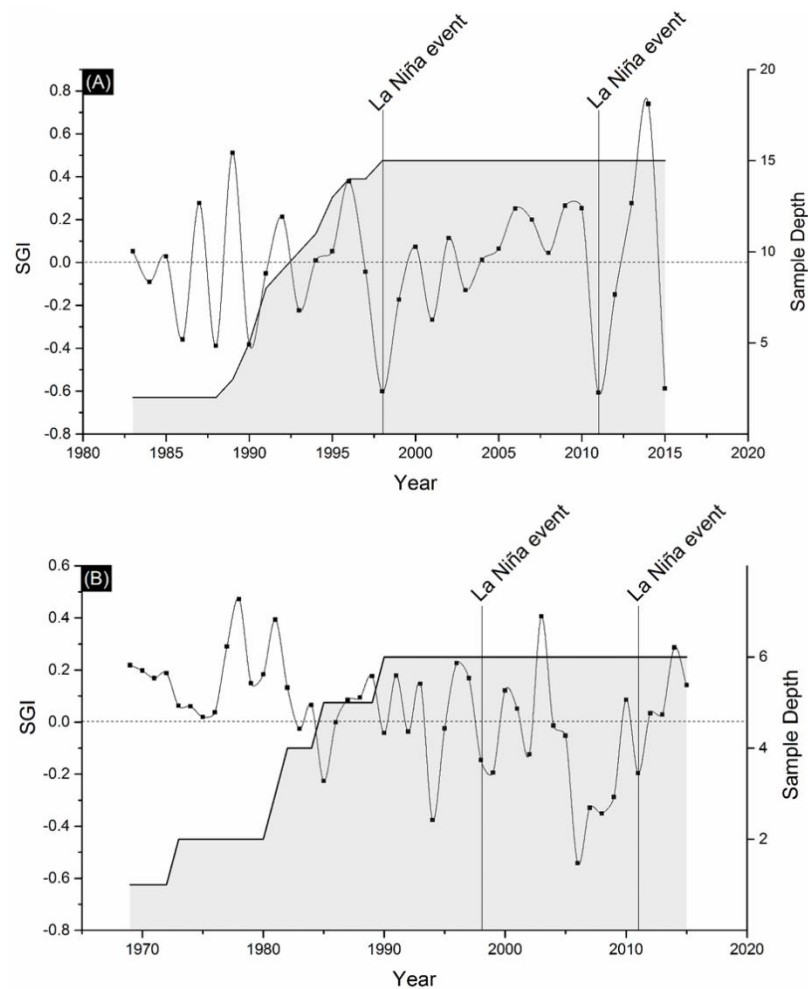
Fig. 4 Master chronology of (A) 15 *Alathyria profuga* and (B) 6 *Cucumerunio novaehollandiae* shells and the respective sample depths. La Niña events are marked by lines.

For *A. profuga,* regression coefficients between SGI and summer and winter air temperature were positive (Table 2), while they are negative between SGI and annual rainfall (Table 2).

Further, multiple linear regression showed that annual rainfall and winter temperature were significant predictors of SGI for *A. profuga* ($F_{2,18}$ = 5.29, p < 0.01) but not for *C. novaehollandiae* ($F_{2, 43}$ = 0.77, p < 0.5) (Table 2).

3.3.3 Oxygen and carbon isotopes

ANOVA, adjusted for serial correlation, revealed significant seasonal variation in $\delta^{18}O$ and $\delta^{13}C$ values in the four measured *A. profuga* shells (example for the two longest series AP04: $F_{2,51}$ = 14.27, p < 0.001 and AP10: $F_{2,55}$ = 10.82, p < 0.001; Fig. S6). Apparent nonlinear trends in shell $\delta^{18}O$ were not significant when autocorrelation was modelled by first-order autoregressive errors for shells (eg; AP04 ϕ = 0.668, s.e. 0.101 and AP10 ϕ = 0.622, s.e. 0.103). Converting these data to water temperature using equation (1), resulted in cyclic patterns with high temperatures in dark layers (maximum 30˚C) and low temperatures in lighter layers (minimum 9˚C; Fig 5). Projected temperatures in the younger portion of shells (within first 10 years) corresponded more closely with measured air temperatures (± 0.1˚C) but diverging by more than 10 ˚C in older sections of the shell with small growth increments. (Fig. 5B).
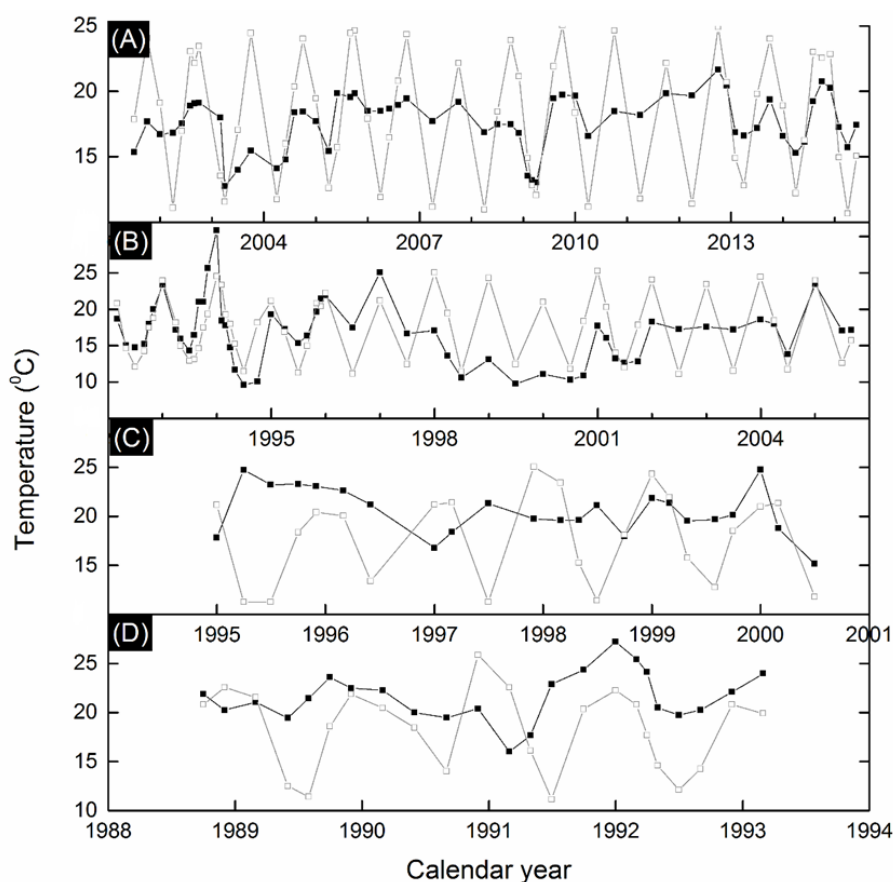
Fig. 5 Comparison between instrumental temperature (open squares) and temperature calculated from the $\delta^{18}O$ values of sample AP10 (A) AP04 (B) AP08 (C) and AP14 (D) (filled squares).

Table 2. Goodness of fit statistics for regression models of Standardised Growth Increment (SGI) and Metal/Ca ratio versus different environmental variables for *Alathyria profuga* and *Cucumerunio novaehollandiae*. (s.e. = standard error, RSQ = coefficient of determination, winter = June to August, summer = December to February). Values significant at 0.05 are in bold and italic. *p*-values in parenthesis are the p-values of predictor variables in multiple regression.

	regression coefficient (s.e.)	p- value	RSQ
Alathyria profuga			
SGI vs summer temperature	0.05 (0.33)	0.30	0.05
SGI vs winter temperature	0.08 (0.32)	0.16	0.10
SGI vs annual rainfall	*0.36* (0.27)	0.00	0.36
SGI vs River discharge	0.17 (0.31)	0.05	0.18
SGI vs Water level	*0.23* (0.30)	0.02	0.23
SGI vs winter temperature + annual rainfall	*0.44* (0.28)	0.01 (0.13,0.01)	0.37
SGI vs winter temperature + annual rainfall + River discharge	*0.44* (0.28)	0.04 (0.11,0.01,0.56)	0.37
Sr/Ca vs temperature	*0.23* (0.46)	0.00	0.23
Ba/Ca vs rainfall	0.03 (0.01)	0.00	0.03
Ba/Ca vs River discharge	0.00 (0.01)	0.97	0.00
Ba/Ca vs rainfall (one month lag)	0.01 (0.01)	0.15	0.01
Ba/Ca vs rainfall (Chichester Dam)	0.02 (0.01)	0.01	0.02
Cucumerunio novaehollandiae			
SGI vs summer temperature	0.03 (0.21)	0.26	0.03
SGI vs winter temperature	0.00 (0.21)	0.70	0.00
SGI vs annual rainfall	0.01 (0.21)	0.55	0.00
SGI vs River discharge	0.16 (0.22)	0.12	0.12
SGI vs Water level	0.12 (0.22)	0.12	0.12
SGI vs winter temperature + annual rainfall	0.01 (0.21)	0.76 (0.66,0.53)	0.01
SGI vs winter temperature + annual rainfall + River discharge	0.16 (0.22)	0.50 (0.92,0.76,0.43)	0.12
Sr/Ca vs temperature	*0.20* (0.66)	0.00	0.20
Ba/Ca vs rainfall	0.02 (0.02)	0.18	0.02
Ba/Ca vs River discharge	0.00 (0.12)	0.34	0.00
Ba/Ca vs rainfall (one month lag)	0.01 (0.02)	0.05	0.01
Ba/Ca vs rainfall (Chichester Dam)	0.04 (0.02)	0.00	0.04

The δ ^{13}C values range between -8.7 ‰ and of -12.2 ‰ (Fig. 3, Table 4), similar to what has been reported in other freshwater mussel studies (Dettman et al., 1999; Versteegh et al., 2010; Yoshimura et al., 2015). Further, the δ ^{13}C series are in phase with δ^{18}O in sections of the dataset, but have a lag of 2-3 months in others (Fig 3). This is similar to what is recorded for other mussel shells (Carré et al., 2005; Surge et al., 2013; Yoshimura et al., 2015), while some other species show no seasonality in δ^{13}C at all (Foster et al., 2009; Versteegh et al., 2010).

3.3.4 Trace element composition

All three mussel species displayed clear cyclic patterns of Sr/Ca, Ba/Ca and Mn/Ca ratios in their shells along the direction of growth (Fig. 6 and S8). Maxima in Sr/Ca and Ba/Ca ratios are synchronous, while they coincide with minima of Mn/Ca ratios by a small lag (Figs. 6 and 7). Sr/Ca ratios increased with ontogenetic age in *A. profuga* and *C. novaehollandiae* (Fig. 7) suggesting that factors additional to purely environmental parameters (e.g. growth rates or metabolic factors (Schöne et al., 2011) may play a role in the uptake of strontium in shells of this species. In contrast, Ba/Ca increased with ontogenetic age in *A. profuga* but decreased with age in *C. novaehollandiae* (Fig. 7). Lastly, Mn/Ca does not change considerably within the lifespan of the measured mussels (Fig. 7).

Sr/Ca maxima in *A. profuga* shell sections occur immediately preceding each growth line in late summer (Fig. 6). Average monthly Sr/Ca, calculated by combining data from two *A. profuga* shells (AP04 and AP10) spanning 22 years (Fig. 7A), showed a slight, positive relationship with temperature ($F_{1,273}$=80.6, $p < 0.01$; Fig. S9A, Table 2) similarly to Sr/Ca ratios for the *C. novaehollandiae* shell, which also had a positive relationship with temperature (Fig. S9B, Table 2).

Table 3. Average δ ^{18}O and δ ^{13}C (ranges in parentheses) of selected *Alathyria profuga* shells (VPDB) and water samples from Williams River collected in October 2016 (VSMOW).

	δ ^{18}O (‰)	δ ^{13}C (‰)
A. profuga (AP04) (n = 66)	-3.08 (-4.01, -1.96)	-10.50 (-12.21, -8.77)
A. profuga (AP10) (n = 63)	-2.90 (-6.14, -1.23)	-9.01 (-11.06, -6.56)
River water 01 (n = 2)	-3.65 (-3.6, -3.7)	
River water 02 (n = 2)	-3.45 (-3.4, -3.5)	
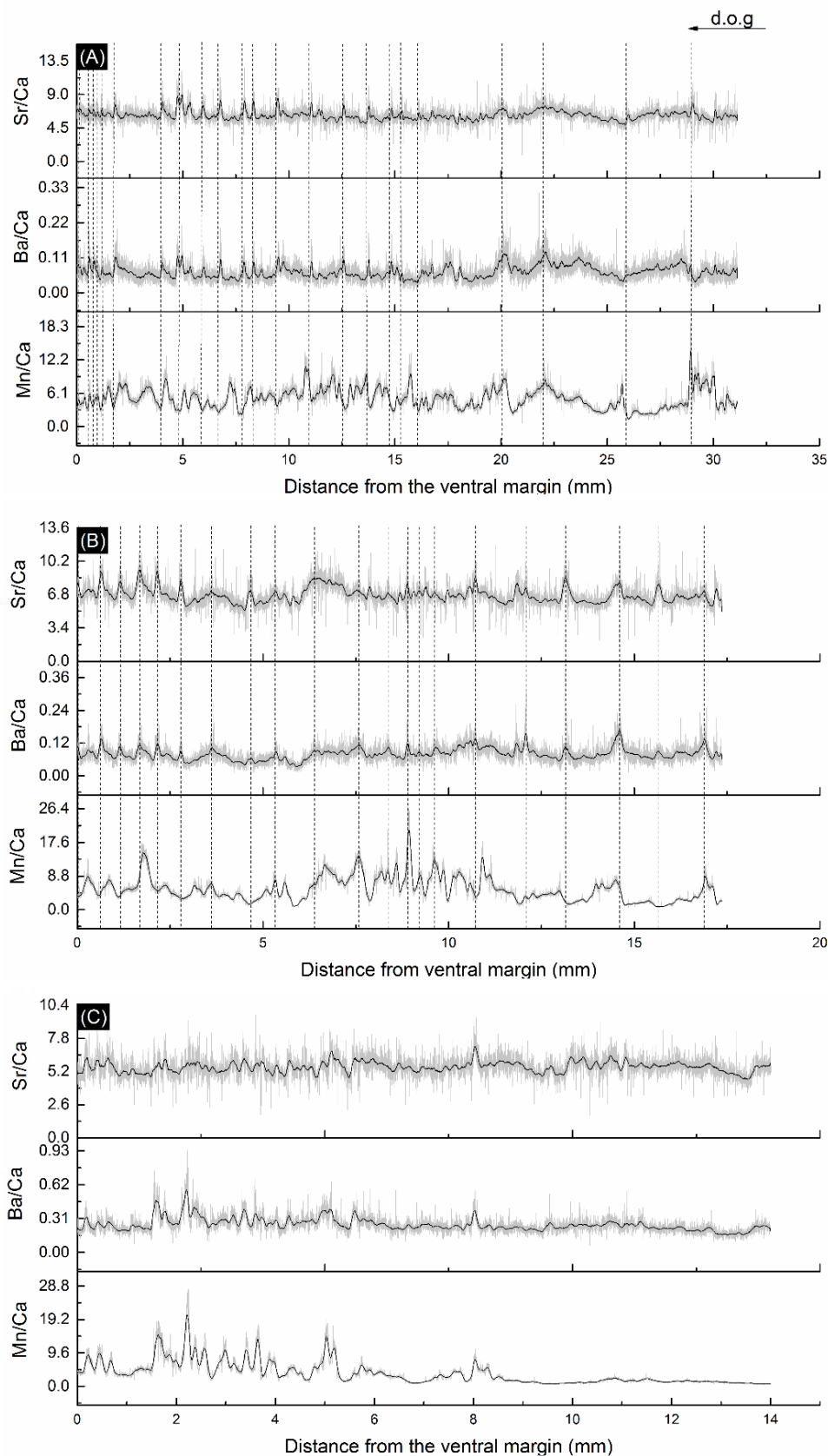
Fig. 6 Element/Ca in the nacre layer of representative individuals of *Alathyria profuga* (top), *Cucumerunio novaehollandiae* (centre) and *Hyridella drapeta* (bottom). The solid dark line indicates the 50 point moving average, while the dashed lines show the locations of the growth lines in *A. profuga* and *C. novaehollandiae*. All element ratios are given in mmol/mol. (dog = direction of growth)
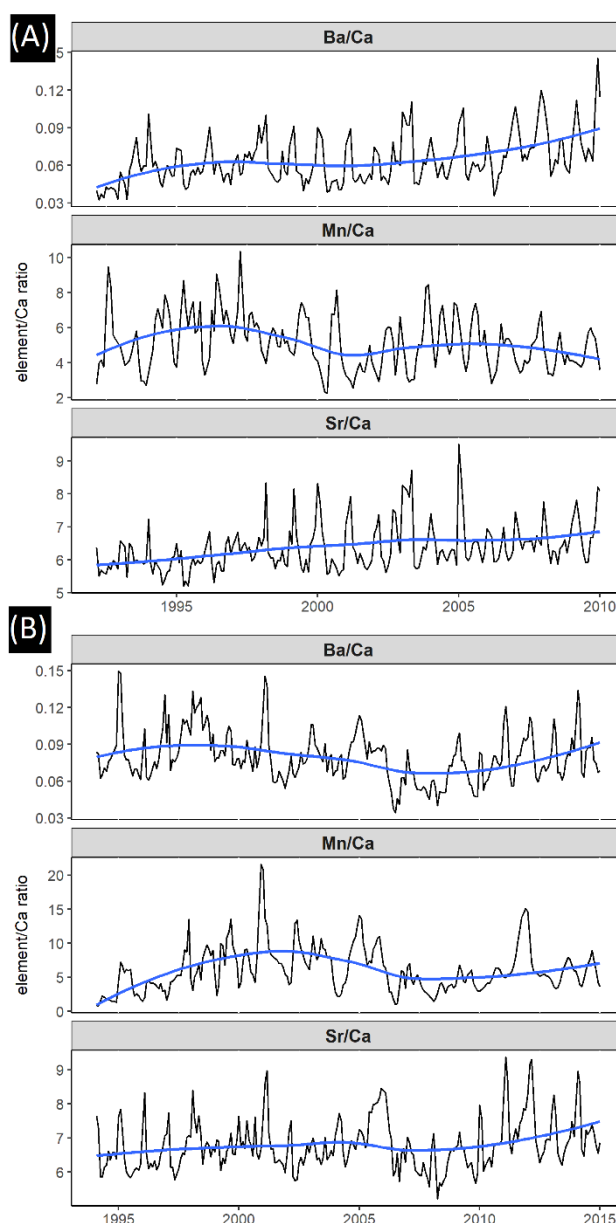
Fig. 7 Monthly averaged Sr/Ca, Ba/Ca and Mn/Ca (in mmol/mol) in the nacre layer of (A) *Alathyria profuga* shell (AP04) and (B) *Cucumerunio novaehollandiae* shell (CN02), showing the variation in Sr/Ca and Ba/Ca throughout the age of the mussel. Blue lines indicate the smoothing curve (more details in the supplementary material). Grey lines show the synchronous maxima in Sr/Ca and Ba/Ca and the inconsistent lag in Mn/Ca.

3.4 Discussion

Sr/Ca ratios in both *A. profuga* and in *C. novaehollandiae* shells have a positive relationship with temperature. Nevertheless, the monthly average Sr/Ca ratios show only a slight positive relationship with instrumental temperature (Fig. S9, Table 2). These correlation coefficient values (which are less than 0.5) are low compared to marine bivalve (Yan et al., 2014) and coral (DeLong et al., 2011) studies which frequently observe values at around 0.9. Laboratory studies showed that Sr/Ca in inorganic aragonite decrease with increasing

temperature (Beck et al., 1992), and Sr/Ca ratios in aragonitic bivalve shells have been used as a thermometer (Yan et al., 2015). However, the behaviour of Sr/Ca ratios varies significantly among different bivalve species: some show negative (Yan et al., 2014) while others have positive (Gillikin et al., 2005; Elliot et al., 2009) correlations with temperature, and some other species do not display any correlation with temperature (Freitas et al., 2005; Schöne et al., 2011). These observations suggest that the incorporation of Sr into aragonitic shells is governed by more than just one variable. Complex biological influences on element intake (Gillikin et al., 2005), growth rate, calcification rate, ontogenetic age, localized organics and crystal morphology (Yan et al., 2014) are some factors that can control Sr/Ca ratios in *A. profuga* and *C. novaehollandiae*, which resulted in low regression coefficient values of Sr/Ca ratios with temperature.

Some studies proposed that Sr/Ca in shells do not directly reflect water temperature, but are rather a function of the growth rate, which in turn depends on temperature (Schöne et al., 2011). This was also seen in the Sr/Ca ratios in *A. profuga* and in *C. novaehollandiae* where the ratios decrease towards the growth break (Fig. 7).

All Ba/Ca maxima in *A. profuga* and in *C. novaehollandiae* are in phase with the Sr/Ca maxima (r = 0.78, p < 0.01; Fig. 6 and 7), indicating that the further are also annual maxima occurring in January. In contrast, marine bivalve species often form irregular Ba/Ca spikes corresponding to riverine discharge (Montaggioni et al., 2006) and allow Ba/Ca ratios to be used as a proxy for freshwater runoff or upwelling in marine settings (Schmitz, 1987; McCulloch et al., 2003; Gillikin et al., 2006; Paytan, 2007). In freshwater environments, in contrast, weathering of surrounding rocks is the main source of Ba during the wetter summer months from terrestrial runoff (Montaggioni et al., 2006). This results in regular seasonal Ba/Ca maxima in freshwater shells (Carroll and Romanek, 2008), which are usually not disturbed by occasional large peaks as in marine shells.

Rainfall in the Hunter river basin is slightly skewed to austral summer, which explains the maxima in January. However, Ba/Ca correlated neither with rainfall nor with river discharge (Table 3) in any of the studied shells. Rainfall data with a one-month lag and rainfall at Chichester Dam (30 km upstream) also remained only weakly correlated with Ba/Ca (Table 3), showing that the lack of correlation was not caused by a lag owing to the large capacity of the Williams River. These results imply that Ba/Ca ratios in *A. profuga* and *C. novaehollandiae* do not vary substantially with changes in Ba concentration in river water or

the relative Ba content in Williams River does not change considerably during wetter summer months.

Riverine runoff alone cannot explain Ba fluxes in freshwater shells (Izumida et al., 2011; Zhao et al., 2017), but factors such as biogenic activity, food supply and temperature are also of influence. In addition, elevated Ba levels can also reflect ingestion of Ba-rich phytoplankton, i.e. primary productivity in the stream (Poulain et al., 2015), which could also explain the formation of maxima during summer in our dataset.

Although there was a slight periodicity in the young shells (Fig. 6), Mn/Ca maxima in *A. profuga* and *C. novaehollandiae* do not follow the same pattern as Sr/Ca and Ba/Ca (Fig. 7) but have an irregular lag. Jeffree, et al. (1995) reported a lag of several days between exposure to elevated environmental Mn concentrations and its expression in the shell. This could possibly be attributed to different metabolic pathways for strontium and manganese (Markich and Jeffree, 1994). However, in the absence of frequent water Mn measurements, this irregularity potentially complicates the use of Mn as a proxy unless the lag time is known.

All Ba/Ca maximums in *A. profuga* and in *C. novaehollandiae* are in phase with the Sr/Ca maximums (r = 0.78, p < 0.01; Fig. 6 and 7), which suggests that these are also annual maximums occurring in January. In contrast, marine species form irregular Ba/Ca spikes, which correspond to riverine discharge (Montaggioni et al., 2006). Therefore, in marine settings, Ba/Ca in biogenic carbonates are mainly used as a proxy for freshwater runoff or upwelling (Schmitz, 1987; McCulloch et al., 2003; Gillikin et al., 2006; Paytan, 2007). However, in freshwater environments, the main source of Ba is the weathering of surrounding rocks, which supplies Ba during wetter summer months from terrestrial runoff (Montaggioni et al., 2006). This results in regular seasonal Ba/Ca maximums in freshwater shells (Carroll and Romanek, 2008), which are usually not disturbed by occasional large maximums.

Rainfall in the Hunter river basin is slightly skewed to austral summer, which explains the maximums in January. However, Ba/Ca correlated neither with rainfall nor with river discharge (Table 3) in any of the studied shells. Rainfall data with a one-month lag and rainfall at Chichester Dam (30 km upstream) also remained only weakly correlated with Ba/Ca (Table 3), showing that the lack of correlation was not caused by a lag owing to the

117

large capacity of the Williams River. These results suggest that Ba/Ca in *A. profuga* and *C. novaehollandiae* do not vary substantially with changes in Ba concentration in river water or the relative Ba content in Williams River does not change considerably during the rainy season. In addition, Ba levels can also reflect ingestion of Ba-rich phytoplankton, i.e. primary productivity in the stream (Thébault et al., 2009; Poulain et al., 2015), which could also explain the formation of maximums during summer. The riverine runoff and primary productivity alone cannot explain Ba fluxes in freshwater shells (Izumida et al., 2011; Zhao et al., 2017), but factors such as biogenic activity, food supply and temperature are also of influence. Information on changes in primary productivity and Ba concentration in the Williams River can assist to improve the understanding of Ba/Ca in the shell in the future.

Although there was a slight periodicity in the young shells (Fig. 6), Mn/Ca maximums in *A. profuga* and *C. novaehollandiae* do not follow the same pattern as Sr/Ca and Ba/Ca (Fig. 7), but have an irregular lag. Jeffree, et al. (1995) reported a lag of several days between exposure to elevated environmental Mn concentrations and its expression in the shell. This could possibly be attributed to different metabolic pathways for strontium and manganese (Markich and Jeffree, 1994). However, in the absence of frequent water Mn measurements, this irregularity potentially complicates the use of Mn as a proxy unless the lag time is known.

3.4.1 Stable isotope variations

The $\delta^{13}C$ series in *A. profuga* follows a cyclic pattern but the frequency of maxima is irregular; some coincide with $\delta^{18}O$ maxima in winter, but others indicate a lag of 2 - 3 months. This is consistent with freshwater (Versteegh et al., 2010) and marine (Foster et al., 2009) bivalve studies, which do not show any seasonal variation in $\delta^{13}C$. Apart from the cyclic pattern, $\delta^{13}C$ values in *A. profuga* shells exhibit sharp fluctuations at several points (Fig. 3), similar to observations for other bivalve species (Grottoli and Eakin, 2007; McConnaughey and Gillikin, 2008; Foster et al., 2009) which are attributed to preferential removal of ^{12}C from the dissolved carbon pool by phytoplankton photosynthesis.

Bivalves primarily use dissolved inorganic carbon (DIC) for the construction of their carbonate shells (Schöne et al., 2005; McConnaughey and Gillikin, 2008), although both, respired CO_2 and ambient DIC, contribute to molluscan shell formation (Yoshimura et al., 2015). Therefore, variation in $\delta^{13}C$ values of bivalve shells mainly indicates changes in food

supply or in primary productivity of the water (Surge et al., 2013), which is also apparent from the elevated $\delta^{13}C$ levels in summer in *A. profuga.* Unfortunately, no information on primary productivity for the Williams River was available to explore this further.

Oxygen isotope variation in bivalve shells is a proxy commonly used in paleoclimate reconstructions (Gillikin et al., 2005), because it is usually deposited in the shell in equilibrium with water and can be used as a paleo-thermometer (Dettman et al., 1999). Calculated temperature values using shell $\delta^{18}O$ here corresponded more accurately with measured air temperatures in the younger portion of shells than in older sections of the shell, which have smaller growth increments. Most likely this inaccuracy originates from insufficient sampling resolution using powder sample collection by micro-drilling. This causes mixing of shell material formed in a larger time window, resulting in reconstructed temperature values that approximately average out over several months. Employing *in-situ* methods in the future, such as secondary ion mass spectrometry (Herath et al., 2017), could improve the sampling resolution in these shells. Nevertheless, the correlation between instrumental and calculated temperatures for both measured shells was r = 0.5 (p < 0.001), which indicates that the calculated temperature follows the same seasonal cyclic pattern as the instrumental temperatures, despite the averaging errors. This indicates that $\delta^{18}O$ in *A. profuga* can indeed be used as an accurate paleo-thermometer once sampling resolution is improved.

Further, the dependency of the temperature reconstruction on the $\delta^{18}O$ values of river water may also impact on the accuracy of oxygen isotope thermometers, because $\delta^{18}O$ values in freshwater often show substantial seasonal variation due to varying river discharge, rainfall and evaporation (Versteegh et al., 2010; Burchell et al., 2013). This is evident from the 15 ‰ range in Darling River water $\delta^{18}O$ values per year measured in Bourke (~ 800 km North West of Dungog) and the approximately 5 ‰ variations in Condamine River water (~ 700 km North of Dungog) (Meredith et al., 2009; Martinez et al., 2015). Monthly water monitoring would be needed to improve our understanding of $\delta^{18}O$ variability leading to more accurate temperature reconstructions.

3.4.2 Climate signals recorded in the shell growth

The master chronology of *A. profuga* suggests that growth rate has a negative relationship with rainfall but is positively correlated with temperature and shows that *A. profuga* shell

growth increase with temperature and decrease with rainfall. This was confirmed by linear regression of the data from 1995 to 2015 (Table 2), which showed that standardized growth increments were significantly negatively associated with rainfall ($R^2 = 0.36$, $p < 0.01$), while summer and winter air temperatures show a small positive relationship with SGI ($R^2 = 0.05$, $p < 0.5$ and $R^2 = 0.08$, $p < 0.5$ respectively). Further, both, water level and river discharge of the Williams River were negatively correlated with shell growth (Table 2) which could be due to the reduction of primary productivity, and thus food availability, during high flow events (Humphrey and Simpson, 1985). In contrast, rainfall and winter temperature both showed small but negative regression coefficient values with SGI in *C. novaehollandiae* (Table 2). Regression coefficient showed a slight increase (up to $R^2 = 0.44$; $p < 0.01$) and the AIC value a slight decrease in *A. profuga* when both rainfall and winter temperature were considered together. No improvement to regression models was observed when river discharge data was added. The same increase in regression coefficients was not observed in *C. novaehollandiae* where linear regression between SGI and the combination of rainfall and winter temperature resulted in $R^2 = 0.01$ ($p < 0.5$).

The resulting linear regression of SGI with combined winter temperature (June – August) and annual average rainfall explained about 37% of the variation in the SGI data ($R^2 = 0.37$; $p < 0.01$) in *A. profuga*. Factors such as the nutrient content of the water and the largely unknown metabolic control on shell precipitation could be contributing to the portion that is not described by this model. Nevertheless, these results suggest that the shell growth rates of *A. profuga* are reliable indicators for winter temperature and rainfall in the Hunter Basin. The same environmental variables explained only about 2% of the variation in growth in *C. novaehollandiae*.

Sea surface temperature in the Pacific, which is frequently influenced by the El Nino Southern Oscillation (ENSO), is the single most important factor in determining climate in eastern Australia (McCulloch et al., 1994). Similarly, the Southern Annular Mode (SAM) also has a major influence on temperatures from the mid-latitudes to the South polar region (Abram et al., 2014). During La Niña events Australia typically experiences an increase in the amount of rainfall and below average temperature through winter and spring (Miralles et al., 2014). Considering the regression coefficient between high rainfall and low temperature, shell growth in *A. profuga* is most likely reduced during these events.

Throughout 2010-12 Australia experienced record high rainfalls, related to a strong La Niña event and a strong positive phase of the SAM (Lim et al., 2016). This event is clearly recorded by the characteristically slow growth in the shells collected from the Williams River (Fig. 4A). Another distinctive low growth phase occurred in the shells in 1997 (Fig. 4A), which was also a La Niña event in Australia (Bureau of Meteorology, Australia). Contrastingly, shell growth did not differ significantly from average growth rates for El Niño years such as 1994, 1997 and 2002 which caused reduced rainfall in the area. Since the resulting regression coefficient values were insufficiently low, a comparison between regional climatic variables such as ENSO or SAM was not attempted for *C. novaehollandiae*.

3.5 Conclusions

This study identified that both *A. profuga* and *C. novaehollandiae* have good potential for future sclerochronology studies. Further, results provided the first age estimations for *A. profuga* from the Hunter River basin with an average age of 25 in the studied population and a maximum lifespan of 33 years. Shell growth rates of *A. profuga* are an indicator of winter temperature and annual rainfall in the Williams River and these variables explained 37 % of the variations in shell growth. Further, the shells also recorded several strong La Niña and SAM events indicating the usefulness of *A. profuga* in recognizing local and regional climatic events.

None of the element to calcium ratios of either *A. profuga* or *C. novaehollandiae* provided significant relationships with temperature, suggesting that the metabolic influence over trace element incorporation is stronger than that of the ambient environment. In contrast, calculated $\delta^{18}O$ temperatures were accurate (± 0.1 ˚C) in the shells. In addition to functioning as a thermometer, the seasonal variation of oxygen isotopic values can be used to verify the season in which the growth lines are formed as shown by this study.

Both *A. profuga* and *C. novaehollandiae* have shorter life spans compared to northern hemisphere bivalve proxy archives such as *Arctica islandica* (Schöne and Surge, 2012).. However, owing to their relatively larger shell size and distinct growth breaks together with promising results from this study, *A. profuga* has the potential to become an environmental proxy archive. However, improving statistical analysis by considering a large population for *C. novaehollandiae* and development of different staining methods for *H. drapeta* could increase the prospects for using these species in the future.

3.6 References

Abram, N.J., Mulvaney, R., Vimeux, F., Phipps, S.J., Turner, J. and England, M.H., 2014. Evolution of the Southern Annular Mode during the past millennium. Nature Climate Change, 4(7): 564-569.

Ariztegui, D., Bösch, P. and Davaud, E., 2007. Dominant ENSO frequencies during the Little Ice Age in Northern Patagonia: the varved record of proglacial Lago Frias, Argentina. Quaternary International, 161(1): 46-55.

Beck, J.W., Edwards, R.L., Ito, E., Taylor, F.W., Recy, J., Rougerie, F., Joannot, P. and Henin, C., 1992. Sea-surface temperature from coral skeletal strontium/calcium ratios. Science, 257(5070): 644-647.

Black, B.A., Griffin, D., Sleen, P., Wanamaker, A.D., Speer, J.H., Frank, D.C., Stahle, D.W., Pederson, N., Copenheaver, C.A. and Trouet, V., 2016. The value of crossdating to retain high-frequency variability, climate signals, and extreme events in environmental proxies. Global change biology, 22(7): 2582-2595.

Bliss, C.I., 1970. Statistics in biology. Vol. 2. Statistics in biology. Vol. 2.

Brockwell, P.J. and Davis, R.A., 2006. Introduction to time series and forecasting. Springer International Publishing, Basel.

Burchell, M., Cannon, A., Hallmann, N., Schwarcz, H. and Schöne, B., 2013. Refining estimates for the season of shellfish collection on the Pacific Northwest coast: Applying higyh-resolution stable oxygen isotope analysis and schlerochronology. Archaeometry, 55(2): 258-276.

Butler, P.G. and Schöne, B.R., 2017. New research in the methods and applications of sclerochronology. Palaeogeography, Palaeoclimatology, Palaeoecology, 465: 295-299.

Byrne, M. and Vesk, P.A., 2000. Elemental composition of mantle tissue granules in *Hyridella depressa* (Unionida) from the Hawkesbury-Nepean River system, Australia: inferences from catchment chemistry. Marine and freshwater research, 51(2): 183-192.

Campbell, V., 1972. Some Radiocarbon Dates for Aboriginal Shell Middens in the Lower Macleay River Valley, New South Wales. Mankind, 8(4): 283-286.

Carré, M., Bentaleb, I., Blamart, D., Ogle, N., Cardenas, F., Zevallos, S., Kalin, R.M., Ortlieb, L. and Fontugne, M., 2005. Stable isotopes and sclerochronology of the bivalve *Mesodesma donacium*: potential application to Peruvian paleoceanographic reconstructions. Palaeogeography, Palaeoclimatology, Palaeoecology, 228(1): 4-25.

Carroll, M. and Romanek, C.S., 2008. Shell layer variation in trace element concentration for the freshwater bivalve *Elliptio complanata*. Geo-Marine Letters, 28(5-6): 369-381.

Cook, E. and Holmes, R., 1996. Guide for computer program ARSTAN. The international tree-ring data bank program library version, 2(0): 75-87.

DeLong, K.L., Flannery, J.A., Maupin, C.R., Poore, R.Z. and Quinn, T.M., 2011. A coral Sr/Ca calibration and replication study of two massive corals from the Gulf of Mexico. Palaeogeography, Palaeoclimatology, Palaeoecology, 307(1): 117-128.

Dettman, D.L., Reische, A.K. and Lohmann, K.C., 1999. Controls on the stable isotope composition of seasonal growth bands in aragonitic fresh-water bivalves (*Unionidae*). Geochimica et Cosmochimica Acta, 63(7): 1049-1057.

Elliot, M., Welsh, K., Chilcott, C., McCulloch, M., Chappell, J. and Ayling, B., 2009. Profiles of trace elements and stable isotopes derived from giant long-lived *Tridacna gigas* bivalves: potential applications in paleoclimate studies. Palaeogeography, Palaeoclimatology, Palaeoecology, 280(1): 132-142.

Erskine, W. and Livingstone, E., 1999. In-channel benches: the role of floods in their formation and destruction on bedrock-confined rivers. Varieties of fluvial form: 445-475.

Erskine, W.D., 2001. Geomorphic evaluation of past river rehabilitation works on the Williams River, New South Wales. Ecological Management and Restoration, 2(2): 116-128.

Featherstone, A.M., Butler, P.G., Peharda, M., Chauvaud, L. and Thébault, J., 2017. Influence of riverine input on the growth of *Glycymeris glycymeris* in the Bay of Brest, North-West France. PloS one, 12(12): e0189782.

Foster, L., Allison, N., Finch, A., Andersson, C. and Ninnemann, U., 2009. Controls on δ18O and δ13C profiles within the aragonite bivalve *Arctica islandica*. The Holocene, 19(4): 549-558.

Fox, J. and Weisberg, S., 2011. An R companion to applied regression, 2nd edn Sage Publications. Thousand Oaks, CA.

Freitas, P., Clarke, L.J., Kennedy, H., Richardson, C. and Abrantes, F., 2005. Mg/Ca, Sr/Ca, and stable-isotope (δ18O and δ13C) ratio profiles from the fan mussel *Pinna nobilis*: Seasonal records and temperature relationships. Geochemistry, Geophysics, Geosystems, 6(4).

Fritts, A.K., Fritts, M.W., Haag, W.R., DeBoer, J.A. and Casper, A.F., 2017. Freshwater mussel shells (*Unionidae*) chronicle changes in a North American river over the past 1000 years. Science of The Total Environment, 575: 199-206.

Garvey, J., 2015. Australian Aboriginal freshwater shell middens from late Quaternary northwest Victoria: Prey choice, economic variability and exploitation. Quaternary International.

Gillikin, D.P., Dehairs, F., Lorrain, A., Steenmans, D., Baeyens, W. and André, L., 2006. Barium uptake into the shells of the common mussel *(Mytilus edulis)* and the potential for estuarine paleo-chemistry reconstruction. Geochimica et Cosmochimica Acta, 70(2): 395-407.

Gillikin, D.P., Lorrain, A., Navez, J., Taylor, J.W., André, L., Keppens, E., Baeyens, W. and Dehairs, F., 2005. Strong biological controls on Sr/Ca ratios in aragonitic marine bivalve shells. Geochemistry, Geophysics, Geosystems, 6(5).

Graf, D.L. and Cummings, K.S., 2006. Palaeoheterodont diversity (Mollusca: *Trigonioida+ Unionoida*): what we know and what we wish we knew about freshwater mussel evolution. Zoological Journal of the Linnean Society, 148(3): 343-394.

Griffin, W., Powell, W., Pearson, N. and O'reilly, S., 2008. GLITTER: data reduction software for laser ablation ICP-MS. Laser Ablation-ICP-MS in the earth sciences. Mineralogical association of Canada short course series, 40: 204-207.

Grossman, E.L. and Ku, T.-L., 1986. Oxygen and carbon isotope fractionation in biogenic aragonite: temperature effects. Chemical Geology: Isotope Geoscience Section, 59: 59-74.

Grottoli, A.G. and Eakin, C.M., 2007. A review of modern coral δ ^{18}O and δ ^{14}C proxy records. Earth-Science Reviews, 81(1): 67-91.

Herath, D., Stern, R., Jacob, D., Clearwater, S. and Fallon, S., 2017. High resolution seasonal signals in bivalve shells from Lake Rotorua, New Zealand, Goldschmidt 2017, Paris, France.

Humphrey, C. and Simpson, R., 1985. The biology and ecology of *Velesunio angasi* (Bivalvia: *Hyriidae*) in the Magela Creek, Northern Territory. Supervising Scientist for the Alligator Rivers Region.

Izumida, H., Yoshimura, T., Suzuki, A., Nakashima, R., Ishimura, T., Yasuhara, M., Inamura, A., Shikazono, N. and Kawahata, H., 2011. Biological and water chemistry controls on Sr/Ca, Ba/Ca, Mg/Ca and δ 18 O profiles in freshwater pearl mussel *Hyriopsis* sp. Palaeogeography, Palaeoclimatology, Palaeoecology, 309(3): 298-308.

Jeffree, R., Markich, S., Lefebvre, F., Thellier, M. and Ripoll, C., 1995. Shell microlaminations of the freshwater bivalve *Hyridella depressa* as an archival monitor of manganese water concentration: Experimental investigation by depth profiling using secondary ion mass spectrometry (SIMS). Experientia, 51(8): 838-848.

Jochum, K.P., Nohl, U., Herwig, K., Lammel, E., Stoll, B. and Hofmann, A.W., 2005. GeoReM: a new geochemical database for reference materials and isotopic standards. Geostandards and Geoanalytical Research, 29(3): 333-338.

Jones, H., Simpson, R. and Humphrey, C., 1986. The reproductive cycles and glochidia of fresh-water mussels (Bivalvia: *Hyriidae*) of the Macleay River, Northern New South Wales, Australia. Malacologia, 27(1): 185-202.

Jones, H.A. and Byrne, M., 2010. The impact of catastrophic channel change on freshwater mussels in the Hunter River system, Australia: a conservation assessment. Aquatic conservation: marine and freshwater ecosystems, 20(1): 18-30.

Jones, H.A. and Byrne, M., 2014. Changes in the distributions of freshwater mussels (*Unionoida*: *Hyriidae*) in coastal south-eastern Australia and implications for their conservation status. Aquatic Conservation: Marine and Freshwater Ecosystems, 24(2): 203-217.

Jones, W. and Walker, K., 1979. Accumulation of iron, manganese, zinc and cadmium by the Australian freshwater mussel *Velesunio ambiguus* (Phillipi) and its potential as a biological monitor. Marine and Freshwater Research, 30(6): 741-751.

Kesler, D. and Downing, J., 1997. Internal shell annuli yield inaccurate growth estimates in the freshwater mussels *Elliptio complanata* and Lampsilis radiata. Freshwater Biology, 37(2): 325-332.

Khandakar, Y. and Hyndman, R.J., 2008. Automatic time series forecasting: the forecast Package for R. Journal of Statistical Software, 27(03).

Kleinbaum, D.G., 1998. Survival Analysis, a Self-Learning Text. Biometrical Journal, 40(1): 107-108.

Lim, E.-P., Hendon, H.H., Arblaster, J.M., Chung, C., Moise, A.F., Hope, P., Young, G. and Zhao, M., 2016. Interaction of the recent 50 year SST trend and La Niña 2010: amplification of the Southern Annular Mode and Australian springtime rainfall. Climate Dynamics: 1-19.

Markich, S., 2017. Sensitivity of the glochidia (larvae) of freshwater mussels (Bivalvia: *Unionida: Hyriidae*) to cadmium, cobalt, copper, lead, nickel and zinc: Differences between metals, species and exposure time. The Science of the total environment, 601: 1427.

Markich, S.J. and Jeffree, R.A., 1994. Absorption of divalent trace metals as analogues of calcium by Australian freshwater bivalves: an explanation of how water hardness reduces metal toxicity. Aquatic toxicology, 29(3): 257-290.

Markich, S.J., Jeffree, R.A. and Burke, P.T., 2002. Freshwater bivalve shells as archival indicators of metal pollution from a copper-uranium mine in tropical northern Australia. Environmental science & technology, 36(5): 821-832.

Martinez, J.L., Raiber, M. and Cox, M.E., 2015. Assessment of groundwater–surface water interaction using long-term hydrochemical data and isotope hydrology: Headwaters of the Condamine River, Southeast Queensland, Australia. Science of the Total Environment, 536: 499-516.

McConnaughey, T.A. and Gillikin, D.P., 2008. Carbon isotopes in mollusk shell carbonates. Geo-Marine Letters, 28(5-6): 287-299.

McCulloch, M., Fallon, S., Wyndham, T., Hendy, E., Lough, J. and Barnes, D., 2003. Coral record of increased sediment flux to the inner Great Barrier Reef since European settlement. Nature, 421(6924): 727-730.

McCulloch, M.T., Gagan, M.K., Mortimer, G.E., Chivas, A.R. and Isdale, P.J., 1994. A high-resolution Sr/Ca and δ18O coral record from the Great Barrier Reef, Australia, and the 1982–1983 El Nino. Geochimica et Cosmochimica Acta, 58(12): 2747-2754.

McMichael, D.F. and Hiscock, I.D., 1958. A monograph of the freshwater mussels (Mollusca: *Pelecypoda*) of the Australian region. Australian Journal of Marine and Freshwater Research, 9(3): 372-527.

Meredith, K., Hollins, S., Hughes, C., Cendón, D., Hankin, S. and Stone, D., 2009. Temporal variation in stable isotopes (18 O and 2 H) and major ion concentrations within the Darling River between Bourke and Wilcannia due to variable flows, saline groundwater influx and evaporation. Journal of Hydrology, 378(3): 313-324.

Miralles, D.G., van den Berg, M.J., Gash, J.H., Parinussa, R.M., de Jeu, R.A., Beck, H.E., Holmes, T.R., Jiménez, C., Verhoest, N.E. and Dorigo, W.A., 2014. El Niño–La Niña cycle and recent trends in continental evaporation. Nature Climate Change, 4(2): 122-126.

Montaggioni, L.F., Le Cornec, F., Corrège, T. and Cabioch, G., 2006. Coral barium/calcium record of mid-Holocene upwelling activity in New Caledonia, South-West Pacific. Palaeogeography, Palaeoclimatology, Palaeoecology, 237(2): 436-455.

Negri, A.P. and Jones, G.J., 1995. Bioaccumulation of paralytic shellfish poisoning (PSP) toxins from the cyanobacterium *Anabaena circinalis* by the freshwater mussel Alathyria condola. Toxicon, 33(5): 667-678.

Nolan, A.L., Lawrance, G.A. and Maeder, M., 1995. Phosphorus speciation in the Williams River, New South Wales: Eutrophication and a chemometric analysis of relationships with other water quality parameters. Marine and freshwater research, 46(7): 1055-1064.

O'Neil, D.D. and Gillikin, D.P., 2014. Do freshwater mussel shells record road-salt pollution? Scientific reports, 4.

Paytan, A.G., Elizabeth M, 2007. Marine barite: Recorder of variations in ocean export productivity. Deep Sea Research Part II: Topical Studies in Oceanography, 54(5): 687-705.

Pinheiro, J.C. and Bates, D.M., 2000. Linear mixed-effects models: basic concepts and examples. Mixed-effects models in S and S-Plus: 3-56.

Poulain, C., Gillikin, D., Thébault, J., Munaron, J.-M., Bohn, M., Robert, R., Paulet, Y.-M. and Lorrain, A., 2015. An evaluation of Mg/Ca, Sr/Ca, and Ba/Ca ratios as environmental proxies in aragonite bivalve shells. Chemical Geology, 396: 42-50.

Roman-Gonzalez, A., Scourse, J.D., Butler, P.G., Reynolds, D.J., Richardson, C.A., Peck, L.S., Brey, T. and Hall, I.R., 2016. Analysis of ontogenetic growth trends in two marine Antarctic bivalves *Yoldia eightsi* and *Laternula elliptica*: Implications for sclerochronology. Palaeogeography, Palaeoclimatology, Palaeoecology.

Rypel, A.L., Haag, W.R. and Findlay, R.H., 2008. Validation of annual growth rings in freshwater mussel shells using cross dating. Canadian Journal of Fisheries and Aquatic Sciences, 65(10): 2224-2232.

Schmitz, B., 1987. Barium, equatorial high productivity, and the northward wandering of the Indian continent. Paleoceanography, 2(1): 63-77.

Schöne, B.R., 2003. A 'clam-ring' master-chronology constructed from a short-lived bivalve mollusc from the northern Gulf of California, USA. The Holocene, 13(1): 39-49.

Schöne, B.R., 2008. The curse of physiology—challenges and opportunities in the interpretation of geochemical data from mollusk shells. Geo-Marine Letters, 28(5-6): 269-285.

Schöne, B.R., Fiebig, J., Pfeiffer, M., Gleβ, R., Hickson, J., Johnson, A.L., Dreyer, W. and Oschmann, W., 2005. Climate records from a bivalved Methuselah (*Arctica islandica*, Mollusca; Iceland). Palaeogeography, Palaeoclimatology, Palaeoecology, 228(1): 130-148.

Schöne, B.R. and Gillikin, D.P., 2013. Unraveling environmental histories from skeletal diaries—advances in sclerochronology. Palaeogeography, Palaeoclimatology, Palaeoecology, 373: 1-5.

Schöne, B.R., Page, N.A., Rodland, D.L., Fiebig, J., Baier, S., Helama, S.O. and Oschmann, W., 2007. ENSO-coupled precipitation records (1959–2004) based on shells of freshwater bivalve mollusks (*Margaritifera falcata*) from British Columbia. International Journal of Earth Sciences, 96(3): 525-540.

Schöne, B.R. and Surge, D.M., 2012. Part N, Revised, Volume 1, Chapter 14: Bivalve sclerochronology and geochemistry. Treatise online, 46: 1-24.

Schöne, B.R., Zhang, Z., Radermacher, P., Thébault, J., Jacob, D.E., Nunn, E.V. and Maurer, A.-F., 2011. Sr/Ca and Mg/Ca ratios of ontogenetically old, long-lived bivalve shells (*Arctica islandica*) and their function as paleotemperature proxies. Palaeogeography, Palaeoclimatology, Palaeoecology, 302(1): 52-64.

Scourse, J., Richardson, C., Forsythe, G., Harris, I., Heinemeier, J., Fraser, N., Briffa, K. and Jones, P., 2006. First cross-matched floating chronology from the marine fossil record: data from growth lines of the long-lived bivalve mollusc *Arctica islandica*. The Holocene, 16(7): 967-974.

Shumway, R.H. and Stoffer, D.S., 2010. Time series analysis and its applications: with R examples. Springer Science & Business Media.

Soldati, A., Jacob, D., Schöne, B., Bianchi, M. and Hajduk, A., 2009. Seasonal periodicity of growth and composition in valves of *Diplodon chilensis patagonicus* (d'Orbigny, 1835). Journal of Molluscan Studies, 75(1): 75-85.

Surge, D., Wang, T., Gutierrez-Zugasti, I. and Kelley, P.H., 2013. Isotope sclerochronology and season of annual growth line formation in limpet shells (*Patella vulgata*) from warm-and cold-temperate zones in the eastern North Atlantic. Palaios, 28(6): 386-393.

Taylor, J.D., 1973. The structural evolution of the bivalve shell. Palaeontology, 16(3): 519-534.

Team, R.C., 2017. R: A language and environment for statistical computing [Internet]. Vienna, Austria; 2014.

Thébault, J., Chauvaud, L., L'Helguen, S., Clavier, J., Barats, A., Jacquet, S., Pécheyran, C. and Amouroux, D., 2009. Barium and molybdenum records in bivalve shells: Geochemical proxies for phytoplankton dynamics in coastal environments? Limnology and Oceanography, 54(3): 1002-1014.

Venables, W. and Ripley, B., 2002. Random and mixed effects, Modern applied statistics with S. Springer, pp. 271-300.

Versteegh, E.A., Vonhof, H.B., Troelstra, S.R., Kaandorp, R.J. and Kroon, D., 2010. Seasonally resolved growth of freshwater bivalves determined by oxygen and carbon isotope shell chemistry. Geochemistry, Geophysics, Geosystems, 11(8).

Walker, K., 1981. Ecology of freshwater mussels in the River Murray. Australian Water Resources Council Technical Paper No. 63. Ecology of freshwater mussels in the River Murray. Australian Water Resources Council Technical Paper, 63(63).

Walker, K., 2016. Reproductive phenology of river and lake populations of freshwater mussels (*Unionida: Hyriidae*) in the River Murray. Molluscan Research: 1-14.

Walker, K.F., Byrne, M., Hickey, C.W. and Roper, D.S., 2001a. Freshwater mussels (Hyriidae) of Australasia, Ecology and evolution of the freshwater mussels Unionoida. Springer, pp. 5-31.

Walker, K.F., Byrne, M., Hickey, C.W. and Roper, D.S., 2001b. Freshwater mussels (*Hyriidae*) of Australasia. In: G. Bauer and K. Wächtler (Editors), Ecological Studies. Ecology and evolution of the freshwater mussels Unionoida. Ecological Studies : 145. Springer, Berlin, pp. 5-31.

Walker, K.F., Jones, H.A. and Klunzinger, M.W., 2014. Bivalves in a bottleneck: taxonomy, phylogeography and conservation of freshwater mussels (*Bivalvia: Unionoida*) in Australasia. Hydrobiologia, 735(1): 61-79.

Wells, T., Hancock, G. and Fryer, J., 2008. Weathering rates of sandstone in a semi-arid environment (Hunter Valley, Australia). Environmental geology, 54(5): 1047-1057.

Wigley, T.M., Briffa, K.R. and Jones, P.D., 1984. On the average value of correlated time series, with applications in dendroclimatology and hydrometeorology. Journal of Climate and Applied Meteorology, 23(2): 201-213.

Yan, H., Shao, D., Wang, Y. and Sun, L., 2014. Sr/Ca differences within and among three Tridacnidae species from the South China Sea: Implication for paleoclimate reconstruction. Chemical Geology, 390: 22-31.

Yan, H., Sun, L., Shao, D. and Wang, Y., 2015. Seawater temperature seasonality in the South China Sea during the late Holocene derived from high-resolution Sr/Ca ratios of *Tridacna gigas*. Quaternary Research, 83(2): 298-306.

Yoshimura, T., Izumida, H., Nakashima, R., Ishimura, T., Shikazono, N., Kawahata, H. and Suzuki, A., 2015. Stable carbon isotope values in dissolved inorganic carbon of ambient waters and shell carbonate of the freshwater pearl mussel (*Hyriopsis* sp.). Journal of Paleolimnology, 54(1): 37-51.

Zhao, L., Schöne, B.R. and Mertz-Kraus, R., 2017. Controls on strontium and barium incorporation into freshwater bivalve shells (*Corbicula fluminea*). Palaeogeography, Palaeoclimatology, Palaeoecology, 465: 386-394.

Zuykov, M., Pelletier, E. and Harper, D.A., 2013. Bivalve mollusks in metal pollution studies: from bioaccumulation to biomonitoring. Chemosphere, 93(2): 201-208.

3.7 Supplementary material – Chapter 3

3.7.1 Supplementary - Methods

Overview of ARIMA models

Trace element ratios were log-transformed to remove skewness and stabilise the variance. Locally-weighted polynomial regression (lowess) smoothers were superimposed on time series plots to reveal trends in trace element concentrations with shell age. This was followed by more rigorous ARIMA Time series methods to identify and describe the presence of trends, seasonality and periodicity in temporal profiles of trace element composition in two *Alathyria profuga* shells (AP04 and AP10). Model fitting was aided by an automatic model-fitting algorithm which combines unit root tests, minimization of the AICc and MLE to obtain an ARIMA model (Khandakar and Hyndman, 2008).

An ARMA(p, q) process for the mean-centered [X_t] is given as:

$$X_t - \varphi_1 X_{t-1} - \cdots - \varphi_p X_{t-p} = Z_t + \theta_1 Z_{t-1} + \cdots + \theta_q Z_{t-q},$$

where φ_p and θ_q are the p and q autoregressive and moving average coefficients, respectively. and (Ariztegui et al.) ~ WN(0, σ^2). An important requirement of an ARMA(p, q) process is that the [X_t] are stationary. Trends in the X_t series may be removed to achieve stationarity by differencing (e.g. $\nabla_1 = X_t - X_{t-1}$) to produce an integrated ARMA(p, q) or ARIMA(p, d, q) model.

ARIMA models may be modified to include seasonal parameters to represent periodic model components in a similar way to ARIMA models. Hence, we describe a multiplicative seasonal ARIMA or SARIMA model as:

$$\text{SARIMA}(p, d, q)(P, D, Q)_s$$

where the subscript s denotes the order of seasonality; e.g. *s = 12* for a monthly time series with an annual periodicity. Refer to Brockwell & Davis (2016) or Shumway & Stoffer (2017) for further details of these models.

Regression with correlated errors (Shumway and Stoffer, 2010) was used to examine the relationship of the trace element ratios Sr/Ca, Ba/Ca and Mn/Ca with temperature. The correlation structure of the residuals was identified by fitting a naïve regression model to the data, followed by fitting an ARMA model to the residuals. The regression model was then refitted with the ARMA model as the error term, by maximum likelihood estimation. The residuals were checked for white noise using the Ljung–Box white noise test and ACF plots.

Fitting of ARIMA time series model to trace element ratios
The ACF plot of the Sr/Ca time series revealed a strong seasonal cycle with a 12 month period for both shells (Fig. S7). The seasonal peaks in shell AP04 are strong for the first two seasons then dampen off before becoming indistinguishable after years 6 or 7. In shell AP10 the seasonal peaks taper off after 4-6 years.

ARIMA models were determined using the auto.arima function (library *forecast*) to compare a range of candidate ARIMA and SARIMA models using the AIC to select the best fitting model. The ARIMA models confirmed the presence of trend in the strontium and Barium series but not manganese. There were seasonal cycles for all trace element series in shell AP10.

Fitting of periodic regression models to δ¹⁸O ratios
We fitted semi-parametric, periodic regression models (Welham *et al.*, 2015) with an annual periodicity and included a nonlinear trend modelled by a penalised cubic regression smooth (Wood, 2006) to explore the pattern of trend and seasonality in the δ¹⁸O series with time.

$$y_i = \beta_0 + \beta_1 sin\left(\frac{2\pi t_i}{12}\right) + \beta_2 cos\left(\frac{2\pi t_i}{12}\right) + s(t_i) + e_i$$

where the sine and cosine terms are dummy variables representing a seasonal cycle with a 12 month period, and $s(t_i)$ represents the cubic regression smooth of the monthly observations t_i. The β_is are regression parameters to be estimated from the data.

3.7.2 Supplementary - Tables

Table S1. Seasonal ARIMA models selected based on the AIC criterion among candidate models. Based on the ACF and PACF plots for the time series, seasonal ARIMA models were fit to the data. ns, not significant. $\nabla_1 = X_t - X_{t-1}$

SARIMA model	Ljung test	*Mean*	*AR1* φ_1	*AR2* φ_2	*MA$_1$* θ_1	*MA$_2$* θ_2	*SAR1* Φ_1	*SAR2* Φ_2	Variance
Shell AP04									
Sr $(2,1,1)(2,0,0)_{12}$	ns	∇_1	0.593 (0.069)	-0.146 (0.071)	-0.980 (0.014)		0.287 (0.065)	0.292 (0.068)	0.0055
Ba $(1,1,2)(2,0,0)_{12}$	ns	∇_1	0.518 (0.095)		-0.710 (0.104)	-0.257 (0.096)	0.258 (0.067)	0.316 (0.072)	0.0303
Mn $(1,0,1)(2,0,0)_{12}$	ns	1.570 (0.067)	0.591 (0.066)		0.483 (0.068)		0.194 (0.067)	0.240 (0.069)	0.0271
Shell AP10									
Sr $(1,0,0)(1,0,0)_{12}$	ns	1.785 (0.016)	0.591 (0.060)				0.240 (0.071)		0.0051
Ba $(1,1,1)(1,0,0)_{12}$	ns	∇_1	0.662 (0.060)		-0.991 (0.024)		0.201 (0.075)		0.0401
Mn $(1,0,1)$	ns	1.227 (0.064)	0.604 (0.068)		0.466 (0.074)				0.0577

Table S2. Parameter estimates for regressions with correlated errors of trace element/calcium ratios (log-transformed) predicted by temperature. ARp, autoregressive model of order p; ARMA, autoregressive moving average model. $\hat{\sigma}^2$, error variance. ns, not significant.

Trace element	Intercept	Temperature	Error model	$\hat{\sigma}^2$
Shell AP04				
Strontium	1.646 (0.064)	0.0113 (0.0034)	AR_1 (0.54)	0.0050
Barium	-3.310 (0.104)	0.0294 (0.005)	AR_1 (0.68)	0.0347
Manganese	1.817 (0.123)	-0.0130 (0.007)[ns]	AR_2 (1.07, -0.39)	0.0296
Shell AP10				
Strontium	1.631 (0.036)	0.0084 (0.002)	AR_1 (0.53)	0.0050
Barium	-3.124 (0.109)	0.0182 (0.006)	AR_1 (0.61)	0.0392
Manganese	1.246 (0.160)	-0.0011 (0.008)[ns]	ARMA (0.60, 0.46)	0.0580

3.7.3 Supplementary – Figures
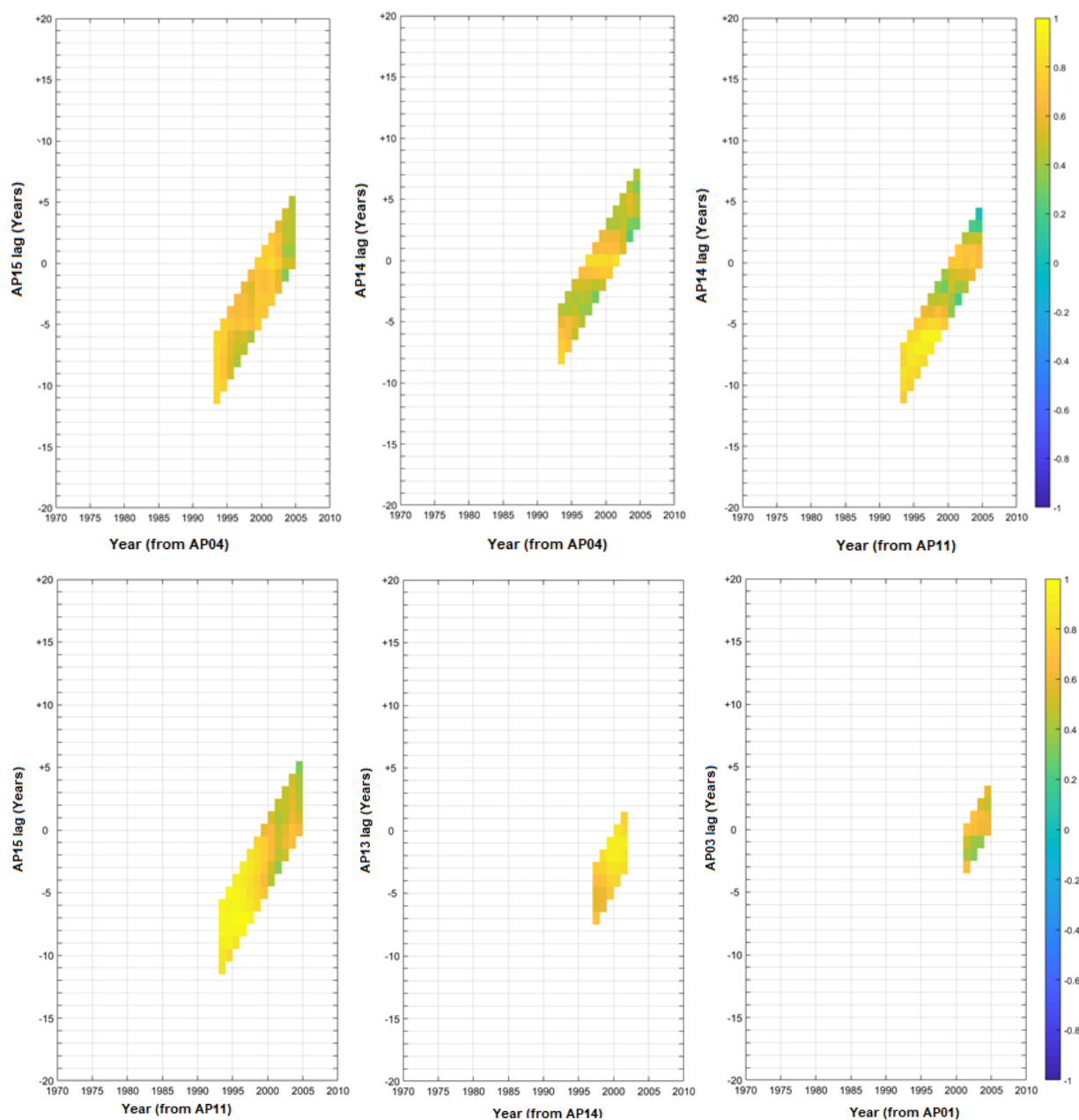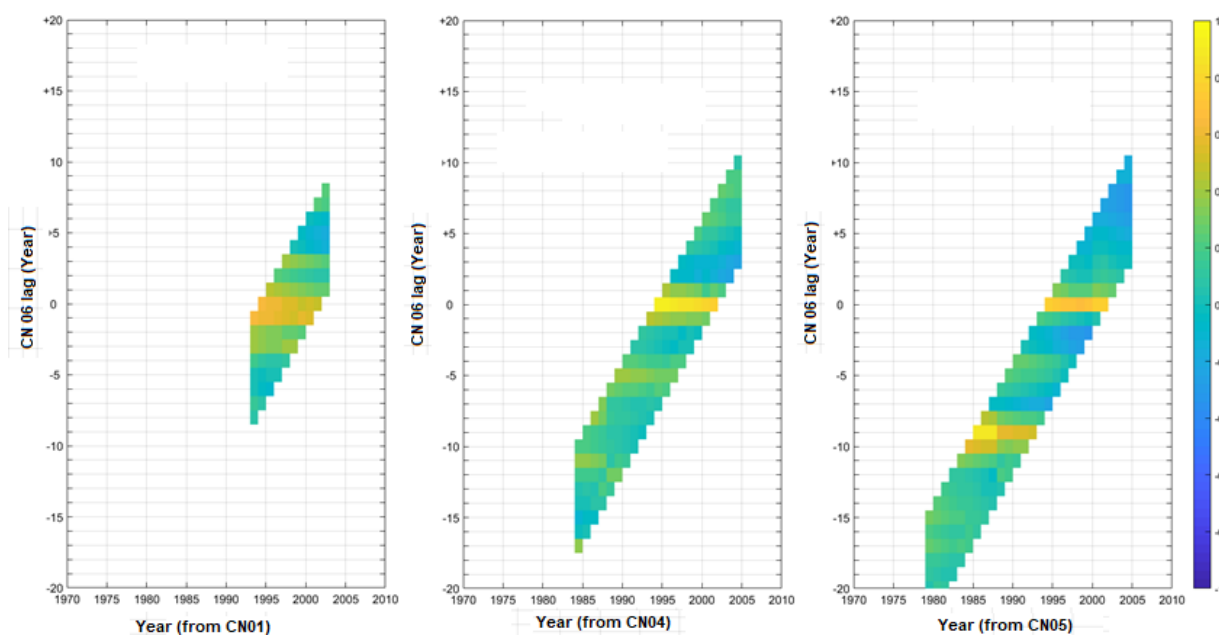
Fig. S1 Selected examples of output from the visual correlation program SHELLCORR. The images show correlation coefficients between pairs of increment width series in a sliding 21-year window at various lags. High positive correlations in yellow, high negative correlations in blue. See Scourse et al. (2006) for more details. Since SHELLCORR produce more than 100 images for the complete sample set, only selected examples from *Alathyria profuga* (top 6) and *Cucumerunio novaehollandiae* (bottom 3) are shown here.

Fig. S2 Cross-sectioned shell of *A. profuga* which indicate where the LA–ICP–MS analysis was done. Black lines indicate example locations of the trenches drilled for oxygen isotope analysis. This image also shows the thickness of the prismatic layer.
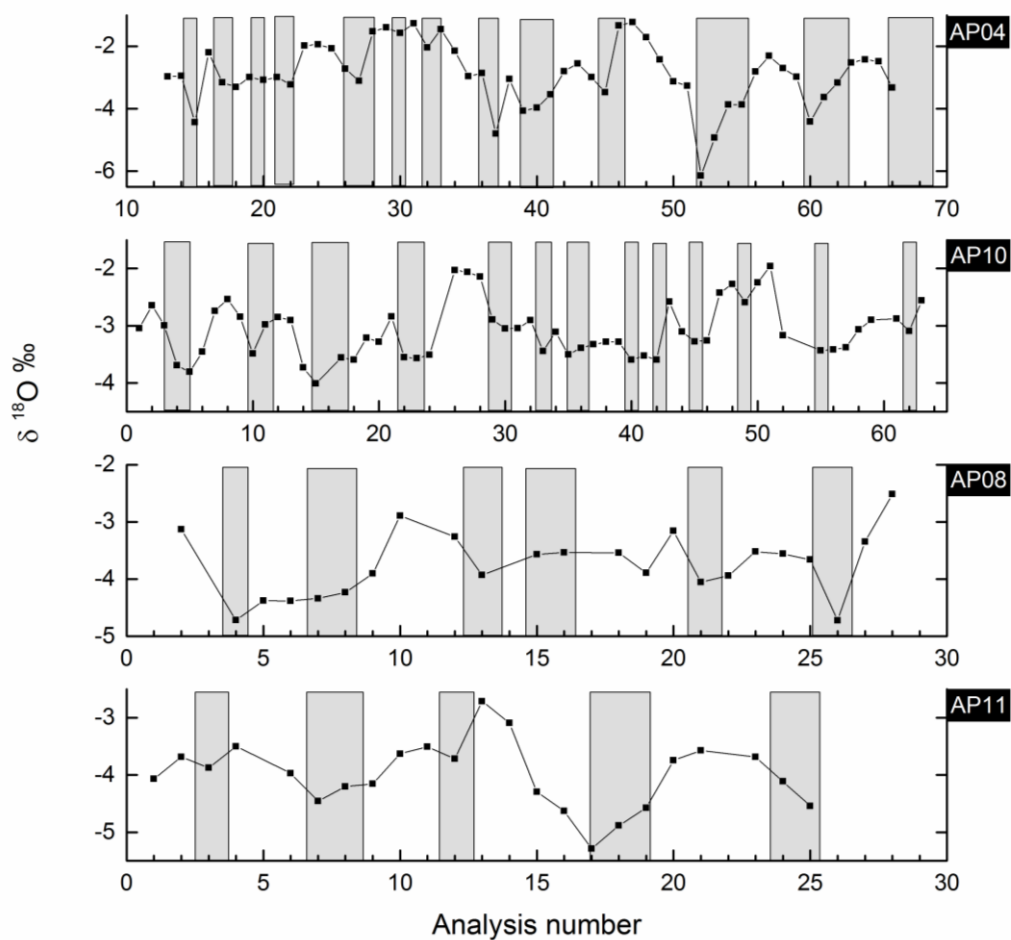
Fig. S3 δ¹⁸O (black line) variation in four *Alathyria profuga* shells indicating seasonal patterns along the direction of growth. Locations of the dark (summer) layer in the shells are indicated by the grey area. (dog = direction of growth).
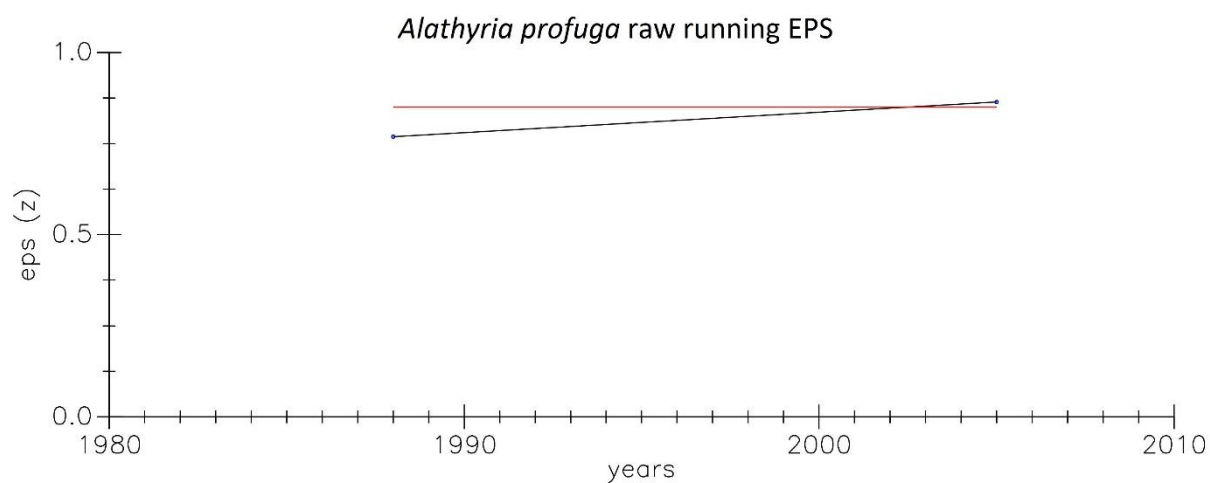
Fig. S4 Expressed population signal (EPS) for *A. profuga* calculated in a 10 year window. EPS value at the start of the window is plotted here. Red line shows the suggested threshold value of 0.85 (Wigley et al., 1984).
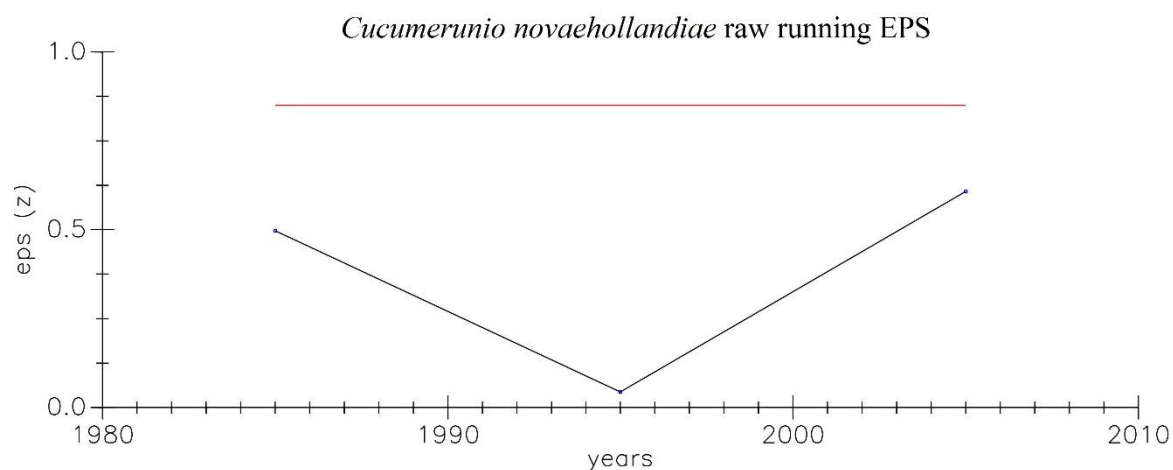
Fig. S5 Expressed population signal (EPS) for *Cucumerunio novaehollandiae* calculated in a 10 year window. EPS value at the start of the window is plotted here. Red line shows the suggested threshold value of 0.85 (Wigley et al., 1984).
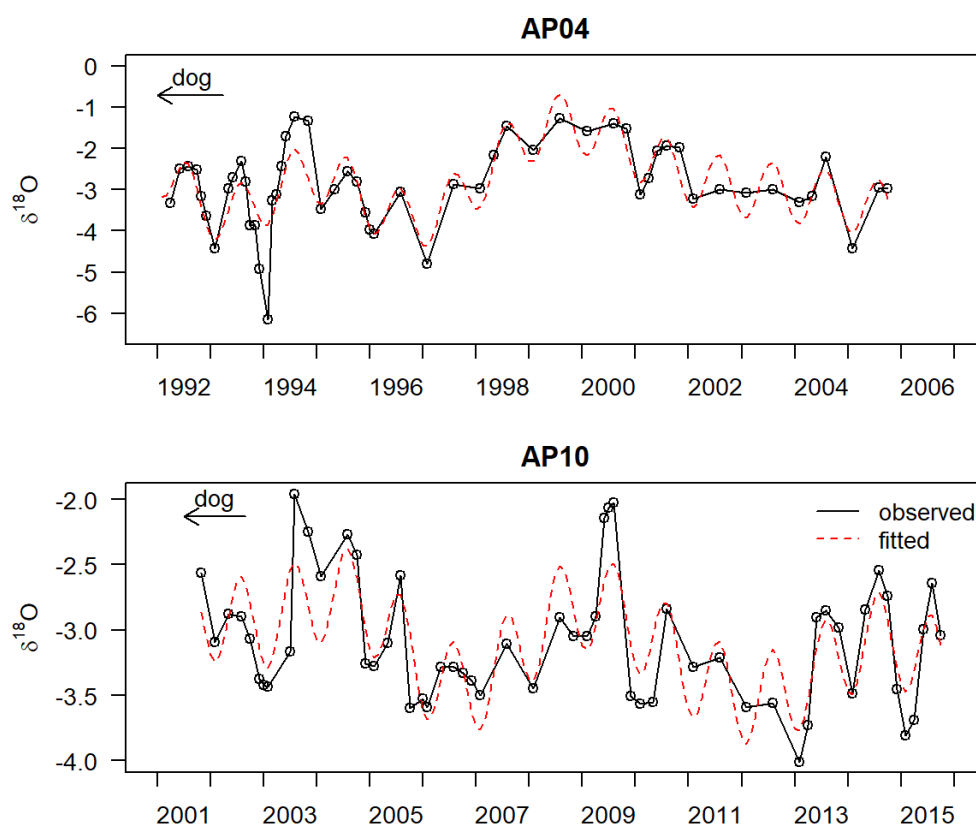
Fig. S6 Observed $\delta^{18}O$ series with fitted values from a periodic regression (with a 12 month period) from two *A. profuga* shells indicating cyclic patterns along the direction of growth. (dog = direction of growth). The period of the sinusoidal components of periodic regression closely matched the peaks and troughs in the cycles for $\delta^{18}O$.
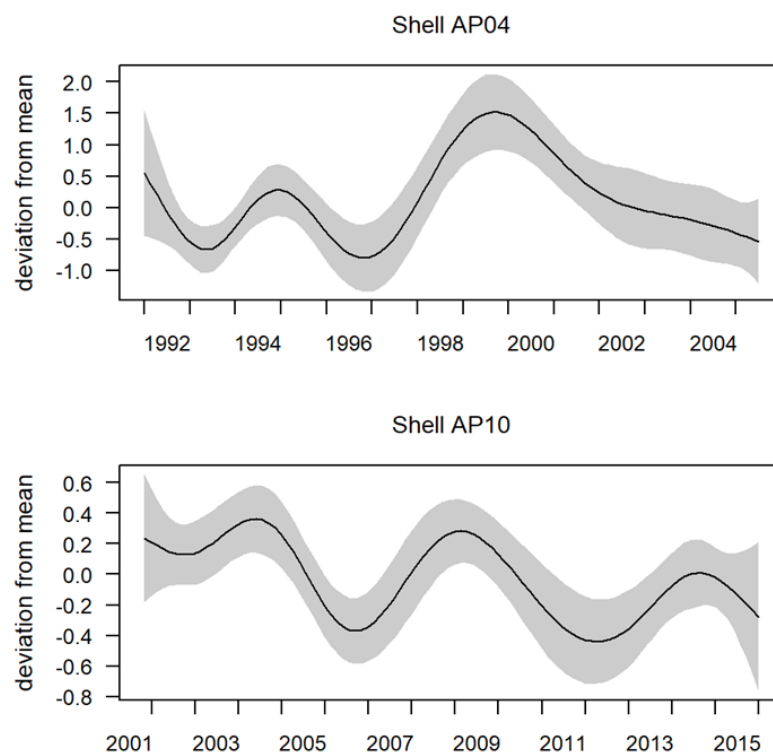
Fig. S7 Non-annual climatic seasonal cycles in δ^{18}O shell profiles
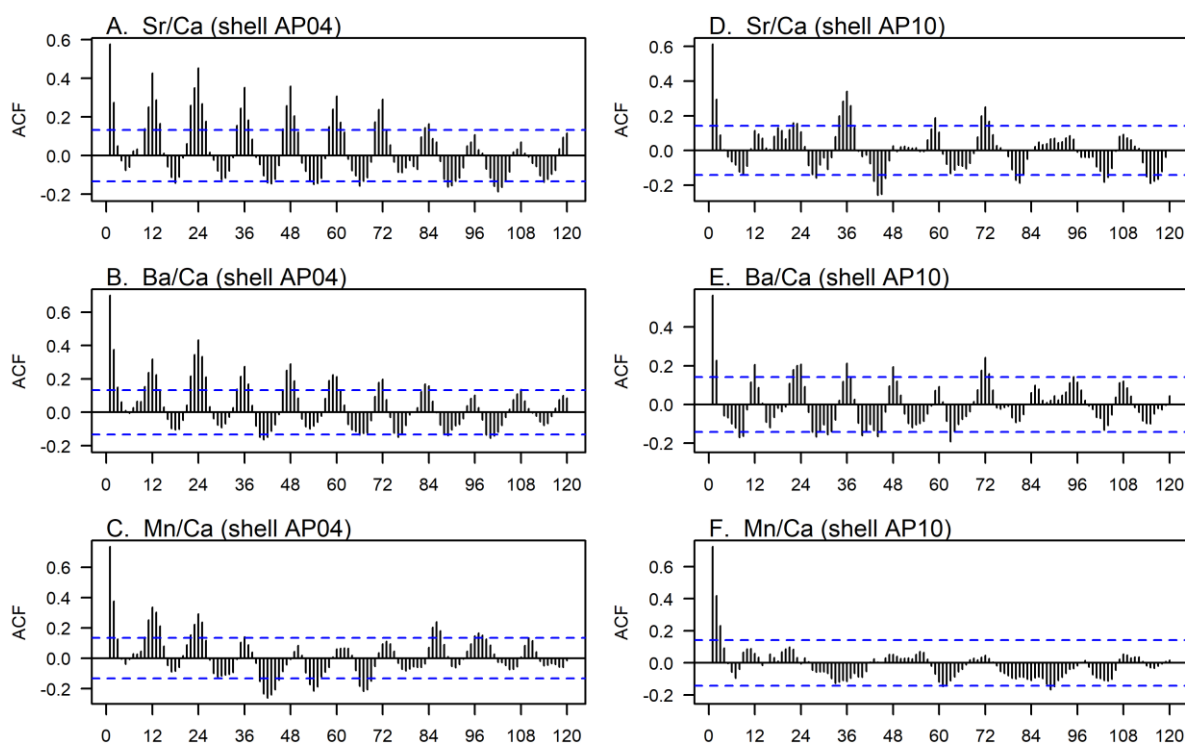
Fig. S8 Plots of the autocorrelation function for trace element ratios in the shell (A,B,C) AP04 and (D,E,F) AP10
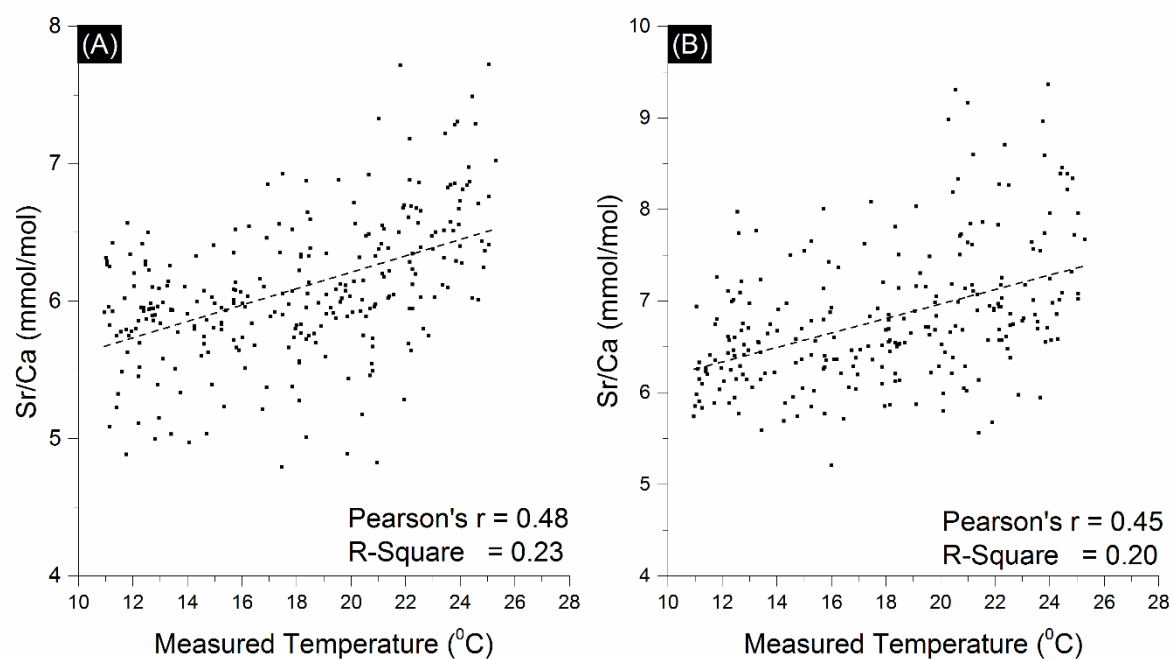
Fig. S9 Monthly averaged Sr/Ca (A) Alathyria profuga (n = 2) and (B) *Cucumerunio novaehollandiae* (n = 1) and measured instrumental temperatures. The dashed lines show the trend line.

CLIMATE SIGNALS IN THE SHELLS OF *Diplodon chilensis patagonicus* (HAAS, 1931) BIVALVES IN NORTHERN PATAGONIA, ARGENTINA

Dilmi Herath[1], Dorrit Jacob[1], Annalia Soldati[2], Maria Bianchi[3,4], Kristine DeLong[5], Adam Hajduk[6]

[1] *Department of Earth and Planetary Science, Macquarie University, Sydney, Australia*

[2] *CONICET, Centro Atómico Bariloche, Av. Bustillo 9500, CP-8400 San Carlos de Bariloche, Argentina*

[3] *Instituto Nacional de Antropología y Pensamiento Latinoamericano, 3 de Febrero 1370, Buenos Aires, Argentina*

[4] *CONICET, Av. Ángel Gallardo 470, Buenos Aires, Argentina*

[5] *Department of Geography and Anthropology and the Coastal Studies Institute, Louisiana State University, Baton Rouge, LA, USA*

[6] *Museo de la Patagonia Dr. Francisco P. Moreno, Centro Cívico S/N, 8400 San Carlos de Bariloche, Argentina*

Abstract

Twenty-seven *Diplodon chilensis patagonicus* shells were collected from four lakes in Northern Patagonia, Argentina presenting the first systematic study on the potential of Patagonian freshwater bivalves as a climate proxy archive. Shells of this species develop a prominent annual growth mark during austral spring simultaneous with the reproduction period. Collected bivalves varied in age from 8 to 67 years with an average of 40 years. The oxygen isotope content in *Diplodon chilensis patagonicus* shells is controlled by evaporation and precipitation in the region, which present the possibility of using *Diplodon chilensis patagonicus* shells as a proxy for precipitation in northern Patagonia. Monthly averaged high-resolution shell Sr/Ca profiles show distinct annual peaks close to the annual growth mark. Although the linear relationship between annual average Sr/Ca and annual average instrumental temperatures is low (r = 0.50, p < 0.05), regressing summer and winter temperatures separately increased the fidelity of reconstructed extreme seasonal temperatures where the summer temperatures show a higher correlation with monthly extreme summer shell Sr/Ca (r = 0.64, p < 0.05). Annual shell growth variability indicates a negative and positive correlation with the El Niño Southern Oscillation and Southern Annular Mode index respectively. Furthermore, results from this study reveal that *Diplodon chilensis patagonicus* shell growth has the ability to record regional climatic events, although this study is not long enough to identify the periodicities with frequency analysis methods, yet does record the occurrence of some regional climatic events.

4.1 Introduction

Understanding natural climate variability remains a challenge in South America due to the scarcity of instrumental records, thus limiting the available data sets used to fine-tune and test climate models (e.g., Collins et al., 2009; Magrin et al., 2014). Therefore, climate proxy records are used to fill these data gaps spatially and temporally. Compared to the northern hemisphere, the number of high-resolution climate proxy records from the southern hemisphere is lower (Villalba et al., 2009; Ahmed et al., 2013; Emile-Geay et al., 2017), and those that exist are mostly annually-resolved tree ring records. Dendrochronological records in South America south of ca. 35°S have yielded reconstructions of annual temperature variability and/or precipitation that cover approximately the last thousand years and are developed mostly from long-lived forest trees (Neukom and Gergis, 2012).

Bivalve shells fulfil the requirements for long-term and seasonally resolved proxy archives, because of periodic incremental shell accretion, worldwide occurrence, and their potential to enable construction of cumulative cross-dated time series (combined individual chronologies from different time periods) (Black et al., 2009; Schöne and Surge, 2012; Yan et al., 2015; Kelemen et al., 2017). Annual, daily as well as ultradian growth patterns in the shells serve as precise time gauges for chemical proxies, such as trace elemental and stable oxygen isotopic ratios ($\delta^{18}O$) that record environmental conditions (Khim et al., 2003; Schöne et al., 2004; Butler et al., 2009; Schöne and Surge, 2012; Yan et al., 2015).

Biological and chemical variables such as growth rate, $\delta^{18}O$ and trace element-to-calcium ratio from bivalve shells have been considered reliable proxies for paleo-environmental changes (Dettman et al., 1999; Yan et al., 2014). However, some studies found that physiological and kinetic effects can affect the usefulness of these archives (Gillikin et al., 2005; Füllenbach et al., 2017; Zhao et al., 2017a). Thus, in contrast to aragonitic corals, interpretation of Sr/Ca signals in bivalve shells can be challenging for reasons that are currently not well understood (Zhao et al., 2017b). In contrast, oxygen isotopic ratios in bivalve shells most often precipitate in equilibrium with water and can be used to reconstruct temperatures (Dettman et al., 1999), although some studies report disequilibrium (Steuber, 1999; de Winter et al., 2017).

Diplodon chilensis patagonicus (Haas, 1931), the subject of this study, occurs abundantly throughout Patagonia (Graf and Cummings, 2007) and is the dominant freshwater bivalve species in the modern environment (Castellanos, 1960; Semenas and Brugni, 2002), as well as in Patagonian archaeological records (Zubimendi, 2007). These *Diplodon chilensis patagonicus* shells were previously identified as a potential archive for this region (Soldati et al., 2009). The present study uses three potential proxies in this archive, namely growth rate, oxygen isotopic ratios and Sr/Ca of these shells in a first systematic study to construct sub-annually resolved environmental conditions with these freshwater bivalve shells in Patagonia. Further, we explore the regional climatic forces in the Southern Pacific area with the potential to complement and provide seasonal information for the extensive tree-ring reconstruction network in South America.

4.1.1 Geographic setting and climate of the study area

South America is the only landmass in the southern hemisphere stretching from tropical climate zones to high latitudes and also the only large inhabited landmass south of 45°S. Patagonia is a particularly climatically sensitive area, due to atmospheric forcing by the position and strengths of southeast Pacific anticyclones and the low pressure belt surrounding Antarctica (Aceituno et al., 1993; Markgraf et al., 2007; Garreaud et al., 2009).

A change in the Pacific sea surface temperature is one of the major factors influencing the climate in Northern Patagonia together with forcing resulting from the proximity to the Antarctic and subpolar regions (Thompson and Solomon, 2002). In fact, the dominant mode of climate variability affecting southern South America is the Southern Annular Mode (SAM). The SAM index reflects changes in the main belt of sub-polar westerly winds at around 60 °S due to air mass exchange between middle and high latitudes in the southern hemisphere (Thompson and Wallace, 2000). Similarly, sea surface temperature in the Pacific Ocean is frequently influenced by the El Niño Southern Oscillation (ENSO), which is a large-scale oceanic warming event in the eastern tropical Pacific Ocean that occurs every 2-7 years (Wang et al., 2017). ENSO events translate into warm summers during El Niño and cold summers during La Niña events in latitudes of Northern Patagonia (Daniels and Veblen, 2004).

Another major factor determining the climate of Patagonia is the morphology of the Andes. The Andes disrupt atmospheric circulation and uplift winds resulting in strong climatic contrasts between their western and eastern slopes (Garreaud et al., 2013). Situated in the rain shadow of the Andes (Fig. 1), our study area at 41°S is characterized by one of the strongest precipitation gradients of southern South America (Prohaska, 1976) including a transition from forest to steppe, which occurs within only 80 km, and is accompanied by a decrease in annual precipitation from 3000 mm in the Andean rainforests to less than 500 mm in the steppe (New et al., 2002). A large number of lakes exist along the eastern slopes of the southern Andes that are mostly relics of Pleistocene glaciation (Tatur et al., 2002) covering a surface area of approximately 15,300 km^2 in total. Temperature and precipitation patterns in the area are distinctly seasonal with the maximum of the precipitation occurring in the austral winter, regulated by the persistent westerly storm tracks and jet stream.
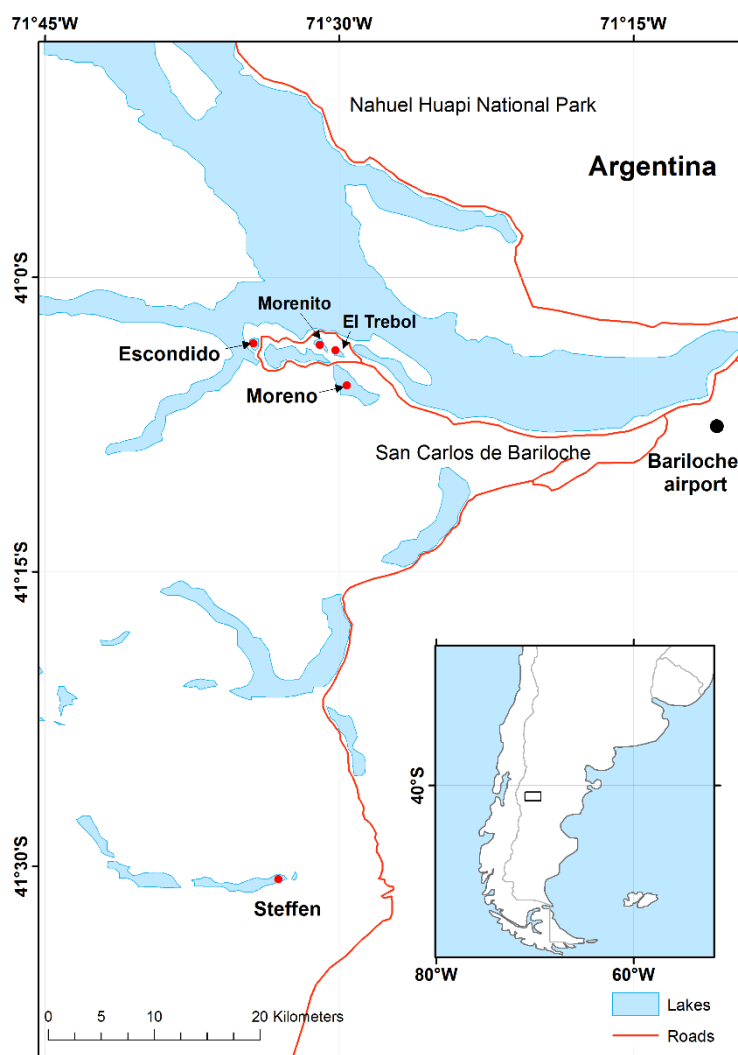
Fig. 1 Map of the Nahuel Huapi National Park in Patagonia, Argentina showing the locations of lakes sampled. Red dots indicate the sampling locations. Inset shows the location of the study area in southern America.

4.2 Methods

4.2.1 Sampling and specimen preparation

Living specimens of *Diplodon chilensis patagonicus* (hereafter *D. patagonicus*) were collected from lake beds of five lakes (Escondido, El Trébol, Moreno, Steffen and Morenito), which are situated at ca. 800 m above sea level in the Nahuel Huapi National Park close to the city San Carlos de Bariloche in Northern Patagonia, Argentina (Fig. 1). Lakes El Trébol (41° 4' S, 71° 30' W) and Escondido (41° 3' S, 71° 33' W) are small (0.30 and 0.13 km^2, respectively) and shallow water bodies (maximum depth 12 and 8 m, respectively) without in or outflowing perennial streams (Massaferro et al., 1999; Gogorza et al., 2002; Pérez et al., 2002). Their hydrological budgets are dominated by groundwater influx and evaporation while human influence is moderate. In contrast, Lake Moreno covers 5.43 km^2 and has a maximum depth of 112 m and is fed by several small streams coming from the nearby mountains (Barriga, 2006). Except for Lake Steffen, the lakes belong to the Nahuel Huapi hydrological system, which discharges into the Atlantic Ocean. In contrast, Lake Steffen belongs to the Río Manso hydrological system, which originates in the Río Manso Glacier and runs through Patagonia to discharge its water into the Pacific Ocean.

D. patagonicus bivalves are abundant in these lakes and live on a sandy-muddy substrate at depths of ca. 2-5 m. Twenty-seven live bivalves were collected from Lakes Escondido, El Trébol, Moreno and Steffen (Table 1), immediately sacrificed and the soft parts were removed. Furthermore, a bimonthly sampling of bivalves from different localities in Lake Morenito (Fig. 1) was carried out over one year to determine the seasons of maximum and minimum shell growth. After drying and coating with metal bisphenol-A-epoxy resin (WIKO), left valves were cut perpendicular to the growth lines and along the minimum growth axis with a Buehler Isomet 1000 low speed saw. Slabs of ca. 3 mm thickness from each specimen were ground in steps with sandpaper (400, 600, 800 and 1200 grit) and eventually polished with 3 and 1 µm diamond pastes.

4.2.2 Increment width measurements and chronology construction

Digital photomicrographs of the polished shell sections were taken under a reflected light binocular microscope at high magnification before and after staining the shells with Alcian Blue (Schöne et al., 2005). Shell annual increment lengths were measured along the complete

shell sections on these photomicrographs with the computer software `Panopea` (©Peinl and Schöne 2004). The width of an individual annual increment was defined as the perpendicular distance between two adjacent growth lines (sharp blue lines in the stained sample, Fig. 2). As the annual growth lines formed at around October (see below), the incomplete increment at the ventral margin of the shell was assigned to the year of sample collection. Growth increment widths were first visually cross-matched with each other and then verified using the visual correlation tool SHELLCORR following the methods outlined in Bušelić et al. (2015). SHELLCORR visualizes the Pearson correlation coefficients between two time series at various lags in a sliding window of twenty-one years. Since growth lines in this species can be subtle, this method of using both, visual and SHELLCORR-based cross-matching facilitated identification of missing and false increments, which led to the re-evaluation of the shell digital images for these shells.

The software package `ARSTAN` (version 44h3) for windows (Cook and Holmes, 1996), which is routinely used in dendrochronology was used to build individual chronologies for each of the four lakes. `ARSTAN` power transforms and detrends individual increment-width series and applies a biweight robust mean function to the indices to build the chronology. Increment widths for individual shells showed a strong ontogenetic trend of declining growth rates with increasing age of the animal (Fig. S1). Therefore, the "general negative exponential function" in the software was used for the detrending before building the chronology. In all cases, `ARSTAN` indicated that the negative exponential function provides the best fit and no evidence of autocorrelation (Fig S2). Out of three versions of the master chronologies form `ARSTAN`, the standardized master chronology was selected for all further analysis since there were no significant differences between it and the residual and ARSTAN types.

Further, `ARSTAN` was also used to calculate separate chronology statistics for each lake such as R*bar* (mean of all correlations between pairs of increment-width series) and Expressed Population Signal (EPS) (Wigley et al., 1984). R*bar* indicates the strength of the common signal in the chronology, while EPS indicates whether the common variance in the chronology is a sufficiently good expression of the common variance in the population. Since the age span of the *D. patagonicuss* was less than 60 years, a window length of 15 years with 5-year window overlap was selected for the EPS calculations. Only the lakes with high EPS values were selected for the creation of master chronology.

4.2.3 Environmental data collection and analysis

Instrumental data for air temperature and precipitation were obtained from Argentinean public institutions (Sevicio Meteorológico Nacional Argentino, Airport station and Instituto Nacional de Tecnología Agropecuaria San Carlos de Bariloche). Air temperatures used in this study were measured at the Bariloche airport (ca. 30 km west and ca. 50 m higher than Lakes Escondido and El Trébol; Fig. 1). Additionally, the water temperature in Lake El Trébol was continuously measured between March 2008 and March 2009 using a temperature sonde deployed adjacent to the mussel bed in the lake. Ordinary least square regression and multiple regression analysis between the standardized master chronology and annual climatic variables of the area were calculated using the statistical software R (Team, 2017). The standardized master chronology was also compared with the summer SAM index of the current and previous year as well as the ENSO index (Nino 3.4 index values are obtained from *www.cpc.ncep.noaa.gov*).

4.2.4 Oxygen and carbon isotope compositions

Stable oxygen and carbon isotopic ratios were measured in three younger shells from Lake El Trébol (ET05 – 12 years, ET08 – 18 years and ET11 – 8 years), as these shells enabled sampling at reasonably high resolution due to higher shell growth rates at ontogenetically young ages. Micromill sampling of shell cross-sections was carried out using a 300 µm drill bit parallel to the growth lines in the nacreous middle shell layer under a binocular microscope at intra-annual resolution, following the axis of minimum shell growth from the ventral margin to the umbo (Fig. S3). Samples were milled approximately equidistantly and were compared to the intact mirror shell section with stained growth lines for assignment of calendar years. *D. patagonicus* shells consist completely of aragonite (Soldati et al., 2009), therefore isotopic differences among different $CaCO_3$ polymorphs are not an issue.

Oxygen and carbon isotopic ratios ($\delta^{18}O$ and $\delta^{13}C$) were determined at the University of Frankfurt using a Finnigan MAT 253 continuous flow isotope ratio mass spectrometer equipped with a GasBench II following the protocol elaborated by Spötl and Vennemann (2003). The $\delta^{18}O$ values were reported relative to Vienna Pee-Dee Belemnite (VPDB) standard based on measurements of NBS-19 ($\delta^{18}O$ = -2.20 ‰) and calibrated Carrara marble ($\delta^{18}O$ = -1.74 ‰). Internal precision (1 sigma) was usually better than ± 0.08 ‰ for $\delta^{18}O$ and

± 0.06 ‰ for $\delta^{13}C$, respectively. The stable isotope composition of surface water samples collected monthly for twelve months from March 2008 to March 2009 were measured at the Leibniz-Laboratory for Radiometric Dating and Stable Isotope Research, University of Kiel, Germany with a Finnigan Delta E mass spectrometer equipped with a Kiel DICI device and an equilibration bath. Analytical precision (1 sigma) based on four replicates each were ± 0.08 ‰ for $\delta^{18}O$ and ± 0.3 ‰ for $\delta^{13}C$.

4.2.5 Elemental analysis

Strontium, Mn, Ba and Ca (measured as ^{88}Sr, ^{55}Mn, ^{137}Ba and ^{43}Ca) concentrations in five polished cross-sections of samples from Lake El Trébol (ET01, 05, 06, 08 and 11) were measured by Laser Ablation Inductively Coupled Plasma Mass Spectrometry (LA-ICP-MS) using an Agilent 7700 quadrupole ICP-MS coupled to a Photon Machines excimer laser (193 nm wavelength) laser ablation system. Measurements were carried out with laser energy density of 4.05 J/cm^2 at 5 Hz and helium/argon as carrier gas (flow rate = 0.8 l/min). To obtain trace element time series, continuous curved lines of differing lengths were ablated in the nacreous layer along the direction of growth (laser spot diameter 30 μm; scanning speed 5 μm/s) after pre-ablation (laser spot diameter 50 μm; scanning speed 125 μm/s) (Fig. S3). Backgrounds were measured for 60 s prior to each analysis. ^{43}Ca was used as the internal standard with NIST SRM 612 glass as the external standard. Data reduction was carried out with the commercial software `GLITTER 4.5b` (Griffin et al., 2008). NIST SRM 610 glass and U.S. Geological Survey reference glass BCR-2G were measured as unknowns to monitor accuracy and instrumental drift. Values for all reference materials were taken from the GeoReM database preferred values (Jochum et al., 2005). Detection limits (99% confidence level) for the measurements were Sr = 0.01 μg/g, Mn = 0.18 μg/g, and Ba = 0.11 μg/g. The reproducibility for BCR-2G (n = 11) and NIST SRM 610 (n = 21) were > 95% and > 98% for all measured elements, respectively.

All data series were divided by Ca to create trace element/Ca (Me/Ca) series that were first compared to the intact mirror shell section with highlighted growth lines for a rough assignment of calendar years. Afterwards, these series were overlain with the measured $\delta^{18}O$ series of the mirror section of the same shell to improve monthly time assignment. Monthly averaged Sr/Ca time series were then created for ET05, ET08 and ET11 excluding October and November when shell growth is minimal. The Sr/Ca maximums coincided with the dark

summer bands and minimums with light winter bands. Since $\delta^{18}O$ data were not available for ET06 and ET01, Sr/Ca time series were created by assuming the peak formation months based on the observations from three shells with $\delta^{18}O$ data and the data in between was distributed assuming constant growth. All other Me/Ca time series were created by aligning with Sr/Ca time series, since all elements were measured simultaneously.

4.3 Results and Discussion

4.3.1 Shell growth rate and sclerochronology

Ages of the *D. patagonicuss* shells varied from 8 to 67 years with an average of 40 years (Table 1), which is consistent with lifespans determined by Parada et al. (1989) and Risk et al. (2010) for *Diplodon chilensis chilensis,* a Chilean subspecies. Growth increment widths of the shells vary as a function of ontogenetic age (Fig. S1) and are larger (ca. 100 - 4000 µm) in youth portions of shells than in sections formed after about the fifteenth year of life (ca. 30 - 200 µm) with an average growth rate of 120 µm per year overall. Shell growth of molluscs, however, is not constant throughout the year but is reduced for many species before and after the development of the growth line (Clark, 1975; Schöne, 2008). In *D. patagonicus,* this line develops annually and represents a visible thin band of less mineralized material in the shell (Fig. 2) (Soldati et al., 2009), which in many species is associated with the reproduction period (Ropes et al., 1984).

Analysis of sixty shells (not shown) sampled bi-monthly from different locations in Lake Morenito confirmed that prominent growth lines develop annually during austral spring (October-November) and shell growth rate is extremely low until the end of November or the beginning of December in a period that is simultaneous with the reproduction period of *D. patagonicus* in this area (Parada et al., 1990; Lara and Parada, 1991; Semenas and Brugni, 2002). Apart from this period, shells grow throughout the year developing a light-coloured band in winter and a dark band in summer (Fig. 2). It is notable that the width of the light-coloured winter band in many shells is comparable to the dark summer band, indicating that growth rates in winter can be similar to those in summers for this species. While we cannot currently identify the threshold-temperature for the cessation of shell growth in *D. patagonicus*, shell growth is maintained below 4 °C albeit at much lower rates as demonstrated by the small but yet detectable winter growth in 2002 where the air temperatures of 0.8 and 0.3 °C in June and July are reported.

146
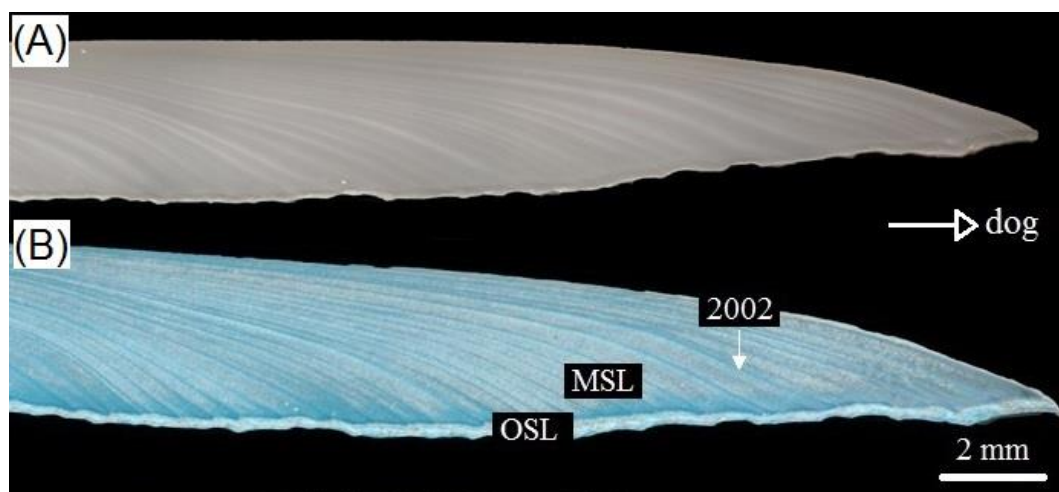
Fig. 2 (A) Internal annual growth increments in polished cross sections of *Diplodon chilensis patagonicus* cut along the axis of minimum growth. (B) The same shell section after staining with Alcian Blue. Organic-rich, growth lines are stained dark blue. (*dog,* direction of growth; *OSL,* outer shell layer consisting of aragonite prisms; *MSL,* middle shell layer consisting of nacre).

According to Wigley et al. (1984), EPS values higher than 0.85 indicate that the signal in the chronology is a sufficiently good representation for the signal in the whole population for tree ring studies. However, bivalve shells frequently show EPS values lower than 0.85 at low sample depths but higher values with increasing sample depth (Featherstone et al., 2017). High R*bar* and EPS values for the bivalve populations in the smaller groundwater fed Lakes Escondido and El Trébol suggest that these shell populations show a common environmental signal (Table 1; Fig. 3). Further, no significant evidence of auto-correlation was detected in these chronologies during chronology construction using ARSTAN (Fig. S2). In contrast, shell sample suites from Lakes Moreno and Steffen both resulted in a low R*bar* and EPS (Table 1; Fig. 3). Hence, the lack of a common signal for the shell populations from Lake Steffen and Lake Moreno led us to exclude these two datasets from further discussion and interpretation here. Both lakes are relatively large, fed by several small streams and thus, are likely to have a more complex mixing dynamics, which likely to affect any common signal in the sample suite. Further, Lakes Steffen is approximately 50 km south of other studied lakes in a region characterised by a rapid transition from forest to steppe, which occurs within only 80 km. This and the fact that it belongs to a different hydrological system indicate that the environment in Lakes Steffen could be completely variable to that of lakes in Nahuel Huapi region. Therefore, more robust studies in future are needed to identify the suitability of *D. patagonicus* as an environmental archive from these lakes. This also suggests that *D. patagonicus* shells are only suitable as an environmental archive in a smaller region.

The running EPS for Lake Escondido until around 1980s is lower than the commonly used threshold of 0.85, however, it gradually increases with increasing sample depth and higher than 0.85 after sample depth reach 5. In contrast, the Lake El Trébol sample suite has a running EPS < 0.85 throughout most of the chronology but the EPS values are higher than 0.7 after around 1975 (sample depth = 2) and remain constant as sample depth increases (Fig. 3).
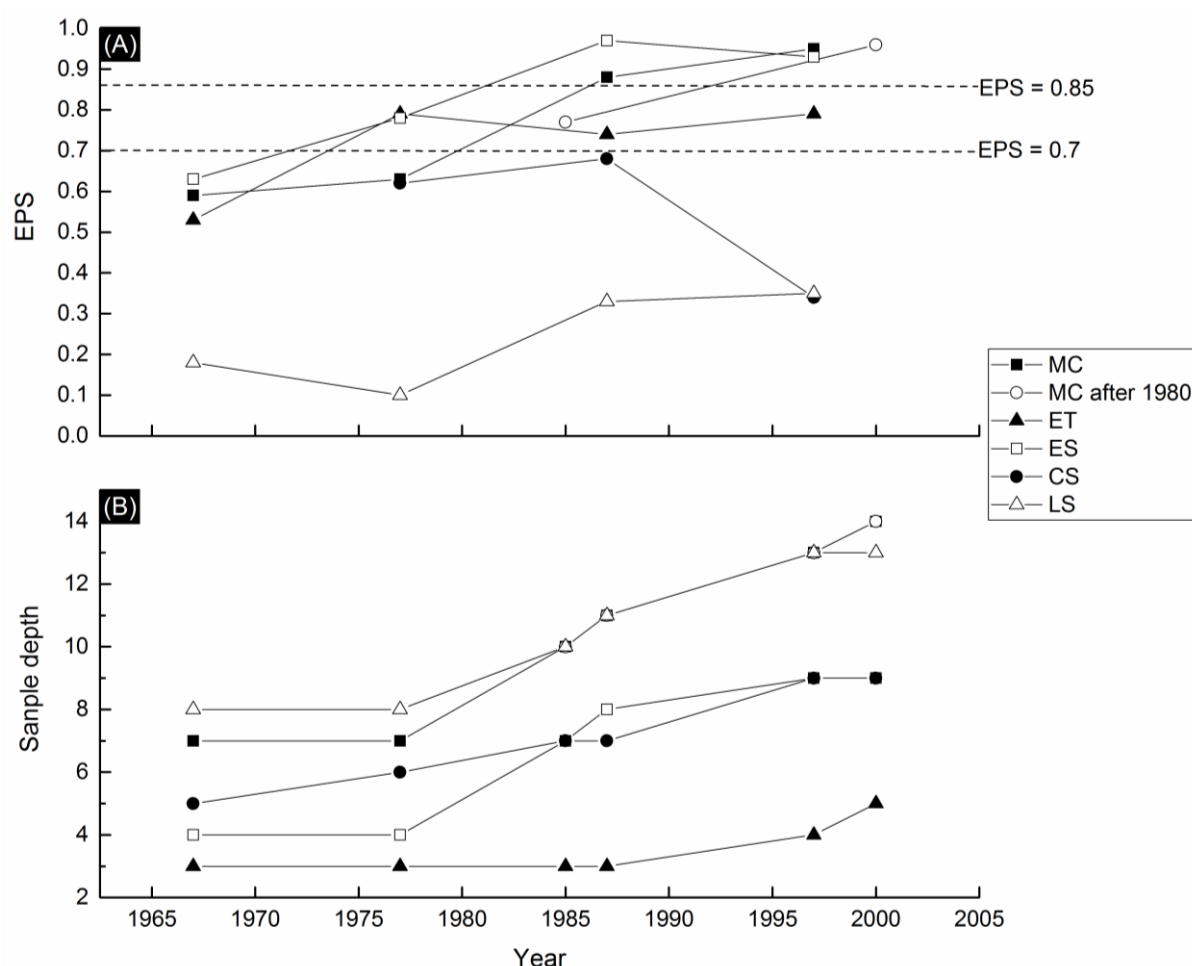
Fig. 3 (A) Variation in the Expressed Population Signal (EPS) and (B) corresponding sample depth of *D. patagonicus* shell chronologies from four lakes in the Nahuel Huapi National Park in Patagonia, Argentina. EPS value is plotted at the start of the time interval. Dash lines indicate the accepted threshold valve of 0.85 and 0.7 (Wigley et al., 1984). MC = Master chronology, ET = El Trébol, ES = Escondido, CS = Moreno and LS = Steffen.

Since Lake Escondido and Lake El Trébol resulted in R_{bar} and EPS values > 0.85 and ≥ 0.70 respectively, only those two lakes were selected for the master chronology construction. Therefore, ARSTAN was used again to create the master chronology using 14 individual chronologies from these two lakes (Fig. 4; Table 1) and this master chronology has an EPS value > 0.7 after 1980 (sample depth = 11), which is close, but slightly under the generally accepted value of 0.85 for tree ring studies. Table 1 shows that individual lake chronologies

have high EPS values that all increase with sample depth, hence it is clear that higher sample depth for the master chronology undoubtedly would yield EPS values above 0.85, and the master chronology shows common environmental signals for the two lake's population.

Table 1. Chronology information and chronology statistics of *D. patagonicus* shell growth chronologies from different lakes in northern Patagonia. Master chronology is constructed using shells from Lakes Escondido and El Trébol.

Lake	Span	No of years	*n*	R_{bar}	EPS 1967	1977	1987	1997
Escondido	1940-2006	67	9	0.58	0.62	0.78	0.97	0.93
El Trébol	1949-2006	58	5	0.38	0.52	0.78	0.73	0.79
Moreno	1952-2006	55	9	0.13		0.61	0.68	0.64
Steffen	1950-2006	57	12	-0.03	0.18	0.10	0.33	0.35
Master	1940-2006	67	14	0.46	0.58	0.63	0.88	0.95
Master (after 1980)	1980-2006	27	14	0.53			0.76	0.96
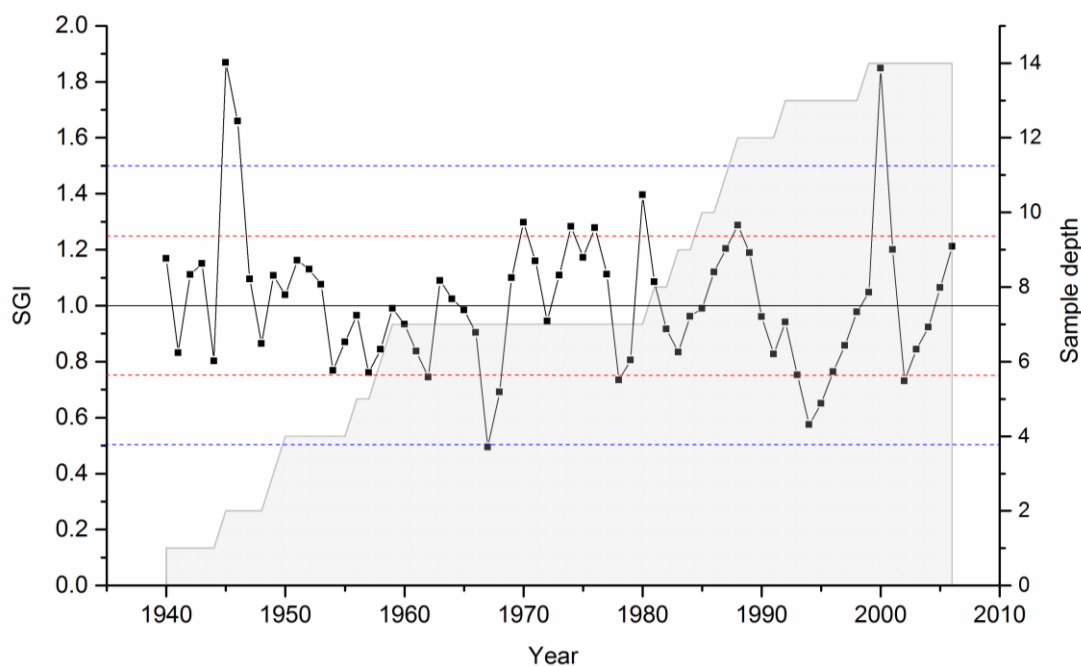
Fig. 4 Master chronology of *D. patagonicus* shells collected from Nahuel Huapi National Park in Patagonia, Argentina (Lake Escondido and Lake El Trébol; Table 1) and the sample depth at the back in grey. SGI = Standardized growth increment. Red and blue dash lines indicate the 1SD and 2SD value (0.25 and 0.5) respectively.

Distinctive years of increased standardised growth, such as 2000 and 1980, were found in the master chronology while lower than average standardised growth was recorded in 1967, 1978, 1995 and 2002 (Fig. 4). Linear correlations were calculated between the shell growth master chronology and annual average temperature and precipitation (excluding the growth break period of October- November). The master chronology indicates an insignificant

correlation with both annual as well as seasonal temperature and precipitation (Table 2). Since the EPS values at the start of the master chronology are low, only the time period after 1980 (when the EPS > 0.7) was compared with annual average and seasonal temperatures and precipitation (Table 2). The only significant correlations (r = 0.24, p < 0.05) observed was between the master chronology and annual precipitation. These observations suggest that high precipitation, which mainly occurs in winters in this area, favours shell growth while the influence of temperature on shell growth is minimal.

Shell growth rates in bivalves depend on a combination of many external factors including temperature, precipitation, food supply and nutrient levels in water (Witbaard, 1996; Sosdian et al., 2006; Schöne and Surge, 2012) as well as on metabolic control. Multiple regression analysis does not identify a significant effect of temperature and precipitation combined (r = 0.06; p < 0.05), neither for the complete master chronology nor for the master chronology after 1980 (r = 0.03; p < 0.05). As both lakes are oligotrophic, i.e. nutrient-poor and oxygen-saturated (Diaz and Pedrozo, 1996; Diaz et al., 2000), we suggest that in these lakes nutrient supply is an additional important parameter for shell growth.

Table 2. Pearson correlation coefficients between the master growth chronology of *D. patagonicus* shells and different environmental variables measured at the San Carlos de Bariloche airport, Argentina. (n = 66, r > 0.25 to be significant at 5% interval for Master Chronology, n = 26, r > 0. 39, to be significant at 5% interval for 1980-2006). Winter = June, July and August; summer = December, January, February. Items in italics are significant at the 5% level.

	Master Chronology	Master Chronology (after 1980)
Annual average temperature	0.09	-0.09
Summer temperature	0.05	0.17
Winter temperature	0.11	0.01
Annual average precipitation	*0.24*	-0.12
Summer precipitation	0.01	0.11
Winter precipitation	0.17	0.24
Southern annular mode (from 1979)	-	0.08
El- Niño southern oscillation (from 1950)	*-0.33*	*-0.51*

4.3.2 Stable isotope signals

Notably, the $\delta^{18}O_{water}$ values do not follow the temperature pattern in the area, but show a 2 to 3 month lag between the peak air temperature and peak $\delta^{18}O_{water}$ values. Oxygen isotopic ratios in Lake El Trébol measured monthly from March 2008 to March 2009 varied between -8.8 and -6.6 ‰ with the highest values recorded (in May) at the end of the dry season in the austral summer and the lowest values recorded (in October; Fig. 5) after the peak precipitation in winter to early spring. This pattern, and the lack of correlation with water temperatures suggest that evaporation and precipitation act as the major controls on the isotopic variation in Lake El Trebol. Evaporation leads to enrichment in ^{18}O in shallow lakes such as Lake El Trebol, resulting in relatively higher $\delta^{18}O_{water}$ values during the dry and windy summer months. Moisture-bringing air masses in eastern Patagonia mostly originate from west of the Andes (Stern and Blisniuk, 2002) and are increasingly depleted in ^{18}O due to Rayleigh distillation during rainout of the ascending clouds, leading to relatively lower $\delta^{18}O_{water}$ values in lakes during the winter months. This rainout effect is reflected in the oxygen isotopic composition of precipitation in this area, which fluctuates between -7.53‰ in the austral summer and -14.03 ‰ in winter when precipitation is usually at its maximum (Global Network for Isotopes in Precipitation and Isotope Hydrology Information System, Station 8776501 Bariloche; *www-naweb.iaea.org/napc/ih/index.html*).
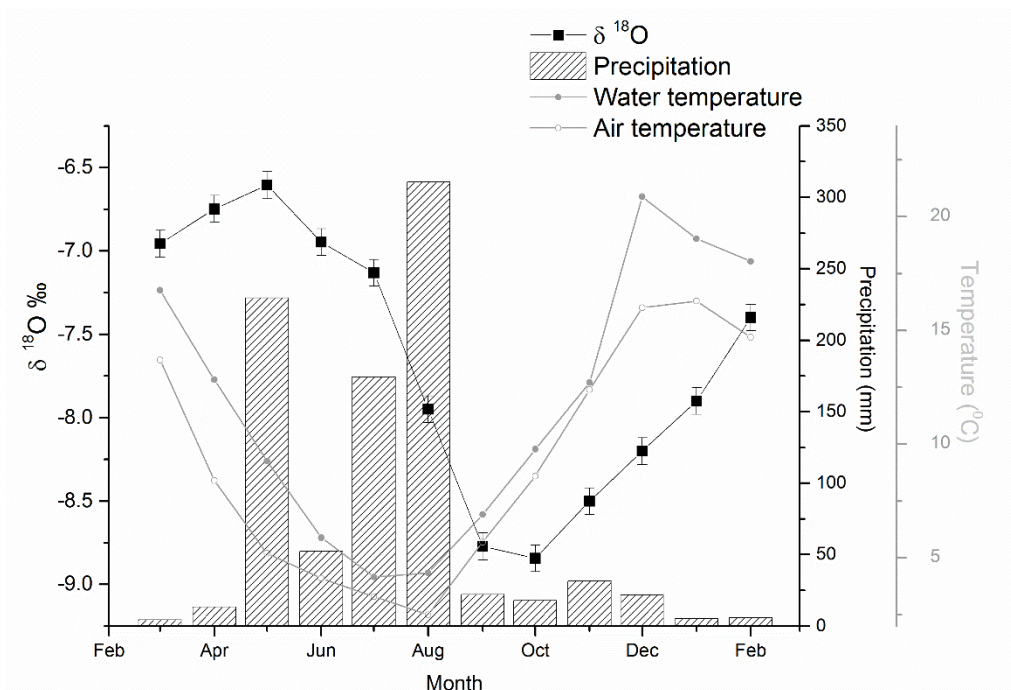
Fig. 5 Variation in water $\delta^{18}O$ values in Lake El Trébol water with instrumental data for lake water temperature as well as air temperature and precipitation from Bariloche airport near the lake for the time interval from March 2008 to March 2009.

Unionid bivalves such as *D. patagonicus* precipitate shell oxygen isotopes in an equilibrium with the $\delta^{18}O_{water}$ in the ambient aquatic environment (Dettman et al., 1999; Kelemen et al., 2017). This is evident in this dataset from the $\delta^{18}O_{shell}$ values measured in shells ET05, ET08 and ET11 (Fig. 6A), which indicate seasonal patterns that follow the lake $\delta^{18}O_{water}$ pattern with highest values every year in late autumn (April-May) and lowest values in early spring (September). To overcome the problems from physiological effects in individual bivalves, it is recommended to use several bivalves with varying age to build a composite time series that will have a higher possibility in capturing the full range of environmental conditions (Kelemen et al., 2017). The composite time series was developed by averaging the shell $\delta^{18}O$ values for the three samples (Fig. 6B). This composite time series does not have significant correlations with monthly air temperature as well as monthly precipitation in the region (Table 3). Nevertheless, the correlation increases with a time lag and significant positive and negative correlations resulted with monthly air temperature and monthly precipitation, respectively, with a three months lag (Table 3). Similar to growth analysis, oxygen isotopic ratios do not result in a significant correlation upon multiple regression analysis of temperature and precipitation (r = 0.06; p < 0.05).
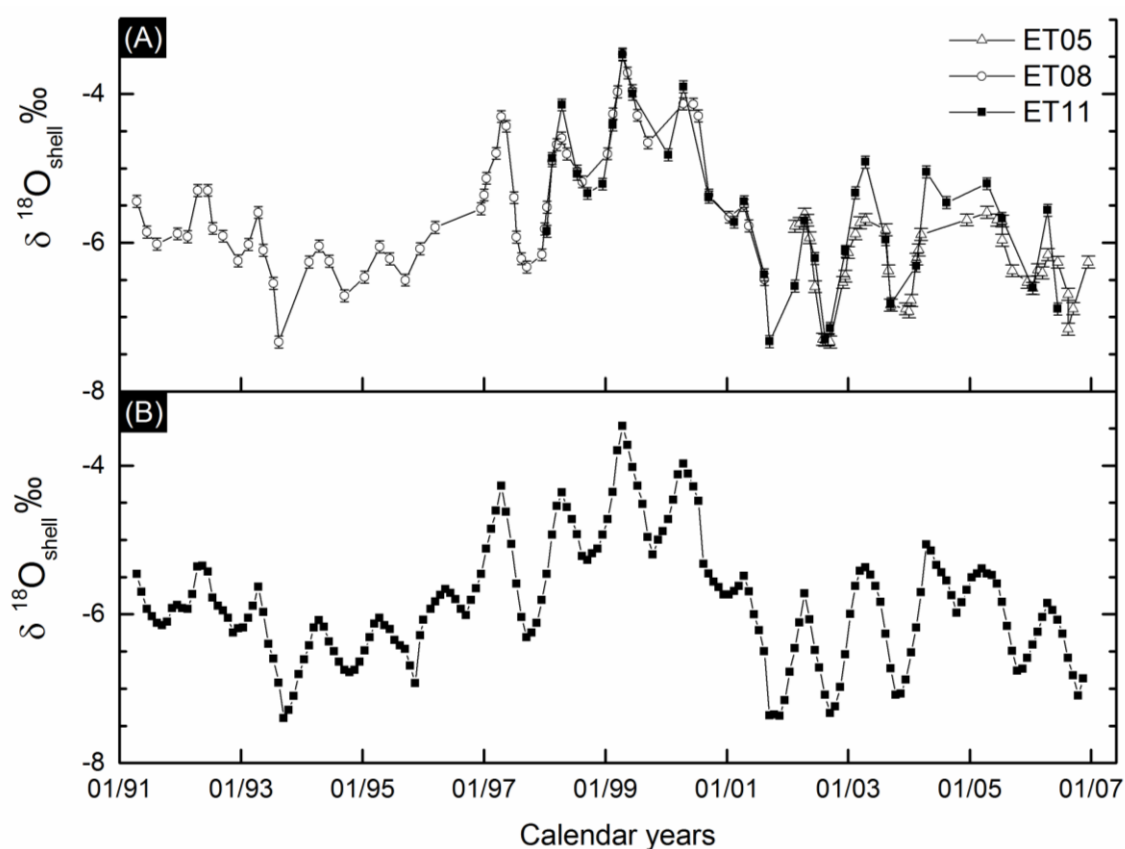
Fig. 6 (A) The $\delta^{18}O_{shell}$ variation in three measured shells from Lake El Trébol and (B) Master $\delta^{18}O_{shell}$ chronology covering fifteen years from combining three shells collected from Lake El Trébol. Individual time series were aligned in time space and then averaged together to create the master time series.

Table 3. Pearson correlation coefficients between composite shell $\delta^{18}O$ as well as different metal/calcium with environmental variables measured at the San Carlos de Bariloche airport, Argentina. Items in italics are significant at the 5% level.

	n	r
$\delta^{18}O_{shell}$ vs monthly precipitation	136	0.02
$\delta^{18}O_{shell}$ vs monthly temperature	156	0.02
$\delta^{18}O_{shell}$ vs monthly precipitation (3 months lag)	129	*0.51*
$\delta^{18}O_{shell}$ vs monthly temperature (3 months lag)	153	*0.41*
Sr/Ca_{shell} vs monthly temperature (linear)	120	*0.50*
Sr/Ca_{shell} vs monthly temperature (polynomial)	120	*0.56*
Sr/Ca_{shell} vs monthly temperature (summer)	76	*0.64*
Sr/Ca_{shell} vs monthly temperature (winter)	44	0.05
Ba/Ca_{shell} vs monthly temperature (linear)	119	0.28
Ba/Ca_{shell} vs monthly precipitation	119	-0.23
Ba/Ca_{shell} vs monthly precipitation (1 month lag)	119	-0.23
Ba/Ca_{shell} vs monthly precipitation (3 month lag)	119	0.02

These low correlations, which increase with time could be attributed to several reasons. Due to smaller growth increments in the *D. patagonicus* shell sections (ca. 100 - 4000 µm in younger shells), there can be time assignment uncertainties when assigning shell formation dates to the drilled samples due to an inadequate sampling resolution, which may lead to lower correlations with seasonal environmental variables. Progress in using high resolution *in situ* sampling methods for shell oxygen isotopes, for example by using secondary ion microprobe (Saenger et al., 2017), will allow for sampling at a higher resolution and better assignment of calendar dates for shells with smaller growth increments. Furthermore, Lake El Trebol does not have in or outflowing perennial streams but has a groundwater influx that dominates the hydrological budget. The time lag for groundwater to reach the lake could cause a delay between precipitation and the recording of that signal in the shell, such as seen in Fig. 5.

The $\delta^{13}C_{shell}$ are generally seasonally in phase (r > 0.4, p < 0.001) with $\delta^{18}O_{shell}$ and shows similar seasonal variations at higher variability with values ranging between − 4.0 and − 9.1 ‰ (Fig. S4). Notably, $\delta^{13}C$ values extend down to − 9.1 ‰, while measured values for dissolved inorganic carbon (DIC) in water only range between − 3.5 and − 5.1 ‰. For the freshwater bivalve *Anodontites trapesiales,* Kaandorp et al. (2003) calculated a systematic offset of − 4 ‰ (± 0.7 ‰) between $\delta^{13}C_{shell}$ and $\delta^{13}C_{HCO_3^-}$, which is similar to the mismatch between $\delta^{13}C_{shell}$ and $\delta^{13}C_{DIC}$ for *D. patagonicus* (− 4.0 ‰ ± 0.3 ‰) observed here. This suggests that only a part of the shell carbonate is derived from DIC with additions from metabolic carbon (Yoshimura et al., 2015).

4.3.3 Trace elements

The overall average shell values for five measured *D. patagonicus* shells from Lake El Trébol for Sr, Mn and Ba were 670, 200 and 20 µg/g respectively, note the shells have different lifespans. All element/Ca show periodic variations over the lifetime and an annual peak is visible in the Sr/Ca and Ba/Ca series after each annual growth break which overlaps approximately with January (Fig. 7), supporting earlier observations in the literature for *D. patagonicus* shells (Soldati et al., 2009; Risk et al., 2010). Further, Sr/Ca and Ba/Ca are in-phase (r = 0.8, p < 0.01, *n* = 130) whereas Mn/Ca show a more irregular pattern without distinct annual peaks (Fig. 7C).

Similar to marine bivalves (Gillikin et al., 2005; Schöne et al., 2010) and corals (DeLong et al., 2011; Wu et al., 2014), freshwater bivalves show clear seasonal variations in Sr/Ca series (Carroll et al., 2006; Izumida et al., 2011). In contrast, elevated Sr/Ca in *D. patagonicus* occur in summer, while low winter temperatures are not reflected (Fig. 7A). Monthly resolved Sr/Ca analysis suggest that air temperature explains only 25% of the Sr/Ca variance in *D. patagonicus* shells. This was evident by the positive correlation between measured air temperature and the composite time series created by taking the average of five *D. patagonicus* shells from Lake El Trébol (r = 0.50, p < 0.05, Table 3). However, an increased correlation between temperature and shell Sr/Ca with the 2nd order polynomial regression (r = 0.56, p < 0.05, Table 3) shows that temperature explains 32% of the Sr/Ca variance in the shell. Further, this also exhibits that the Sr/Ca in shells decrease with the temperature at temperatures below 5 °C and start to increase with increasing temperature after 5 °C as shown by the axis of symmetry value of the polynomial curve (Fig. 8). Therefore, two separate linear regressions were considered for summer and winter months with a cut-off of 5 °C. Linear regression between Sr/Ca and monthly summer temperatures resulted in a higher significant correlation (r = 0.64, p < 0.05, equation 1) than winter that show no significant correlation (r = 0.05, p < 0.05) with measured monthly temperature. Since shell potions formed during summer and winter can be easily identified by the colour (dark and light), this can be also used in fossil shells were the formation season is unknown.

$$Sr/Ca_{(shell)} = 0.03 \, x \, Temp. \, [°C] + 2.53 \hspace{3cm} (1)$$

Correlations between the Sr/Ca and instrumental temperature in bivalves vary considerably among species possibly depending on their growth rates and environments, for example between, slow growing cold water species *Arctica islandica* (r = -0.64; Schöne et al., 2011) and warm water fast growing *Tridacnidae* species (r > 0.8; Yan et al., 2014). The correlation for Sr/Ca with summer temperatures in *D. patagonicus* shells is similar to those for the freshwater species *Corbicula fluminea* (Zhao et al., 2017a) of r = 0.7 (p < 0.001).

Bivalve shell Ba/Ca are usually considered as a proxy of both particulate and dissolved Ba in the ambient water (Gillikin et al., 2006). The main source of Ba in freshwater systems is the weathering of Ba-rich rocks in the catchment, which adds Ba into the lakes and rivers during the rainy season (Montaggioni et al., 2006). This often results in regular seasonal Ba/Ca peaks in freshwater shells during the precipitation season (Carroll and Romanek, 2008). Precipitation in northern Patagonia is seasonal and peaks in July during austral winter. In contrast, the annual Ba/Ca peaks in *D. patagonicus* shells occur in January, a relatively dry period of the year. This implies that the influence of Ba added by runoff on lake water Ba concentration is minimal. Linear regression analysis of precipitation and Ba/Ca with a 2-3 month time lag only resulted in low correlation values (Table 3).

Variation in primary productivity and temperature can also influence the Ba intake into freshwater shells (Izumida et al., 2011; Zhao et al., 2017a). Bivalves ingest Ba-rich particles with diatom or phytoplankton due to their filter feeding nature, thus the Ba/Ca is often used as a proxy for primary productivity in the ambient water (Thébault et al., 2009). Lake El Trébol is an oligotrophic lake (Diaz and Pedrozo, 1996; Diaz et al., 2000) with its nutrient budget dominated by silica, while the limiting factor for phytoplankton growth was shown to be nitrogen rather than phosphorus (Diaz et al., 2007). Nutrient replenishment in the lake is achieved by precipitation as well as during a single complete mixing period in spring when temperature differences between surface and bottom water diminish (Queimaliños et al., 1998). Therefore, nutrient supply is an influential factor for bivalve shell growth in this environment and acts synergistically with temperature. The dominant influence of nutrient supply over precipitation could be the reason for the formation of Ba/Ca peaks during summer when temperature and food supply are at their highest.

Mn concentration in freshwater environments (average ~ 8 μgkg^{-1}) is typically higher than in marine environments (average ~ 0.2 μgkg^{-1}). Aragonitic freshwater shells can act as

archives of dissolved Mn associated with riverine anthropogenic inputs (Jeffree et al., 1995; Markich et al., 2002), as well as particulate Mn concentrations associated with lacustrine upwelling and associated changes in phytoplankton productivity (Langlet et al., 2007). Similarly to Ba, Mn incorporation into carbonate shells is mainly controlled by the dissolved and/or particulate Mn^{2+} in water while the physiological control is minimal (Zhao et al., 2017c). However, unlike Sr and Ba, Mn does not exhibit any seasonal variation but irregular elevations of concentrations in the shells studied here (Fig. 7). Irregular phytoplankton blooms could be a reason for the observed peaks in shell Mn/Ca.
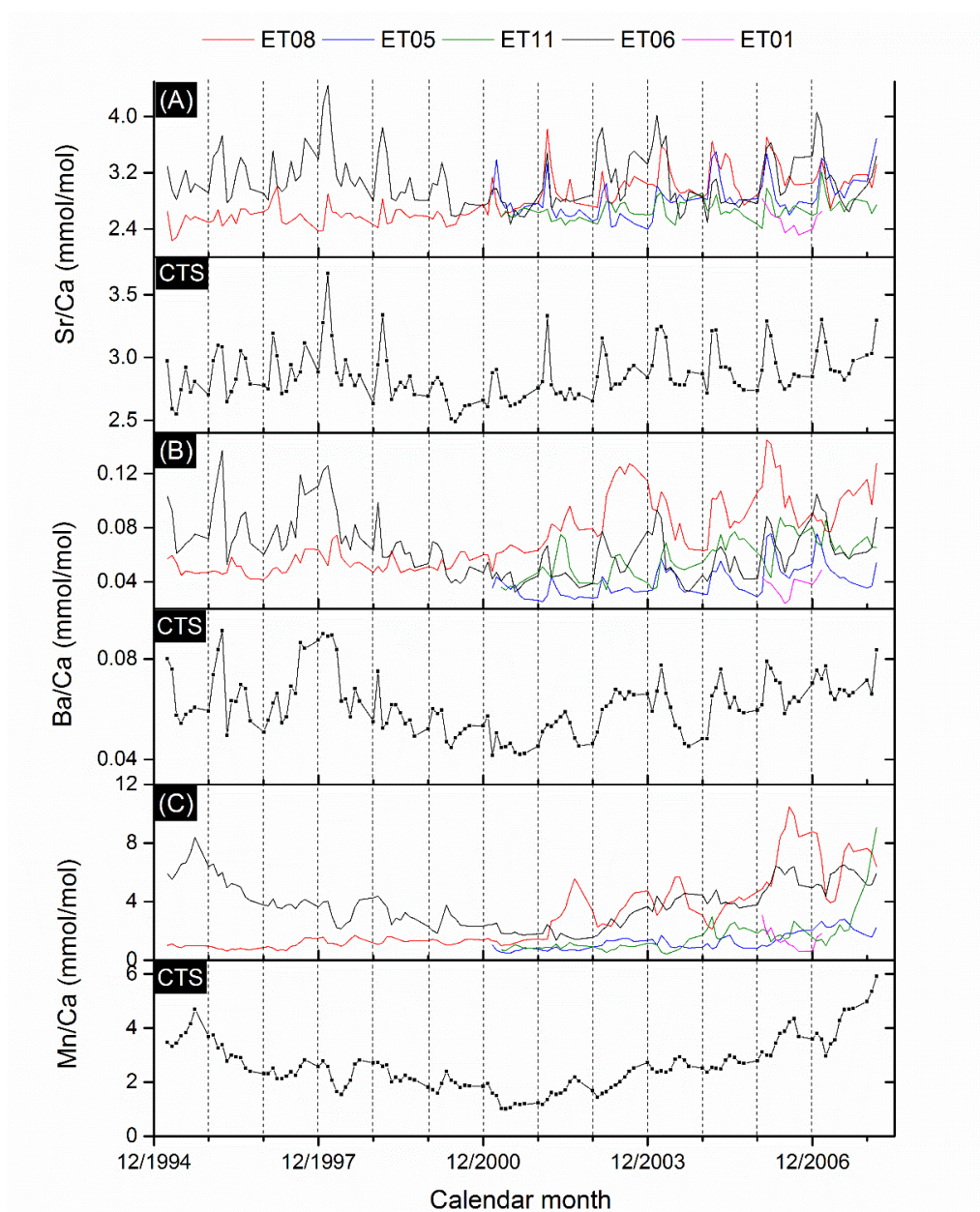
Fig. 7 Monthly variations of (A) Sr/Ca, (B) Ba/Ca and (C) Mn/Ca in the nacreous layer along the direction of minimum growth of four *D. patagonicus* shells from Lake El Trébol and the Composite Time Series (CTS) created by taking the weighted average of five *D. patagonicus* shells. Shell ET01 is not presented in the figure due to its relatively short lifespan. The vertical lines are inserted as a guide and mark the approximate location of the growth line in the shell.
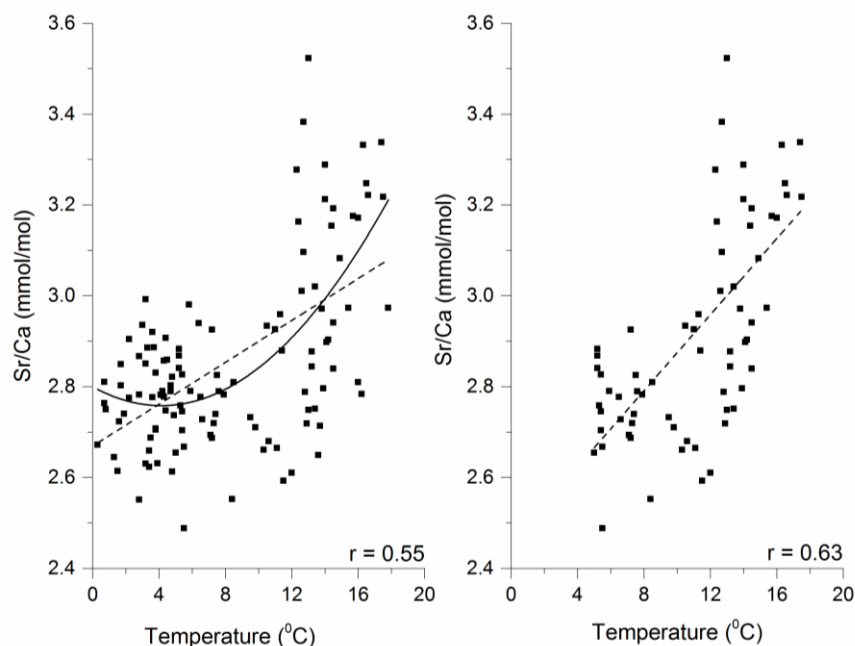
Fig. 8 Scatterplots of monthly averaged shell Sr/Ca of the composite time series of *D. patagonicus* shells from Lake El Trebol with measured air temperature (A) for temperatures from 0 – 20 °C and (B) for temperatures from 5 – 20 °C. Dash lines represent the linear regression line while the solid line represents the polynomial regression line.

4.3.4 Regional and global climate signals in the shell chronology

The El Nino Southern Oscillation (ENSO) is the largest source of global inter-annual climate variability, with near worldwide impacts on temperature, rainfall, and climate events (Yan et al., 2017). Due to the relatively low frequency of ENSO (2–7 years), skeletal bicarbonates are considered to be one of the best high resolution archives of ENSO (Hallmann et al., 2008), and marine and freshwater bivalves have been used in extracting ENSO signals from the temperature records (Schöne et al., 2007; Welsh et al., 2011; Yan et al., 2017). Similarly, *D. patagonicus* shells from Lake El Trébol indicate a significant negative correlation with the Nino 3.4 index (*www.cpc.ncep.noaa.gov)*, especially after 1980 (r = -0.51, p < 0.05, Table 2). This was confirmed by the occurrence of negative anomalies in the master chronology (e.g. 1994, 1978, and 1967; Fig. 9) around El-Niño years (1991-1995, 1976/7/8 and 1965/6,) (*www.cpc.ncep.noaa.gov*). In contrast, positive anomalies in the growth chronology (e.g. 2000, 1980, and 1970; Fig. 9) are associated with main La Niña events (1998-2000, and 1970/2 Fig 9). However, not all El Nino and La Niña events are recorded in the shells, particularly El Nino events in the 1980s and La Niña events in the 1950s are not recorded.

157

The master chronology demonstrates a significant positive correlation with the summer SAM index (*www.cpc.ncep.noaa.gov*) of the previous year (r = 0.4, p < 0.05, Table 2). For instance, the highest recorded positive shift in SAM in 1999 (Marshall, 2003) was followed by the highest shell growth in the year 2000 (Fig. 9). Further, above average shell growth is recorded in the mid 1970s to the mid 1990s, except for 1978/1979, coinciding with the continued positive trend in the SAM in the southern hemisphere (Villalba et al., 2003). In Patagonia, a strong and continued La Niña event was reported during 1998 and 1999 (Suarez et al., 2004), a time during which SAM also recorded its highest values (1998-1999; (Marshall, 2003). Influence of this positive SAM phase intensified by the La Niña event can be put forward as the reason for the extreme above average growth observed in the shells in the year 2000 (Fig. 4). This anomalous event was also recorded in *Nothofagus sp.* trees by increased tree mortality in 1998/1999 (Suarez et al., 2004) as well as a drought in Patagonian streamflow reconstructions using *Austrocedrus sp.* trees (Lara et al., 2008).
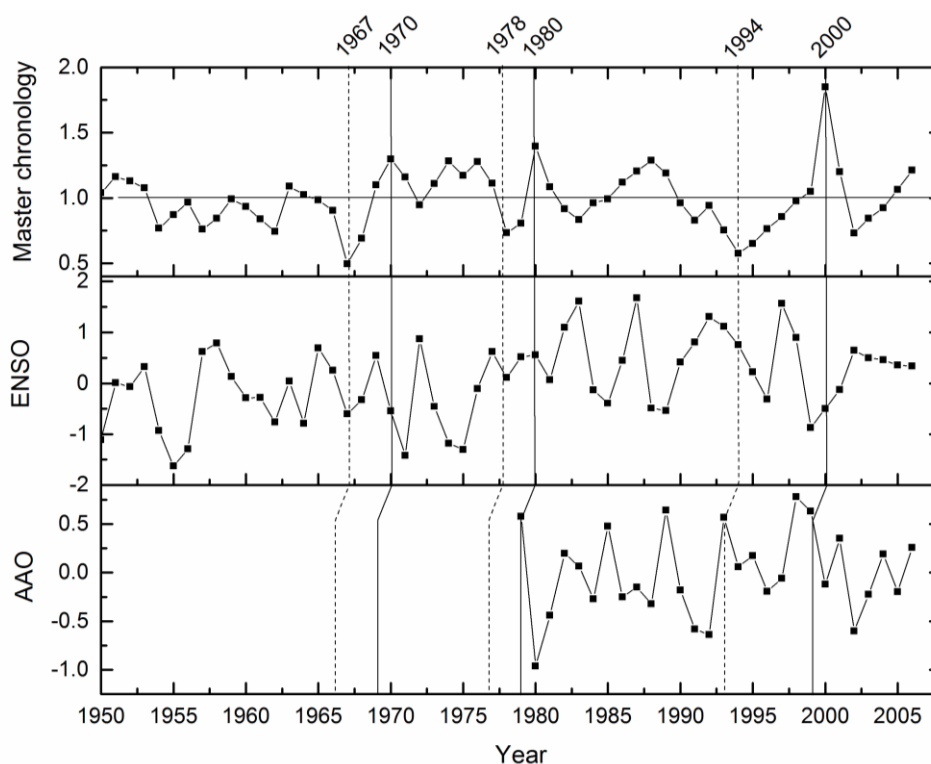
Fig. 9 Master chronology of *D. patagonicus* shells collected from Nahuel Huapi National Park in Patagonia, Argentina compared with the El Niño Southern Oscillation (ENSO) and the Southern Annular Mode (SAM). Dash lines represent the years with anomalous shell growth which are specially mentioned in the text.

Many continental proxy archives have been used to understand the climatic and environmental variability in the Patagonian region, for example tree rings (Boninsegna et al., 2009; Villalba et al., 2012; Álvarez et al., 2015), tree mortality (Suarez et al., 2004), wildfire

activities (Holz and Veblen, 2011; Holz et al., 2012), variability of lake levels (Pasquini et al., 2008) as well as varved sediment cores in proglacial lakes in Patagonia (Ariztegui et al., 2007). Unlike tree rings, lake levels and varved sediment cores have a low temporal resolution (usually decadal or longer), while tree mortality and wildfire activities record only anomalous events. Therefore, *D. patagonicus* shells provide a more detailed insight into environmental change with seasonal detail than those archives with maximally annual resolution.

In contrast to *D. patagonicus* shells, tree growth consistently indicates a positive (negative) relationship with the warm (cold) phase of the ENSO in Patagonia (Daniels and Veblen, 2004; Lara et al., 2008; Christie et al., 2009; Álvarez et al., 2015), hence an opposite response to ENSO events to that of the freshwater bivalve shells. However, the relationship of SAM and tree ring growth differs with location and can show either, positive (in the western Andes: Álvarez et al., 2015) as well as negative correlations (in the eastern Andes: Daniels and Veblen, 2004; Lara et al., 2008). Since all lakes considered in this study are located East of the Andes, this suggests that the response to SAM could be complementary between *D. patagonicus* shells and trees, similar to their response to ENSO events. Hence, a combined use of tree ring and *D. patagonicus* shell proxy archives in the future could lead to a more detailed reconstruction of both ENSO phases. Furthermore, due to continued growth during the Patagonian winter, *D. patagonicus* shells can be used to reconstruct monthly resolved temperature variations throughout the year, while tree ring reconstructions usually are restricted to their growing season that excludes the winter months.

4.4. Conclusions

Adding *D. patagonicus* shells as a new independent continental proxy archive to regional climatic records can potentially improve our understanding of the paleo-environment in the southern hemisphere considerably. Since *D. patagonicus* is the dominant freshwater bivalve species in modern and fossil assemblages in South America, their shells can act as a supplementary archive to the well-developed tree ring database. One of the disadvantages of this new proxy archive, namely the shorter lifetime of the bivalves compared to trees, can be overcome by cross-dating of several individuals collected at different times, thus creating master chronologies covering longer time periods expanding into several centuries.

The oxygen isotope content in Lake El Trebol water is controlled by evaporation and precipitation, not temperature, which indicates that the oxygen isotope ratio in *D. patagonicus* shells also reflects the evaporation and precipitation patterns in the region. In contrast, the resulted in relatively higher correlation indicate that Sr/Ca in *D. patagonicus* shells can act as a proxy of summer temperature in the region. The use of two seasonally separate empirical equations improved the reliability of temperatures calculated with shell Sr/Ca. This approach could enhance the usefulness of bivalve species like *D. patagonicus* in South America, where temperature proxies with monthly resolution are otherwise scarce.

We see the strength of this new biogenic climate archive in its similar temporal resolution to tree-ring archives and the possibility to use this in complementing and supporting tree ring studies. The method of combining different proxies has been shown to yield highly resolved, consistent and more precise reconstructions of past climate conditions (Black et al., 2009) that are clearly needed in order to improve climate models.

4.5. References

Aceituno, P., Fuenzalida, H. and Rosenblüth, B., 1993. Climate along the extratropical west coast of South America. Earth system responses to global change, edited by: Mooney, HA, Fuentes, ER, and Kronberg, BI, Academic Press, San Diego: 61-69.

Ahmed, M., Anchukaitis, K.J., Asrat, A., Borgaonkar, H.P., Braida, M., Buckley, B.M., Büntgen, U., Chase, B.M., Christie, D.A. and Cook, E.R., 2013. Continental-scale temperature variability during the past two millennia. Nature Geoscience, 6(5): 339.

Álvarez, C., Veblen, T.T., Christie, D.A. and González-Reyes, Á., 2015. Relationships between climate variability and radial growth of Nothofagus pumilio near altitudinal treeline in the Andes of northern Patagonia, Chile. Forest Ecology and Management, 342: 112-121.

Ariztegui, D., Bösch, P. and Davaud, E., 2007. Dominant ENSO frequencies during the Little Ice Age in Northern Patagonia: the varved record of proglacial Lago Frias, Argentina. Quaternary International, 161(1): 46-55.

Barriga, J., 2006. La distribución espacio-temporal, el crecimiento y la alimentación de larvas y juveniles de Galaxias (*Pisces, Galaxiidae*) en lagos y rıos patagónicos, Ph. D. Thesis, Universidad Nacional del Comahue, Bariloche.

Black, B.A., Copenheaver, C.A., Frank, D.C., Stuckey, M.J. and Kormanyos, R.E., 2009. Multi-proxy reconstructions of northeastern Pacific sea surface temperature data from trees and Pacific geoduck. Palaeogeography, Palaeoclimatology, Palaeoecology, 278(1): 40-47.

Boninsegna, J.A., Argollo, J., Aravena, J., Barichivich, J., Christie, D., Ferrero, M., Lara, A., Le Quesne, C., Luckman, B. and Masiokas, M., 2009. Dendroclimatological reconstructions in South America: a review. Palaeogeography, Palaeoclimatology, Palaeoecology, 281(3): 210-228.

Butler, P.G., Scourse, J.D., Richardson, C.A., Wanamaker, A.D., Bryant, C.L. and Bennell, J.D., 2009. Continuous marine radiocarbon reservoir calibration and the ^{13}C Suess effect in the Irish Sea: Results from the first multi-centennial shell-based marine master chronology. Earth and Planetary Science Letters, 279(3): 230-241.

Carroll, M., Romanek, C. and Paddock, L., 2006. The relationship between the hydrogen and oxygen isotopes of freshwater bivalve shells and their home streams. Chemical Geology, 234(3): 211-222.

Carroll, M. and Romanek, C.S., 2008. Shell layer variation in trace element concentration for the freshwater bivalve *Elliptio complanata*. Geo-Marine Letters, 28(5-6): 369-381.

Castellanos, Z.d., 1960. Almejas nacaríferas de la República Argentina género Diplodon (MollMutélidos). Publicación Miscelánea. 421. 40 p.

Christie, D.A., Lara, A., Barichivich, J., Villalba, R., Morales, M.S. and Cuq, E., 2009. El Niño-Southern Oscillation signal in the world's highest-elevation tree-ring chronologies from the Altiplano, Central Andes. Palaeogeography, Palaeoclimatology, Palaeoecology, 281(3): 309-319.

Clark, G., 1975. Periodic growth and biological rhythms in experimentally grown bivalves. Growth rhythms and the history of the earth's rotation, London, John Wiley & Sons: 103-117.

Collins, J.M., Chaves, R.R. and da Silva Marques, V., 2009. Temperature variability over South America. Journal of climate, 22(22): 5854-5869.

Cook, E. and Holmes, R., 1996. Guide for computer program ARSTAN. The international tree-ring data bank program library version, 2(0): 75-87.

Daniels, L.D. and Veblen, T.T., 2004. Spatiotemporal influences of climate on altitudinal treeline in northern Patagonia. Ecology, 85(5): 1284-1296.

De Winter, N.J., Goderis, S., Dehairs, F., Jagt, J.W., Fraaije, R.H., Van Malderen, S.J., Vanhaecke, F. and Claeys, P., 2017. Tropical seasonality in the late Campanian (late Cretaceous): Comparison between multiproxy records from three bivalve taxa from Oman. Palaeogeography, Palaeoclimatology, Palaeoecology.

DeLong, K.L., Flannery, J.A., Maupin, C.R., Poore, R.Z. and Quinn, T.M., 2011. A coral Sr/Ca calibration and replication study of two massive corals from the Gulf of Mexico. Palaeogeography, Palaeoclimatology, Palaeoecology, 307(1): 117-128.

Dettman, D.L., Reische, A.K. and Lohmann, K.C., 1999. Controls on the stable isotope composition of seasonal growth bands in aragonitic fresh-water bivalves (*Unionidae*). Geochimica et Cosmochimica Acta, 63(7): 1049-1057.

Diaz, M., Pedrozo, F. and Baccala, N., 2000. Summer classification of southern hemisphere temperate lakes (Patagonia, Argentina). Lakes & Reservoirs: Research & Management, 5(4): 213-229.

Diaz, M., Pedrozo, F., Reynolds, C. and Temporetti, P., 2007. Chemical composition and the nitrogen-regulated trophic state of Patagonian lakes. Limnologica-Ecology and Management of Inland Waters, 37(1): 17-27.

Diaz, M.M. and Pedrozo, F.L., 1996. Nutrient limitation in Andean-Patagonian lakes at latitude 40-41 S. Archiv für Hydrobiologie, 138(1): 123-143.

Emile-Geay, J., McKay, N.P., Kaufman, D.S., Von Gunten, L., Wang, J., Anchukaitis, K.J., Abram, N.J., Addison, J.A., Curran, M.A. and Evans, M.N., 2017. A global multiproxy database for temperature reconstructions of the Common Era. 2052-4463.

Featherstone, A.M., Butler, P.G., Peharda, M., Chauvaud, L. and Thébault, J., 2017. Influence of riverine input on the growth of *Glycymeris glycymeris* in the Bay of Brest, North-West France. PloS one, 12(12): e0189782.

Füllenbach, C.S., Schöne, B.R., Shirai, K., Takahata, N., Ishida, A. and Sano, Y., 2017. Minute co-variations of Sr/Ca ratios and microstructures in the aragonitic shell of Cerastoderma edule (Bivalvia)–Are geochemical variations at the ultra-scale masking potential environmental signals? Geochimica et Cosmochimica Acta, 205: 256-271.

Garreaud, R., Lopez, P., Minvielle, M. and Rojas, M., 2013. Large-scale control on the Patagonian climate. Journal of Climate, 26(1): 215-230.

Garreaud, R.D., Vuille, M., Compagnucci, R. and Marengo, J., 2009. Present-day south american climate. Palaeogeography, Palaeoclimatology, Palaeoecology, 281(3): 180-195.

Gillikin, D.P., Dehairs, F., Lorrain, A., Steenmans, D., Baeyens, W. and André, L., 2006. Barium uptake into the shells of the common mussel (*Mytilus edulis*) and the potential for estuarine paleo-chemistry reconstruction. Geochimica et Cosmochimica Acta, 70(2): 395-407.

Gillikin, D.P., Lorrain, A., Navez, J., Taylor, J.W., André, L., Keppens, E., Baeyens, W. and Dehairs, F., 2005. Strong biological controls on Sr/Ca ratios in aragonitic marine bivalve shells. Geochemistry, Geophysics, Geosystems, 6(5).

Gogorza, C., Sinito, A., Lirio, J., Nuñez, H., Chaparro, M. and Vilas, J., 2002. Paleosecular variations 0–19,000 years recorded by sediments from Escondido Lake (Argentina). Physics of the Earth and Planetary Interiors, 133(1): 35-55.

Graf, D.L. and Cummings, K.S., 2007. Review of the systematics and global diversity of freshwater mussel species (*Bivalvia: Unionoida*). Journal of Molluscan Studies, 73(4): 291-314.

Griffin, W., Powell, W., Pearson, N. and O'reilly, S., 2008. GLITTER: data reduction software for laser ablation ICP-MS. Laser Ablation-ICP-MS in the earth sciences. Mineralogical association of Canada short course series, 40: 204-207.

Hallmann, N., Schöne, B.R., Strom, A. and Fiebig, J., 2008. An intractable climate archive— sclerochronological and shell oxygen isotope analyses of the Pacific geoduck,

Panopea abrupta (bivalve mollusk) from Protection Island (Washington State, USA). Palaeogeography, Palaeoclimatology, Palaeoecology, 269(1-2): 115-126.

Holz, A., Kitzberger, T., Paritsis, J. and Veblen, T.T., 2012. Ecological and climatic controls of modern wildfire activity patterns across southwestern South America. Ecosphere, 3(11): 1-25.

Holz, A. and Veblen, T.T., 2011. Variability in the Southern Annular Mode determines wildfire activity in Patagonia. Geophysical Research Letters, 38(14).

Izumida, H., Yoshimura, T., Suzuki, A., Nakashima, R., Ishimura, T., Yasuhara, M., Inamura, A., Shikazono, N. and Kawahata, H., 2011. Biological and water chemistry controls on Sr/Ca, Ba/Ca, Mg/Ca and δ 18 O profiles in freshwater pearl mussel *Hyriopsis* sp. Palaeogeography, Palaeoclimatology, Palaeoecology, 309(3): 298-308.

Jeffree, R., Markich, S., Lefebvre, F., Thellier, M. and Ripoll, C., 1995. Shell microlaminations of the freshwater bivalve *Hyridella depressa* as an archival monitor of manganese water concentration: Experimental investigation by depth profiling using secondary ion mass spectrometry (SIMS). Experientia, 51(8): 838-848.

Jochum, K.P., Nohl, U., Herwig, K., Lammel, E., Stoll, B. and Hofmann, A.W., 2005. GeoReM: a new geochemical database for reference materials and isotopic standards. Geostandards and Geoanalytical Research, 29(3): 333-338.

Kaandorp, R.J., Vonhof, H.B., Del Busto, C., Wesselingh, F.P., Ganssen, G.M., Marmól, A.E., Pittman, L.R. and van Hinte, J.E., 2003. Seasonal stable isotope variations of the modern Amazonian freshwater bivalve *Anodontites trapesialis*. Palaeogeography, Palaeoclimatology, Palaeoecology, 194(4): 339-354.

Kelemen, Z., Gillikin, D.P., Graniero, L.E., Havel, H., Darchambeau, F., Borges, A.V., Yambélé, A., Bassirou, A. and Bouillon, S., 2017. Calibration of hydroclimate proxies in freshwater bivalve shells from Central and West Africa. Geochimica et Cosmochimica Acta, 208: 41-62.

Khim, B.K., Krantz, D.E., Cooper, L.W. and Grebmeier, J.M., 2003. Seasonal discharge of estuarine freshwater to the western Chukchi Sea shelf identified in stable isotope profiles of mollusk shells. Journal of Geophysical Research: Oceans, 108(C9).

Langlet, D., Alleman, L., Plisnier, P.-D., Hughes, H. and André, L., 2007. Manganese content records seasonal upwelling in Lake Tanganyika mussels. Biogeosciences, 4(2): 195-203.

Lara, A., Villalba, R. and Urrutia, R., 2008. A 400-year tree-ring record of the Puelo River summer–fall streamflow in the Valdivian Rainforest eco-region, Chile. Climatic Change, 86(3-4): 331-356.

Lara, G. and Parada, E., 1991. Seasonal changes in the condition index of *Diplodon chilensis* chilensis (Gray, 1828) in sandy and muddy substrata, Villarrica Lake, Chile (39◦ 18 S; 72◦ 05 W). Boletín Sociedad de Biología de Concepción, 62: 99-106.

Magrin, G., Marengo, J., Boulanger, J., Buckeridge, M., Castellanos, E., Poveda, G., Scarano, F. and Vicuña, S., 2014. Central and South America. Climate change: 1499-1566.

Markgraf, V., Whitlock, C. and Haberle, S., 2007. Vegetation and fire history during the last 18,000 cal yr BP in Southern Patagonia: Mallín Pollux, Coyhaique, Province Aisén (45 41′ 30 ″S, 71 50′ 30 ″W, 640 m elevation). Palaeogeography, Palaeoclimatology, Palaeoecology, 254(3): 492-507.

Markich, S.J., Jeffree, R.A. and Burke, P.T., 2002. Freshwater bivalve shells as archival indicators of metal pollution from a copper− uranium mine in tropical Northern Australia. Environmental science & technology, 36(5): 821-832.

Marshall, G.J., 2003. Trends in the Southern Annular Mode from observations and reanalyses. Journal of Climate, 16(24): 4134-4143.

Massaferro, M., Massaferro, J., Ross, G.R., Amos, A. and Lami, A., 1999. Late Pleistocene and early Holocene ecological response of Lake El Trébol (Patagonia, Argentina) to environmental changes. Journal of Paleolimnology, 22(2): 137-148.

Montaggioni, L.F., Le Cornec, F., Corrège, T. and Cabioch, G., 2006. Coral barium/calcium record of mid-Holocene upwelling activity in New Caledonia, South-West Pacific. Palaeogeography, Palaeoclimatology, Palaeoecology, 237(2): 436-455.

Neukom, R. and Gergis, J., 2012. Southern Hemisphere high-resolution palaeoclimate records of the last 2000 years. The Holocene, 22(5): 501-524.

New, M., Lister, D., Hulme, M. and Makin, I., 2002. A high-resolution data set of surface climate over global land areas. Climate research, 21(1): 1-25.

Parada, E., Peredo, S. and Gallardo, C., 1990. Tácticas reproductivas y dinámica poblacional de *Diplodon chilensis* (Gray, 1828)(Bivalvia: Hyriidae). Revista Chilena de Historia Natural, 63: 23-35.

Pasquini, A.I., Lecomte, K.L. and Depetris, P.J., 2008. Climate change and recent water level variability in Patagonian proglacial lakes, Argentina. Global and Planetary Change, 63(4): 290-298.

Pérez, G.L., Queimaliños, C.P. and Modenutti, B.E., 2002. Light climate and plankton in the deep chlorophyll maxima in North Patagonian Andean lakes. Journal of Plankton Research, 24(6): 591-599.

Prohaska, F., 1976. The climate of argentina, Paraguay and Uruguay. Climates of Central and South America, 12: 13-112.

Queimaliños, C.P., Modenutti, B.E. and Balseiro, E.G., 1998. Phytoplankton responses to experimental enhancement of grazing pressure and nutrient recycling in a small Andean lake. Freshwater Biology, 40(1): 41-49.

Ropes, J.W., Jones, D., Murawski, S., Serchuk, F. and Jearld, A., 1984. Documentation of annual growth lines in ocean quahogs, *Arctica-islandica* linne. Fishery Bulletin, 82(1): 1-19.

Saenger, C., Gabitov, R.I., Farmer, J., Watkins, J.M. and Stone, R., 2017. Linear correlations in bamboo coral δ ^{13}C and δ ^{18}O sampled by SIMS and micromill: Evaluating paleoceanographic potential and biomineralization mechanisms using δ ^{11}B and Δ_{47} composition. Chemical Geology, 454: 1-14.

Schöne, B.R., 2008. The curse of physiology—challenges and opportunities in the interpretation of geochemical data from mollusk shells. Geo-Marine Letters, 28(5-6): 269-285.

Schöne, B.R., Dunca, E., Fiebig, J. and Pfeiffer, M., 2005. Mutvei's solution: an ideal agent for resolving microgrowth structures of biogenic carbonates. Palaeogeography, Palaeoclimatology, Palaeoecology, 228(1): 149-166.

Schöne, B.R., Dunca, E., Mutvei, H. and Norlund, U., 2004. A 217-year record of summer air temperature reconstructed from freshwater pearl mussels (*M. margarifitera*, Sweden). Quaternary Science Reviews, 23(16): 1803-1816.

Schöne, B.R., Page, N.A., Rodland, D.L., Fiebig, J., Baier, S., Helama, S.O. and Oschmann, W., 2007. ENSO-coupled precipitation records (1959–2004) based on shells of freshwater bivalve mollusks (*Margaritifera falcata*) from British Columbia. International Journal of Earth Sciences, 96(3): 525-540.

Schöne, B.R. and Surge, D.M., 2012. Part N, Revised, Volume 1, Chapter 14: Bivalve sclerochronology and geochemistry. Treatise online, 46: 1-24.

Schöne, B.R., Zhang, Z., Jacob, D., Gillikin, D.P., Tütken, T., Garbe-Schönberg, D. and SOLDATI, A., 2010. Effect of organic matrices on the determination of the trace element chemistry (Mg, Sr, Mg/Ca, Sr/Ca) of aragonitic bivalve shells (*Arctica islandica*)—Comparison of ICP-OES and LA-ICP-MS data. Geochemical journal, 44(1): 23-37.

Semenas, L. and Brugni, N., 2002. Características poblacionales y ciclo de vida de *Diplodon chilensis* (d'Orbigny, 1835)(Hyriidae, Bivalvia) en el lago Gutiérrez (Patagonia, Argentina). Ecología austral, 12: 29-40.

Soldati, A., Jacob, D., Schöne, B., Bianchi, M. and Hajduk, A., 2009. Seasonal periodicity of growth and composition in valves of *Diplodon chilensis patagonicus* (d'Orbigny, 1835). Journal of Molluscan Studies, 75(1): 75-85.

Sosdian, S., Gentry, D.K., Lear, C.H., Grossman, E.L., Hicks, D. and Rosenthal, Y., 2006. Strontium to calcium ratios in the marine gastropod *Conus ermineus*: Growth rate effects and temperature calibration. Geochemistry, Geophysics, Geosystems, 7(11).

Spötl, C. and Vennemann, T.W., 2003. Continuous-flow isotope ratio mass spectrometric analysis of carbonate minerals. Rapid communications in mass spectrometry, 17(9): 1004-1006.

Stern, L.A. and Blisniuk, P.M., 2002. Climate and Dynamics (ACL)-ACL 3 Stable isotope composition of precipitation across the southern Patagonian Andes (DOI 10.1029/2002JD002509). Journal of Geophysical Research-Part D-Atmospheres, 107(23).

Steuber, T., 1999. Isotopic and chemical intra-shell variations in low-Mg calcite of rudist bivalves (*Mollusca-Hippuritacea*): disequilibrium fractionations and late Cretaceous seasonality. International Journal of Earth Sciences, 88(3): 551-570.

Suarez, M.L., Ghermandi, L. and Kitzberger, T., 2004. Factors predisposing episodic drought-induced tree mortality in Nothofagus–site, climatic sensitivity and growth trends. Journal of Ecology, 92(6): 954-966.

Tatur, A., del Valle, R., Bianchi, M.-M., Outes, V., Villarosa, G., Niegodzisz, J. and Debaene, G., 2002. Late Pleistocene palaeolakes in the Andean and Extra-Andean Patagonia at mid-latitudes of South America. Quaternary International, 89(1): 135-150.

Team, R.C., 2017. R: A language and environment for statistical computing. Vienna, Austria: R Foundation for Statistical Computing; 2017.

Thébault, J., Chauvaud, L., L'Helguen, S., Clavier, J., Barats, A., Jacquet, S., Pécheyran, C. and Amouroux, D., 2009. Barium and molybdenum records in bivalve shells: Geochemical proxies for phytoplankton dynamics in coastal environments? Limnology and Oceanography, 54(3): 1002-1014.

Thompson, D.W. and Solomon, S., 2002. Interpretation of recent Southern Hemisphere climate change. Science, 296(5569): 895-899.

Thompson, D.W. and Wallace, J.M., 2000. Annular modes in the extratropical circulation. Part I: month-to-month variability*. Journal of Climate, 13(5): 1000-1016.

Villalba, R., Grosjean, M. and Kiefer, T., 2009. Long-term multi-proxy climate reconstructions and dynamics in South America (LOTRED-SA): state of the art and perspectives. Palaeogeography, Palaeoclimatology, Palaeoecology, 281(3): 175-179.

Villalba, R., Lara, A., Boninsegna, J.A., Masiokas, M., Delgado, S., Aravena, J.C., Roig, F.A., Schmelter, A., Wolodarsky, A. and Ripalta, A., 2003. Large-scale temperature changes across the southern Andes: 20th-century variations in the context of the past 400 years, Climate Variability and Change in High Elevation Regions: Past, Present & Future. Springer, pp. 177-232.

Villalba, R., Lara, A., Masiokas, M.H., Urrutia, R., Luckman, B.H., Marshall, G.J., Mundo, I.A., Christie, D.A., Cook, E.R. and Neukom, R., 2012. Unusual Southern Hemisphere tree growth patterns induced by changes in the Southern Annular Mode. Nature Geoscience, 5(11): 793-798.

Wang, C., Deser, C., Yu, J.-Y., DiNezio, P. and Clement, A., 2017. El Niño and Southern Oscillation (ENSO): A Review, Coral Reefs of the Eastern Tropical Pacific. Springer, pp. 85-106.

Welsh, K., Elliot, M., Tudhope, A., Ayling, B. and Chappell, J., 2011. Giant bivalves (*Tridacna gigas*) as recorders of ENSO variability. Earth and Planetary Science Letters, 307(3-4): 266-270.

Wigley, T.M., Briffa, K.R. and Jones, P.D., 1984. On the average value of correlated time series, with applications in dendroclimatology and hydrometeorology. Journal of Climate and Applied Meteorology, 23(2): 201-213.

Witbaard, R., 1996. Growth variations in *Arctica islandica* L.(Mollusca): a reflection of hydrography-related food supply. ICES Journal of Marine Science, 53(6): 981-987.

Wu, H.C., Moreau, M., Linsley, B.K., Schrag, D.P. and Corrège, T., 2014. Investigation of sea surface temperature changes from replicated coral Sr/Ca variations in the eastern equatorial Pacific (Clipperton Atoll) since 1874. Palaeogeography, Palaeoclimatology, Palaeoecology, 412: 208-222.

Yan, H., Liu, C., Zhang, W., Li, M., Zheng, X., Wei, G., Xie, L., Deng, W. and Sun, L., 2017. ENSO variability around 2000 years ago recorded by *Tridacna gigas* δ^{18}O from the South China Sea. Quaternary International, 452: 148-154.

Yan, H., Shao, D., Wang, Y. and Sun, L., 2014. Sr/Ca differences within and among three *Tridacnidae* species from the South China Sea: Implication for paleoclimate reconstruction. Chemical Geology, 390: 22-31.

Yan, H., Sun, L., Shao, D. and Wang, Y., 2015. Seawater temperature seasonality in the South China Sea during the late Holocene derived from high-resolution Sr/Ca ratios of *Tridacna gigas*. Quaternary Research, 83(2): 298-306.

Yoshimura, T., Izumida, H., Nakashima, R., Ishimura, T., Shikazono, N., Kawahata, H. and Suzuki, A., 2015. Stable carbon isotope values in dissolved inorganic carbon of ambient waters and shell carbonate of the freshwater pearl mussel (*Hyriopsis* sp.). Journal of Paleolimnology, 54(1): 37-51.

Zhao, L., Schöne, B.R. and Mertz-Kraus, R., 2017a. Controls on strontium and barium incorporation into freshwater bivalve shells (*Corbicula fluminea*). Palaeogeography, Palaeoclimatology, Palaeoecology, 465: 386-394.

Zhao, L., Schöne, B.R. and Mertz-Kraus, R., 2017b. Delineating the role of calcium in shell formation and elemental composition of *Corbicula fluminea* (Bivalvia). Hydrobiologia, 790(1): 259-272.

Zhao, L., Walliser, E.O., Mertz-Kraus, R. and Schöne, B.R., 2017c. Unionid shells (*Hyriopsis cumingii*) record manganese cycling at the sediment-water interface in a shallow eutrophic lake in China (Lake Taihu). Palaeogeography, Palaeoclimatology, Palaeoecology.

Zubimendi, M., 2007. Discusión sobre las malacofaunas presentes en sitios arqueológicos de la Patagonia Continental Argentina. Publicación digital en el CD de las VI Jornadas de Arqueología e Historia de las Regiones Pampeana y Patagónica, 232.

4.6 Supplementary material – Chapter 4

4.6.2 Supplementary – Tables

Table S1. The incremental width of 14 *D. patagonicus* shells collected from Lake Escondido (ES) and Lake El Trébol (ET) which are used in the master chronology.

Year	ET 05	ET 06	ET 07	ET 08	ET 12	ES 01	ES 02	ES 03	ES 05	ES 06	ES 07	ES 08	ES 09	ES 10
1940								0.13						
1941								0.09						
1942								0.12						
1943								0.13						
1944								0.09						
1945							0.03	0.15						
1946							0.08	0.08						
1947							0.06	0.09						
1948							0.05	0.08						
1949		0.22					0.07	0.10						
1950		0.28					0.09	0.08					0.17	
1951		0.29					0.09	0.15					0.17	
1952		0.13					0.12	0.12					0.21	
1953		0.07					0.10	0.14					0.21	
1954		0.08					0.09	0.08					0.15	
1955		0.10					0.11	0.10					0.15	
1956		0.10	0.17				0.13	0.12					0.12	
1957		0.06	0.15				0.17	0.07					0.13	
1958		0.13	0.10		0.17		0.07	0.06					0.19	
1959		0.20	0.15		0.21		0.10	0.05	0.13				0.16	
1960		0.24	0.14		0.13		0.16	0.09	0.13				0.15	
1961		0.21	0.09		0.14		0.08	0.10	0.06				0.18	
1962		0.05	0.10		0.13		0.12	0.10	0.08				0.13	
1963		0.08	0.14		0.13		0.22	0.12	0.24				0.18	
1964		0.12	0.12		0.10		0.21	0.08	0.20				0.23	
1965		0.15	0.10		0.19		0.17	0.12	0.11				0.13	
1966		0.17	0.10		0.23		0.09	0.12	0.03				0.09	
1967		0.03	0.07		0.06		0.04	0.10	0.14				0.04	
1968		0.10	0.07		0.05		0.14	0.07	0.28				0.14	
1969		0.16	0.08		0.09		0.20	0.11	0.27				0.19	
1970		0.16	0.11		0.19		0.24	0.11	0.26				0.18	
1971		0.14	0.17		0.13		0.26	0.10	0.19				0.16	

Year	ET 05	ET 06	ET 07	ET 08	ET 12	ES 01	ES 02	ES 03	ES 05	ES 06	ES 07	ES 08	ES 09	ES 10
1973		0.13	0.15		0.19		0.21	0.10	0.11				0.21	
1974		0.11	0.15		0.15		0.25	0.15	0.14				0.28	
1975		0.07	0.09		0.11		0.26	0.14	0.20				0.25	
1976		0.08	0.10		0.07		0.30	0.16	0.25				0.23	
1977		0.09	0.08		0.06		0.28	0.13	0.19				0.18	
1978		0.07	0.09		0.10		0.07	0.15	0.08				0.11	
1979		0.07	0.11		0.06		0.19	0.11	0.12				0.07	
1980		0.19	0.28		0.13		0.25	0.10	0.19				0.15	
1981		0.16	0.15		0.13	0.07	0.24	0.07	0.14				0.14	
1983		0.05	0.14		0.03	0.04	0.23	0.09	0.16	0.07			0.12	
1984		0.10	0.13		0.07	0.11	0.20	0.06	0.14	0.12			0.11	
1985		0.14	0.14		0.08	0.12	0.20	0.06	0.10	0.10			0.15	0.14
1986		0.11	0.17		0.14	0.23	0.19	0.04	0.15	0.06			0.12	0.18
1987		0.15	0.21		0.09	0.24	0.17	0.07	0.13	0.14		0.14	0.11	0.20
1988		0.19	0.20		0.08	0.28	0.20	0.06	0.09	0.13	0.14	0.17	0.11	0.21
1989		0.15	0.21		0.09	0.25	0.20	0.04	0.10	0.09	0.09	0.15	0.11	0.23
1990		0.13	0.20		0.16	0.19	0.11	0.03	0.05	0.06	0.10	0.15	0.03	0.15
1991		0.17	0.12		0.06	0.16	0.08	0.03	0.07	0.07	0.13	0.10	0.04	0.11
1992		0.11	0.11	0.29	0.14	0.16	0.09	0.02	0.08	0.08	0.13	0.12	0.06	0.12
1993		0.09	0.12	0.24	0.07	0.09	0.09	0.02	0.07	0.05	0.09	0.10	0.05	0.11
1994		0.08	0.12	0.35	0.04	0.04	0.07	0.02	0.04	0.05	0.05	0.06	0.06	0.07
1995		0.08	0.11	0.42	0.08	0.04	0.05	0.02	0.03	0.06	0.07	0.07	0.08	0.03
1996		0.10	0.14	0.34	0.08	0.05	0.06	0.01	0.04	0.07	0.08	0.09	0.05	0.13
1997		0.10	0.10	0.23	0.08	0.07	0.04	0.04	0.04	0.09	0.07	0.11	0.09	0.10
1998		0.11	0.20	0.25	0.07	0.05	0.08	0.04	0.07	0.09	0.07	0.14	0.07	0.08
1999	0.25	0.14	0.12	0.50	0.07	0.07	0.08	0.05	0.05	0.09	0.06	0.15	0.05	0.10
2000	0.28	0.21	0.24	0.35	0.11	0.20	0.13	0.14	0.09	0.19	0.19	0.23	0.10	0.15
2001	0.25	0.20	0.20	0.23	0.06	0.10	0.09	0.03	0.05	0.10	0.12	0.15	0.06	0.08
2002	0.31	0.06	0.09	0.13	0.03	0.03	0.05	0.05	0.04	0.03	0.06	0.12	0.03	0.03
2003	0.38	0.10	0.08	0.08	0.04	0.06	0.03	0.02	0.02	0.09	0.08	0.07	0.04	0.04
2004	0.32	0.11	0.12	0.14	0.03	0.05	0.04	0.02	0.04	0.02	0.06	0.07	0.02	0.04
2005	0.16	0.07	0.12	0.13	0.04	0.04	0.06	0.02	0.02	0.06	0.06	0.07	0.04	0.02
2006	0.27	0.05	0.06	0.13	0.05	0.03	0.05	0.02	0.02	0.06	0.03	0.06	0.03	0.02

4.6.2 Supplementary - Figures
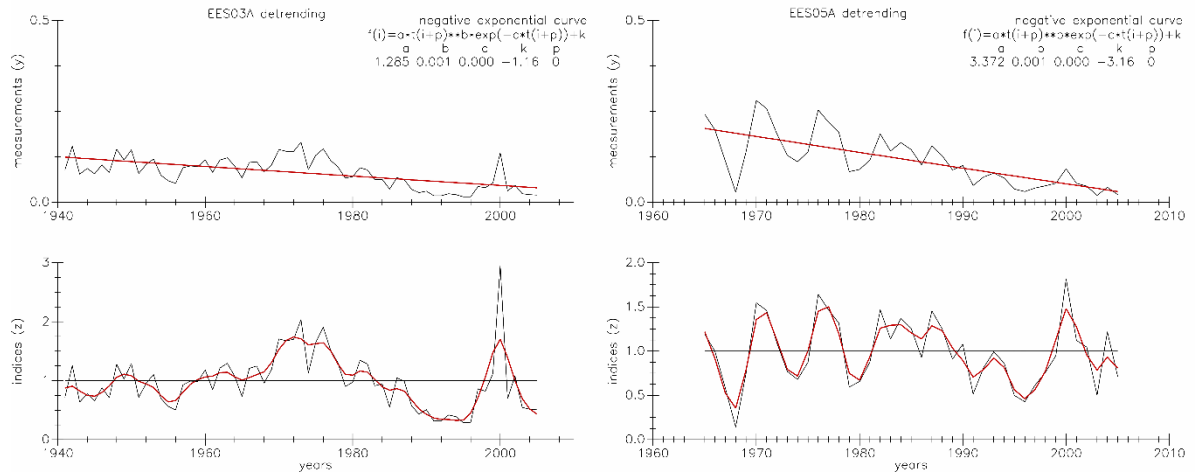
Fig. S1 Two representative shell growth increment time series from Lake Escondido before (top) and after detrending (bottom) using a negative exponential function in ARSTAN. The red curve on the bottom indicates the fitted curve using the general exponential function.
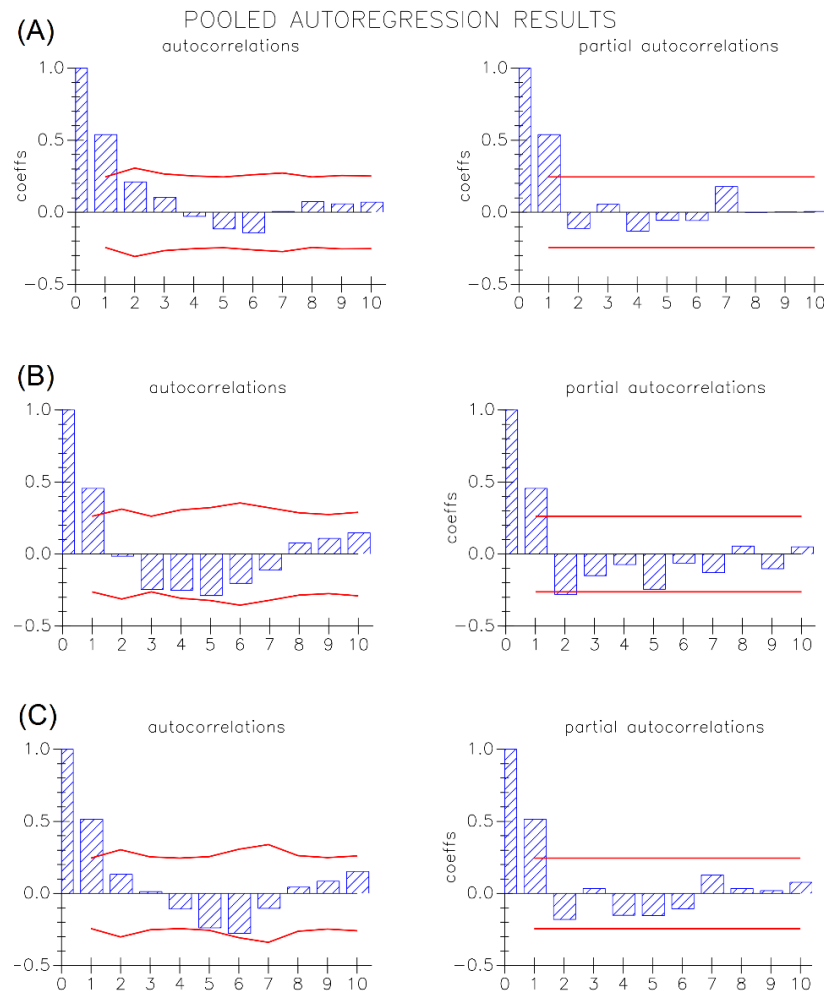
Fig. S2 The autocorrelation functions of (A) Lake Escondido, (B) El Trébol, and (C) master chronology of *Diplodon* shell collected from Nahuel Huapi National Park in Patagonia, Argentina.

169
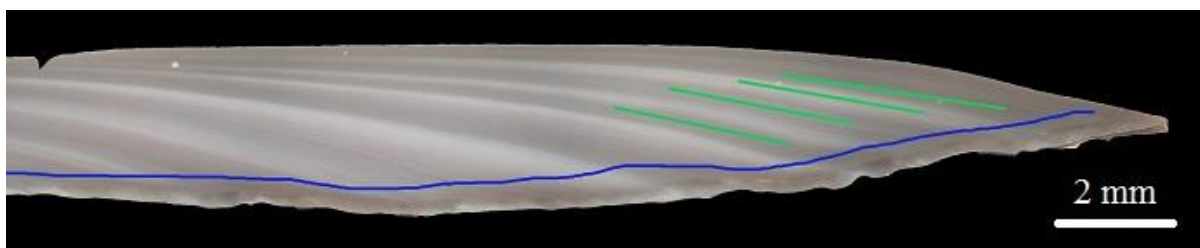
Fig. S3 Image shows representative locations of micro mill paths for stable isotope sampling (green lines) and laser ablation path (blue line) of *Diplodon* shell collected from Patagonia, Argentina.
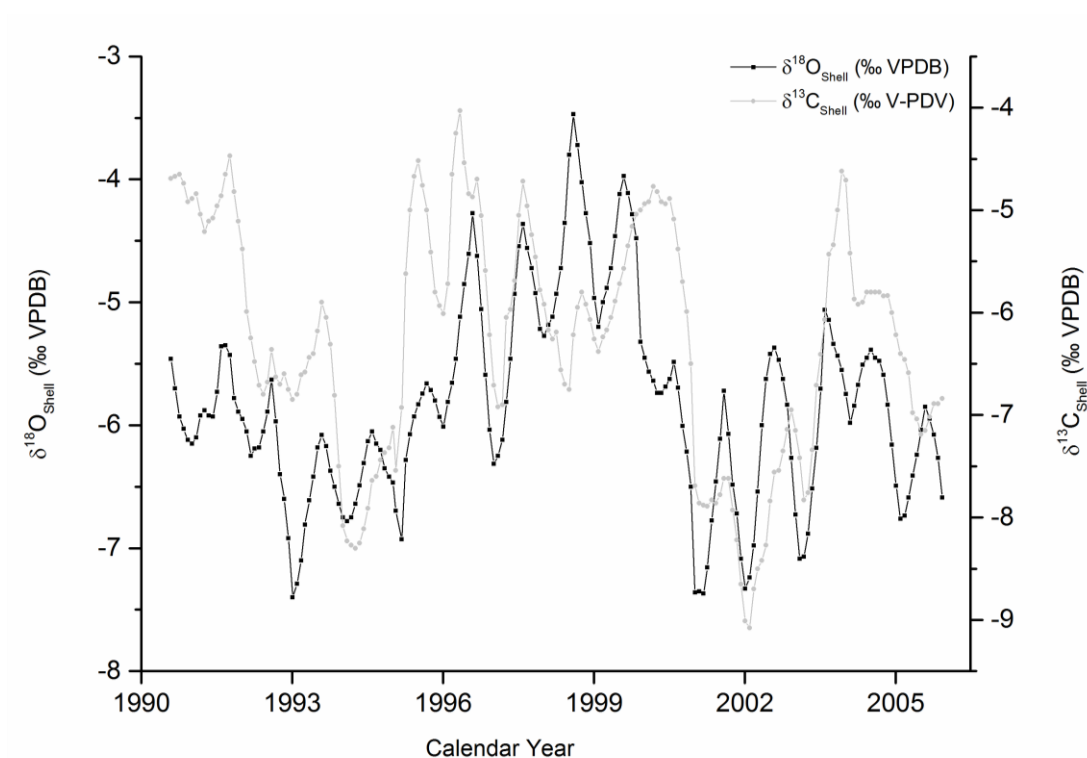
Fig. S4 Master $\delta^{18}O_{shell}$ and $\delta^{13}C_{shell}$ chronologies covering fifteen years created by combining three *Diplodon* shells from Lake El Trébol (ET05, ET08 and ET11).

Chapter 5

MEDIEVAL CLIMATIC ANOMALY SIGNALS IN FOSSIL *Diplodon chilensis patagonicus* (HAAS, 1931) SHELLS FROM NORTHERN PATAGONIA

Dilmi Herath[1], Dorrit Jacob[1], Analia Soldati[2], Stewart Fallon[3], María Bianchi[4], Adam Hajduk[5]

[1] Department of Earth and Planetary Science, Macquarie University, Sydney, Australia

[2] CONICET, Centro Atómico Bariloche, Av. Bustillo 9500, CP-8400 San Carlos de Bariloche, Argentina

[3] Research School of Earth Sciences, Australian National University, Canberra, ACT, Australia

[4] CONICET, Instituto Nacional de Antropología y Pensamiento LatinoAmericano, 3 de febrero 1370, Buenos Aires, Argentina

[5] Museo de la Patagonia Dr. Francisco P. Moreno, Centro Cívico S/N, 8400 San Carlos de Bariloche, Argentina

Abstract

Calibrated ages of 29 *Diplodon chilensis patagonicus* (Haas, 1931) shell, 8 bone and 3 charcoal samples from El Trébol and Puerto Tranquilo archaeological sites in northern Patagonia were determined. These are the first calibrated ages for Holocene freshwater bivalve shells in Argentinean Patagonia. Results indicate that the El Trébol site was occupied by humans from ca. 5500 BC to ca. 1400 AD, while Puerto Tranquilo was occupied only for the last 2000 years. Initial observations suggest that shellfish consumption was restricted to summer and during climatic anomalies only. Paleo-environmental conditions could be reconstructed using stable oxygen isotope and strontium/calcium in the shells. Elevated Sr/Ca during the medieval period suggests warmer temperatures in northern Patagonia during the 14th century than today, consistent with the Medieval Climatic Anomaly (MCA). These results are the first evidence from freshwater bivalve shells for the existence of MCA in South America and are consistent with dendrochronological data. Further, lower oxygen isotope ratio in the shells suggest a higher precipitation rate in the area during the late Holocene than today. Based on these observations, we suggest that *Diplodon chilensis patagonicus* shells could be developed as a terrestrial paleo proxy archive for the Patagonian region suitable for hemispheric scale climate reconstructions for the southern hemisphere.

5.1 Introduction

Bivalve shell archives offer highly time-resolved records (Kawakubo et al., 2014; Poulain et al., 2015), but are currently underrepresented in climate reconstructions of the past millennia. Particularly in continental areas reconstructions depend mostly on tree-rings, which offer similar time-resolution as bivalve shells (Helama et al., 2007), but respond differently to climate forcing. These tree ring records would benefit from being combined with other paleo proxy archives that record similar climatic phenomena which can potentially improve available proxy networks, thus enhancing the precision of climate reconstructions (Black et al., 2009).

Bivalves record environmental conditions through variations in the chemistry of their shells (Leng and Lewis, 2015), which are formed by incremental growth with annual growth breaks. Although bivalves are shorter-lived than coral colonies or trees, it is possible to cover longer periods expanding into centuries by combining time series from several bivalve individuals (Butler et al., 2013). Freshwater bivalve shells (Bivalvia: Unionoida) are a common constituent in shell middens and archaeological sites around the world (Peacock and Seltzer, 2008; Leng and Lewis, 2015). Therefore, shells from archaeological and geological contexts have been used in paleo-environmental studies employing morphometric, trace element, and stable isotope analysis (Panarello, 1987; Peacock and Seltzer, 2008; Scartascini et al., 2015). Furthermore, understanding the seasonality in bivalve collection can infer past changes in climate and environmental impact on human behaviour (Surge et al., 2013).

Here I explore past environmental conditions during the late Holocene using the freshwater bivalve *Diplodon chilensis patagonicus* (Haas, 1931), a common constituent in the modern and fossil inland shell assemblages in Patagonia. In addition, here I present the first calibrated ages using freshwater bivalve shells in the northern Patagonian region in Argentina and attempt to identify the historic shellfish consumption in northern Patagonia.

5.1.1 *Diplodon chilensis patagonicus*

Diplodon chilensis (Family – Hyriidae) is the most abundant freshwater bivalve species on both sides of the Andes mountains (Soldati et al., 2009) and includes two subspecies *Diplodon chilensis chilensis* (Gray, 1828) and *Diplodon chilensis patagonicus* (Haas, 1931).

Diplodon chilensis patagonicus (hereafter *D. patagonicus*), common in northern Patagonia, forms alternating dark and light-coloured bands in the shell cross section which are forming in summer and winter respectively (Soldati *et al.,* 2009). Further, these shells form throughout the year with a distinct annual growth break during October and November which overlaps with the reproduction period of the bivalve (Chapter 4). While individual freshwater shells are common in archaeological excavations in Argentinean Patagonia, freshwater shell middens, as such, are not known in the region. Here shells from two archaeological excavations in northern Patagonia are used to reconstruct paleo-temperature and precipitation using two independent proxies; oxygen isotope ratio ($\delta^{18}O$) and strontium/calcium (Sr/Ca).

This study builds on previous studies on modern *D. patagonicus* shells from northern Patagonia, which demonstrated that these shells record ambient environmental conditions (Soldati et al., 2009 and Chapter 4). In contrast to other freshwater bivalves (Carroll et al., 2006; Izumida et al., 2011) and corals (DeLong et al., 2011; Wu et al., 2014), the Sr/Ca in *D. patagonicus* shells do not show clear seasonal cycles but regular peaks during summer, suggesting a positive relationship between Sr/Ca intake and temperature (Chapter 4). Linear regression analysis shows that summer air temperature explained 41 % of the variation in Sr/Ca of *D. patagonicus* shells (r = 0.64, p < 0.05; Chapter 4). This indicated that Sr/Ca in *D. patagonicus* shells has the potential to be a proxy of ambient summer air temperature. The $\delta^{18}O$ values in *D. patagonicus* shells showed seasonal variations (Soldati et al., 2009) and increased at the end of the dry season in the late austral summer (April-May) and the minimum values were recorded after the major peak of precipitation in winter to early spring (September-October; Fig 5 in Chapter 4). This demonstrated that the $\delta^{18}O$ in *D. patagonicus* shells varied with the evaporation and precipitation pattern of the region.

5.2 Study area

Northern Patagonia, located between 37 °S and 46 °S in South America, is characterised by the Andes mountains which act as a climatic barrier with wet conditions to the west and dry conditions to the east (Garreaud et al., 2009). This is evident by the 1500 mm/year precipitation on the Chilean coast which reduces to 300 mm/year precipitation at the Patagonian steppe at around 40 °S (Boninsegna et al., 2009). Further, Patagonia is a temperate region with a mean annual temperature of 12 °C in the north (Paruelo et al., 1998).

Forest/steppe interface regions like northern Patagonia are among the most dynamic ecosystems on Earth and are highly vulnerable to changes in climate (Iglesias and Whitlock, 2014). Therefore, this area is intensively studied for its climate during Holocene and the longest tree-ring chronologies of South America which extend over 2500 years were obtained from this region (Villalba, 1990; Lara and Villalba, 1993; Boninsegna et al., 2009). However, other continental paleo-climatic archives from this region such as bio carbonates, speleothems and lake sediments are scarce (Neukom and Gergis, 2012).

The Patagonian climate is dominated by westerly air flows and the sea surface temperatures in the equatorial Pacific (Aravena and Luckman, 2009). The Westerlies are winds characteristic to the middle latitudes of Earth, blowing from west to east between the high-pressure areas of the subtropics and the low-pressure areas over the poles (Toggweiler, 2009). Strong westerly winds that blow in Patagonia decrease the mean annual temperature (Paruelo et al., 1998) while a shift in Westerlies historically produced drastic changes in climate (Kreutz et al., 1997; Toggweiler, 2009). Evidences for shifts in the Westerlies were found throughout the Holocene especially during the last glacial maximum, the Little Ice Age and past 50 years (Kreutz et al., 1997; Mayr et al., 2007b; Toggweiler, 2009). Therefore, northern Patagonia is particularly interesting for Holocene climate reconstructions since it is located in the zone of major influence of the westerly winds (Álvarez et al., 2015).

5.2.1 Archaeological setting

D. patagonicus shell samples were collected from two archaeological sites namely El Trébol and Puerto Tranquilo (Fig. 1). Both sites are located at the eastern flank of the Andes in a forested lacustrine environment of the Nahuel Huapi National Park, Argentina, near the forest/steppe ecotone; a zone of transition between adjacent ecological systems of forest and steppe (McArthur and Sanderson, 1999). El Trébol is the first site in the Argentine Patagonian forest to yield extinct fauna and one of the few in Argentina with evidence that humans exploited them (Hajduk et al., 2006). This site, where most of the samples are from, is a cave close to a lake with the same name. It has an interior surface of ca. 110 m^2 and was excavated to a depth of 5 m during 2002, 2004 and 2006 (for more details see Hajduk et al., 2006). The first occupation of the cave was dated back to 10,570 years cal. yr. BP using dermal bones of an extinct animal, the ground sloth (*Mylodon sp.*, Family - *Mylodontidae*) (Hajduk et al., 2006). Only three badly preserved *D. patagonicus* shells were registered at levels more than 250 cm below the surface. The Puerto Tranquilo site is situated on the island

Isla Victoria (Fig. 1) in the Nahuel Huapi Lake and its oldest archaeologically evidence dates to 1980 ± 60 cal. yr. BP as given by radiocarbon dating (Hajduk, personal communication).
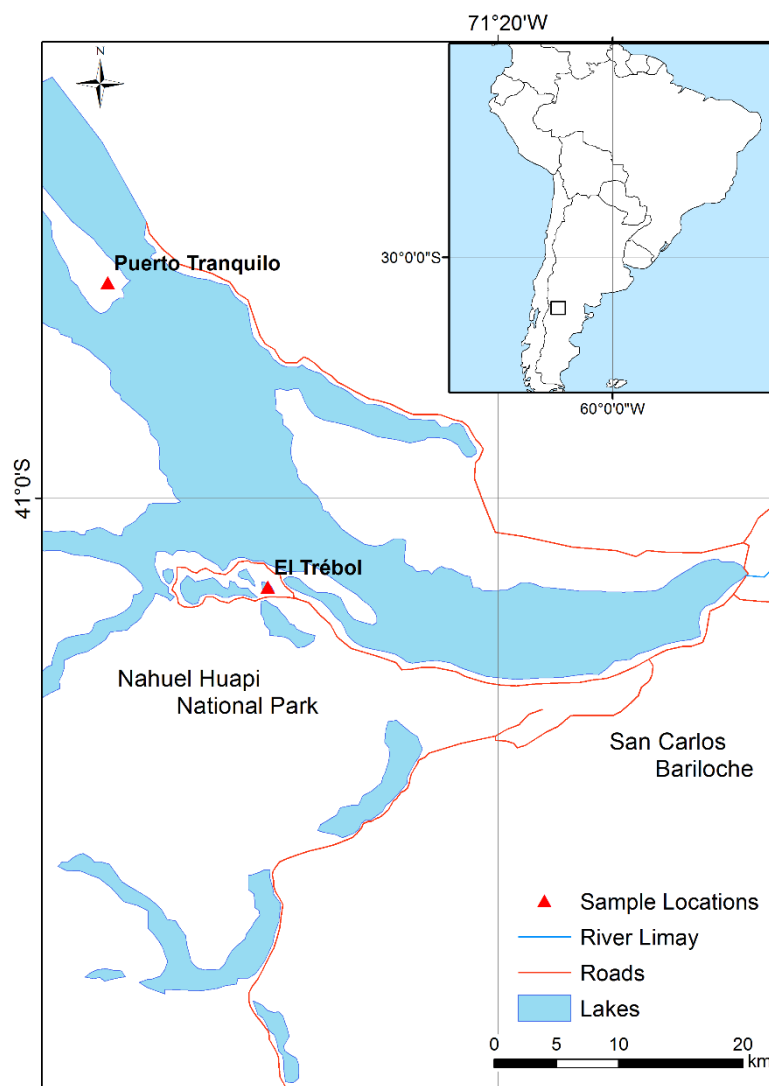
Fig. 1 Map of Argentinean Patagonia showing the locations (red triangles) of the archaeological sites where the specimens were collected.

First human groups populated Patagonia about 13,000 years ago (Hajduk et al., 2007b; Borrero, 2008), and persisted for thousands of years until almost the nineteenth century. However, during the late Holocene, these hunter-gatherer communities were mainly hunting for guanaco (*Lama guanicoe*), which is evident by the presence of guanaco bones at most archaeological sites in the region (Borrero, 2014). These communities changed into less hard and less abrasive diets in late Holocene mainly due to differences in food processing methods, for example, the use of ground stone tools (Bernal et al., 2007). In addition to guanaco, red fox (*Lycalopex culpaeus*), rodent (*Lagidium sp.*), hairy armadillo (*Chaetophractus villosus*), birds (*Milvago sp.*), swan (*Cygnus sp.*), freshwater fish and clams

176

were present in the El Trébol site (Adán et al., 2008). Fish consumption was present only in forest and ecotone sites in Patagonia, and it is in these that the freshwater bivalves are used to a greater extent than in neighbouring steppe sites (Hajduk et al., 2007a).

5.3 Material and methods

5.3.1 Radiocarbon analysis

Twenty-nine (29) *D. patagonicus* shells from both archaeological sites, eight bone samples from El Trébol and three charcoal samples from Puerto Tranquilo were selected for Accelerated Mass Spectrometry (AMS) radiocarbon analysis (Table 1 and 2). The shell exterior was cleaned, ~20mg of shell material was removed and broken into small chunks. 0.01M HCl was used to remove the outer 20% of the shell material and 7-10 mg of cleaned shell material was loaded into glass Vacutainer™ blood tubes, evacuated and CO_2 gas was evolved using 85% orthophosphoric acid (Fallon et al., 2010).

Bone samples were first tested for %N on a Sercon 20-20 ER-IRMS and only when %N > 0.2%, radiocarbon dating sample preparation proceeded (Brock et al., 2012). Surface discolouration and any soft bone material were removed with a drill, and ~300-500 mg of bone powder was drilled for the analysis. These were then washed with chloroform and methanol solvent. The mineral component was removed with a 0.5M HCl (wash overnight) and then alkali-soluble organics were removed with 0.1M NaOH, finished with an acid wash with 0.5M HCl at room temperature. Collagen was gelatinized using 0.001M HCl at 70 $^{\circ}$C for 20 hours for large insoluble contaminants to be removed by Ezee™ filter (45-90 µm). Small soluble contaminants were removed with a 30 kDa molecular weight cut-off Vivaspin™ 15 ultrafilter. 2-3mg of cleaned collagen was loaded into quartz tube with CuO and silver capsules, evacuated and combusted at 900 $^{\circ}$C. Charcoal samples were mechanically cleaned and then subject to standard Acid:Base:Acid pre-treatment with 1M HCl:1M NaOH: 1M HCl, with multiple clean water rinses (18 MΩ) between each treatment. Approximately 1.5 mg of cleaned charcoal was loaded into 6 mm OD quartz tubes with CuO and silver capsules evacuated, sealed and combusted at 900 $^{\circ}$C for 6 hours. CO_2 was then cryogenically purified and samples were converted to graphite using hydrogen and Fe as a catalyst (Fallon and Guilderson, 2008). Graphite targets were analysed at the Radiocarbon Laboratory, Research School of Earth Sciences, Australian National University on the single stage Accelerator Mass Spectrometer (AMS) (Fallon et al., 2010). The results include online

δ^{13}C correction for isotope fractionation and a blank subtraction based on ^{14}C-free calcite. The ^{14}C AMS dates were calibrated using `OxCal 4.2` (Ramsey, 2009) and the radiocarbon calibration curve for the southern hemisphere ShCal 13 (Hogg et al., 2013).

5.3.2 Stable isotope analyses

Six *D. patagonicus* shells were selected for stable isotope analysis (Table 3), representing different time periods with different calibrated ages. All shells were tested for diagenetic recrystallization of the original aragonite into calcite by Raman spectroscopy and were found to consist entirely of aragonite. Raman spectra were collected at room temperature using a Horiba Jobin Yvon LabRAM HR Evolution confocal spectrometer with 473 nm laser excitation. All Raman spectra (5-10 spots per shell) were recorded in the 100–1600 cm^{-1} wavenumber range using a spectral acquisition time of 12 seconds and four accumulations. A grating with 1800 grooves/mm was used with a slit width of 100 μm to ensure a high spectral resolution of approximately 0.8 cm^{-1}.

All selected bivalve shells were cut along the minimum growth axis of the left valve to produce thick sections (~ 3 mm), which were then polished to create shell sections following the methods described in Soldati et al., (2009) for isotope and trace element analysis. After geo-chemical analysis, these shells were stained with Alcian Blue stain to verify the growth lines (Schöne et al., 2005). Powdered samples with weights of around 1 mg from each shell section were drilled out under a binocular microscope using a 400 μm drill bit. One sample was collected from the dark (summer) layer closest to the ventral margin (hereafter ventral margin sample) while 2 − 5 additional samples were collected from rest of the shell cross-cutting both winter and summer layers. All samples were collected from the middle of the shell section (nacreous shell layer) to avoid any possible alteration along the inner and outer areas. Shell samples were transferred into 5.9 ml Labco Exetainer vials, flushed with He gas, reacted with 0.2 ml of 99.9 % phosphoric acid and finally heated to 70 °C before being rested for two hours. Analyses of oxygen and carbon isotopes were carried using a SerCon 20-22 stable isotope ratio mass spectrometer equipped with a carbonate device at the Research School of Earth Sciences, The Australian National University. Values of δ^{18}O are reported relative to the Vienna Pee-Dee Belemnite (VPDB) reference material based internal reference material, calibrated Carrara marble and NBS-18. External precision (1 SD) is better

than ± 0.1 ‰ based on multiple measurements of the ANU-M1 and other secondary reference materials.

Table 1. AMS radiocarbon ages and respective calibrated years for *Diplodon* shells obtained from two sites in northern Patagonia. All ^{14}C AMS dates are calibrated using OxCal 4.2 (Ramsey, 2009) and the radiocarbon calibration curve for the southern hemisphere ShCal 13 (Hogg et al., 2013). The depth and thickness of layers are given in cm and related to the present surface level. The sequence of the samples is in stratigraphic order.

Location	Sample no	Depth (cm)	Condition	[14]C Age	Error±	Cal Yr (BC/AD) To	From	Median
El Trébol	ET-37	10-20	fragment	845	25	1158	1256	1199
El Trébol	ET-38	'' ''	fragment	605	30	1297	1406	1348
El Trébol	ET-33	20-55	fragment	1195	25	728	893	828
El Trébol	ET-32	'' ''	valve	605	30	1297	1406	1348
El Trébol	ET-31	'' ''	valve	600	25	1299	1407	1347
El Trébol	ET-30	'' ''	valve	565	70	1285	1445	1362
El Trébol	ET-34	'' ''	fragment	2885	25	-1190	-979	-1063
El Trébol	ET-36	55-67	valve	2915	25	-1207	-1021	-1104
El Trébol	ET-35	55-67	valve	2895	25	-1193	-1003	-1076
El Trébol	ET-28	71-93	valve	3020	25	-1388	-1134	-1264
El Trébol	ET-27	'' ''	valve	3075	25	-1411	-1271	-1341
El Trébol	ET-26	'' ''	fragment	3010	30	-1386	-1128	-1250
El Trébol	ET-24	'' ''	fragment	3005	25	-1376	-1129	-1243
El Trébol	ET-25	'' ''	fragment	2930	25	-1217	-1045	-1132
El Trébol	ET-23	93-104	fragment	3020	30	-1391	-1131	-1266
El Trébol	ET-39	239-259	valve	6540	45	-5615	-5382	-5506
El Trébol	ET-40	'' ''	fragment	6015	30	-4995	-4810	-4906
El Trébol	ET-41	'' ''	fragment	5950	25	-4908	-4742	-4824
P Tranquilo	PT-05	21-30	valve	425	25	1428	1610	1453
P Tranquilo	PT-06	'' ''	valve	375	25	1447	1631	1503
P Tranquilo	PT-04	'' ''	valve	405	25	1437	1618	1467
P Tranquilo	PT-03	30-35	valve	785	30	1193	1280	1245
P Tranquilo	PT-02	'' ''	valve	420	35	1421	1624	1465
P Tranquilo	PT-01	'' ''	valve	350	35	1457	1637	1553
P Tranquilo	PT-07	35-45	valve	540	70	1285	1462	1386
P Tranquilo	PT-08	35-45	valve	585	35	1298	1416	1349
P Tranquilo	PT-09	48-80	fragment	1690	25	258	412	360
P Tranquilo	PT-11	'' ''	fragment	1805	25	131	322	209
P Tranquilo	PT-10	80-100	fragment	1650	30	264	533	398

The stable isotope composition of surface water samples collected from El Trébol monthly for twelve months from March 2008 to March 2009 were measured at the Leibniz-Laboratory for Radiometric Dating and Stable Isotope Research, University of Kiel, Germany with a Finnigan Delta E mass spectrometer equipped with a Kiel DICI device and an equilibration bath. Analytical precision (1 sigma) based on four replicates each were $\pm$ 0.08 ‰ for δ^{18}O and $\pm$ 0.3 ‰ for δ^{13}C.

5.3.3 Trace element analyses

In situ Laser Ablation Inductively Coupled Plasma Mass Spectrometer (LA-ICP-MS) was used to measure the Sr and Ca concentrations (measured as ^{88}Sr and ^{43}Ca) in the same 6 *D. patagonicus* shells selected for stable isotope analysis using an Agilent 7700 quadrupole ICP-MS coupled to a Photon Machines excimer laser (193 nm wavelength) system. Measurements were carried out with laser energy densities of 4.05 J/cm^2 at 5 Hz with helium as carrier gas (flow rate − 0.8 l/min). Spots of 30 µm diameter were ablated at the dark (summer) layer closest to the ventral margin (ventral margin sample) and at 5 other locations (coinciding with powder sample collection locations) in the nacreous layer for 120 s with backgrounds measured for 60 s prior to each ablation. ^{43}Ca was used as the internal standard and SRM NIST 612 glass was used as the external standard while data reduction was carried out with the commercial software `GLITTER 4.5b` (Griffin et al., 2008). USGS BCR-2G and SRM NIST 610 were used as secondary standards and values for NIST SRM 612 and 610 as well as USGS BCR-2G were taken from the GeoReM preferred values database (Jochum et al., 2005). The detection limit (99% confidence level) for the measurements of Sr was 0.01 µg/g whereas the relative standard deviation based on multiple measurements on USGS BCR-2G (n = 6) was < 1.5 % while the reproducibility of USGS BCR-2G was > 96 %.

5.4 Results

Thick sections of fossil *D. patagonicus* shells show alternating dark and light-coloured bands (Fig. 2) which represent summers and winters, respectively (Soldati *et al.* 2009). Organic-rich growth lines are clearly stained in dark blue, while growth increments appear in lighter blue after being treated with Alcian Blue staining method (Schöne et al., 2005), (Fig. 2).

Notably, no difference in growth rates was observed in these shells compared to modern *D. patagonicus* shells.
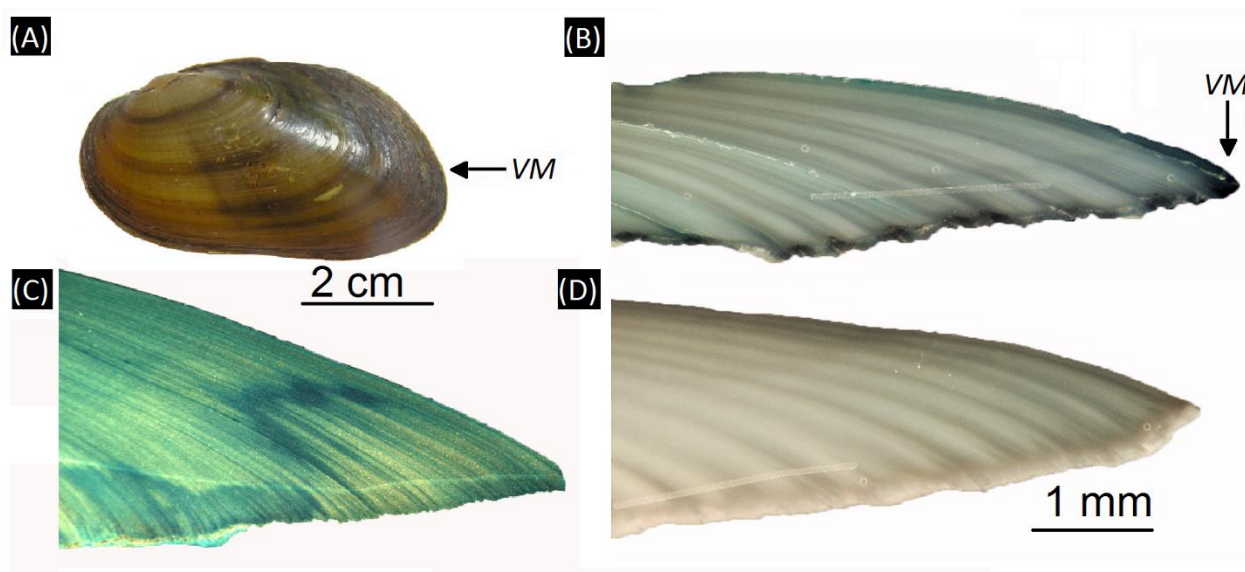

Fig. 2 (A) External surface of a left valve of a *Diplodon chilensis patagonicus* shell from El Trebol. (B and D) Cross sections of valves showing annual growth increments. Dark areas represent summer while light areas represent winter. (C) Shell section of a different shell after staining with Alcian Blue. Organic-rich, growth lines are stained dark blue while growth increments appear in lighter blue. (dog, the direction of growth; VM, ventral margin)

Radiocarbon dating indicates that the stratigraphic sequences were undisturbed during at least last 7000 years as evident by the sequential increase in age with depth in both locations (Fig. 3 and 4). The shells from El Trébol cover a wide range of ages over the strata with the oldest shells from around 5000 BC and the youngest from around 1400 AD (Fig. 3 and Table 1). These shells belong to three age groups; one cluster at around 1300 AD, another at around 1100 BC while only three shells were from around 5000 BC (Fig. 3). Contrastingly, bone samples, which are all from the El Trébol site, show approximately continuous age variation from more than 4800 BC to 1400 AD (Fig. 4, Table 2). At Puerto Tranquilo the uppermost archaeological strata produced calibrated ages between 400 AD to recent, while ^{14}C dates from the deepest deposits are around 200 AD (Fig. 3). All measured charcoal samples from Puerto Tranquilo also have calibrated ages within last 2000 years (Fig. 4, Table 2).

Table 2. AMS radiocarbon ages and respective calibrated years for mammal bones and charcoal samples obtained from two sites in northern Patagonia. All ^{14}C AMS dates are calibrated using `OxCal 4.2` (Ramsey, 2009) and the radiocarbon calibration curve for the southern hemisphere ShCal 13. The sequence of the samples is in stratigraphic order.

Location	Sample no	Sample Type	[14]C age	Error±	Cal.yr. (BC/AD) from	to	median
El Trébol	ET-B3	Bone - Guanaco	280	30	1498	1795	1577
El Trébol	ET-B4	Bone - Guanaco	2965	30	-1268	-1056	-1178
El Trébol	ET-B5	Bone - Mouse	3490	30	-1893	-1700	-1816
El Trébol	ET-B6	Bone - Guanaco	4040	30	-2832	-2474	-2551
El Trébol	ET-B7	Bone - Guanaco	4050	30	-2835	-2476	-2573
El Trébol	ET-B8	Bone - Guanaco	5810	30	-4764	-4553	-4666
El Trébol	ET-B9	Bone - Guanaco	5710	30	-4668	-4461	-4542
El Trébol	ET-B10	Bone - Guanaco	5745	30	-4689	-4517	-4593
P Tranquilo	PT-C1	Charcoal	375	35	1444	1634	1514
P Tranquilo	PT-C4	Charcoal	1585	40	395	560	480
P Tranquilo	PT-C5	Charcoal	325	35	1473	1645	1562

The $\delta^{18}O$ value of shells varies between -4.86 and -9.15 ‰ ($n = 35$ from 10 shells) with the lowest values coming from 1199 and 1348 AD (Table 3, Fig. 5). The Sr/Ca in the same shells vary between 1.96 and 3.45 mmol/mol ($n = 29$ from 10 shells) while in contrast to oxygen isotope ratio, the highest values of Sr/Ca came from 1199 and 1348 AD. Notably, Sr/Ca form a mirror pattern of the $\delta^{18}O$ values in all measured shells (Fig. 5). Additionally, the $\delta^{18}O$ and Sr/Ca of three modern shells collected from Lake El Trébol on March 2009 were also measured during this study for comparison. The Sr/Ca in modern shells are collected from continues ablation of the final dark layer of the shell whereas the $\delta^{18}O$ values are coming from the powder samples collected from the edge (dark band) of the shell. Both modern shells show identical $\delta^{18}O$ (-5.5 ‰) and Sr/Ca values (2.6 mmol/mol) (Fig. 5, Table 3).
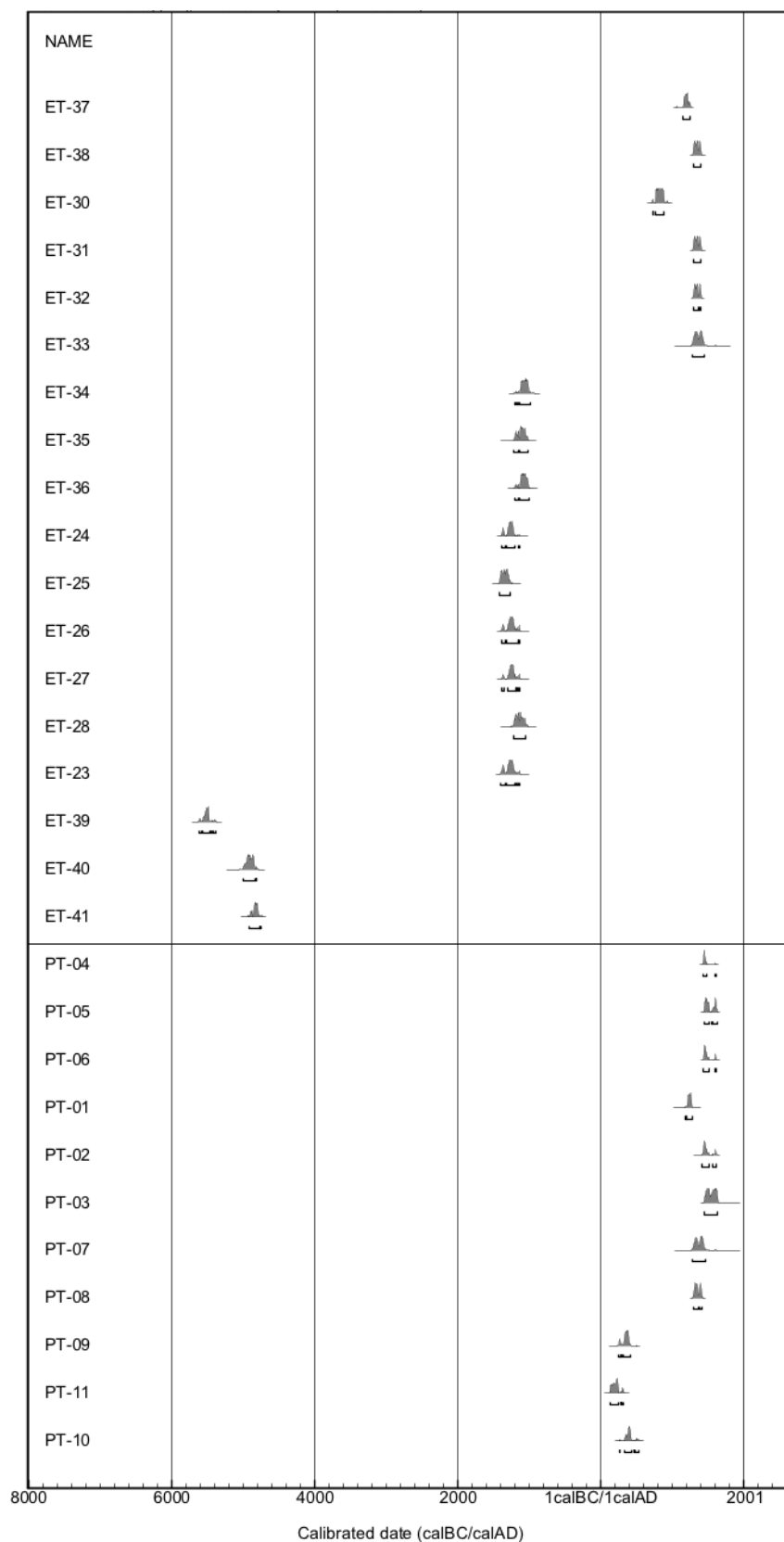
Fig. 3 Calibrated probability distributions for the ^{14}C determinations obtained from 29 *Diplodon chilensis patagonicus* shell specimens collected in this study. Details about sample locations and depth are given in Table 1. All values are calibrated using ShCal13 calibration curve as implemented in `OxCal 4.2` (Ramsey, 2009). ET = El Trebol, PT = Puerto Tranquilo
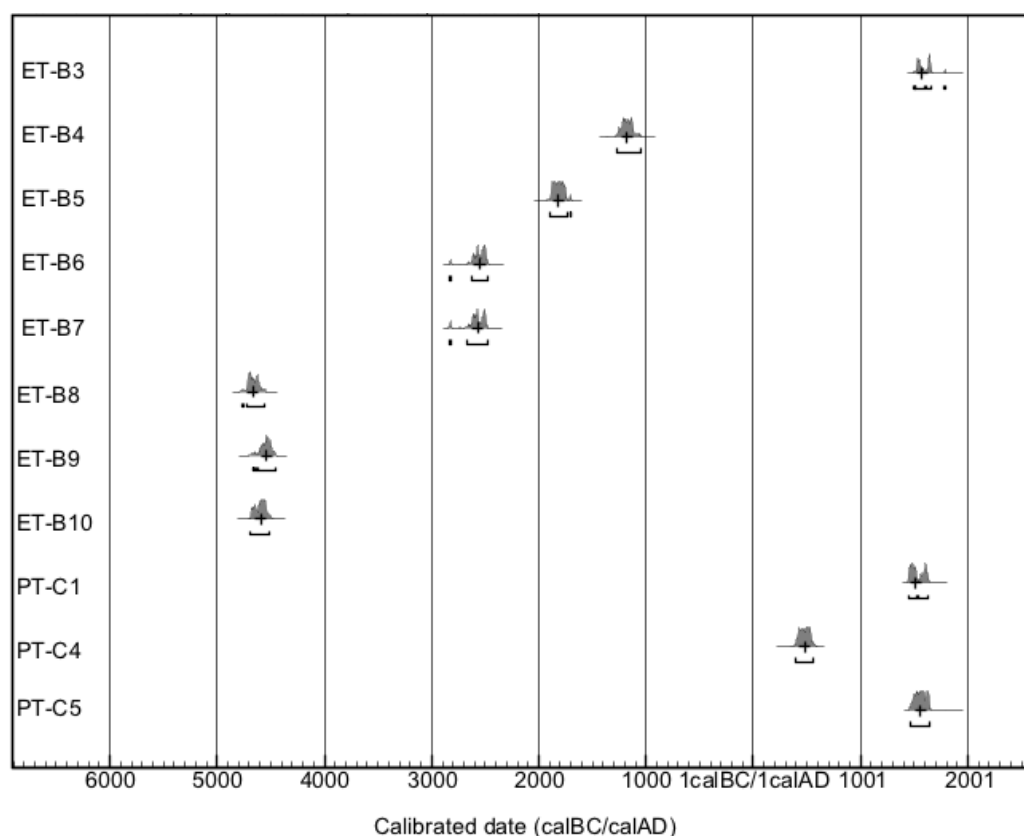
183

Fig. 4 Calibrated probability distributions for the ^{14}C determinations obtained from 8 Guanaco (*Lama guanicoe*) bones and 3 charcoal samples. All values are calibrated using ShCal13 calibration curve as implemented in `OxCal 4.2` (Ramsey, 2009). B = bone, C = Charcoal

5.5 Discussion

5.5.1 Historic shellfish consumption in northern Patagonia

Historically, archaeological studies in Patagonia have been mostly conducted within the steppe region while the forest environment has been less studied (Hajduk et al., 2007a). Consequently, more work is required in order to characterise the behaviour of the people that inhabited the forested-lacustrine area over time. Results obtained in this study are useful in understanding the relationship of hunter-gatherer communities in the region maintained with various environmental aspects both within a short and a broader time scale. Although many collected fossil shells are fragments (Table 1), undamaged shell valves show that the area closer to the ventral margin is almost always a dark layer (Fig. 2). This indicates that these animals were captured during summer, after the formation of the annual growth line. This agrees well with the findings of Hajduk et al. (2006) who suggested, mainly due to lack of archaeological remains, that El Trébol was used for seasonal occupation by small human groups. Some of the smaller lakes in the Nahuel Huapi region reach temperatures close to 0

ºC during winter (Chapter 4), which also limits access to bivalve beds a couple of meters below the water surface, which is otherwise easily accessible in summer due to water level fluctuations (Tessone et al., 2009).

A considerable gap in ages of collected shells between 4700 BC and 1100 BC (Table 1, Fig. 3) suggests either a discontinuity in human occupation in El Trébol or unavailability of bivalves in these lakes. This could also be due to partial removal of sediment and rocks by later occupants in order to lower the floor and thereby gain access to protected spaces within the rock shelter (Hajduk et al., 2006). However, radiocarbon dates of the mammal bones from the same location present a continuing chronological sequence indicating that the site was occupied continuously from at least around 5000 BC to recent years. This suggests that shellfish, in contrast to mammals, was only an occasional food source for the hunter-gatherer communities in the Nahuel Huapi region. Episodic bivalve consumption by humans is also recorded from other parts of the world such as from coastal tropics of Australia (Brockwell et al., 2013) and river estuaries in New Zealand (Anderson and Smith, 1996) within 1000 cal. yr. BP. These are attributed to human behavioural variability as a result of climate change (Brockwell et al., 2013) or the proximity to resource environments until those resources decline (Anderson and Smith, 1996). It is likely that under extreme climatic conditions human groups clustered their settlements in those places that provided critical resources such as water, firewood, and presence of good sheltering (Tessone et al., 2009). Since both fossil shell clusters are from periods of well-known cold climate anomalies (1300 AD – little ice age and 1100 BC - bronze age cold epoch), this suggests that climate change could be responsible for the diet behavioural changes in these occupants.

5.5.2 Environmental variations recorded in fossil *D. patagonicus* shells

The Sr/Ca in *D. patagonicus* shells increase with increasing temperature which was evident by the significant positive correlation between the Sr/Ca and summer temperature in the region (r = 0.64, p < 0.05, Chapter 4) and the increase of Sr/Ca within summer dark bands (Soldati et al., 2009). Observed results indicate that the calcification temperature of studied fossil *D. patagonicus* shells remains approximately constant throughout the studied time periods except for a drastic increase during 1199 and 1347 AD which is followed by a decrease in temperature at 1467 AD. This was demonstrated by the similar Sr/Ca values (around 2.4 to 2.6 mmol/mol) in most measured fossil *D. patagonicus* shells as well as the

modern shells, except an increase in Sr/Ca (3.2 to 3.4 mmol/mol) in shells from 1199 and 1347 AD. This suggests that the northern Patagonian region had relatively stable temperature conditions during the late Holocene with the exception of the 13th to mid-14th century, which was warmer than modern day Patagonia. This condition terminated when modern environmental conditions started towards the end of the 15th century.

The δ^{18}O in modern shells follow the precipitation pattern in the area with high values after the dry periods due to excessive evaporation, and lower values after the wet periods due to the addition of ^{16}O by precipitation (Chapter 4). The fossil δ^{18}O indicates that the environment in Patagonia was wetter than the modern environment since all fossil shells have lower δ^{18}O values than modern shells (Fig. 5). Further, the 13th to mid-14th century was the wettest period in the studied time periods and was followed by a relatively dry time towards the end of the 14th century.
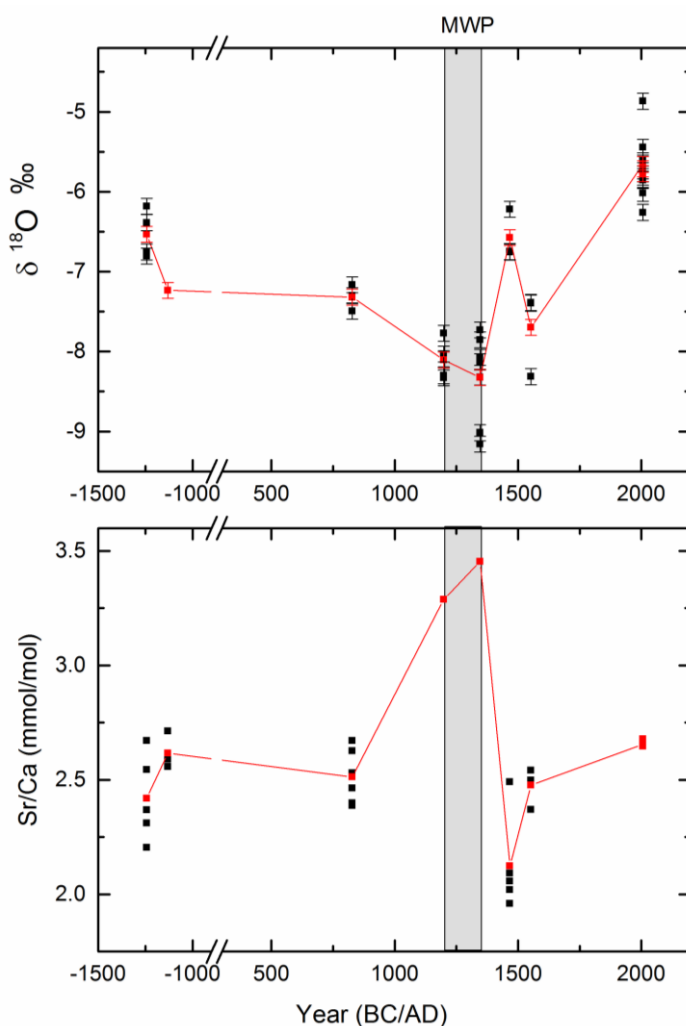

Fig. 5 The Sr/Ca ± 0.01 (mmol/mol) and δ^{18}O ± 0.1 ‰ obtained from modern and fossil *Diplodon chilensis patagonicus* shells plotted against age (calBC/AD). The red squares represent the mean value for a shell. Gray area represent the Medieval Warm Period (MWP).

Table 3. Measured $\delta^{18}O$ and Sr/Ca values of 6 fossils and 2 modern shells from northern Patagonia. All ^{14}C AMS dates are calibrated using `OxCal 4.2` (Ramsey, 2009) and the radiocarbon calibration curve for the southern hemisphere ShCal 13. (* = modern shells from Chapter 4)

Sample name	Location	Cal yr (BC/AD)	$\delta^{18}O$ ‰	Sr/Ca (mmol/mol)
ET-27	El Trébol	-1243	-6.53	2.41
ET-28	El Trébol	-1132	-7.23	2.61
ET-30	El Trébol	828	-7.31	2.51
ET-37	El Trébol	1199	-8.10	3.28
ET-32	El Trébol	1347	-8.32	3.45
PT-06	Puerto Tranquilo	1467	-6.57	2.12
PT-03	Puerto Tranquilo	1553	-7.69	2.47
ET-05*	El Trébol	2009	-5.65	2.65
ET-08*	El Trébol	2009	-5.77	2.67
ET-11*	El Trébol	2009	-5.71	2.64

5.5.3 Medieval climatic signals in Sr/Ca of *D. patagonicus* shells

The medieval warm period refers to a period from approximately 900 to 1300 AD during which temperatures in the North Atlantic region (especially Europe) exceeded those of the late 20th century (Mann, 2002). This period was followed by a period of cooling (also known as little ice age) over the extratropical northern hemisphere continents during the 16th to mid-19th centuries (Reinemann et al., 2014; Xoplaki et al., 2015). Similarly, southern hemisphere climatic reconstructions for the past millennium also show a warm phase of approximately 150 years starting at 1200 AD (Neukom et al., 2014) which was followed by a cold period from approximately 1350 to 1850 AD. While these medieval climatic anomalies are commonly recorded in northern hemisphere archives, records from the southern hemisphere for this time period are limited (Villalba, 1994). Further, these events are regionally complex and their timing, magnitude, and nature have not yet been clearly outlined in southern South America (Moy et al., 2009).

Based on the evidence of Sr/Ca variation in *D. patagonicus* shells, the climate in the Nahuel Huapi region remained stable and close to modern conditions during the studied time periods except for during the medieval climatic anomalies (Fig. 5). This implies that during the northern hemisphere medieval warm period, the temperature in the Nahuel Huapi region was

also higher than those of the modern-day summer temperatures. Further, results also suggest that this warm period terminated towards the mid-15th century or at the start of the little ice age, during which the minimum Sr/Ca (2.1 mmol/mol) was recorded (in 1467 AD). This provides the first records for the occurrence of medieval climatic anomalies derived from freshwater bivalve shells from Patagonia.

The medieval warm period is clearly recorded in dendrochronological data from northern Patagonia, for example, a warm period from 1080 to 1250 AD was observed in *Fitzroya cupressoides* tree rings (Villalba, 1994). Other than these high-resolution records, some low-resolution archives from South America also identify the medieval warm period. For instance a period of extreme drought without strong flooding was identified in flood records from Peru (3000 km north of El Trébol) from 800 AD to 1250 AD (Rein et al., 2004) while warm and dry climate from the mid-13th century until the early 15th is recorded in lake levels in southern Patagonia (1000 km south of El Trébol) (Haberzettl et al., 2005). The medieval warm period was followed by the little ice age which corresponds to relatively cold hemispheric conditions during 1400 to 1700 AD (Mann et al., 2009). This was also recorded in *Fitzroya cupressoides* tree ring data from northern Patagonia (100 km south west of El Trébol) where a long interval with below-average temperatures was recorded from 1490 to 1700 AD (Lara and Villalba, 1993). These results suggest that the Sr/Ca in *D. patagonicus* shell records the same climatic anomaly similar to other proxy archives from the Patagonian region.

5.5.4 Evaporation and precipitation variations as recorded in *D. patagonicus* shells

The $\delta^{18}O$ values in Lake El Trebol water vary inter-annually with the evaporation and precipitation pattern in the region (Chapter 4). Evaporation leads to enrichment of ^{18}O in the lake, resulting in high $\delta^{18}O_{water}$ values during the dry and windy austral summer months. Moisture-bringing air masses in eastern Patagonia mostly originate from west of the Andes (Stern and Blisniuk, 2002) and are increasingly depleted in ^{18}O due to Rayleigh distillation during rainout of the ascending clouds, leading to low $\delta^{18}O_{water}$ values in Lake El Trebol during the winter months. Since Unionoid bivalves such as *D. patagonicus* precipitate shell oxygen isotopes at equilibrium with $\delta^{18}O_{water}$ in the ambient aquatic environment (Dettman et al., 1999; Kelemen et al., 2017), the variations in $\delta^{18}O$ in *D. patagonicus* shells can be used to identify the past evaporation and precipitation variations in the Nahuel Huapi region. Since the $\delta^{18}O$ values of the live-collected samples provide a baseline, the resulted in lower

δ^{18}O values throughout the studied periods than the modern ^{18}O values indicate that the precipitation dominates the evaporation and this time-period was wetter than the modern Patagonian environment. These trends are consistent with other studies from South America which identify the late Holocene (4000 cal. yr. BP to present) as wetter than the present environment which is mainly attributed to a strengthening and equatorward shift of the westerlies (Lamy et al., 2001; Álvarez et al., 2015).

Our results are consistent with bivalve shell data from Patagonia where, similar to *D. patagonicus,* a decrease in δ^{18}O values during 1200 to 1500 AD was observed in three different taxa of molluscs (*Lymnaeidae, Sphaeriidae*, and *Planorbidae* families) from the eastern Andes in Chile (1000 km south of El Trebol) (Álvarez et al., 2015). This wet period is attributed to a less than normal influence of the westerlies, possibly due to a weakening or a displacement to a poleward position of the westerlies. Similarly, increased precipitation after approximately 1200 AD was also observed in northern Patagonia by various authors using high resolution (tree-ring) as well as low resolution (sediment layers) proxies (Villalba, 1994; Rebolledo et al., 2008). Similar to Álvarez et al. (2015), these increased precipitation events are also typically credited as associated with a shift in the Southern Westerlies.

5.5.5 Comparison of *D. patagonicus* shell δ^{18}O with other medieval proxy records

The lower δ^{18}O values observed during the medieval warm period, which point towards a wet phase are in apparent contrast to findings from other archival records from Patagonia for the same period. For example, a long period of drought from 1280 to 1450 AD was identified in Chile using *Austrocedrus chilensis* tree rings (Boninsegna, 1988) and according to various tree ring data from central Chile, the period between 1280 and 1380 AD experienced lower than the average precipitation (Villalba, 1994). Although a number of studies created long tree ring chronologies from northern Patagonia to identify the precipitation variations (Villalba et al., 1998a; Villalba et al., 1998b; Lara et al., 2008), none of these reaches back to the medieval period.

Several reasons can be put forward for the discrepancy between the precipitation records from *D. patagonicus* shell and other medieval climate records from the region. Although this region is subjected to a long-term climatic variation during the medieval climatic anomalies there can be local and seasonal exceptions as evident by similar low δ^{18}O in three different taxa of molluscs from the eastern Andes in Chile (Álvarez et al., 2015). In addition, the late

Holocene after 3000 years cal. yr. BP appears to have been characterized by high variability of climate, marked by fluctuations in the influence of the Southern Westerly Winds (SWW) (Veit, 1996). As the SWW largely control the precipitation pattern along the southern Andes (Gilli et al., 2005) and as the position of SWW decide the wind direction, a shift in westerlies can change the origin of moisture-bringing air masses which in modern environments originate from west of the Andes (Stern and Blisniuk, 2002). The air masses coming from eastern directions, in general, have significantly higher $\delta^{18}O$ values than from western directions due to rainout effects of air-masses passing the southern Andes (Mayr et al., 2007a). As the oxygen isotopic composition of the clouds during rainout influence the $\delta^{18}O$ in lake water, clouds originating from the east could add higher amounts of ^{18}O which consecutively change the negative relationship the $\delta^{18}O$ in *D. patagonicus* shells currently have to a positive relationship. This would point towards a drought during the medieval warm period as recorded by other proxy archives in the region.

Another possible reason could be that, in contrast to modern shells, the influence of ambient temperature during the late Holocene on the $\delta^{18}O$ variation of *D. patagonicus* shells was stronger than the influence by the precipitation and evaporation. Since $\delta^{18}O$ in bio-carbonates has a negative relationship with ambient temperature (Dettman et al., 1999), the resulting $\delta^{18}O$ variation in *D. patagonicus* shells would result the same temperature variation resulted in the Sr/Ca variation with high temperatures during the medieval warm period and low temperatures during the little ice age. However, without $\delta^{18}O$ data from additional shells from the medieval period, these results must be treated with caution and, at this stage, our interpretations are only introductory.

5.6 Conclusions

This study provides the first calibrated ages using freshwater bivalve shells in the northern Patagonian region in Argentina. Results calibrated ages from bivalve shells and mammal bones indicate that the archaeological site El Trébol was occupied continuously at least for the last 7000 years. However, a discontinuous bivalve record between 4700 BC and 1100 BC years suggests that bivalves were used as a food source during climatic anomalies only. Further, the shell growth band data suggest that early occupants in northern Patagonia collected *D. patagonicus* only during the summer. The medieval climatic anomalies were recorded by Sr/Ca in the *D. patagonicus* shells studied, supporting a similar finding in other

paleo proxy archive in Argentinean Patagonia such as tree rings, lake levels and flood records. The δ^{18}O in *D. patagonicus* shells showed that the late Holocene was wetter than the modern day environment, while exhibiting contrasting results to other medieval climatic archives.

We suggest that *D. patagonicus* shells could be developed as a terrestrial paleo proxy archive for the Patagonian region suitable for hemispheric scale climate reconstructions for the southern hemisphere. Further, this study opens up the possibility of identifying seasonality in *D. patagonicus* consumption which will make it possible to reconstruct the seasonal movements, seasonal occupations and adaptive responses to environmental changes that have occurred throughout Holocene.

5.7 References

Adán, H., María, A.A., Lezcano, M.J., de La Patagonia, E.d.M. and Moreno, F., 2008. Arqueología del área del lago Nahuel Huapi. La problemática del uso del medio ambiente boscoso-lacustre cordillerano y su relación con el de estepa y ecotono vecinos.

Álvarez, D., Fagel, N., Araneda, A., Jana-Pinninghoff, P., Keppens, E. and Urrutia, R., 2015. Late Holocene climate variability on the eastern flank of the Patagonian Andes (Chile): A $\delta^{18}O$ record from mollusks in Lago Cisnes (47° S). The Holocene: 0959683615580859.

Anderson, A. and Smith, I., 1996. The transient village in southern New Zealand. World Archaeology, 27(3): 359-371.

Aravena, J.C. and Luckman, B.H., 2009. Spatio-temporal rainfall patterns in southern South America. International Journal of Climatology, 29(14): 2106-2120.

Bernal, V., Novellino, P., Gonzalez, P.N. and Perez, S.I., 2007. Role of wild plant foods among late Holocene hunter-gatherers from Central and North Patagonia (South America): An approach from dental evidence. American Journal of Physical Anthropology, 133(4): 1047-1059.

Black, B.A., Copenheaver, C.A., Frank, D.C., Stuckey, M.J. and Kormanyos, R.E., 2009. Multi-proxy reconstructions of northeastern Pacific sea surface temperature data from trees and Pacific geoduck. Palaeogeography, Palaeoclimatology, Palaeoecology, 278(1): 40-47.

Boninsegna, J., 1988. Santiago de Chile winter rainfall since 1220 as being reconstructed by tree rings. Quaternary of South America and Antarctic Peninsula, 6: 67-87.

Boninsegna, J.A., Argollo, J., Aravena, J., Barichivich, J., Christie, D., Ferrero, M., Lara, A., Le Quesne, C., Luckman, B. and Masiokas, M., 2009. Dendroclimatological reconstructions in South America: a review. Palaeogeography, Palaeoclimatology, Palaeoecology, 281(3): 210-228.

Borrero, L.A., 2008. Early occupations in the southern cone, The Handbook of South American Archaeology. Springer, pp. 59-77.

Borrero, L.A., 2014. 18 Fuego-Patagonian bone assemblages and the problem of communal guanaco hunting. Hunters of the recent past, 20: 373.

Brock, F., Wood, R., Higham, T.F., Ditchfield, P., Bayliss, A. and Ramsey, C.B., 2012. Reliability of nitrogen content (% N) and carbon: nitrogen atomic ratios (C: N) as indicators of collagen preservation suitable for radiocarbon dating. Radiocarbon, 54(3-4): 879-886.

Brockwell, S., Marwick, B., Bourke, P., Faulkner, P. and Willan, R., 2013. Late Holocene climate change and human behavioural variability in the coastal wet-dry tropics of northern Australia: Evidence from a pilot study of oxygen isotopes in marine bivalve shells from archaeological sites. Australian Archaeology, 76(1): 21-33.

Butler, P.G., Wanamaker, A.D., Scourse, J.D., Richardson, C.A. and Reynolds, D.J., 2013. Variability of marine climate on the North Icelandic Shelf in a 1357-year proxy archive based on growth increments in the bivalve *Arctica islandica*. Palaeogeography, Palaeoclimatology, Palaeoecology, 373: 141-151.

Carroll, M., Romanek, C. and Paddock, L., 2006. The relationship between the hydrogen and oxygen isotopes of freshwater bivalve shells and their home streams. Chemical Geology, 234(3): 211-222.

DeLong, K.L., Flannery, J.A., Maupin, C.R., Poore, R.Z. and Quinn, T.M., 2011. A coral Sr/Ca calibration and replication study of two massive corals from the Gulf of Mexico. Palaeogeography, Palaeoclimatology, Palaeoecology, 307(1): 117-128.

Dettman, D.L., Reische, A.K. and Lohmann, K.C., 1999. Controls on the stable isotope composition of seasonal growth bands in aragonitic fresh-water bivalves (*Unionidae*). Geochimica et Cosmochimica Acta, 63(7): 1049-1057.

Fallon, S., Fifield, L.K. and Chappell, J., 2010. The next chapter in radiocarbon dating at the Australian National University: status report on the single stage AMS. Nuclear Instruments and Methods in Physics Research Section B: Beam Interactions with Materials and Atoms, 268(7-8): 898-901.

Fallon, S.J. and Guilderson, T.P., 2008. Surface water processes in the Indonesian throughflow as documented by a high-resolution coral $\Delta^{14}C$ record. Journal of Geophysical Research: Oceans, 113(C9).

Garreaud, R.D., Vuille, M., Compagnucci, R. and Marengo, J., 2009. Present-day south american climate. Palaeogeography, Palaeoclimatology, Palaeoecology, 281(3): 180-195.

Gilli, A., Ariztegui, D., Anselmetti, F.S., McKenzie, J.A., Markgraf, V., Hajdas, I. and McCulloch, R.D., 2005. Mid-Holocene strengthening of the southern westerlies in South America—sedimentological evidences from Lago Cardiel, Argentina (49 S). Global and Planetary Change, 49(1-2): 75-93.

Griffin, W., Powell, W., Pearson, N. and O'reilly, S., 2008. GLITTER: data reduction software for laser ablation ICP-MS. Laser Ablation-ICP-MS in the earth sciences. Mineralogical association of Canada short course series, 40: 204-207.

Haberzettl, T., Fey, M., Lücke, A., Maidana, N., Mayr, C., Ohlendorf, C., Schäbitz, F., Schleser, G.H., Wille, M. and Zolitschka, B., 2005. Climatically induced lake level changes during the last two millennia as reflected in sediments of Laguna Potrok Aike, southern Patagonia (Santa Cruz, Argentina). Journal of Paleolimnology, 33(3): 283-302.

Hajduk, A., Albornoz, A. and Lezcano, M., 2006. Levels with extinct fauna in the forest rockshelter El trébol (Northwest Patagonia, Argentina). Current Research in the Pleistocene, 23(5).

Hajduk, A., Albornoz, A. and Lezcano, M., 2007a. Nuevos pasos en pos de los primeros barilochenses. Arqueología del Parque Nacional Nahuel Huapi. Patrimonio Cultural: la gestión, el arte, la arqueología y las ciencias exactas aplicadas: 175-194.

Hajduk, A., Albornoz, A., Lezcano, M., Vázquez, C. and Palacios, O., 2007b. Nuevos pasos en pos de los primeros barilochenses. Arqueología del Parque Nacional Nahuel Huapi. Patrimonio Cultural: la gestión, el arte, la arqueología y las ciencias exactas aplicadas: 175-194.

Helama, S., Schöne, B.R., Kirchhefer, A.J., Nielsen, J.K., Rodland, D.L. and Janssen, R., 2007. Compound response of marine and terrestrial ecosystems to varying climate: pre-anthropogenic perspective from bivalve shell growth increments and tree-rings. Marine Environmental Research, 63(3): 185-199.

Hogg, A.G., Hua, Q., Blackwell, P.G., Niu, M., Buck, C.E., Guilderson, T.P., Heaton, T.J., Palmer, J.G., Reimer, P.J. and Reimer, R.W., 2013. SHCal13 Southern Hemisphere calibration, 0–50,000 years cal BP. Radiocarbon, 55(4): 1889-1903.

Iglesias, V. and Whitlock, C., 2014. Fire responses to postglacial climate change and human impact in northern Patagonia (41–43° S). Proceedings of the National Academy of Sciences, 111(51): E5545-E5554.

Izumida, H., Yoshimura, T., Suzuki, A., Nakashima, R., Ishimura, T., Yasuhara, M., Inamura, A., Shikazono, N. and Kawahata, H., 2011. Biological and water chemistry controls on Sr/Ca, Ba/Ca, Mg/Ca and δ 18 O profiles in freshwater pearl mussel *Hyriopsis* sp. Palaeogeography, Palaeoclimatology, Palaeoecology, 309(3): 298-308.

Jochum, K.P., Nohl, U., Herwig, K., Lammel, E., Stoll, B. and Hofmann, A.W., 2005. GeoReM: a new geochemical database for reference materials and isotopic standards. Geostandards and Geoanalytical Research, 29(3): 333-338.

Kawakubo, Y., Yokoyama, Y., Suzuki, A., Okai, T., Alibert, C., Kinsley, L. and Eggins, S., 2014. Precise determination of Sr/Ca by laser ablation ICP-MS compared to ICP-AES and application to multi-century temperate corals. Geochemical Journal, 48(2): 145-152.

Kelemen, Z., Gillikin, D.P., Graniero, L.E., Havel, H., Darchambeau, F., Borges, A.V., Yambélé, A., Bassirou, A. and Bouillon, S., 2017. Calibration of hydroclimate proxies in freshwater bivalve shells from Central and West Africa. Geochimica et Cosmochimica Acta, 208: 41-62.

Kreutz, K., Mayewski, P., Meeker, L., Twickler, M., Whitlow, S. and Pittalwala, I., 1997. Bipolar changes in atmospheric circulation during the Little Ice Age. Science, 277(5330): 1294-1296.

Lamy, F., Hebbeln, D., Röhl, U. and Wefer, G., 2001. Holocene rainfall variability in southern Chile: a marine record of latitudinal shifts of the Southern Westerlies. Earth and Planetary Science Letters, 185(3): 369-382.

Lara, A. and Villalba, R., 1993. A 3620-year temperature record from Fitzroya cupressoides tree rings in southern South America. Science-New York Then Washington-, 260: 1104-1104.

Lara, A., Villalba, R. and Urrutia, R., 2008. A 400-year tree-ring record of the Puelo River summer–fall streamflow in the Valdivian Rainforest eco-region, Chile. Climatic Change, 86(3-4): 331-356.

Leng, M.J. and Lewis, J.P., 2015. Oxygen isotopes in Molluscan shell: Applications in environmental archaeology. Environmental Archaeology: 1-12.

Mann, M.E., 2002. Medieval climatic optimum. Encyclopedia of Global environmental change, 1: 514-516.

Mann, M.E., Zhang, Z., Rutherford, S., Bradley, R.S., Hughes, M.K., Shindell, D., Ammann, C., Faluvegi, G. and Ni, F., 2009. Global signatures and dynamical origins of the Little Ice Age and Medieval Climate Anomaly. Science, 326(5957): 1256-1260.

Mayr, C., Lücke, A., Stichler, W., Trimborn, P., Ercolano, B., Oliva, G., Ohlendorf, C., Soto, J., Fey, M. and Haberzettl, T., 2007a. Precipitation origin and evaporation of lakes in semi-arid Patagonia (Argentina) inferred from stable isotopes (δ ^{18}O, δ ^{2}H). Journal of Hydrology, 334(1): 53-63.

Mayr, C., Wille, M., Haberzettl, T., Fey, M., Janssen, S., Lücke, A., Ohlendorf, C., Oliva, G., Schäbitz, F. and Schleser, G.H., 2007b. Holocene variability of the Southern Hemisphere westerlies in Argentinean Patagonia (52 S). Quaternary Science Reviews, 26(5): 579-584.

McArthur, E.D. and Sanderson, S.C., 1999. Ecotones: introduction, scale, and big sagebrush example. ED McArthur, WK Ostler, and CL Wambolt [compilers]. Proceedings: shrubland ecotones. Ogden, UT: USDA Forest Service, Rocky Mountain Research Station. Proceedings RMRS-P-11: 3-8.

Moy, C.M., Moreno, P.I., Dunbar, R.B., Kaplan, M.R., Francois, J.-P., Villalba, R. and Haberzettl, T., 2009. Climate change in southern South America during the last two millennia, Past climate variability in South America and surrounding regions. Springer, pp. 353-393.

Neukom, R. and Gergis, J., 2012. Southern Hemisphere high-resolution palaeoclimate records of the last 2000 years. The Holocene, 22(5): 501-524.

Neukom, R., Gergis, J., Karoly, D.J., Wanner, H., Curran, M., Elbert, J., González-Rouco, F., Linsley, B.K., Moy, A.D. and Mundo, I., 2014. Inter-hemispheric temperature variability over the past millennium. Nature Climate Change, 4(5): 362-367.

Panarello, H.O., 1987. Oxygen-18 temperatures on present and fossil invertebrated shells from Tunel Site, Beagle Channel, Argentina. Quaternary oj South America and Antarctic Península, 5: 83-91.

Paruelo, J.M., Beltrán, A., Jobbagy, E., Sala, O.E. and Golluscio, R.A., 1998. The climate of Patagonia: general patterns and controls on biotic processes. Ecología Austral, 8(2): 85-101.

Peacock, E. and Seltzer, J.L., 2008. A comparison of multiple proxy data sets for paleoenvironmental conditions as derived from freshwater bivalve (Unionid) shell. Journal of Archaeological Science, 35(9): 2557-2565.

Poulain, C., Gillikin, D., Thébault, J., Munaron, J.-M., Bohn, M., Robert, R., Paulet, Y.-M. and Lorrain, A., 2015. An evaluation of Mg/Ca, Sr/Ca, and Ba/Ca ratios as environmental proxies in aragonite bivalve shells. Chemical Geology, 396: 42-50.

Ramsey, C.B., 2009. Bayesian analysis of radiocarbon dates. Radiocarbon, 51(01): 337-360.

Rebolledo, L., Sepúlveda, J., Lange, C.B., Pantoja, S., Bertrand, S., Hughen, K. and Figueroa, D., 2008. Late Holocene marine productivity changes in Northern Patagonia-Chile inferred from a multi-proxy analysis of Jacaf channel sediments. Estuarine, Coastal and Shelf Science, 80(3): 314-322.

Rein, B., Lückge, A. and Sirocko, F., 2004. A major Holocene ENSO anomaly during the Medieval period. Geophysical Research Letters, 31(17).

Reinemann, S.A., Porinchu, D.F., MacDonald, G.M., Mark, B.G. and DeGrand, J.Q., 2014. A 2000-yr reconstruction of air temperature in the Great Basin of the United States with specific reference to the Medieval Climatic Anomaly. Quaternary Research, 82(2): 309-317.

Scartascini, F.L., Sáez, M. and Volpedo, A.V., 2015. Otoliths as a proxy for seasonality: The case of *Micropogonias furnieri* from the northern coast of San Matías Gulf, Río Negro, Patagonia, Argentina. Quaternary International, 373: 136-142.

Schöne, B.R., Dunca, E., Fiebig, J. and Pfeiffer, M., 2005. Mutvei's solution: an ideal agent for resolving microgrowth structures of biogenic carbonates. Palaeogeography, Palaeoclimatology, Palaeoecology, 228(1): 149-166.

Soldati, A., Jacob, D., Schöne, B., Bianchi, M. and Hajduk, A., 2009. Seasonal periodicity of growth and composition in valves of *Diplodon chilensis patagonicus* (d'Orbigny, 1835). Journal of Molluscan Studies, 75(1): 75-85.

Stern, L.A. and Blisniuk, P.M., 2002. Climate and Dynamics (ACL)-ACL 3 Stable isotope composition of precipitation across the southern Patagonian Andes (DOI 10.1029/2002JD002509). Journal of Geophysical Research-Part D-Atmospheres, 107(23).

Surge, D., Wang, T., Gutierrez-Zugasti, I. and Kelley, P.H., 2013. Isotope sclerochronology and season of annual growth line formation in limpet shells (*Patella vulgata*) from warm-and cold-temperate zones in the eastern North Atlantic. Palaios, 28(6): 386-393.

Tessone, A., Zangrando, A.F., Barrientos, G., Goñi, R., Panarello, H. and Cagnoni, M., 2009. Stable isotope studies in the Salitroso Lake Basin (southern Patagonia, Argentina): assessing diet of Late Holocene hunter-gatherers. International Journal of Osteoarchaeology, 19(2): 297-308.

Toggweiler, J., 2009. Shifting westerlies. Science, 323(5920): 1434-1435.

Veit, H., 1996. Southern Westerlies during the Holocene deduced from geomorphological and pedological studies in the Norte Chico, Northern Chile (27–33 S). Palaeogeography, Palaeoclimatology, Palaeoecology, 123(1-4): 107-119.

Villalba, R., 1990. Climatic fluctuations in northern Patagonia during the last 1000 years as inferred from tree-ring records. Quaternary Research, 34(3): 346-360.

Villalba, R., 1994. Tree-ring and glacial evidence for the Medieval Warm Epoch and the Little Ice Age in southern South America, The Medieval Warm Period. Springer, pp. 183-197.

Villalba, R., Cook, E.R., Jacoby, G.C., D'Arrigo, R.D., Veblen, T.T. and Jones, P.D., 1998a. Tree-ring based reconstructions of northern Patagonia precipitation since AD 1600. The Holocene, 8(6): 659-674.

Villalba, R., Grau, H.R., Boninsegna, J.A., Jacoby, G.C. and Ripalta, A., 1998b. Tree-ring evidence for long-term precipitation changes in subtropical South America. International Journal of Climatology, 18(13): 1463-1478.

Wu, H.C., Moreau, M., Linsley, B.K., Schrag, D.P. and Corrège, T., 2014. Investigation of sea surface temperature changes from replicated coral Sr/Ca variations in the eastern equatorial Pacific (Clipperton Atoll) since 1874. Palaeogeography, Palaeoclimatology, Palaeoecology, 412: 208-222.

Xoplaki, E., Fleitmann, D., Luterbacher, J., Wagner, S., Haldon, J.F., Zorita, E., Telelis, I., Toreti, A. and Izdebski, A., 2015. The Medieval Climate Anomaly and Byzantium: a review of the evidence on climatic fluctuations, economic performance and societal change. Quat. Sci. Rev, 22.

CONCLUSIONS

General conclusions

In this thesis, freshwater bivalves were studied from three different localities at similar latitudes (around 40 °S) in the southern hemisphere, namely northern New Zealand, eastern Australia and northern Patagonia, to identify the potential of five different species as new environmental proxy archives. Physical and chemical characteristics in three species *Echyridella menziesii*, from New Zealand's North Island, *Alathyria profuga* from Australia's Hunter Valley and *Diplodon chilensis patagonicus* from Argentinean Patagonia have the potential to be used as proxy archives of various environmental and climatic parameters. Two further species from the Hunter Valley, Australia: *Cucumerunio novaehollandiae* and *Hyridella drapeta* were studied and are found to be less fitting for this purpose.

The individual data of *Echyridella menziesii* and *Alathyria profuga* shows the potential of using oxygen isotope ratios of the shell as a temperature proxy while the oxygen isotope ratios of *Diplodon chilensis patagonicus* follows the precipitation and evaporation pattern in the region. The Sr/Ca in *Echyridella menziesii* and *Diplodon chilensis patagonicus* show significant correlations (r = 0.63 and r = 0.64 at p < 0.05 respectively) indicating the capacity to be a proxy of temperature. The growth rate of *Alathyria profuga* has a significant correlation with precipitation (r = -0.6, p < 0.05), and thus shows the possibility for use as a proxy of precipitation. In addition, these three species exhibit distinct growth variations responding to regional climatic phenomena such as the El Niño–Southern Oscillation (ENSO) and Southern Annular Mode (SAM). *Echyridella menziesii* and *Diplodon chilensis patagonicus* show a distinctive reduction in growth rate during El Niño years contrary to tree ring data from these regions which show higher growth rates during El Niño years. In comparison, *Alathyria profuga* indicates a characteristic growth reduction during La Niña years.

The lifespans of these bivalve species have been determined only in a few studies. For example, Soldati et al. (2009) for *Diplodon chilensis patagonicus* and Grimmond (1968); Roper and Hickey (1994) for *Echyridella menziesii*, but no lifespan determinations were available for *Alathyria profuga* before this study. Furthermore, no systematic study of frequency and timing of the growth line formation is available on these species. Therefore, this is the first study that identified the growth lines as annual and forming in February in shells of *Echyridella menziesii* and *Alathyria profuga* and in October-November in *Diplodon*

chilensis patagonicus shells. Another important outcome is the introduction of two different empirical equations for summer and winter temperature reconstructions using Sr/Ca in *Diplodon chilensis patagonicus* (Chapter 4). This improves the reliability in temperature reconstruction which, to my knowledge, has not been published in the literature.

Significance

Throughout the last century dendrochronology has grown to be one of the biggest contributors to climate studies due to longer lifespans, seasonally resolved growth patterns, and the possibilities to build cross dated chronologies extending over millennia (Stokes, 1996). The temperate southern hemisphere is well-represented in dendrochronological studies where for example, *Nothofagus pumilio* and *Fitzroya cupressoides* from South America and *Agathis australis* from New Zealand has long been considered faithful recorders of environmental variables such as temperature, precipitation, river discharge, drought events and fire history (Lara and Villalba, 1993; Boninsegna et al., 2009; Fowler et al., 2012). Similarly, these tree species are used in reconstructing global climate phenomena such as ENSO, SAM and Pacific decadal oscillation (Fowler et al., 2008; Villalba et al., 2012). Combining different proxy archives has been shown to yield highly resolved, consistent and more precise reconstructions of past climate conditions that are clearly needed in order to improve climate models (Black et al., 2009). This thesis identified three different freshwater bivalve species from the same localities with a similar temporal resolution to tree-ring archives and with the potential to record environmental variables as well as regional climate. Given the scarcity of instrumental records in the southern hemisphere, and particularly the limited studies regarding freshwater ecosystems, identifying new environmental and paleoclimate proxy archives opens the possibility to advance our understanding of freshwater environmental changes in the past in this understudied region.

Trees typically grow in summer and spring in contrast to studied bivalve species that grow throughout the winter and have a possible growth break during summer. This indicates freshwater bivalves, of course, record environmental variability during a season in the year which is usually not captured in dendrochronology. In contrast to most tree rings, that record climate at an annual resolution, freshwater bivalves can be developed to record data at a weekly resolution as established by secondary ion mass spectrometric analysis of *Echyridella menziesii* (Chapter 2). Such high resolution is not reached in most terrestrial archives such

as speleothems, sediment sequences and lake levels. Further, these bio-carbonate archives commonly use various chemical proxies, which enhance the added advantage of using multi-proxy approaches in environmental reconstructions as demonstrated by this study (Chapter 2, 3 and 4).

Limitations

One of the major disadvantages of these new proxy archives is the shorter lifetime of these bivalves: *Echyridella menziesii* (10 years)*, Alathyria profuga* (26 years) and *Diplodon chilensis patagonicus* (46 years) compared to marine bivalves (*Arctica islandica* – 405 years; Wanamaker et al., 2008, *Panopea abrupta* – 100-160 years; Strom et al. 2004, *Margritifera margritifera* – 127; Schöne et al., 2004) and to trees (*Agathis australis* – over 600 years; Fowler et al., 2012). However, this can be overcome by cross-dating of several individuals collected at different times, thus creating master chronologies covering longer time periods expanding into several centuries.

Since all sets of geochemical analysis in this thesis are coming from a few samples (n < 5), the results must be treated with caution. Whilst acknowledging that there are challenges presented by the low number of samples, however, I believe that these can serve as a guideline as to which environmental and climate archives should be studied in more detail in subsequent studies from the region.

Future directions and recommendations

Although the ENSO originates in the tropical Pacific region, its effects on ecosystems, agriculture, and other severe weather events are worldwide. Further, under the influence of global warming, the mean climate of the Pacific region is expected to undergo significant changes such as weakening of the tropical easterly trade winds, warming of the southern ocean and steepening of temperature gradients across the thermocline (Collins et al., 2010). However, these changes are regionally complex and their timing, magnitude, and nature differ from location to location that is not yet been clearly outlined (Moy et al., 2009). Therefore, a broad spatial coverage in well-established archival data can improve the accuracy of future climate models.

This thesis establishes the enormous potential of using freshwater bivalves from Hyriidae; a family that is native to Oceania and South America (Bogan, 2008), for environmental reconstructions and demonstrate the importance of identifying new environmental archives from the southern hemisphere. Although there are many freshwater bivalve species of Hyriidae family recorded from these regions (Bogan, 2008; Marshall et al., 2014; Walker et al., 2014), only very few of these species have been studied to date (Soldati et al., 2009), underscoring the vast potential to develop many more environmental and climate proxy archives. Due to its presence in the high latitudes, temperate climate and lack of instrumental data, southernmost South America can be suggested as a well-suited region for a similar study.

Combining different climate proxy archives could assist in building more precise reconstructions of past climate conditions. As the southern Pacific has yielded a wealth of dendrochronological data, combining these with bivalve archival data from this and other studies could be another direction to persist since no such study has been reported from the southern hemisphere. This can follow similar studies conducted in other regions such as Rypel et al. (2009), Black et al. (2015), Black et al. (2009) and Helama et al. (2007).

Further, this thesis is the first to use carbonate clumped isotope analysis on freshwater bivalves from the southern hemisphere and one of the few in the world (Csank et al., 2011; Tobin et al., 2014). Therefore, this opens the possibility to study more bio-carbonates from this region using carbonate clumped isotopes; a relatively new and more reliable temperature proxy than oxygen isotope ratios. Since Oceania is well known for marine carbonate climate archives such as *Tridacna sp.* (Driscoll et al., 2014; Duprey et al., 2015) and corals (Alibert and McCulloch, 1997; Quinn et al., 1998; Thresher et al., 2016), carbonate clumped isotope thermometry can be used to create reliable, long-term climate reconstructions from the southern Pacific.

The work in this thesis is a starting point for closing the vital gap in environmental reconstructions of the mid to high latitude zone of the southern hemisphere. Therefore, the results herein will encourage new sclerochronological research from Oceania and South America and enhance the amazing potential of using freshwater bivalves as environmental archives in future.

References

Alibert, C. and McCulloch, M.T., 1997. Strontium/calcium ratios in modern Porites corals from the Great Barrier Reef as a proxy for sea surface temperature: calibration of the thermometer and monitoring of ENSO. Paleoceanography, 12(3): 345-363.

Black, B.A., Copenheaver, C.A., Frank, D.C., Stuckey, M.J. and Kormanyos, R.E., 2009. Multi-proxy reconstructions of northeastern Pacific sea surface temperature data from trees and Pacific geoduck. Palaeogeography, Palaeoclimatology, Palaeoecology, 278(1): 40-47.

Black, B.A., Dunham, J.B., Blundon, B.W., Brim-Box, J. and Tepley, A.J., 2015. Long-term growth-increment chronologies reveal diverse influences of climate forcing on freshwater and forest biota in the Pacific Northwest. Global change biology, 21(2): 594-604.

Bogan, A.E., 2008. Global diversity of freshwater mussels (Mollusca, Bivalvia) in freshwater. Hydrobiologia, 595(1): 139-147.

Boninsegna, J.A., Argollo, J., Aravena, J., Barichivich, J., Christie, D., Ferrero, M., Lara, A., Le Quesne, C., Luckman, B. and Masiokas, M., 2009. Dendroclimatological reconstructions in South America: a review. Palaeogeography, Palaeoclimatology, Palaeoecology, 281(3): 210-228.

Collins, M., An, S.-I., Cai, W., Ganachaud, A., Guilyardi, E., Jin, F.-F., Jochum, M., Lengaigne, M., Power, S. and Timmermann, A., 2010. The impact of global warming on the tropical Pacific Ocean and El Niño. Nature Geoscience, 3(6): 391.

Csank, A.Z., Tripati, A.K., Patterson, W.P., Eagle, R.A., Rybczynski, N., Ballantyne, A.P. and Eiler, J.M., 2011. Estimates of Arctic land surface temperatures during the early Pliocene from two novel proxies. Earth and Planetary Science Letters, 304(3-4): 291-299.

Driscoll, R., Elliot, M., Russon, T., Welsh, K., Yokoyama, Y. and Tudhope, A., 2014. ENSO reconstructions over the past 60 ka using giant clams (*Tridacna* sp.) from Papua New Guinea. Geophysical Research Letters, 41(19): 6819-6825.

Duprey, N., Lazareth, C.E., Dupouy, C., Butscher, J., Farman, R., Maes, C. and Cabioch, G., 2015. Calibration of seawater temperature and δ 18Oseawater signals in Tridacna maxima's δ 18Oshell record based on in situ data. Coral Reefs, 34(2): 437-450.

Fowler, A.M., Boswijk, G., Gergis, J. and Lorrey, A., 2008. ENSO history recorded in *Agathis australis* (kauri) tree rings. Part A: kauri's potential as an ENSO proxy. International Journal of Climatology, 28(1): 1-20.

Fowler, A.M., Boswijk, G., Lorrey, A.M., Gergis, J., Pirie, M., McCloskey, S.P., Palmer, J.G. and Wunder, J., 2012. Multi-centennial tree-ring record of ENSO-related activity in New Zealand. Nature Climate Change, 2(3): 172.

Grimmond, N.M.W., 1968. Observations on growth and age of *Hyridella menziesi* Gray (MolluscaBivalvia) in a freshwater tidal lake, University of Otago.

Helama, S., Schöne, B.R., Kirchhefer, A.J., Nielsen, J.K., Rodland, D.L. and Janssen, R., 2007. Compound response of marine and terrestrial ecosystems to varying climate: pre-anthropogenic perspective from bivalve shell growth increments and tree-rings. Marine Environmental Research, 63(3): 185-199.

Lara, A. and Villalba, R., 1993. A 3620-year temperature record from Fitzroya cupressoides tree rings in southern South America. SCIENCE-NEW YORK THEN WASHINGTON-, 260: 1104-1104.

Marshall, B.A., Fenwick, M.C. and Ritchie, P.A., 2014. New Zealand Recent Hyriidae (Mollusca: Bivalvia: Unionida). Molluscan Research, 34(3): 181-200.

Moy, C.M., Moreno, P.I., Dunbar, R.B., Kaplan, M.R., Francois, J.-P., Villalba, R. and Haberzettl, T., 2009. Climate change in southern South America during the last two

millennia, Past climate variability in South America and surrounding regions. Springer, pp. 353-393.

Quinn, T.M., Crowley, T.J., Taylor, F.W., Henin, C., Joannot, P. and Join, Y., 1998. A multicentury stable isotope record from a New Caledonia coral: Interannual and decadal sea surface temperature variability in the southwest Pacific since 1657 AD. Paleoceanography, 13(4): 412-426.

Roper, D.S. and Hickey, C.W., 1994. Population structure, shell morphology, age and condition of the freshwater mussel *Hyridella menziesi* (Unionacea: Hyriidae) from seven lake and river sites in the Waikato River system. Hydrobiologia, 284(3): 205-217.

Rypel, A.L., Haag, W.R. and Findlay, R.H., 2009. Pervasive hydrologic effects on freshwater mussels and riparian trees in southeastern floodplain ecosystems. Wetlands, 29(2): 497-504.

Schöne, B.R., Dunca, E., Mutvei, H. and Norlund, U., 2004. A 217-year record of summer air temperature reconstructed from freshwater pearl mussels (*M. margarifitera*, Sweden). Quaternary Science Reviews, 23(16): 1803-1816.

Soldati, A., Jacob, D., Schöne, B., Bianchi, M. and Hajduk, A., 2009. Seasonal periodicity of growth and composition in valves of *Diplodon chilensis patagonicus* (d'Orbigny, 1835). Journal of Molluscan Studies, 75(1): 75-85.

Stokes, M.A., 1996. An introduction to tree-ring dating. University of Arizona Press.

Strom, A., Francis, R.C., Mantua, N.J., Miles, E.L. and Peterson, D.L., 2004. North Pacific climate recorded in growth rings of geoduck clams: a new tool for paleoenvironmental reconstruction. Geophysical Research Letters, 31(6).

Thresher, R.E., Fallon, S.J. and Townsend, A.T., 2016. A "core-top" screen for trace element proxies of environmental conditions and growth rates in the calcite skeletons of bamboo corals (*Isididae*). Geochimica et Cosmochimica Acta, 193: 75-99.

Tobin, T.S., Wilson, G.P., Eiler, J.M. and Hartman, J.H., 2014. Environmental change across a terrestrial Cretaceous-Paleogene boundary section in eastern Montana, USA, constrained by carbonate clumped isotope paleothermometry. Geology, 42(4): 351-354.

Villalba, R., Lara, A., Masiokas, M.H., Urrutia, R., Luckman, B.H., Marshall, G.J., Mundo, I.A., Christie, D.A., Cook, E.R. and Neukom, R., 2012. Unusual Southern Hemisphere tree growth patterns induced by changes in the Southern Annular Mode. Nature Geoscience, 5(11): 793-798.

Walker, K.F., Jones, H.A. and Klunzinger, M.W., 2014. Bivalves in a bottleneck: taxonomy, phylogeography and conservation of freshwater mussels (*Bivalvia: Unionoida*) in Australasia. Hydrobiologia, 735(1): 61-79.

Wanamaker, A.D., Heinemeier, J., Scourse, J.D., Richardson, C.A., Butler, P.G., Eiríksson, J. and Knudsen, K.L., 2008. Very long-lived mollusks confirm 17th century AD tephra-based radiocarbon reservoir ages for North Icelandic shelf waters. Radiocarbon, 50(3): 399-412.

PROPORTION OF CONTRIBUTIONS TO THE CHAPTERS

Co-authored and submitted chapters	Study concept and design (%)	Acquisition of data (%)	Analysis and interpretation (%)	Drafting of manuscript (%)
Chapter 1: The freshwater bivalve *Echyridella Menziesii*: a new environmental archive from Lake Rotorua, New Zealand.	90	80	90	90
Chapter 2: Temperature reconstructions by clumped isotopes, $\delta^{18}O$ and Sr/Ca using freshwater bivalve *Echyridella menziesii* from New Zealand	90	80	90	90
Chapter 3: The potential of three East Australian freshwater bivalve species as environmental proxy archives	90	90	80	90
Chapter 4: Climate signals in the shells of *Diplodon chilensis patagonicus* (Haas, 1931) bivalves in northern Patagonia, Argentina	60	40	60	50
Chapter 5: Medieval climatic anomaly signals in fossil *Diplodon chilensis patagonicus* (Haas, 1931) shells from Northern Patagonia	80	70	90	90

***